ABSTRACT

A modified Redlich-Kwong equation of state was employed for the prediction and extrapolation of vapor-liquid equilibrium data from limited information for the purpose of saving the cost and labor of experimental determinations.

A detailed calculation procedure was proposed for the determination of the equilibrium vapor composition and saturated pressure of the system from the given liquid composition and system temperature. Its applicability was tested on eleven binary systems at eighteen isothermal conditions. The agreement obtained between the predicted and literature data was very good with the exception of the system methane-ethylene. Further experimental investigation was required to substantiate the validity of the proposed method. For this reason, vapor-liquid equilibrium data were measured in this investigation for the methane-ethylene system at -193.1°, -173.1° and -156.1° F, the methane-ethane system at -173.1° F, and the methane-ethylene-ethane ternary system at -173.1° F and at pressures up to 330 p.s.i.a. by means of a forced-recirculation apparatus. The experimental results agreed well with the values predicted by the proposed method. In addition, adjustable activity coefficients were evaluated by means of the modified Redlich-Kwong equation of state and correlated by the Redlich-Kister equations.

The Redlich-Kwong equation of state was further extended to the supercritical region for the sake of prediction of gas solubilities, volumetric properties and phase equilibria of normal fluid mixtures with one supercritical component. The temperature-dependent parameters of the Redlich-Kwong equation were established for pure

component methane from its critical temperature, -115.78° F, up to 160° F. Solubilities of methane in various solvents have been successfully predicted. The proposed method has been satisfactorily applied to the prediction of vapor-liquid equilibrium data for five binary and three ternary systems. Molal and partial molal volumes of seven binary systems have also been evaluated.

In addition, values of excess enthalpy of mixing, excess Gibbs free energy of mixing and excess entropy of mixing for the hydrogen-nitrogen binary system over the complete concentration range between 170° and 290°K, and up to 95 atm., were evaluated by using a limited amount of information; and a method for determining the limiting slopes of the binary vapor-liquid equilibrium composition curve was also proposed.

ACKNOWLEDGEMENT

The author is deeply indebted to his supervisor, Dr. Benjamin C. -Y. Lu, for the advise, guidance, encouragement and personal understanding throughout the course of this investigation. He wishes to express his gratitude to Dr. F. D. F. Talbot for providing the gas partitioner, and to Dr. Shinn-der Chang for the helpful suggestions from time to time.

The author also wishes to acknowledge all the faculty members of the Chemical Engineering Department for their interest in this work, and to extend the appreciation to Mr. G. Gasperetti for his willing assistance in the construction of the equipment.

He is also indebted to the Government of the Province of Ontario for an Ontario Graduate Fellowship.

Finally, the author would like to express his most sincere gratitude to his wife, Sherly, whose faith, patience and encouragement made this work possible.

TABLE OF CONTENTS

			Page
ABSTRACT			i
ACKNOWLEDGEMENT			iii
TABLE OF CONTENTS			iv
LIST OF TABLES			vii
LIST OF FIGURES			xii
NOMENCLATURE			xvii
CHAPTER I	-	INTRODUCTION	1
CHAPTER II	-	LITERATURE REVIEW	3
2.1	-	CORRELATIONS BASED ON THE BENEDICT-WEBB-RUBIN EQUATION OF STATE	3
2.2	-	CORRELATIONS WITH THE REDLICH-KWONG EQUATION OF STATE	9
CHAPTER III	-	PREDICTION OF VAPOR-LIQUID EQUILIBRIA OF NORMAL FLUID MIXTURES WITH THE REDLICH-KWONG EQUATION OF STATE	25
3.1	-	EQUATION OF STATE IN PHASE EQUILIBRIA CALCULATIONS	25
3.2	-	REDLICH-KWONG EQUATION OF STATE	27
3.3	-	CALCULATION OF FUGACITY COEFFICIENTS	30
3.4	-	PREDICTION OF VAPOR-LIQUID EQUILIBRIA	31
3.5	-	COMPARISON WITH LITERATURE DATA	33

			Page
3.6	-	CONCLUSIONS	52
CHAPTER IV	-	EXPERIMENTAL STUDY OF VAPOR-LIQUID EQUILIBRIA: SYSTEM METHANE-ETHYLENE-ETHANE	60
4.1	-	APPARATUS	60
4.2	-	MATERIALS	69
4.3	-	EXPERIMENTAL PROCEDURES	69
4.4	-	MEASUREMENT ERRORS	71
4.5	-	RESULTS AND DISCUSSIONS	72
CHAPTER V	-	CORRELATION OF VAPOR-LIQUID EQUILIBRIA	87
5.1	-	CONSTANT-PRESSURE AND CONSTANT-TEMPERATURE ACTIVITY COEFFICIENT	87
5.2	-	PARTIAL MOLAL VOLUME	90
5.3	-	CORRELATION OF ACTIVITY COEFFICIENTS WITH THE REDLICH-KISTER EQUATION	91
5.4	-	RESULTS AND DISCUSSIONS	94
CHAPTER VI	-	PREDICTION OF GAS SOLUBILITIES AND PHASE EQUILIBRIA OF NORMAL FLUID MIXTURES WITH ONE SUPER-CRITICAL COMPONENT	117
6.1	-	FURTHER MODIFICATION OF THE REDLICH-KWONG EQUATION OF STATE	117
6.2	-	PREDICTION OF GAS SOLUBILITIES	119

			Page
6.3	-	PREDICTION OF PHASE EQUILIBRIA WITH ONE SUPERCRITICAL COMPONENT	122
6.4	-	PREDICTION OF VOLUMETRIC PROPERTIES	134
6.5	-	DISCUSSIONS AND CONCLUSIONS	145
CHAPTER VII	-	MISCELLANEOUS WORK	151
7.1	-	EXCESS THERMODYNAMIC PROPERTIES FOR HYDROGEN-NITROGEN MIXTURES	151
7.2	-	DETERMINATION OF LIMITING SLOPES OF BINARY VAPOR-LIQUID EQUILIBRIUM COMPOSITION CURVE	174
CHAPTER VIII	-	SUMMARY AND CONCLUSIONS	182
REFERENCES			185
APPENDIX A	-	PURE-COMPONENT PROPERTIES AND BINARY INTERACTION CONSTANTS	193
APPENDIX B	-	METHOD FOR THE EVALUATION OF Ω_a AND Ω_b FOR A SUBCRITICAL COMPONENT	198
APPENDIX C	-	COMPUTER PROGRAMS	202
APPENDIX D	-	CALIBRATION RESULTS OF THE GAS PARTITIONER	237

LIST OF TABLES

Table		Page
3-1	Comparison of the Benedict-Webb-Rubin Equation of State and the Redlich-Kwong Equation of State	28
3-2	Comparison of Calculated and Experimental Results for the System Benzene (1) - Cyclohexane (2)	35
3-3	Comparison of Calculated and Experimental Results for the System Propane (1) - Butane (2) at 160°F	37
3-4	Comparison of Calculated and Experimental Results for the System Propane (1) - n-Pentane (2) at 160°F	39
3-5	Comparison of Calculated and Experimental Results for the System Propane (1) - n-Decane (2)	41
3-6	Comparison of Calculated and Experimental Results for the System Propane (1) - Carbon Dioxide (2) at 40°F	45
3-7	Comparison of Calculated and Experimental Results for the System Hydrogen Sulfide (1) - n-Butane (2) at 100°F	46
3-8	Comparison of Calculated and Experimental Results for the System Ethane (1) - n-Pentane (2) at 40°F	48
3-9	Comparison of Calculated and Experimental Results for the System Ethane (1) - Propane (2)	50
3-10	Comparison of Calculated and Experimental Results for the System Ethylene (1) - Ethane (2) at -100°F	53

Table		Page
3-11	Predicted Vapor-Liquid Equilibrium Data for the Methane (1) - Ethane (2) System at -150°F	55
4-1	Analysis of Samples	73
4-2	Comparison of Experimental and Calculated Vapor-Liquid Equilibrium Data for the System Methane (1) - Ethylene (2)	80
4-3	Comparison of Experimental and Calculated Vapor-Liquid Equilibrium Data for the System Methane (1) - Ethane (3) at -173.1°F	83
4-4	Comparison of Experimental and Calculated Vapor-Liquid Equilibrium Data for the System Methane (1) - Ethylene (2) - Ethane (3) at -173.1°F	84
5-1	Predicted Vapor-Liquid Equilibrium Data for the System Ethylene (2) - Ethane (3) at -173.1°F	95
5-2	A Summary of Correlation Results for the Binary Systems	96
5-3	Experimental and Calculated Activity Coefficients for the System Methane (1) - Ethylene (2)	101
5-4	Experimental and Calculated Activity Coefficients for the System Methane (1) - Ethane (3) at -173.1°F	104
5-5	Experimental and Calculated Activity Coefficients for the System Methane (1) - Ethylene (2) - Ethane (3) at -173.1°F	106

Table		Page
5-6	Calculated Values of y and lnγ for the System Methane (1) - Ethylene (2) from the Literature Data	114
6-1	Comparison of Calculated and Experimental Results for the Solubility of Methane in Various Solvents	123
6-2	Comparison of Calculated and Experimental Results for the System Methane (1) - n-Butane (2) at 70°F	126
6-3	Comparison of Calculated and Experimental Results for the System Methane (1) - n-Butane (2) at 100°F	127
6-4	Comparison of Calculated and Experimental Results for the System Methane (1) - n-Pentane (2) at 100°F	129
6-5	Comparison of Calculated and Experimental Results for the System Methane (1) - n-Hexane (2) at 25°C	131
6-6	Comparison of Calculated and Experimental Results for the System Methane (1) - n-Heptane (2) at 40°F	133
6-7	Comparison of Calculated and Experimental Results for the System Methane (1) - Hydrogen Sulfide (2) at 40°F	136
6-8	Comparison of Calculated and Experimental Results for the System Methane (1) - Ethane (2) - Propane (3)	137
6-9	Comparison of Calculated and Experimental Results for the System Methane (1) - Propane (2) - n-Butane (3) at 40°F	139
6-10	Comparison of Calculated and Experimental Results for the System Methane (1) - Propane (2) - n-Pentane (3)	140

Table		Page
6-11	Summary of Results of Prediction of Volumetric Behavior	144
7-1	Comparison of Predicted and Experimental H^E Values Using the Method of Gunn et al. for a Gaseous Mixture of 47.5% H_2 and 52.5% N_2	153
7-2	Conditions of Experimental H^E Values Reported in the Literature	157
7-3	Excess Thermodynamic Properties for the H_2-N_2 Mixtures at 170°K	159
7-4	Excess Thermodynamic Properties for the H_2-N_2 Mixture at 180°K	160
7-5	Excess Thermodynamic Properties for the H_2-N_2 Mixtures at 190°K	161
7-6	Excess Thermodynamic Properties for the H_2-N_2 Mixtures at 200°K	162
7-7	Excess Thermodynamic Properties for the H_2-N_2 Mixtures at 210°K	163
7-8	Excess Thermodynamic Properties for the H_2-N_2 Mixtures at 220°K	164
7-9	Excess Thermodynamic Properties for the H_2-N_2 Mixtures at 230°K	165
7-10	Excess Thermodynamic Properties for the H_2-N_2 Mixtures at 240°K	166
7-11	Excess Thermodynamic Properties for the H_2-N_2 Mixtures at 250°K	167

Table		Page
7-12	Excess Thermodynamic Properties for the H_2-N_2 Mixtures at 260°K	168
7-13	Excess Thermodynamic Properties for the H_2-N_2 Mixtures at 270°K	169
7-14	Excess Thermodynamic Properties for the H_2-N_2 Mixtures at 280°K	170
7-15	Excess Thermodynamic Properties for the H_2-N_2 Mixtures at 290°K	171
A-1	Critical Constants and Acentric Factor of Pure Fluids	194
A-2	Values of Ω_a and Ω_b	195
A-3	Binary Interaction Constants k_{12}	197

LIST OF FIGURES

Figure		Page
3-1	Schematic Diagram of Bubble Point Calculation	34
3-2	Comparison of Calculated and Experimental Vapor-Liquid Equilibria of the Propane - n-Butane System at 160°F	38
3-3	Comparison of Calculated and Experimental Vapor-Liquid Equilibria of the Propane - n-Pentane System at 160°F	40
3-4	Comparison of Calculated and Experimental Vapor-Liquid Equilibria of the Propane - n-Decane System at 160°F	42
3-5	Comparison of Calculated and Experimental Vapor-Liquid Equilibria of the Propane - Carbon Dioxide System at 40°F	44
3-6	Comparison of Calculated and Experimental Vapor-Liquid Equilibria of the Hydrogen Sulfide - n-Butane System at 100°F	47
3-7	Comparison of Calculated and Experimental Vapor-Liquid Equilibria of the Ethane - n-Pentane System at 40°F	49
3-8	Comparison of Calculated and Experimental Vapor-Liquid Equilibria of the Ethylene-Ethane System at -100°F	54
3-9	Comparison of Calculated and Experimental Vapor-Liquid Equilibria of the Methane-Ethane System at -150°F	56

Figure		Page
3-10	Comparison of Calculated and Experimental Vapor-Liquid Equilibria of the Methane - Ethylene System at -104°C	57
3-11	Comparison of Calculated and Experimental Vapor-Liquid Equilibria of the Methane - Ethylene System at -146.06°C	58
4-1	Schematic Diagram of Experimental Apparatus	61
4-2	Front View of the Equipment Assembly	62
4-3	Side View of the Equipment Assembly	63
4-4	A View of Equilibrium Cell	65
4-5	Electric Circuit of Electromagnetic Pump	66
4-6	Schematic Diagram of Sampling System	68
4-7	Vapor-Liquid Equilibrium Data for the Methane-Ethylene System at -156.1°F	76
4-8	Vapor-Liquid Equilibrium Data for the Methane-Ethylene System at -173.1°F	77
4-9	Vapor-Liquid Equilibrium Data for the Methane-Ethylene System at -193.1°F	78
4-10	Vapor-Liquid Equilibrium Data for the Methane-Ethane System at -173.1°F	79
5-1	Comparison of Experimental and Calculated γ Values for the Methane-Ethylene System at -156.1°F	97
5-2	Comparison of Experimental and Calculated γ Values for the Methane-Ethylene System at -173.1°F	98

Figure		Page
5-3	Comparison of Experimental and Calculated γ Values for the Methane-Ethylene System at -193.1°F	99
5-4	Comparison of Experimental and Calculated γ Values for the Methane-Ethane System at -173.1°F	100
5-5	Area-test for the Methane-Ethylene System at -156.1°F	108
5-6	Area-test for the Methane-Ethylene System at -173.1°F	109
5-7	Area-test for the Methane-Ethylene System at -193.1°F	110
5-8	Area-test for the Methane-Ethane System at -173.1°F.	111
5-9	ln γ_1/γ_2 vs. x_1 Plot for the Literature Data	116
6-1	Temperature Dependent Characteristics of Ω_a and Ω_b of Methane in the Supercritical Region	120
6-2	Comparison of Calculated and Experimental Vapor-Liquid Equilibria of the Methane - n-Butane System at 70°F	124
6-3	Comparison of Calculated and Experimental Vapor-Liquid Equilibria of the Methane-n-Butane System at 100°F	125
6-4	Comparison of Calculated and Experimental Vapor-Liquid Equilibria of the Methane-n-Pentane System at 100°F	128
6-5	Comparison of Calculated and Experimental Vapor-Liquid Equilibria of the Methane-n-Hexane System at 25°C	130

Figure		Page
6-6	Comparison of Calculated and Experimental Vapor-Liquid Equilibria of the Methane-n-Heptane System at 40°F	132
6-7	Comparison of Calculated and Experimental Vapor-Liquid Equilibria of the Methane - Hydrogen Sulfide System at 40°F	135
6-8	Comparison of Calculated and Experimental K-Values for the Methane-Propane-n-Pentane System at 100°F.	141
6-9	Comparison of Calculated and Experimental K-Values for the Methane-Propane-n-Pentane System at 160°F.	142
6-10	Values of $\bar{V}^{\infty}_{CH_4}$ as a function of $(T_r)_{CH_4}$	146
6-11	Comparison of Calculated and Experimental Partial Molal Volumes of the Methane-n-Heptane System at 40°F	147
6-12	A Plot of $\bar{V}^{\infty}_{CH_4}$ vs. the Number of Carbon Atoms of the Aliphatic Hydrocarbon Solvents at 25°C	148
6-13	Correlation of k_{12} for the Methane-n-Alkane Binary Mixtures	150
7-1	Calculated Excess Thermodynamic Properties for the H_2-N_2 Mixtures at 200°K and 80 atm.	172
7-2	Comparison of the Experimental H^E Values with the Calculated Results for y_{H_2} = 0.475 Mixture	173
7-3	Correlation of log a and log a' with Temperature	179
7-4	Comparison of Predicted and Experimental Equilibrium Compositions for the Binary System n-Heptane - p-Dioxane at 80°C	180

Figure		Page
B-1	Schematic Diagram for Comparison of Original and Modified R-K Equation of State	201
D-1	Calibration of Gas Partitioner for the Methane-Ethylene System	238
D-2	Calibration of Gas Partitioner for the Methane-Ethylene System	239
D-3	Calibration of Gas Partitioner for the Ethylene-Methane System	240
D-4	Calibration of Gas Partitioner for the Ethylene-Methane System	241
D-5	Calibration of Gas Partitioner for the Methane-Ethane System	242
D-6	Calibration of Gas Partitioner for the Ethane-Methane System	243
D-7	Calibration of Gas Partitioner for the Ethane-Methane System	244
D-8	Calibration of Gas Partitioner for the Ethylene-Ethane System	245
D-9	Calibration of Gas Partitioner for the Ethane-Ethylene System	246

NOMENCLATURE

A_o, B_o, C_o, a, b, c, α, γ	=	constants in the Benedict-Webb-Rubin equation of state
A, B, a, b	=	parameters in the Redlich-Kwong equation of state
A', B'	=	binary parameters in equations (2-52) and (2-53)
A, B, A', B'	=	constants (equations (7-17) and (7-18))
a, b, a', b'	=	constants in the Clark equation (equations (7-13) and (7-14))
B_{12}, C_{12}, D_{12} B_{23}, C_{23}, D_{23} B_{31}, C_{31}, D_{31}	=	constants in the Redlich-Kister equation for binary systems
C	=	number of components
C, D_1, D_2, D_3	=	ternary constants in the Redlich-Kister equation (equation (5-13))
C_{ij}	=	interaction constant for pair of components i and j (equation (2-59))
c_1, c_2, c_3	=	constants in the Prahl equation (equation (7-19))
d_1, d_2, d_3	=	constants in equation (7-20)
f	=	fugacity
G	=	molal Gibbs free energy
H	=	molal enthalpy
h	=	dummy parameter in the Redlich-Kwong equation of state (equation (2-17))

K	=	vaporization equilibrium ratio, y/x
k	=	temperature-independent parameter in equation (2-32)
k_{ij}	=	binary interaction constant
n	=	number of moles or empirical constant in equations (2-46) and (2-47)
P	=	pressure
P'	=	vapor pressure of pure component
p_i	=	partial pressure of component i
Q	=	excess free energy function
R	=	gas constant
r	=	molecular size ratio (equation (2-45))
S	=	molal entropy
T	=	temperature
V	=	molal volume
x	=	liquid mole fraction
y	=	vapor mole fraction
Z	=	compressibility factor
z	=	number of nearest neighbour (equation (2-44))
z_i	=	mole fraction of the component i, either in the vapor phase or in the liquid phase
α	=	Bunsen absorption coefficient (equation (6-3))
$\alpha_{22(1)}$	=	self-interaction constant of molecules 2 in the environment of molecules 1 (equations (2-52) and (2-53))

β	=	second virial coefficient or adjustable constant of the modified B-W-R equation of state of Lin and Naphtali (equation (2-14))
γ	=	activity coefficient
Δ	=	difference
δ	=	solubility parameter
$\eta_{2(1)}$	=	dilation constant of solute 2 in solvent 1 (equation (2-53))
φ	=	fugacity coefficient
Φ	=	volume fraction (equation (2-45))
χ	=	energy parameter (equation (2-46))
ρ	=	density
θ_{ij}	=	temperature-independent parameter in equation (2-33)
μ	=	chemical potential
Ω_a, Ω_b	=	characteristic parameters of the Redlich-Kwong equation of state
ω	=	acentric factor

Superscripts

E	=	excess
id	=	ideal
r	=	reference state (equation (2-49))
o	=	reference state

^	=	fugacity or fugacity coefficient in the solution
−	=	partial molal quantity
∞	=	infinite dilution property
*	=	unsymmetric convention of normalization for activity coefficients

Subscripts

c	=	critical property
i, j, 1, 2, 3	=	component identification
L	=	liquid phase
V	=	vapor phase
r	=	reduced state
T	=	total property

CHAPTER I

INTRODUCTION

The design of industrial equipment for separation processes requires information on phase equilibrium properties of the system concerned. Frequently, the prevailing conditions of temperature, pressure and composition are different from those for which experimental data may be available. On the other hand, the high cost and time consumption of experimental investigation prevent us from making many measurements. For rational design, therefore, it is necessary to calculate phase equiiibrium relationships by reducing and generalizing the available but limited experimental data. To perform such calculations with confidence, suitable tools provided by thermodynamics must be utilized. It is most desirable if the phase equilibrium relationships could be represented by means of a suitable equation of state.

The Redlich-Kwong equation of state[1] is recognized as the best simple equation available[2] which can be used to represent fluid properties in both gaseous and liquid states[3, 4]. For this reason, the Redlich-Kwong equation of state with a certain modification[5] is chosen to be employed for the prediction and extrapolation of vapor-liquid equilibrium data from the limited information. The attention is restricted to normal fluid mixtures such as those encountered in the petroleum and related industries. The definition of normal fluid is that given by Pitzer[6]. In a simple statement[7], a normal fluid is one which is either nonpolar or else slightly polar, and which does not associate strongly (e. g., by hydrogen bonding); further, it is a fluid whose configurational properties can be evaluated to a sufficiently good approximation by classical, rather than quantum, statistical

mechanics. Hence, the following attempts are made in the present study:

(1) to propose a detailed calculation procedure for the determination of the equilibrium vapor composition and saturated pressure of the system from the given liquid composition and system temperature,

(2) to obtain experimental vapor-liquid equilibrium data for further justification of the proposed method,

(3) to correlate the experimental vapor-liquid equilibrium data, and

(4) to extend the Redlich-Kwong equation of state to the supercritical region for the prediction of gas solubilities, volumetric properties and phase equilibria of normal fluid mixtures involving one supercritical component.

CHAPTER II

LITERATURE REVIEW

A rather detailed review on the subject of vapor-liquid equilibria has recently been given by Chang[8]. An extensive review on the engineering applications of various equations of state was also made by many prominent workers - for instance, Shah and Thodos[2], Stewart and Timmerhaus[9], Martin[10], and recently, Tsonopoulos and Prausnitz[11]. In this thesis, only those publications which are pertinent to the present study are briefly reviewed and discussed in this chapter.

Many methods have been proposed to utilize equations of state for the correlation and/or prediction of vapor-liquid equilibria. In any of the equation-of-state methods, an equation of state is used to calculate either the values of the vapor-phase fugacity coefficient or the values of the vapor-phase as well as the liquid-phase fugacity coefficient. The method places great demands on the equation of state because it must be capable of representing the fluid properties, such as P-V-T behaviour.

Of the many empirical equations of state, the Benedict-Webb-Rubin equation[12] and the Redlich-Kwong equation[1] are widely used in the calculation of vapor-liquid equilibria.

2.1 CORRELATIONS BASED ON THE BENEDICT-WEBB-RUBIN EQUATION OF STATE

In 1940, Benedict and co-workers presented an equation of state with eight adjustable constants[12]:

$$P = RT\rho + (B_o RT - A_o - \frac{C_o}{T^2})\rho^2 + (bRT - a)\rho^3 + a\alpha\rho^6 + \frac{c\rho^3(1+\gamma\rho^2)\exp(-\gamma\rho^2)}{T^2} \quad (2\text{-}1)$$

where A_o, B_o, C_o, a, b, c, α, γ are the adjustable constants and ρ is the density.

The equation represents satisfactorily volumetric properties of nonpolar gases and liquids to densities up to about 1.8 times the critical[11]. Benedict and co-workers were primarily interested in applying their equation to hydrocarbon mixtures for calculation of K-values and enthalpies; combining rules for the eight constants were proposed in 1942[13]:

$$A_o = \left[\sum_i z_i (A_{oi})^{\frac{1}{2}}\right]^2 \quad (2\text{-}2)$$

$$B_o = \sum_i z_i B_{oi} \quad (2\text{-}3)$$

$$C_o = \left[\sum_i z_i (C_{oi})^{\frac{1}{2}}\right]^2 \quad (2\text{-}4)$$

$$a = \left[\sum_i z_i (a_i)^{\frac{1}{3}}\right]^3 \quad (2\text{-}5)$$

$$b = \left[\sum_i z_i (b_i)^{\frac{1}{3}}\right]^3 \quad (2\text{-}6)$$

$$c = \left[\sum_i z_i (c_i)^{\frac{1}{3}}\right]^3 \quad (2\text{-}7)$$

$$a = \left[\sum_i z_i (a_i)^{\frac{1}{3}}\right]^3 \tag{2-8}$$

$$\gamma = \left[\sum_i z_i (\gamma_i)^{\frac{1}{2}}\right]^2 \tag{2-9}$$

where z_i is the mole fraction of component i in the vapor or liquid phase.

Constants for twelve light hydrocarbons from methane through n-heptane were given by Benedict, Webb and Rubin in 1951[14] and their utility for calculating vapor-liquid equilibria was demonstrated[15, 16]. The K-value is calculated by means of the equation:

$$K_i = \frac{\hat{f}_{iL}/x_i}{\hat{f}_{iV}/y_i} \tag{2-10}$$

In which $\hat{f}_{iL}/x_i$ and $\hat{f}_{iV}/y_i$ are evaluated through the equation:

$$RT \ln (\hat{f}_i/z_i) = RT \ln[\rho RT] + \int_0^\rho \left[\left(\frac{\partial PV_T}{\partial n_i}\right)_{n, V_T, T} - RT\right] d \ln \rho \tag{2-11}$$

By substituting Equations (2-1) to (2-9) in Equation (2-11) gives

$$RT \ln (\hat{f}_i/z_i) = RT \ln[\rho RT] + \left[(B_o + B_{oi})RT - 2 (A_o A_i)^{\frac{1}{2}} - 2 (C_o C_{oi})^{\frac{1}{2}}/T^2\right]\rho + 3/2 \left[RT (b^2 b_i)^{\frac{1}{3}} - (a^2 a_i)^{\frac{1}{3}}\right]\rho^2$$

$$+ \frac{3}{5}\left[a\,(a^2 a_i)^{\frac{1}{3}} + a\,(a^2 a_i)^{\frac{1}{3}}\right]\rho^5$$

$$+ 3\rho^2\,(c^2 c_i)^{\frac{1}{3}}\left[\frac{1-\exp(-\gamma\rho^2)}{\gamma\rho^2} - \frac{\exp(-\gamma\rho^2)}{2}\right]/T^2$$

$$-\frac{2\rho^2 c}{T^2}\left(\frac{\gamma_i}{\gamma}\right)^{\frac{1}{2}}\left[\frac{1-\exp(-\gamma\rho^2)}{\gamma\rho^2} - \exp(-\gamma\rho^2) - \frac{\gamma\rho^2\exp(-\gamma\rho^2)}{2}\right] \qquad (2\text{-}12)$$

It should be noted that Equation (2-12) is applied to the liquid and the vapor phases. Combining Equations (2-10) and (2-12), the K-value is therefore calculated.

Because of its complexity, the correlation based on the Benedict-Webb-Rubin (B-W-R) equation of state is usually reduced to chart form to facilitate engineering application. Well-known correlations, such as Kellogg charts[16, 17] and DePriester's correlation[18] were therefore brought out.

2.1.1 Kellogg Charts[17]

A set of 324 charts was published by the M. W. Kellogg Company in 1950. The preparation of these charts was based on the B-W-R equation of state. The molal average boiling point (MABP) expressed in degrees Fahrenheit was chosen as the composition-dependent parameter. The charts cover a temperature range from -100° F to +400° F and a range of molal average boiling points from -255° F to +180° F. At 26 pressures between 14.7 and 1000 psia., the charts represent the dependence of the equilibrium distribution ratio (K-value), for twelve hydrocarbons,-namely, methane, ethylene, ethane, propylene, propane, i-butane, i-butylene, n-butane, i-pentane, n-pentane, n-hexane and

n-heptane,- on the temperature and MABP of the vapor and liquid phases. The Kellogg correlation gives an average deviation from experimental data of 7.1%.

2.1.2 DePriester's Correlation[18]

Linear or nearly linear relations between the two fugacity functions, $\hat{f}_{iL}/Px_i$ and $Py_i/\hat{f}_{iV}$, and pressure were found by DePriester[18]. Therefore, the Kellogg charts[17] were condensed into a more manageable form. This contains two sets of charts, the pressure-temperature-composition (P. T. C.) charts and the generalized correlation charts. The P. T. C. charts show K-values as the product of the vapor-phase fugacity function ($Py_i/\hat{f}_{iV}$) and liquid-phase fugacity function ($\hat{f}_{iL}/Px_i$) for temperatures from -100°F to +400°F, pressures up to 1000 p. s. i. a., and a range of phase compositions. K-values for twelve light hydrocarbons from methane through n-heptane are shown on twenty-four charts. The generalized correlation was presented on two nomographs, one for the temperature range from -100°F to 70°F and the other for the temperature range from 20°F to 400°F. The nomographs show K-values as a function of temperature and pressure only and were developed for use in preliminary calculations. The P. T. C. charts give an average deviation from experimental data of 6.4%. The generalized correlation is inherently less accurate than the P. T. C. charts because the effects of phase composition are not correlated. The average absolute deviation from experimental data is 15.0% for the generalized correlation.

Both the Kellogg correlation and the DePriester's correlation are applicable to calculate K-values of light hydrocarbon mixtures of

up to twelve components within the range of pressure, temperature and MABP of the charts with satisfactory results.

Schiller and Canjar[19] have applied the B-W-R equation to predict vapor-liquid equilibria for the nitrogen-carbon monoxide system with satisfactory results. However, the prediction of the K-values of mixtures of nitrogen-methane[20], of propane-carbon dioxide[21] and of light hydrocarbons containing hydrogen[22] were found to be far from satisfactory. Even for the systems consisting purely of light hydrocarbons, the predicted K-values were not satisfactory when the temperature was low and the pressure was high[23].

Several modifications have been suggested to improve the K-value prediction. Stotler and Benedict[20] have made an attempt to modify the combining rule for the constant A_o of the equation for the nitrogen-methane system

$$A_o = z_1^2 A_{o_1} + z_2^2 A_{o_2} + 2.874\, z_1 z_2 \qquad (2\text{-}13)$$

and they considered the constant C_o to be temperature-dependent. Lin and Naphtali[24] modified the B-W-R equation into the following form in order to predict the K-values of the nitrogen-methane, methane-carbon dioxide, propane-carbon dioxide and n-butane-carbon dioxide systems:

$$P = RT\rho + (B_oRT - A_o - C_o/T^{\beta})\,\rho^2 + (bRT - a)\rho^3 + a\alpha\rho^6 + (c\rho^3/T^2)(1 + \gamma\rho^2)\exp(-\gamma\rho^2) \qquad (2\text{-}14)$$

into which another adjustable constant, β, was introduced. Cullen and Kobe[21] also indicated that the lack of success in certain cases outside of the hydrocarbons was thought to be caused by the increased interac-

tion of the molecules of the components in the liquid phase. Therefore, one or more interaction constants are likely required in some cases to give a good overall representation of a binary mixture with the B-W-R equation of state.

Finally, it should be born in mind that, to obtain eight constants for a large number of substances would be a formidable task in view of the complexity of the B-W-R equation[11, 25]. The eight constants obtained from data reduction are probably not unique[11]. Several sets of constants may give equally good representation of the data. The non-uniqueness of the constants is not an important matter as long as attention is restricted to the properties of pure components but it becomes extremely important when pure component constants are used to predict mixture properties[26, 27].

2.2 CORRELATIONS WITH THE REDLICH-KWONG EQUATION OF STATE

A two-parameter equation of state was proposed by Redlich and Kwong in 1949[1] as follows:

$$P = RT/(V-b) - a/T^{\frac{1}{2}}\, V(V+b) \qquad (2\text{-}15)$$

It may be changed to the following form for practical use:

$$Z = 1/(1-h) - \frac{A^2}{B}\left(\frac{h}{1+h}\right) \qquad (2\text{-}16)$$

where:

$$h = BP/Z \qquad (2\text{-}17)$$

$$A^2 = a/R^2T^{2.5} = \Omega_a T_c^{2.5}/P_c T^{2.5} \qquad (2\text{-}18)$$

$$B = b/RT = \Omega_b T_c/P_c T \qquad (2\text{-}19)$$

$$\Omega_a = 0.4278 \qquad (2\text{-}20)$$

$$\Omega_b = 0.0867 \qquad (2\text{-}21)$$

For mixtures, Redlich and Kwong suggested the following combining rules:

$$b = \sum_i z_i b_i \qquad (2\text{-}22)$$

$$a = \sum_i \sum_j a_{ij} z_i z_j \qquad (2\text{-}23)$$

with:

$$a_{ij} = \sqrt{a_{ii} a_{jj}} \qquad (2\text{-}24)$$

The Redlich-Kwong equation of state has been chosen by many workers to represent the nonideality of fluid mixtures. It led to many well-known methods of correlation and/or prediction of vapor-liquid equilibria.

2.2.1 Correlation of Chao and Seader[28]

Chao and Seader[28] calculated the K-values through a combination of three factors:

$$K_i = (f_{iL}/P)\,(\gamma_i)/(\hat{\phi}_{iV}) \qquad (2\text{-}25)$$

The liquid fugacity coefficient of a pure component i, (f_{iL}/P), was correlated within the framework of Pitzer's modified form of the principle of corresponding states[29]. Accordingly, (f_{iL}/P) is given by:

$$\log (f_{iL}/P) = \log (f_{iL}/P)^{(0)} + \omega \log (f_{iL}/P)^{(1)} \qquad (2\text{-}26)$$

The quantities, $(f_{iL}/P)^{(0)}$ and $(f_{iL}/P)^{(1)}$, are dependent only on reduced temperature and reduced pressure. They have been fitted with the following approximating functions:

$$\log (f_{iL}/P)^{(0)} = A_o + A_1/T_r + A_2 T_r + A_3 T_r^2 + A_4 T_r^3 + (A_5 + A_6 T_r + A_7 T_r^2) P_r + (A_8 + A_9 T_r) P_r^2 - \log P_r \qquad (2\text{-}27)$$

$$\log (f_{iL}/P)^{(1)} = -4.23893 + 8.65808 T_r - 1.22060/T_r - 3.15224 T_r^3 - 0.025 (P_r - 0.6) \qquad (2\text{-}28)$$

The liquid activity coefficient, γ_i, was calculated from the theory of regular solutions of Scatchard and Hildebrand[30]:

$$\ln \gamma_i = V_i (\delta_i - \bar{\delta})^2/RT \qquad (2\text{-}29)$$

where

$$\bar{\delta} = \sum_i x_i V_i \delta_i / \sum_i x_i V_i \qquad (2\text{-}30)$$

The solubility parameter, δ_i, was calculated from the heat of vaporization and the liquid molal volume, V_i, at 25°C for most of the hydrocarbons. For hydrogen and for a number of light hydrocarbons, such as methane, ethane, and ethylene, the solubility parameter was treated

as empirical one and determined from the best fitting of experimental vapor-liquid equilibrium data, since these light gases are either in the supercritical region or very close to the critical temperature at the reference temperature of 25°C.

The vapor-phase fugacity coefficient of a component i, $\hat{\varphi}_{iV}$, was calculated using the following equation:

$$\ln \hat{\varphi}_{iV} = (Z - 1)\frac{B_i}{B} - \ln (Z - BP) - \frac{A^2}{B}\left[2\frac{A_i}{A} - \frac{B_i}{B}\right] \ln (1+BP/Z) \qquad (2-31)$$

with the aid of the Redlich-Kwong equation of state.

The correlation could be applied to hydrocarbons including paraffins, olefins, aromatics, and naphthenes. Hydrogen in hydrocarbon mixtures was also correlated. The correlation has failed at low temperatures and high temperatures as well, but Grayson and Streed[31] have extended the applicability range to a higher temperature region. The failure of their method may be due to the following reasons: (1) liquid molal volumes and solubility parameters were considered as temperature-independent, (2) the correlation of the liquid fugacity coefficient of a pure component was not successful at low temperatures, and (3) the correlation of the fugacity of a component in one phase did not possess much in common with the correlation of the behavior of the other phase.

2.2.2 Correlation of Wilson[3]

Wilson[3] proposed a method to correlate vapor-liquid equilibrium data of the methane-nitrogen and helium-hydrogen systems by means of the Redlich-Kwong equation of state with a modified procedure. In

his modification, he suggested that one utilizes the parameter of the equation $\Omega_b = 0.0867$ at all temperatures and makes the parameter a to be temperature-dependent according to the following equations:

$$a_{ii}/RT_{ci}^{1.5} = 4.934 \left[1 + k\left(\frac{1}{T_{r_i}} - 1\right)\right] T_{r_i}^{1.5} b_i \qquad (2\text{-}32)$$

$$a_{ij} = \theta_{ij} a_{ii} + (1 - \theta_{ij}) a_{jj} \qquad (2\text{-}33)$$

where k and θ_{ij} are temperature-independent parameters and T_{r_i} is the reduced temperature of component i. Two vapor pressure points are necessary to determine the temperature dependence.

Vapor-liquid equilibria are calculated from the equation through the application of the thermodynamic conditions of equilibrium, namely, that the pressure be the same in both phases and that the fugacity of each component be the same in both phases. The equation for the fugacity of a component is as follows:

$$\ln \hat{f}_i = \ln \frac{RT\, z_i}{V - b} + \frac{b_i}{b}\left(\frac{PV}{RT} - 1\right) - \frac{a}{RT^{3/2} b}\left[\frac{2\sum_j z_j a_{ij}}{a} - \frac{b_i}{b}\right] \ln\left(1 - \frac{b}{V}\right) \qquad (2\text{-}34)$$

In a recent paper[32] Wilson presents a complicated relation that combines Equations (2-32) and (2-33) and further improves the calculation of mixture properties. Wilson successfully applies his latest modification to the hydrogen-nitrogen system; for some other systems, especially those containing larger hydrocarbons, agreement is less satisfactory.

2. 2. 3 Correlation of Chang, Chappellar and Kobayashi[33]

K-values of methane in paraffinic, naphthenic and aromatic solvents at low temperatures and high pressures were correlated by Chang, Chappellar and Kobayashi[33]. K-values were expressed by an equation identical with the work of Chao and Seader[28],

$$K_i = (f_{iL}/P)\,(\gamma_i)/(\hat{\varphi}_{iV}) \tag{2-25}$$

where the quantity of (f_{iL}/P) was taken from Chao and Seader's work[28].

The vapor-phase fugacity coefficient, $\hat{\varphi}_{iV}$, was evaluated by means of the Redlich-Kwong equation of state with a simplified form of Wilson's modification[32]. The constants of the Redlich-Kwong equation for pure component were given as:

$$a_i = F(Tc/T,\ \omega)\, b_i RT^{1.5} \tag{2-35}$$

$$b_i = 0.0867\, RTc_i/Pc_i \tag{2-36}$$

where:

$$\begin{aligned} F(Tc/T,\ \omega) &= a/(b\,RT^{1.5}) \\ &= 4.934\,[1 + (1.45 + 1.62\,\omega) \\ &\quad (Tc/T - 1.0)]\,(Tc/T)^{0.12} \end{aligned} \tag{2-37}$$

or:

$$A_i^2 = a_i/(R^2 T^{2.5}) \tag{2-38}$$

$$B_i = b_i/RT \tag{2-39}$$

The constants for mixtures were given as:

$$A = \sum_i y_i A_i \tag{2-40}$$

$$B = \sum_i y_i B_i \tag{2-41}$$

Then the vapor-phase fugacity coefficient may be evaluated through Equations (2-16) and (2-17), and through the following equation:

$$\log \hat{\Phi}_{iV} = 0.4343 (Z - 1.0) (B_i/B) - \log (Z - BP) - \left(\frac{A^2}{B}\right)\left(2\frac{A_i}{A} - \frac{B_i}{B}\right) \log (1 + BP/Z) \tag{2-42}$$

The liquid-phase activity coefficient was taken as a sum of the athermal and thermal effects and was written in the form:

$$\ln \gamma_i = \ln \gamma_i^{ath} + \ln \gamma_i^{th} \tag{2-43}$$

The expression of $\ln \gamma_i^{ath}$ was given by Miller-Guggenheim[34, 35] as:

$$\ln \gamma_1^{ath} = \ln \left[(1 - \Phi_2)/x_1 \right] - z/2 \ \ln \left[1 - (1 - \frac{1}{r_1}) 2\Phi_2/z \right] \tag{2-44}$$

where:

$$\Phi_2 = r_1 x_2/(x_1 + r_1 x_2) \tag{2-45}$$

in which r_1 is the molecular size ratio. The number of nearest neighbor sites, z, was chosen as twelve.

The expression of $\ln \gamma^{th}$ was given as

$$\ln \gamma^{th} = \chi \Phi_2^n \tag{2-46}$$

where χ and n were fitted to the experimental data through the equation:

$$\chi = \left[\ln (K_i \hat{\varphi}_{iV}) - \ln (f_{iL}/P) - \ln \gamma_i^{ath}\right] \Phi_2^{-n} \quad . \tag{2-47}$$

The best results were obtained with n = 2.6.

K-values were computed by the combination of Equations (2-46), (2-44), (2-42) and (2-26).

Generally, the K-values of methane were predicted with the deviation falling within $\pm$ 5% of the experimental data up to 0.70 mole fraction of methane in the liquid phase; the failure in predicting the K-value near the critical point was due to the sharp increase of the concentration of methane in the liquid phase. However, the average relative deviation for the heavy component K-values ranged from + 20 to -200%. This failure may be due to the following: (1) the application to low temperatures of the correlation based on Pitzer's corresponding states principle (Equation (2-26))[28] for the liquid fugacity coefficient is not as successful as at high temperatures, (2) the approximate Redlich-Kwong equation of state[4, 32] was unsuccessful in describing the nonideality of the heavy component in the vapor phase, because the vapor-phase fugacity coefficients for the heavy components decreased markedly from unity as the pressure increased. This sharp decrease indicated the importance of the nonideality existing in the vapor phase for heavy components. When the temperature decreased, this behavior became more serious. As pointed out by the authors[33], a further modification for the equation of state would

be the inclusion of the effect of the inter-molecular forces acting between unlike molecules on the mixing rule which relates the constants of a mixture to those of the pure components.

2.2.4 Method of Chueh and Prausnitz[36]

Chueh and Prausnitz[36] presented a method for reducing binary vapor-liquid equilibrium data to thermodynamically significant binary parameters, and predicted the phase behavior of multicomponent mixtures by using these binary parameters.

Their method was mainly based on the following equation:

$$\hat{\Phi}_{iV}\, y_i\, P = \gamma_i\, x_i\, f_i^{\circ} \qquad (2\text{-}48)$$

The vapor-phase fugacity coefficient, $\hat{\Phi}_{iV}$, was evaluated by means of the Redlich-Kwong equation of state with certain modifications. In their modifications, the authors[36] proposed to evaluate the parameters of the Redlich-Kwong equation, Ω_a and Ω_b, for each component by fitting the original equation to the volumetric data of the saturated vapor. The temperature range used was that from the normal boiling point to the critical temperature. The combining rules which relate the parameters of a mixture to those of the pure components will be discussed in the next chapter.

For the liquid phase, the constant-pressure (composition-dependent) activity coefficients were expressed by the modified van Laar's model:

$$\ln \gamma_i(P^r) = A' \Phi_2^2 + B' \Phi_2^4 \qquad (2\text{-}49)$$

$$\ln \gamma_2^{*(P^r)} = A'\left(\frac{Vc_2}{Vc_1}\right)\left(\Phi_2^2 - 2\Phi_2\right) + B'\left(\frac{Vc_2}{Vc_1}\right)\left(\Phi_2^4 - \frac{4}{3}\Phi_2^3\right) \qquad (2\text{-}50)$$

where:

$$\Phi_2 \equiv \frac{x_2 Vc_2}{x_1 Vc_1 + x_2 Vc_2} \qquad (2\text{-}51)$$

$$A' \equiv a_{22(1)} Vc_1 \qquad (2\text{-}52)$$

$$B' \equiv 3\eta_{2(1)} a_{22(1)} Vc_1 \qquad (2\text{-}53)$$

and, subscript 1 refers to the condensable and subscript 2 to the noncondensable component, and the asterisk (*) in Equation (2-50) indicates that the unsymmetric convention has been used for normalization of the activity coefficients. $a_{22(1)}$ is called the self-interaction constant and $\eta_{2(1)}$ is called the dilation constant.

The pressure-dependence of the activity coefficients was calculated with the aid of the liquid-phase partial molal volumes using the following equation:

$$\left(\frac{\partial \ln \gamma_i}{\partial P}\right)_{T,x} = \frac{\bar{V}_i}{RT} \qquad (2\text{-}54)$$

The reference state was taken at a fixed pressure. The liquid-phase partial molal volumes were evaluated by means of the Redlich-Kwong equation of state with the following modification for liquid mixtures: The parameters, Ω_a and Ω_b, of the equation were obtained by fitting the Redlich-Kwong equation to the P-V-T data of the saturated liquid for each pure component. The same combining rules (which will be discussed in the next chapter) as were applied to the calculation of the vapor-phase fugacity coefficient were used, except that the cube-

root average for Vc_{ij} was replaced by the arithmetic mean of Vc_i and Vc_j.

For a solvent component, the standard-state fugacity was the pure liquid fugacity at zero pressure. For a solute component, the standard-state fugacity was Henry's constant in the mixed solvent, corrected to zero pressure.

The vapor-liquid equilibria were therefore predicted by using their equations of binary reduction by the following basic relation:

$$\hat{f}_{iV} = \hat{f}_{iL} \tag{2-55}$$

The vapor-phase fugacities were given by:

$$\hat{f}_{iV} = \hat{\varphi}_{iV}\, y_i\, P \tag{2-56}$$

and the liquid-phase fugacities were given by:

$$\hat{f}_{iL} = \gamma_i^{(P^r)}\, x_i\, f_i^{\circ(P^r)}\, \exp\left[(P - P^r)\, \bar{V}_{iL}/(RT)\right] \tag{2-57}$$

In general, this method can be applied to the systems containing nonpolar (or slightly polar) components and it will give a satisfactory result. The importance of the nonideality which exists in the vapor phase for the heavier component is increased markedly as the temperature decreases. At low temperatures, the equilibrium composition of the heavier component in the vapor phase is small; therefore, the average experimental error is relatively large for the heavier component. In such a case, the activity coefficients of the heavier component, directly evaluated from the vapor-liquid equilibrium compositions, are erratic. For this reason, any empirical expression, such as the modified van Laar's model, can not reliably represent the activity coefficients of the heavier component.

2.2.5 Method of Zudkevitch and Joffe[37]

Zudkevitch and Joffe[37] followed the approach of Wilson[3,4] and extended it to the quantity of Ω_b. They evaluated the Ω_a and Ω_b of the Redlich-Kwong equation of state separately for the saturated vapor phase and saturated liquid phase. In the establishment of the values of Ω_a and Ω_b, the generalized correlation of Lyckman, Eckert and Prausnitz[38] for fugacity coefficients was employed:

$$\log \varphi = (\log \varphi)^{(0)} + \omega (\log \varphi)^{(1)} \qquad (2\text{-}58)$$

where $(\log \varphi)^{(0)}$ and $(\log \varphi)^{(1)}$ are functions of the reduced temperature, tabulated by Lyckman, Eckert and Prausnitz.

It was found that for most compounds the values of Ω_a and Ω_b for the vapor phase ascend rapidly as Tr decreases. In several cases, the vapor-phase values take an erratic course and become negative after passing through a maximum. Therefore, the values of Ω_a and Ω_b evaluated from the saturated liquid properties were finally utilized for both phases.

The parameters of pure components were combined to give that of a mixture in the form of the following relation:

$$a_{ij} = (1 - C_{ij}) (a_{ii}\, a_{jj})^{0.5} \qquad (2\text{-}59)$$

where C_{ij} represents the deviation of a_{ij} from the classical geometric mean assumption. The establishment of C_{ij} was from experimental data.

The K-values for each component were then calculated through the fugacity coefficients in both phases,

$$K_i = \hat{\varphi}_{iL} / \hat{\varphi}_{iV} \qquad (2\text{-}60)$$

$\hat{\varphi}_{iL}$ and $\hat{\varphi}_{iV}$ were obtained from P-T-x-y data by means of the Redlich-Kwong equation of state with the modifications mentioned above. It has been mentioned by Zudkevitch and Joffe[37] that in actual engineering work, the compositions may be arrived at via flash routine. However, in such a case, no actual working example was given to illustrate their proposition.

It should be noticed that the temperature-dependent parameters Ω_a and Ω_b, obtained with their method would not satisfy the fundamental conditions, $\varphi_{iV} = \varphi_{iL}$. This drawback may be attributed to two factors: (1) using generalized fugacity coefficients to evaluate Ω_a and Ω_b, (2) using liquid phase Ω_a and Ω_b for both phases. It may be also mentioned here that the method of Wilson[3, 4] has the same drawback.

Joffe, Schroeder and Zudkevitch[39] recognized the above mentioned pitfalls; subsequently, they proposed an alternative procedure for establishing the pure component Ω_a and Ω_b parameters as temperature functions in their very recent publication. The procedure is essentially similar to the method proposed by Chang and Lu[5] in the calculation of partial molal volumes of liquid mixtures. Lyckman's correlated values of φ_L[38] were avoided by forcing the equalization of the fugacity coefficients in the saturated vapor and the saturated liquid. Therefore, the following relation was derived:

$$\Omega_a = \Omega_b \left[\frac{\ln \left[(V_V - b)/(V_L - b) \right] - P (V_V - V_L)/RT}{(Tc/T)^{3/2} \ln \left[V_V (V_L + b)/V_L (V_V + b) \right]} \right] \qquad (2\text{-}61)$$

Equation (2-61) was solved simultaneously with the Redlich-Kwong equation of state at each temperature below the critical point to yield

values of Ω_a and Ω_b. The solution proceeded by a trial and error procedure. But, Equation (2-61) becomes indeterminate at the critical point. It is therefore necessary to use the previous method to establish the values of Ω_a and Ω_b at the critical point.

2.2.6 Method of Chang and Lu for Prediction of Liquid Partial Molal Volumes[5]

The Redlich-Kwong equation of state was modified for the purpose of obtaining the partial molal volumes of normal fluid mixtures by Chang and Lu[5]. The parameters Ω_a and Ω_b of the equation were treated as temperature-dependent, and were obtained through a rigorous thermodynamic approach. Therefore, the fundamental condition of equilibrium state, $\varphi_{iV} = \varphi_{iL}$, was satisfied. The vapor pressures and saturated liquid densities of the pure components are the necessary information for evaluating the quantities of Ω_a and Ω_b. The detailed procedure of the calculation of the values of Ω_a and Ω_b is presented in Appendix B.

The applicability of treating Ω_a and Ω_b as temperature-dependent parameters for the subcooled liquid was tested using n-heptane as an example. It was shown that this modification did give a considerable improvement for the representation of the behavior of pure liquids at high pressures.

Partial molal volumes of six binary systems, methane-ethane, methane-propane, ethane-propane, nitrogen-oxygen, nitrogen-argon and argon-oxygen, were satisfactorily predicted. The differences between the calculated and experimental $\bar{V}_i$ values are generally less than 0.2%. The success in the prediction of volumetric properties of normal fluid mixtures by employing the modified Redlich-Kwong

equation of state invites a further application, to the prediction of other thermodynamic properties, such as vapor-liquid equilibria, excess thermodynamic properties of mixing, etc.

Although the modified equation may be readily applicable for the evaluation of vapor-liquid equilibria, its application is restricted to the situation when all components are in the subcritical region. It seems to be sufficiently promising to develop a method for the evaluation of the temperature-dependent parameters of the pure component when it is in the supercritical region, so that the modified Redlich-Kwong equation of state can be applied to the prediction of gas solubilities, volumetric properties and phase equilibria of normal fluid mixtures involving one supercritical component.

In summary, the conventional method of correlating vapor-liquid equilibrium data is to separate deviation from ideality into deviations occurring in the vapor phase and deviations occurring in the liquid phase, and then to fit these deviations with separate thermodynamically consistent correlation expressions. By this method deviations from ideality occurring in the vapor are usually calculated from an equation of state and deviations from ideality occurring in the liquid are calculated with reference to the pure liquid component. The Chao and Seader correlation[28], the method of Chang, Chappellar and Kobayashi[33] and the method of Chueh and Prausnitz[36] may be considered to be belonging to this category. The difficulties encountered in the application of this approach are: (1) at temperatures above the critical temperature of a component, a hypothetical pure liquid state is assumed, (2) relationships of liquid phase activity coefficients

must be employed, (3) the critical region is not amenable to treatment because of lack of continuity of the separate vapor and liquid equations. The other method of correlating vapor-liquid equilibria is utilizing a single equation of state which represents both the nonidealities in the vapor and the nonidealities in the liquid. The above mentioned difficulties may be avoided since the equation is continuous in going from vapor to liquid. The Kellogg correlation[16, 17], the DePriester correlation[18], the correlation of Wilson[3, 4] and the correlation of Zudkevitch and Joffe[37] belong to this group. This approach relies greatly on the capability of the equation of state to represent the fluid properties for pure components as well as their mixtures. The equation of state employed, on the other hand, should apply to versatile systems, wide temperature and pressure range, and over the complete concentration range as well. The modified Redlich-Kwong equation of Chang and Lu[5] appears promising to be followed up in predicting vapor-liquid equilibria because of its simplicity and wide application range.

CHAPTER III

PREDICTION OF VAPOR-LIQUID EQUILIBRIA OF NORMAL FLUID MIXTURES WITH THE REDLICH-KWONG EQUATION OF STATE

In view of the limitations of various methods for the correlation and/or prediction of vapor-liquid equilibrium data in the literature[3, 4, 16, 17, 18, 28, 33, 36, 37], it is most desirable to develop a new method for the prediction of vapor-liquid equilibria by means of a suitable equation of state. It also appears desirable to avoid, as much as possible, the difficulties encountered by other workers.

3.1 EQUATION OF STATE IN PHASE EQUILIBRIA CALCULATIONS

The basic relationship for defining phase equilibria is the equality of the chemical potential of each component i when distributed between two phases in equilibrium:

$$\mu_{iV} = \mu_{iL} \tag{3-1}$$

But, for practical engineering work, it is preferable to treat phase equilibria with the aid of fugacities rather than to use the chemical potentials directly[40, 41].

The fugacity of any component i of a solution, $\hat{f}_i$, may be defined by the equation[42]:

$$\begin{cases} \mu_i = \mu_i^\circ + RT \ln \hat{f}_i \\ \dfrac{f_i}{p_i} \to 1 \quad \text{as} \quad P \to 0 \end{cases} \tag{3-2}$$

where μ_i° is a function of T only and has precisely the same value as for the pure component i at the same temperature. If the mole fraction of this component is supposed to be progressively increased until it becomes equal to unity, the quantity μ_i° remains unchanged, because the fugacity has been defined in such a way that μ_i° is a function of temperature only. Therefore, it is the chemical potential of pure i at unit fugacity.

For vapor-liquid equilibrium, substitution of Equation (3-2) into Equation (3-1) gives

$$\hat{f}_{iV} = \hat{f}_{iL} \tag{3-3}$$

The quantity of $\hat{f}_{iV}$ and $\hat{f}_{iL}$ must be represented by a suitable function of temperature, pressure and composition. In doing so, an auxiliary function, the fugacity coefficient, is required, which is defined by:

$$\hat{\varphi}_{iV} = \hat{f}_{iV}/(y_i P) \tag{3-4}$$

and:

$$\hat{\varphi}_{iL} = \hat{f}_{iL}/(x_i P) \tag{3-5}$$

The fugacity coefficient of component i in the mixture, $\hat{\varphi}_i$, is rigorously related to the volumetric properties of the mixture[43, 44] through the following equation:

$$\ln \hat{\varphi}_i = \frac{1}{RT} \int_{V_T}^{\infty} \left[\left(\frac{\partial P}{\partial n_i} \right)_{T, V_T, n_j} - \frac{RT}{V_T} \right] dV_T - \ln Z \tag{3-6}$$

where n_i represents the number of moles of component i, V_T is the total volume of the mixture, and Z is the compressibility factor of the mixture. The total pressure is designated by P, and the absolute temperature by T. The subscript n_j in Equation (3-6) signifies that all mole numbers except n_i must be held constant.

To obtain numerical results from Equation (3-6), an equation of state is required.

Of the many empirical equations of state, only two are widely used in the calculation of phase equilibria. They are the Benedict-Webb-Rubin[12] and Redlich-Kwong[1] equations. These two equations and their applications have been discussed in the previous chapter. A brief comparison of these two equations is given in Table 3-1. In view of the simplicity and the range of applicability, the two-parameter Redlich-Kwong equation is more attrative.

3.2 REDLICH-KWONG EQUATION OF STATE

The working equation originally proposed by Redlich and Kwong[1] is of the following form:

$$Z = \frac{1}{1-h} - \frac{A^2}{B}\left(\frac{h}{1+h}\right) \tag{3-7}$$

where:

$$h = BP/Z \tag{3-8}$$

$$A^2 = a/R^2T^{2.5} = \Omega_a Tc^{2.5}/PcT^{2.5} \tag{3-9}$$

$$B = b/RT = \Omega_b Tc/PcT \tag{3-10}$$

$$\Omega_a = 0.4278 \tag{3-11}$$

$$\Omega_b = 0.0867 \tag{3-12}$$

TABLE 3 - 1

Comparison of the Benedict-Webb-Rubin Equation of State and the Redlich-Kwong Equation of State

	R - K Equation	B - W - R Equation
1)	Two parameters.	Eight parameters.
2)	Applied to normal fluid.	Applied to light paraffinic and olefinic hydrocarbons and their mixtures. (some additional non-hydrocarbons are included)
3)	One single set of constants can best represent the vapor pressure and P-V-T behavior in both gaseous and liquid states.	No unique set of constants can do the same job.
4)	Only saturated liquid properties are required to determine the parameters for pure substances.	One needs much more experimental data to determine the parameters for pure substances.
5)	Less accurate when applied to a pure substance in vapor region but accuracy increases in liquid region.	More accurate up to twice the critical density.
6)	Worked at low temperatures, and high density region.	Failed at low temperatures due to density limitation.
7)	Binary interaction constants are easily introduced.	It is relatively difficult to introduce interaction constants.

The values of Ω_a and Ω_b were obtained originally by setting the first and second partial derivatives of pressure with respect to volume equal to zero at the critical point. Namely, $\left(\frac{\partial P}{\partial V}\right)_{Tc} = 0$ and $\left(\frac{\partial^2 P}{\partial V^2}\right)_{Tc} = 0$. In this investigation, following up the approach of Chang and Lu[5], Ω_a and Ω_b are treated as temperature-dependent parameters rather than the universal constants, and are evaluated for each pure component, below its critical temperature, from the molal volumes and vapor pressures of the pure saturated liquid. The method of evaluation of Ω_a and Ω_b is presented in Appendix B.

When the Redlich-Kwong equation of state is applied to mixtures, the following mixing rules are used[5, 36]:

$$a = \sum_i \sum_j z_i z_j a_{ij} \tag{3-13}$$

$$b = \sum_i z_i b_i \tag{3-14}$$

where z_i represents the mole fraction of the component i, either in the vapor or in the liquid phase. The quantities a_{ij} and b_i are defined by:

$$a_{ij} = \Omega_{a_{ij}} R^2 Tc_{ij}^{2.5}/Pc_{ij} \tag{3-15}$$

$$b_i = \Omega_{b_i} RTc_{ii}/Pc_{ii} \tag{3-16}$$

in which:

$$Tc_{ij} = (Tc_{ii}\, Tc_{jj})^{0.5} (1 - k_{ij}) \tag{3-17}$$

$$\Omega_{a_{ij}} = 0.5 (\Omega_{a_{ii}} + \Omega_{a_{jj}}) \tag{3-18}$$

$$Pc_{ij} = Zc_{ij} R Tc_{ij}/Vc_{ij} \tag{3-19}$$

$$Vc_{ij} = [0.5\,(Vc_i^{\frac{1}{3}} + Vc_j^{\frac{1}{3}})]^3 \tag{3-20}$$

$$Zc_{ij} = 0.291 - 0.08\,\omega_{ij} \tag{3-21}$$

$$\omega_{ij} = 0.5\,(\omega_i + \omega_j) \tag{3-22}$$

It may be mentioned that the quantity k_{ij} in Equation (3-17) is the binary interaction constant, which is a constant characteristic of i-j interaction; as a good approximation, k_{ij} is assumed to be independent of temperature, density, and composition[36]. A minimum of one observation of a binary mixture property, such as vapor-liquid equilibrium data, saturated liquid molal volume, second virial cross coefficient, etc., is needed for evaluating the value of k_{ij}.

Equations (3-13) to (3-22) are identical with those employed by Chang and Lu[5] and Chueh and Prausnitz[36]. If i = j, these equations can be reduced to those of the pure component.

3.3 CALCULATION OF FUGACITY COEFFICIENTS

Upon substituting Equation (3-7) and the mixing rules, Equations (3-13) to (3-22), into Equation (3-6), the fugacity coefficients of component i in a multicomponent mixture for both phases may be expressed as follows:

$$\ln \hat{\varphi}_{iV} = (Z_V - 1)\frac{B_i}{B} - \ln (Z_V)\,(1 - h_V) - \left(\frac{A^2}{B}\right)\left(\frac{2\sum_j y_j A_{ji}^2}{A^2} - \frac{B_i}{B}\right) \ln (1 + h_V) \tag{3-23}$$

and

$$\ln \hat{\varphi}_{iL} = (Z_L - 1)\frac{B_i}{B} - \ln (Z_L)(1 - h_L)$$
$$-\left(\frac{A^2}{B}\right)\left(\frac{2\sum_j x_j A_{ji}^2}{A^2} - \frac{B_i}{B}\right) \ln (1 + h_L) \qquad (3\text{-}24)$$

The compressibility factor Z is one of three roots of Equation (3-7) rearranged in the following form:

$$f(Z) = Z^3 - Z^2 + BP\left(\frac{A^2}{B} - 1 - BP\right)Z - \frac{A^2}{B}(BP)^2 = 0 \qquad (3\text{-}25)$$

The smallest root is taken as the compressibility factor of the saturated liquid, Z_L, and the largest root is taken as that of the saturated vapor, Z_V.

3.4 PREDICTION OF VAPOR-LIQUID EQUILIBRIA

Chang and Lu[5], and Zudkevitch and Joffe[37] have treated Ω_a and Ω_b of the Redlich-Kwong equation of state as the temperature-dependent parameters. However, Chang and Lu[5] applied their modified form of the Redlich-Kwong equation only to the prediction of partial molal volumes of normal fluid mixtures. Zudkevitch and Joffe[37] employed their modified Redlich-Kwong equation to correlate vapor-liquid equilibrium data, but the experimental P-T-x-y data have been used directly in the correlation of K-values.

In the present work, the method of Chang and Lu[5] is extended to predict the vapor phase composition and the saturated pressure from the specified temperature and liquid phase composition.

For vapor-liquid equilibria of a C-component system, the variables of interest are the system temperature, total pressure, (C-1) independent liquid-phase mole fractions and (C-1) independent vapor-phase mole fractions. Therefore, there are 2C variables in total. At equilibrium, the following equation must be satisfied:

$$\hat{f}_{iV} = \hat{f}_{iL}, \qquad i = 1, 2, \ldots\ldots C \tag{3-3}$$

in which:

$$\hat{f}_{iV} = \hat{\varphi}_{iV}\, y_i\, P \tag{3-4}$$

$$\hat{f}_{iL} = \hat{\varphi}_{iL}\, x_i\, P \tag{3-5}$$

If the temperature and (C-1) independent liquid-phase mole fractions are specified, it should be possible to calculate the total pressure and (C-1) independent vapor-phase mole fractions with the aid of Equation (3-3). This is the so-called bubble-point calculation. The C simultaneous equations may be solved by a trial-and-error procedure. Arbitrary values of P and $\hat{\varphi}_{iV}$ are assumed for the first iteration; for example, P = 100 p. s. i. a. and $\hat{\varphi}_{iV} = 1$. From the given x_i's and T, $\hat{\varphi}_{iL}$ is calculated by means of Equation (3-24), the vapor-phase compositions are calculated by:

$$y_i = (\hat{\varphi}_{iL}/\hat{\varphi}_{iV})\, x_i \tag{3-26}$$

and the total pressure is calculated by:

$$P = \sum_{i=1}^{C} \hat{f}_{iL}/\hat{\varphi}_{iV} \tag{3-27}$$

which is then compared with the previously assumed value. If it is different, $\hat{\varphi}_{iV}$'s are recalculated by Equation (3-23) with the newly obtained value of pressure and normalized y_i's, and then $\hat{\varphi}_{iL}$'s are also recalculated with the new value of P. When the pressure is no longer changed within a desired tolerance (in the present investigation, $\Delta P/P = 0.0001$), the relation:

$$\sum_{i=1}^{C} y_i = 1 \qquad (3\text{-}28)$$

is finally tested. Usually this is fulfilled while the pressure remains unchanged. If it is not satisfied, the $\hat{\varphi}_{iV}$'s must be recalculated and the iteration is continued. A schematic diagram of the iteration is shown in Figure 3-1. It may be mentioned that hypothetical standard states are eliminated and any artificial relationships of liquid activity coefficients are avoided in the present study.

3.5 COMPARISON WITH LITERATURE DATA

An extensive comparison was carried out for the results from the proposed prediction method. The systems were normal fluid mixtures and were arbitrarily chosen for the purpose of comparison.

Benzene-Cyclohexane: The predicted results for the benzene-cyclohexane system at 39.99° and 69.96°C are compared with the reported data of Scatchard, Wood and Machel[45] in Table 3-2. The agreement is very good. The average absolute deviation and maximum absolute deviation in pressure are 0.56 mm. Hg. and 1.22 mm. Hg., respectively. The average absolute deviation and maximum absolute deviation in vapor-phase composition are 0.0018 and 0.0055 mole fraction, respectively.

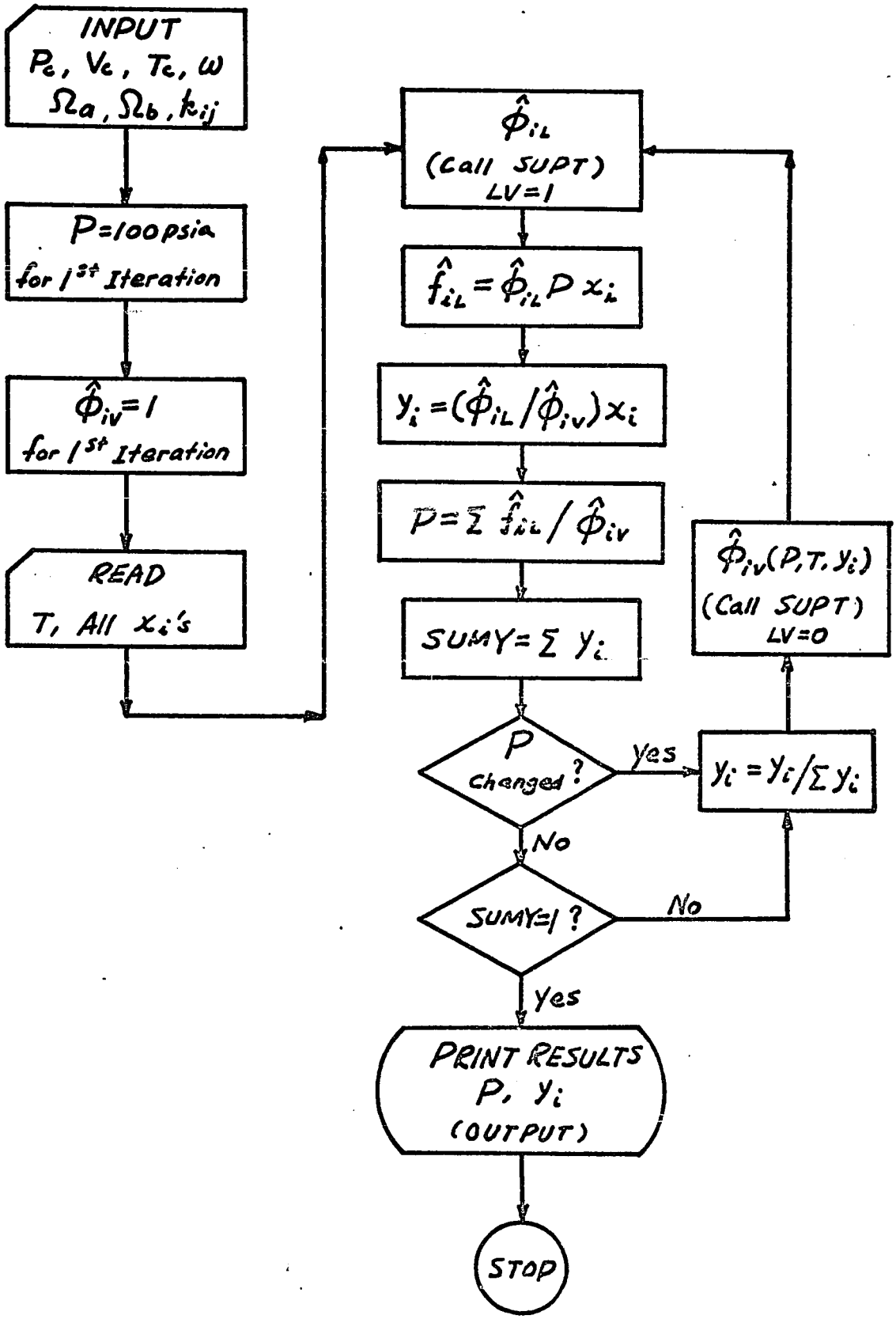

Figure 3-1 Schematic Diagram of Bubble Point Calculation

TABLE 3 - 2

Comparison of Calculated and Experimental Results for the System Benzene (1) - Cyclohexane (2)

$k_{ij} = 0.0095$*

T, °C	x_1	P. mm. Hg.		y_1		Deviation	
		expt.[45]	calc.	expt.[45]	calc.	ΔP	Δy_1
39.99	0.1282	194.94	195.93	0.1657	0.1641	-0.99	0.0016
	0.2354	200.65	201.17	0.2766	0.2759	-0.52	0.0007
	0.3685	204.75	205.05	0.3912	0.3950	-0.30	-0.0038
	0.4932	206.12	206.42	0.4950	0.4958	-0.30	-0.0008
	0.6143	205.18	205.58	0.5909	0.5914	-0.40	-0.0005
	0.7424	201.73	202.16	0.6979	0.6992	-0.43	-0.0013
	0.8656	195.04	195.85	0.8205	0.8205	-0.81	0.0000
69.96	0.1186	567.60	566.66	0.1486	0.1504	0.94	-0.0018
	0.2409	584.90	583.68	0.2805	0.2796	1.22	0.0009
	0.3759	596.16	595.31	0.3982	0.4033	0.85	-0.0051
	0.4945	600.27	599.87	0.4975	0.5030	0.40	-0.0055
	0.6180	599.32	599.18	0.6027	0.6044	0.14	-0.0017
	0.7248	593.48	593.79	0.6962	0.6957	-0.31	0.0005
	0.8659	577.79	578.06	0.8311	0.8324	-0.27	-0.0013

* In this study, all k_{ij}'s were determined from fitting experimental vapor-liquid equilibrium data at one temperature, using one to several experimental values. However, for the binary system under consideration, the same k_{ij} value was employed for predicting vapor-liquid equilibrium data and volumetric properties at other pressures and temperatures.

Propane-n-Butane: The comparison of calculated and experimental[46] K-values for the propane-n-butane system at 160° F is shown in Table 3-3. The calculated P-T-x-y values are also compared with experimental data in Figure 3-2. The average absolute deviation in pressure is 1.69 p.s.i.a. which is less than 1.0%. The average absolute deviation in vapor-phase mole fraction for propane is 0.0213.

Propane-n-Pentane: Good agreement between calculated and experimental values was observed for the system propane-n-pentane at 160° F. The data were taken from Sage and Lacey[47]. The comparison is made in Figure 3-3 and Table 3-4. The average absolute deviation in pressure is 0.38 p.s.i.a. and that in vapor-phase mole fraction is 0.0109.

Propane-n-Decane: The vapor-phase of the propane-n-decane system contains mostly propane. The data were taken from Reamer and Sage[48]. The comparison is made in Table 3-5 for two temperatures, 100° and 160° F. The results of 160° F are also shown in Figure 3-4. Very good agreement between calculated and experimental values was observed. The average absolute deviation in pressure is 1.66 p.s.i.a. and the average absolute deviation in vapor-phase mole fraction is 0.0009.

Propane-Carbon Dioxide: Mixtures of carbon dioxide and hydrocarbons exhibit irregular behavior[49]. Therefore, the system propane-carbon dioxide deserves special attention. Satisfactory results for the prediction have been obtained. The experimental data of Reamer, Sage and Lacey[50] were taken and compared with the calculated results at 40° F. The results are shown in Figure 3-5 and

TABLE 3 - 3

Comparison of Calculated and Experimental Results for the System Propane (1) - n-Butane (2) at 160° F

$k_{ij} = 0.00$

	P, psia		K_1		K_2		Deviation		
x_1	expt.[46]	calc.	expt.[46]	calc.	expt.[46]	calc.	P	K_1	K_2
0.1223	150	151.20	2.22	2.16	0.830	0.839	-1.20	0.06	-0.009
0.3241	200	201.26	1.73	1.66	0.650	0.685	-1.26	0.07	-0.035
0.5158	250	249.63	1.43	1.37	0.542	0.605	0.37	0.06	-0.063
0.6966	300	296.87	1.23	1.19	0.472	0.563	3.13	0.04	-0.091
0.8788	350	347.49	1.08	1.06	0.420	0.543	2.51	0.02	-0.123

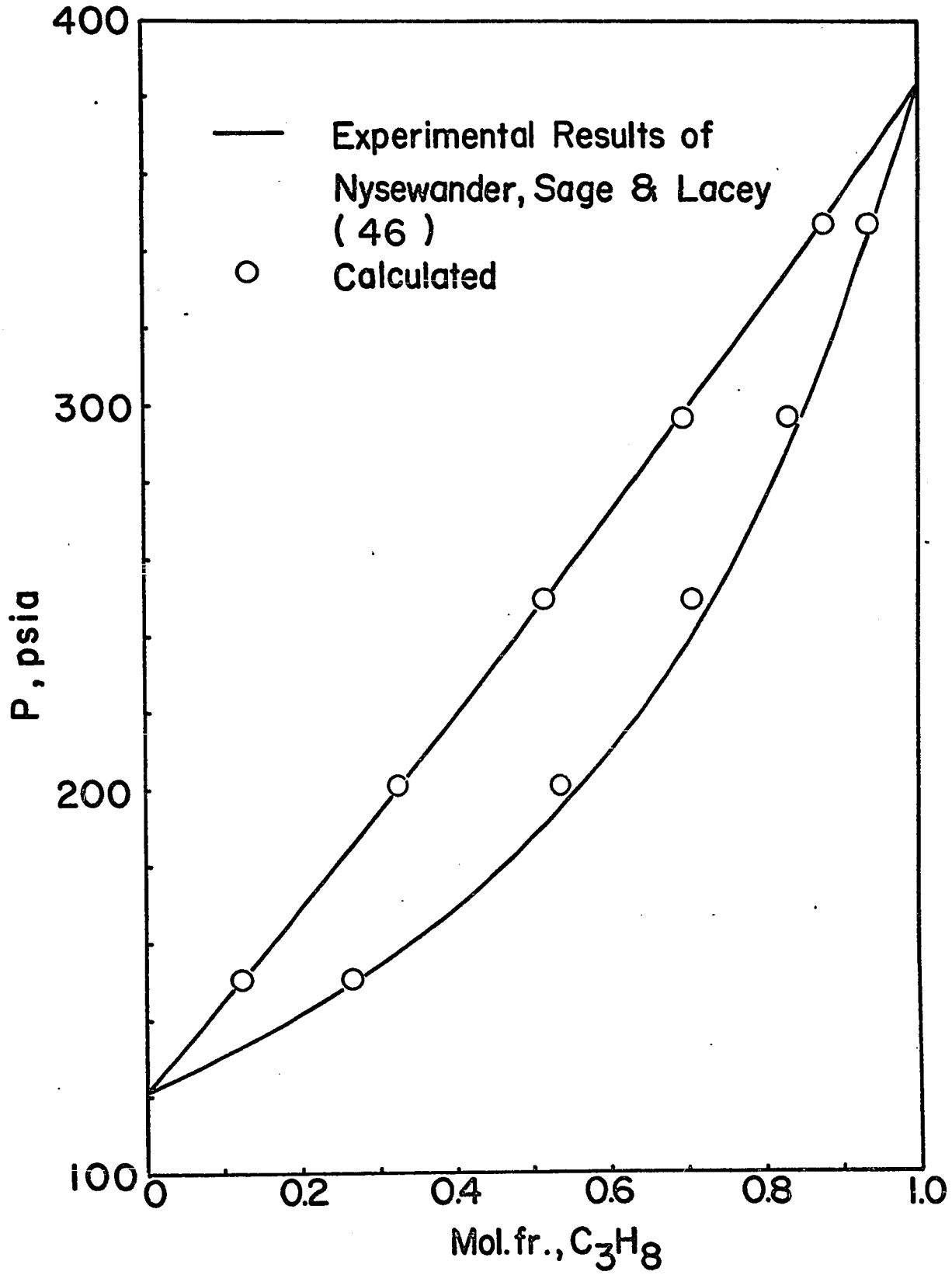

Figure 3-2 Comparison of Calculated and Experimental Vapor-Liquid Equilibria of the Propane-n-Butane System at 160° F

TABLE 3 - 4

Comparison of Calculated and Experimental Results for the System Propane (1) - n-Pentane (2) at 160° F

$k_{ij} = 0.0060$

	P, psia		y_1		Deviation	
x_1	expt.[47]	calc.	expt.[47]	calc.	ΔP	Δy_1
0.058	60	60.12	0.295	0.3099	-0.12	-0.0149
0.124	80	80.28	0.482	0.4996	-0.28	-0.0176
0.189	100	100.23	0.600	0.6136	-0.23	-0.0136
0.270	125	125.26	0.701	0.7066	-0.26	-0.0056
0.350	150	151.20	0.770	0.7697	-1.20	0.0003
0.504	200	199.13	0.863	0.8507	0.87	0.0123
0.657	250	249.76	0.920	0.9051	0.24	0.0149
0.799	300	300.14	0.958	0.9455	-0.14	0.0125
0.925	350	350.05	0.986	0.9790	-0.05	0.0070

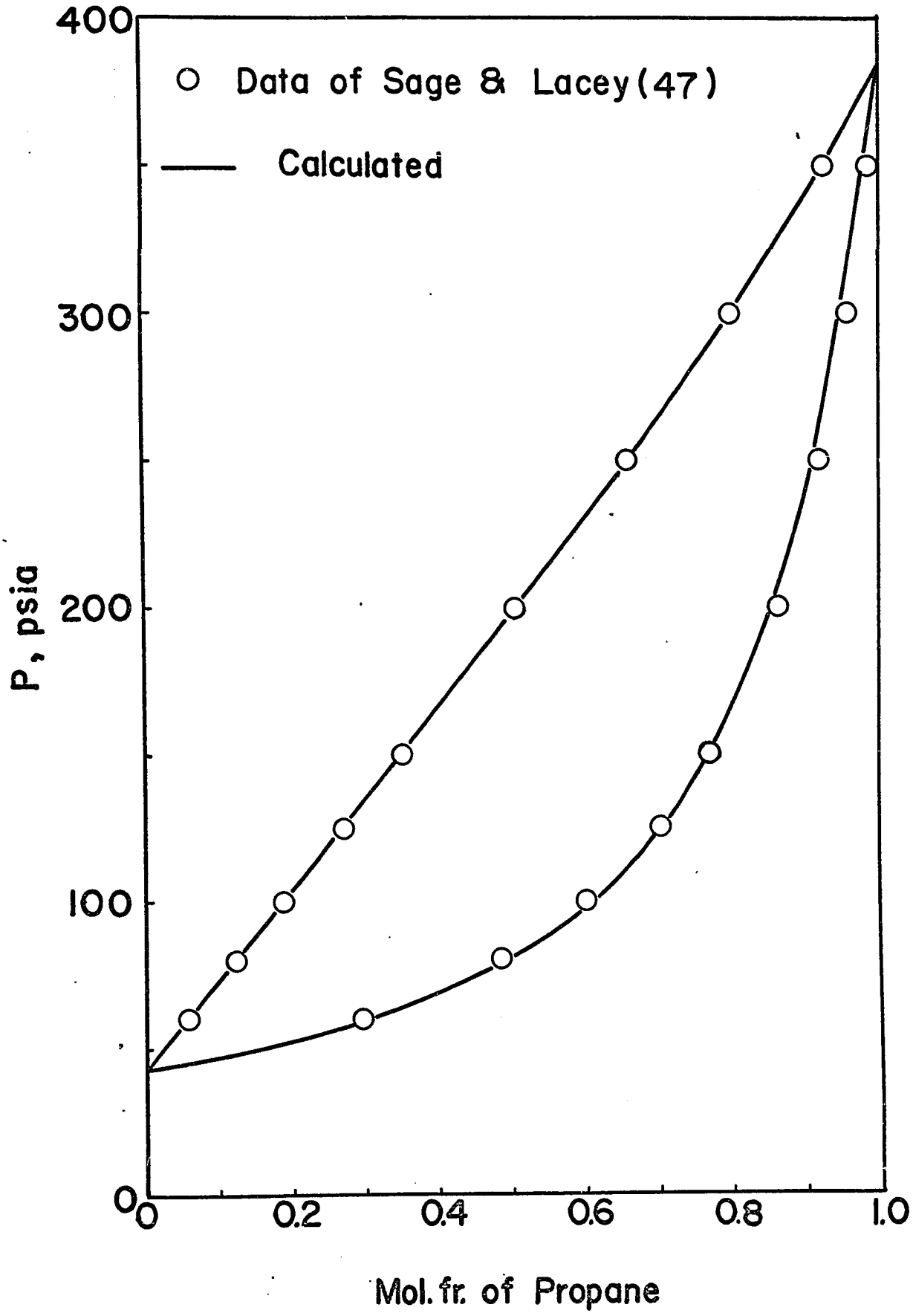

Figure 3-3 Comparison of Calculated and Experimental Vapor-Liquid Equilibria of the Propane-n-Pentane System at 160° F

TABLE 3 - 5

Comparison of Calculated and Experimental Results for the System Propane (1) - n-Decane (2)

$k_{ij} = 0.0450$

		P, psia		y_1		Deviation	
T, °F	x_1	expt.[48]	calc.	expt.[48]	calc.	ΔP	Δy_1
100	0.2973	50	49.44	0.9979	0.9987	0.56	-0.0008
	0.5746	100	100.41	0.9989	0.9995	-0.41	-0.0006
	0.8253	150	150.80	0.9996	0.9998	-0.80	-0.0002
160	0.1652	50	48.61	0.9910	0.9917	1.39	-0.0007
	0.3178	100	98.50	0.9984	0.9959	1.50	0.0025
	0.4584	150	147.44	0.9961	0.9973	2.56	-0.0012
	0.5899	200	196.98	0.9969	0.9981	3.02	-0.0012
	0.8275	300	296.96	0.9985	0.9990	3.04	-0.0005

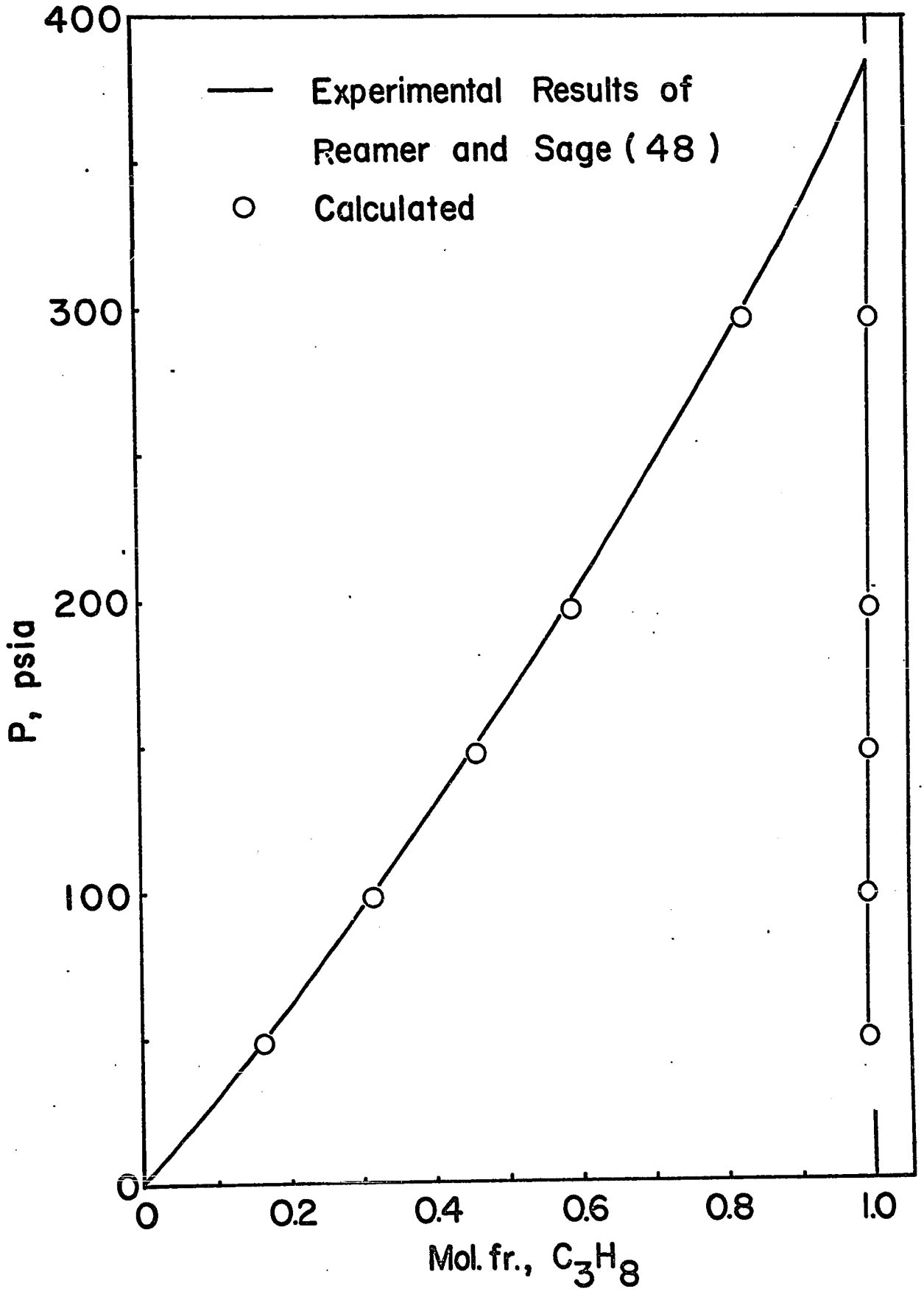

Figure 3-4 Comparison of Calculated and Experimental Vapor-Liquid Equilibria of the Propane-n-Decane System at 160° F

TABLE 3 - 6

Comparison of Calculated and Experimental Results for the System Propane (1) - Carbon Dioxide (2) at 40° F

$k_{ij} = 0.095$

	P, psia		y_1		Deviation	
x_1	expt.[50]	calc.	expt.[50]	calc.	ΔP	Δy_1
0.9753	100	98.47	0.7944	0.8069	1.53	-0.0125
0.9116	150	146.65	0.5324	0.5414	3.35	-0.0090
0.8398	200	197.84	0.3964	0.3969	2.16	-0.0005
0.7598	250	250.74	0.3136	0.3069	- 0.74	0.0067
0.6684	300	305.64	0.2569	0.2436	- 5.64	0.0133
0.5639	350	361.20	0.2124	0.1957	-11.20	0.0167
0.4468	400	415.06	0.1691	0.1569	-15.06	0.0122
0.3286	450	462.07	0.1312	0.1245	-12.07	0.0067
0.2044	500	505.88	0.0898	0.0904	- 5.88	-0.0006
0.0599	550	551.24	0.0298	0.0369	- 1.24	-0.0071

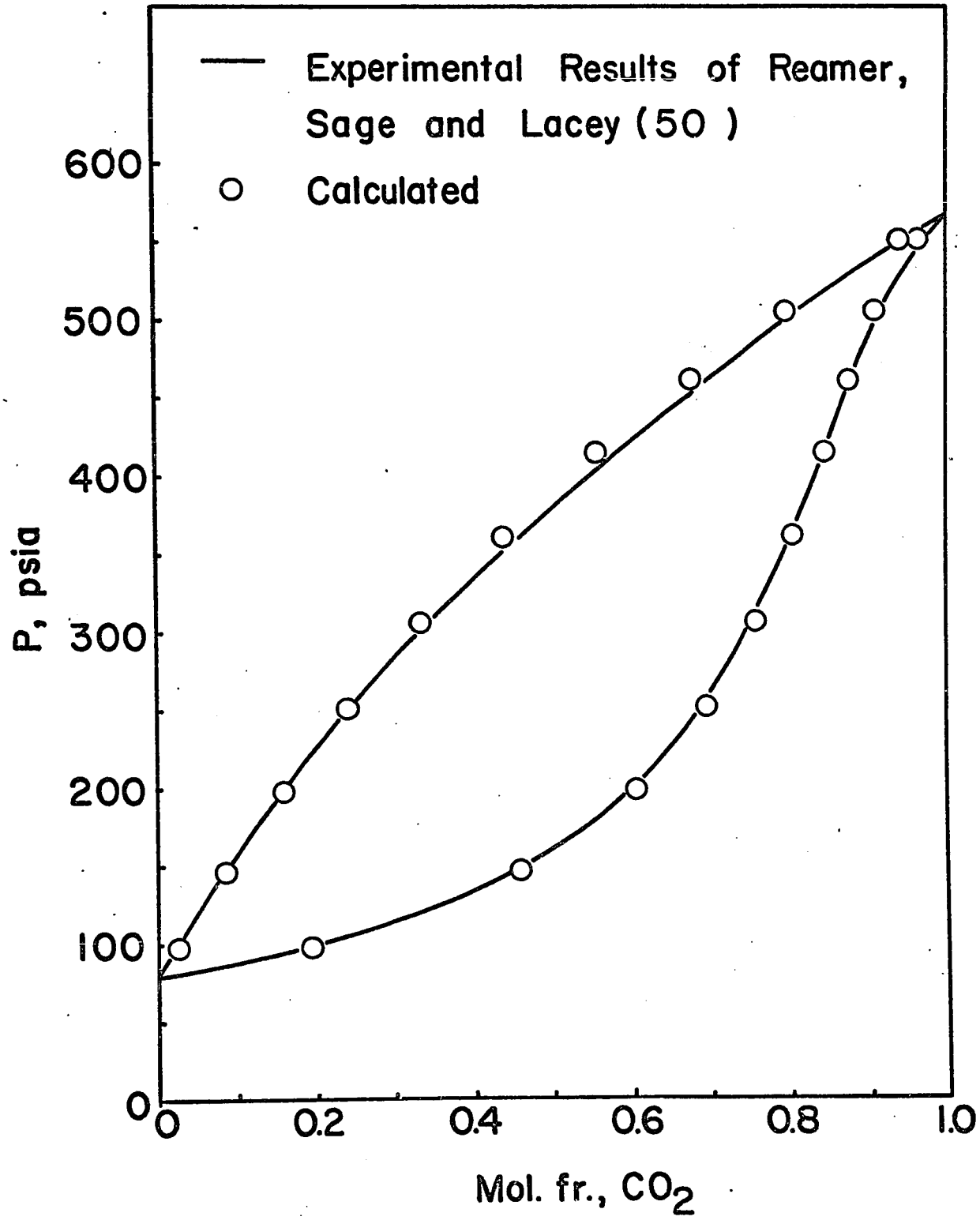

Figure 3-5 Comparison of Calculated and Experimental Vapor-Liquid Equilibria of the Propane-Carbon Dioxide System at 40° F

Table 3-6. The average absolute deviation in pressure is 5.89 p.s.i.a. and that in vapor-phase mole fraction is 0.0085.

Hydrogen Sulfide-n-Butane: The experimental data of Robinson, Hughes and Sandercock[51] were taken and compared with the calculated values for the hydrogen sulfide-n-butane system at 100°F. The results of comparison are shown in Figure 3-6 and Table 3-7. The average absolute deviation in pressure is 3.17 p.s.i.a. and that in vapor-phase mole fraction is 0.014.

Ethane-n-Pentane: The prediction of phase behavior in the ethane-n-pentane system at 40°F was tested against the data of Reamer, Sage and Lacey[52]. The results are listed in Table 3-8 and shown in Figure 3-7. The average absolute deviation in pressure is 1.56 p.s.i.a. and that in vapor-phase composition is 0.0038 mole fraction.

Ethane-Propane: Very recently, Djordjevich and Budenholzer[53] have reported vapor-liquid equilibrium data for the ethane-propane system at low temperatures. These data were compared with the calculated values in Table 3-9 for five temperatures from 0°F to -200°F. The binary interaction constant, k_{ij}, evaluated from this set of data is -0.025 which is different from the value established from the data of Price and Kobayashi[54] at 50°F (k_{ij} = -0.015). The validity of some data points has been questioned. The average deviation in pressure is less than 4% and that in vapor-phase composition for ethane is about 1.5%. It was found that the calculation failed to converge while the pressure lower than 10 mm. Hg. It may be attributed to the supersensitivity of the pure component property to the mixture property.

TABLE 3 - 7

Comparison of Calculated and Experimental Results for the System Hydrogen Sulfide (1) - n-Butane (2) at 100° F

$k_{ij} = 0.062$

	P, psia		y_1		Deviation	
x_1	expt.[51]	calc.	expt.[51]	calc.	ΔP	Δy_1
0.021	60.4	60.63	0.133	0.152	-0.23	-0.019
0.066	84.8	79.83	0.386	0.366	4.97	0.020
0.131	111.0	107.19	0.539	0.540	3.81	-0.001
0.209	146.8	139.35	0.655	0.661	7.45	-0.006
0.355	203.4	197.07	0.763	0.783	6.33	-0.020
0.468	239.3	238.96	0.818	0.838	0.34	-0.020
0.607	283.8	286.36	0.870	0.886	-2.56	-0.016
0.716	315.8	319.83	0.904	0.916	-4.03	-0.012
0.805	343.0	344.63	-	0.938	-1.63	-
0.858	358.8	358.44	-	0.951	0.36	-

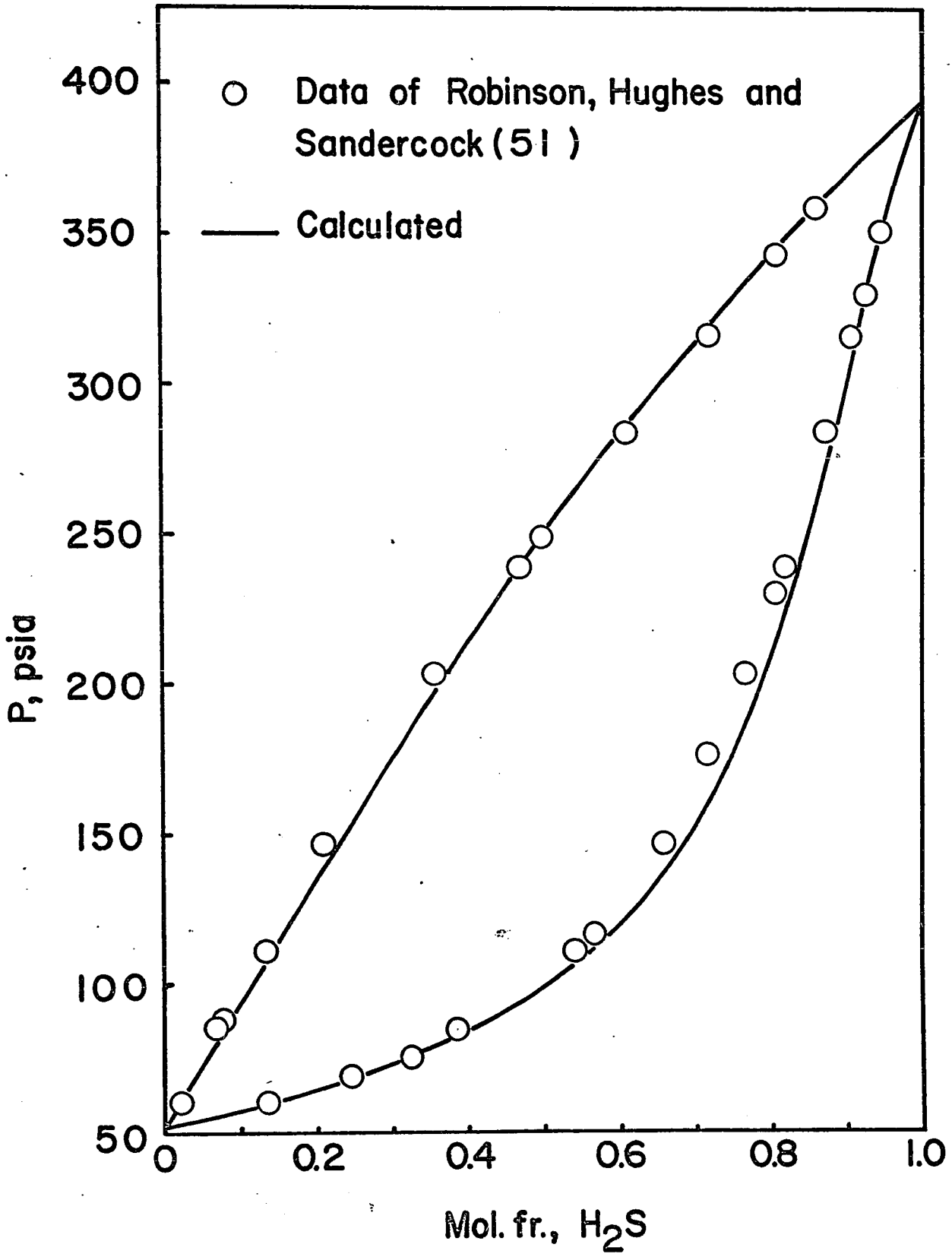

Figure 3-6 Comparison of Calculated and Experimental Vapor-Liquid Equilibria of the Hydrogen Sulfide-n-Butane System at 100° F

TABLE 3 - 8

Comparison of Calculated and Experimental Results for the System Ethane (1) - n-Pentane (2) at 40° F

$k_{ij} = 0.0098$

	P, psia		y_1		Deviation	
x_1	expt.[52]	calc.	expt.[52]	calc.	ΔP	Δy_1
0	4.4	4.40	0	0	0	0
0.1432	50	50.92	0.9158	0.9165	-0.92	-0.0007
0.2891	100	100.13	0.9504	0.9598	-0.13	-0.0094
0.4316	150	150.04	0.9659	0.0752	-0.04	-0.0093
0.5659	200	198.92	0.9763	0.9832	1.08	-0.0069
0.6950	250	247.95	0.9838	0.9886	2.05	-0.0048
0.8141	300	295.90	0.9901	0.9928	4.10	-0.0027
0.9235	350	344.50	0.9960	0.9966	5.50	-0.0006
1.0000	385	384.82	1.0000	1.0000	0.18	0

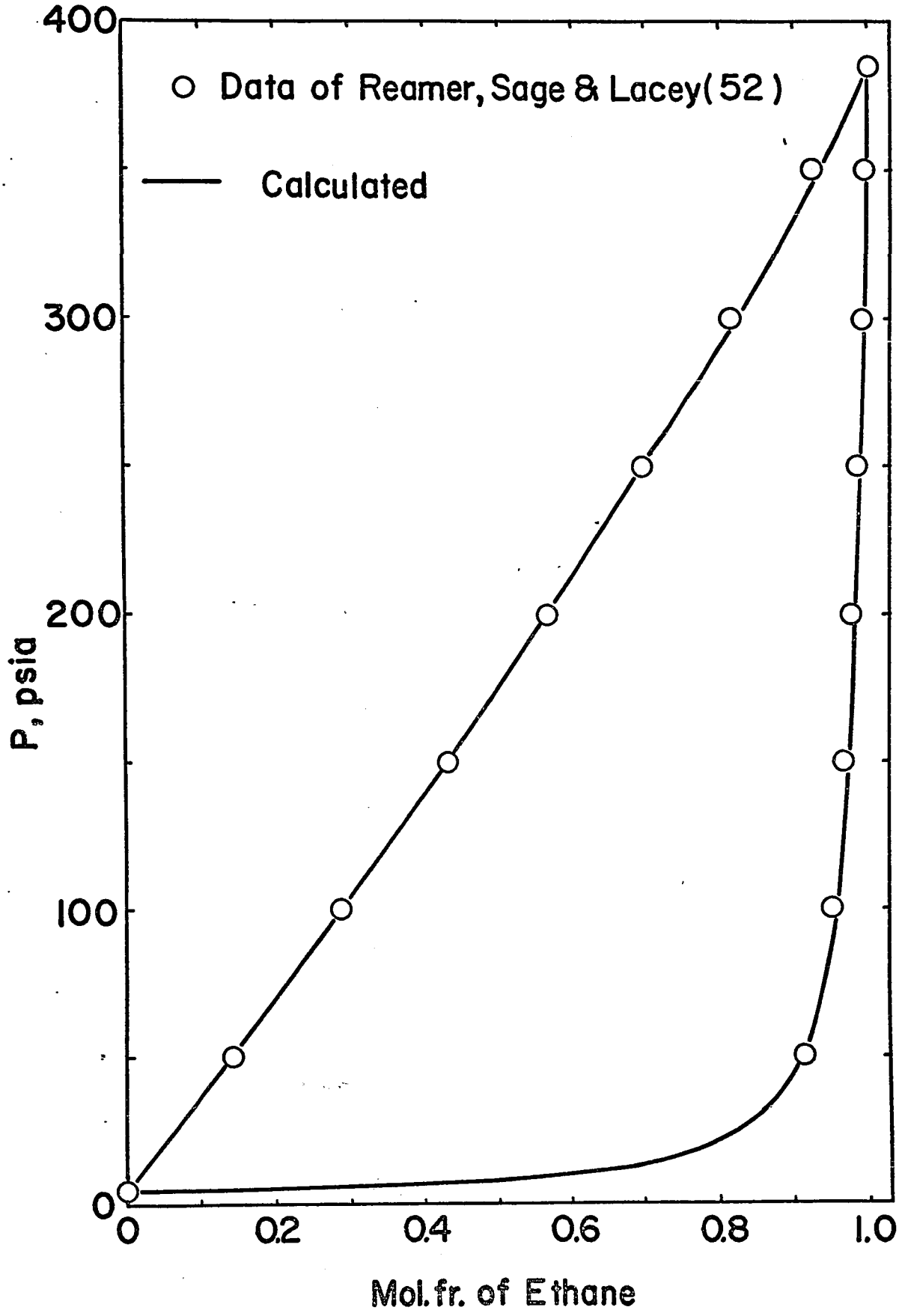

Figure 3-7 Comparison of Calculated and Experimental Vapor-Liquid Equilibria of the Ethane-n-Pentane System at 40° F

TABLE 3 - 9

Comparison of Calculated and Experimental Results for the System Ethane (1) - Propane (2)

$k_{ij} = -0.025$

		P		y_1		Dev. %	
T, °F	x_1	expt.[53]	calc.	expt.[53]	calc.	P	y_1
		psia					
0	0.051	45.3	44.50	0.1966	0.1914	1.75	2.64
	0.2495	75.6	73.91	0.5854	0.5949	2.23	-1.62
	0.3435	90.0	88.91	0.6815	0.6983	1.21	-2.46
	0.5300	120.5	120.84	0.8116	0.8333	- 0.28	-2.67
	0.5370	121.0	122.09	0.8123	0.8372	- 0.90	-3.06
	0.5750	126.1	128.98	0.8357	0.8571	- 2.28	-2.56
	0.6000	131.2	133.58	0.8432	0.8693	- 1.81	-3.09
	0.7460	159.0	161.52	0.8970	0.9286	- 1.59	-3.52
	0.9460	204.8	202.74	0.9818	0.9872	1.00	-0.55
- 50	0.0645	15.03	16.86	0.3020	0.2922	-12.18	3.24
	0.2515	28.00	29.90	0.6766	0.6725	- 6.81	0.60
	0.4424	41.00	44.45	0.8480	0.8324	- 8.41	1.83
	0.5935	54.90	56.81	0.8977	0.9033	- 3.47	-0.62
	0.7245	66.50	68.06	0.9409	0.9450	- 2.35	-0.43
	0.8144	75.00	76.02	0.9631	0.9668	- 1.36	-0.38
-100	0.0705	4.75	4.53	0.4172	0.4119	4.14	1.27
	0.1918	8.00	7.55	0.6923	0.6917	4.81	0.08
	0.4580	15.15	14.79	0.8852	0.8945	1.78	-1.05
	0.6331	19.90	19.94	0.9380	0.9477	- 0.59	-1.03
	0.6365	20.00	20.05	0.9384	0.9485	- 0.60	-1.07
	0.7415	23.00	23.25	0.9596	0.9689	- 1.30	-0.96
	0.9134	28.15	28.56	0.9867	0.9918	- 1.50	-0.51
		mm. Hg					
-150	0.0280	30.0	27.54	0.2997	0.3118	8.19	-4.03
	0.0975	51.0	48.09	0.6135	0.6338	5.70	-3.30
	0.1873	80.0	75.82	0.7754	0.7912	5.22	-2.03
	0.4445	165.0	162.27	0.9246	0.9347	1.65	-1.09
	0.6461	234.0	236.06	0.9633	0.9725	- 0.88	-0.95
	0.8095	291.0	297.84	0.9851	0.9888	- 2.35	-0.37
	0.9470	341.0	349.33	0.9967	0.9975	2.44	-0.08

(. . . continuation . . .) Table 3 - 9

T, °F	x_1	P		y_1		Dev. %	
		expt.[53]	calc.	expt.[53]	calc.	P	y_1
		mm. Hg.					
-200	0.4435	21.0	18.26	0.9444	0.9697	13.04	-2.67
	0.5690	25.5	23.89	0.9791	0.9826	6.30	-0.35
	0.6629	29.5	28.25	0.9862	0.9889	4.23	-0.27
	0.8384	37.0	36.50	0.9948	0.9962	1.35	-0.14

Ethane-Ethylene: The predicted results for the ethane-ethylene system at -100° F are compared with the reported data of Hanson, Hogan, Ruehlen and Cines[55] in Table 3-10 and Figure 3-8. The average absolute deviation in pressure is 0.91 p.s.i.a. and that in vapor-phase composition is 0.0161 mole fraction.

Methane-Ethane: The predicted vapor-liquid equilibrium data for the system methane-ethane at -150° F are listed in Table 3-11. The predicted fugacity coefficients for both components in the vapor and liquid phases are also shown in the table. The calculated results are compared with the experimental data reported by Ellington, Eakin, Parent, Gami and Bloomer[56, 57] in Figure 3-9. It may be seen that very good agreement is obtained.

Methane-Ethylene: The phase equilibria of the methane-ethylene system was studied by Guter, Newitt and Ruhemann[58] and by Volova[59]. The calculated values were tested against these reported data. The comparison is made in Figures 3-10 and 3-11. The disagreement was noted for both sets of data. It is not possible to explain such disagreement with certainty. Therefore, further experimental investigation is required to substantiate the validity of the proposed method with confidence.

3.6 CONCLUSIONS

A detailed calculation procedure has been developed for the determination of the equilibrium vapor composition and saturated pressure of the system from the given liquid composition and system temperature. Only the temperature-dependent parameters of the

TABLE 3 - 10

Comparison of Calculated and Experimental Results for the System Ethylene (1) - Ethane (2) at -100° F

	P, psia		y_1		Deviation	
x_1	expt.[55]	calc.	expt.[55]	calc.	ΔP	Δy_1
0.1100	35.90	36.96	0.2140	0.2357	-1.06	-0.0217
0.1070	36.20	36.82	0.2100	0.2305	-0.62	-0.0205
0.2615	42.60	43.60	0.4240	0.4471	-1.00	-0.0231
0.3840	47.15	48.19	0.5600	0.5695	-1.04	-0.0095
0.6120	54.60	55.42	0.7500	0.7441	-0.82	-0.0059

TABLE 3 - 10

Comparison of Calculated and Experimental Results for the System Ethylene (1) - Ethane (2) at -100° F

	P, psia		y_1		Deviation	
x_1	expt.[55]	calc.	expt.[55]	calc.	ΔP	Δy_1
0.1100	35.90	36.96	0.2140	0.2357	-1.06	-0.0217
0.1070	36.20	36.82	0.2100	0.2305	-0.62	-0.0205
0.2615	42.60	43.60	0.4240	0.4471	-1.00	-0.0231
0.3840	47.15	48.19	0.5600	0.5695	-1.04	-0.0095
0.6120	54.60	55.42	0.7500	0.7441	-0.82	-0.0059

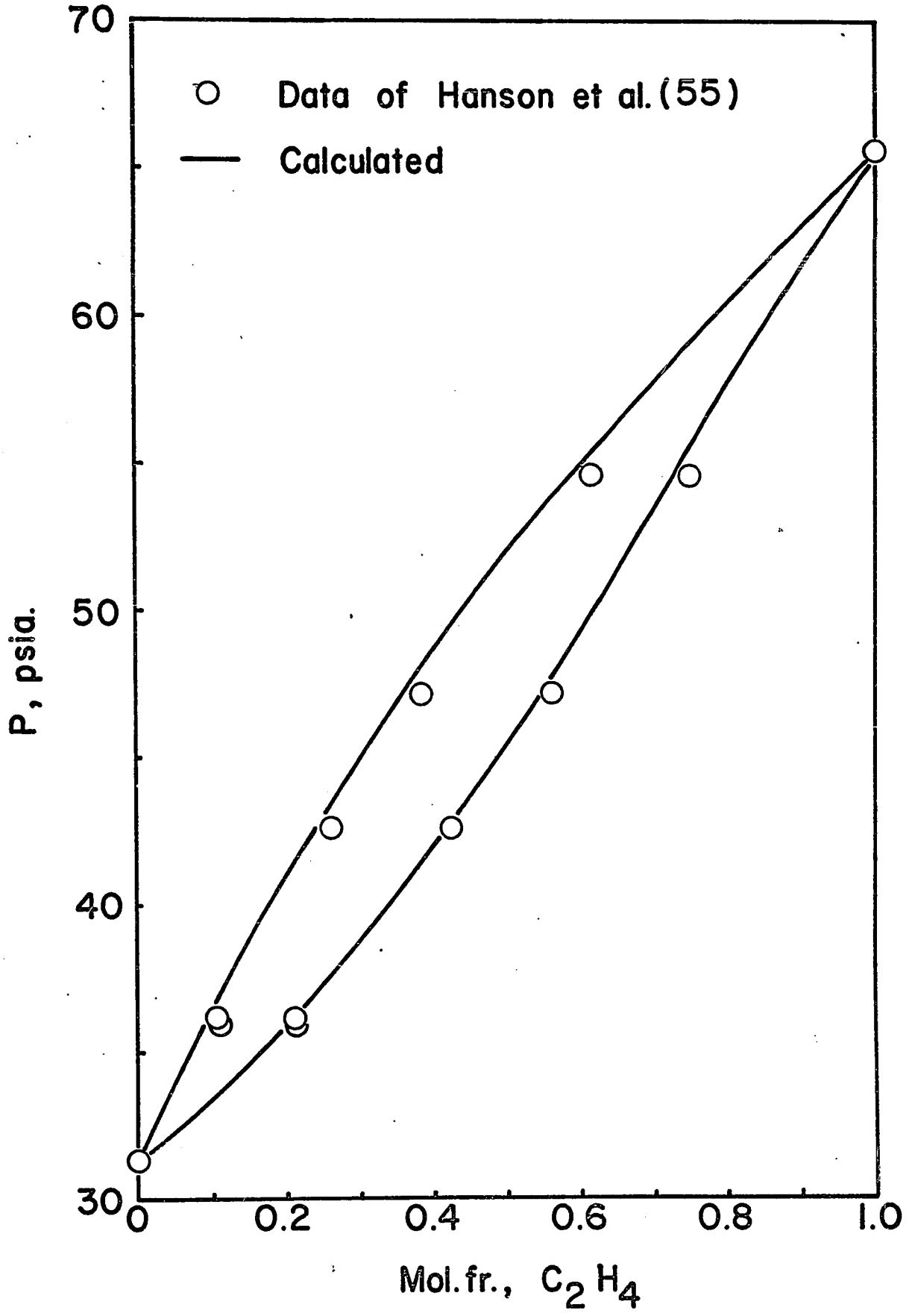

Figure 3-8 Comparison of Calculated and Experimental Vapor-Liquid Equilibria of the Ethylene-Ethane System at -100° F

TABLE 3 - 11

Predicted Vapor-Liquid Equilibrium Data for the Methane (1) - Ethane (2) System at -150°F

P, psia	x_1	y_1	$\hat{\varphi}_{1L}$	$\hat{\varphi}_{2L}$	$\hat{\varphi}_{1V}$	$\hat{\varphi}_{2V}$
11.19	0.01	0.3659	36.4099	0.6248	0.9951	0.9756
15.26	0.02	0.5357	26.5613	0.4586	0.9917	0.9680
23.35	0.04	0.6975	17.1885	0.3005	0.9858	0.9537
31.35	0.06	0.7756	12.6706	0.2244	0.9802	0.9399
39.28	0.08	0.8216	10.0117	0.1796	0.9749	0.9264
47.13	0.10	0.8520	8.2606	0.1502	0.9696	0.9132
66.39	0.15	0.8962	5.7171	0.1076	0.9568	0.8814
85.13	0.20	0.9202	4.3463	0.0849	0.9445	0.8510
103.34	0.25	0.9354	3.4894	0.0708	0.9326	0.8219
121.02	0.30	0.9458	2.9042	0.0614	0.9211	0.7941
138.17	0.35	0.9536	2.4794	0.0548	0.9100	0.7675
154.83	0.40	0.9596	2.1571	0.0500	0.8992	0.7420
171.01	0.45	0.9644	1.9047	0.0464	0.8887	0.7175
186.76	0.50	0.9685	1.7017	0.0438	0.8785	0.6940
202.14	0.55	0.9720	1.5351	0.0418	0.8686	0.6714
217.25	0.60	0.9751	1.3957	0.0405	0.8588	0.6493
232.19	0.65	0.9779	1.2776	0.0397	0.8492	0.6277
247.13	0.70	0.9806	1.1760	0.0393	0.8395	0.6064
262.26	0.75	0.9832	1.0877	0.0394	0.8297	0.5850
277.88	0.80	0.9858	1.0100	0.0400	0.8196	0.5630
294.35	0.85	0.9886	0.9408	0.0411	0.8089	0.5401
312.24	0.90	0.9917	0.8785	0.0429	0.7972	0.5155
332.39	0.95	0.9953	0.8214	0.0455	0.7840	0.4880

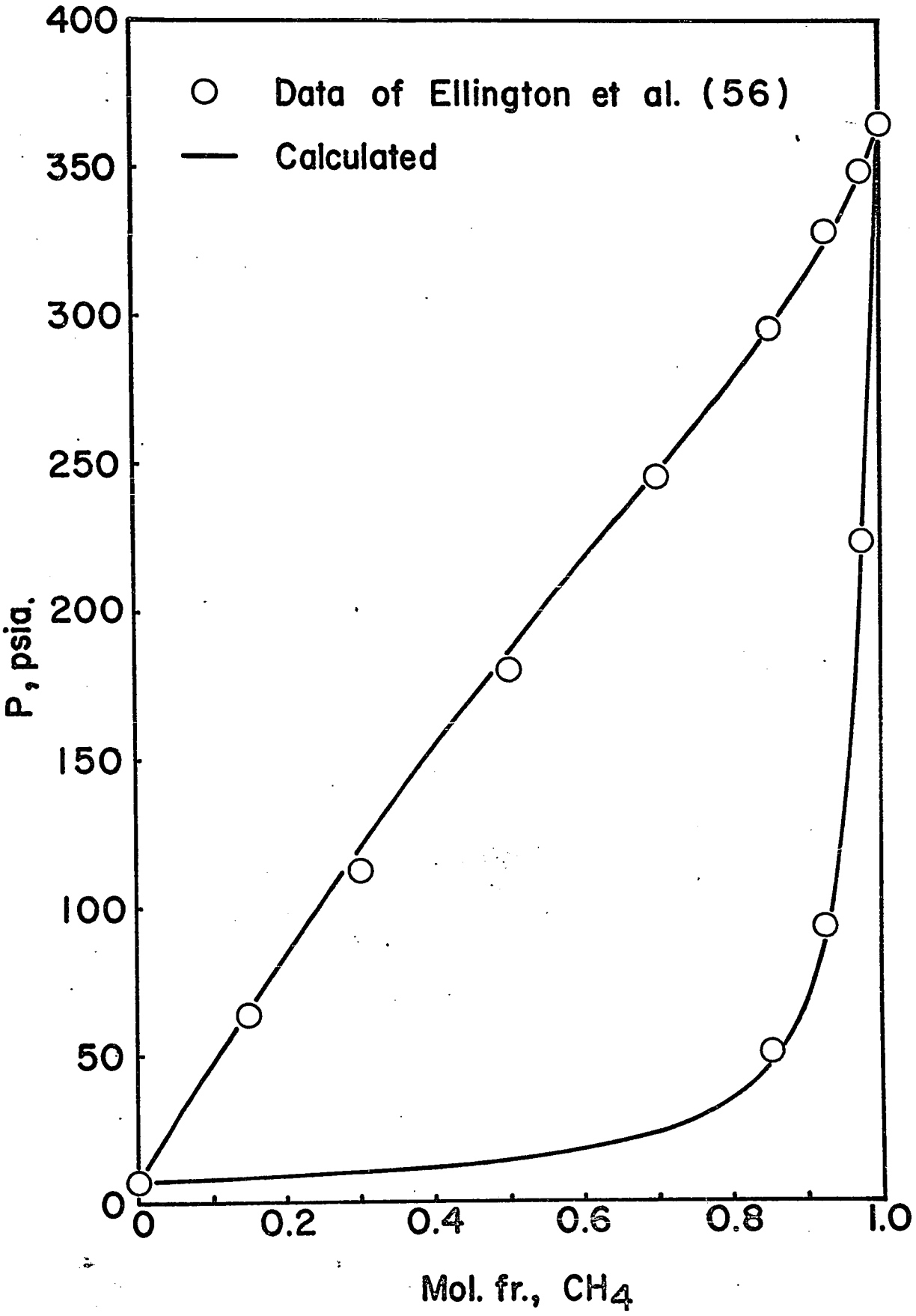

Figure 3-9 Comparison of Calculated and Experimental Vapor-Liquid Equilibria of the Methane-Ethane System at -150° F

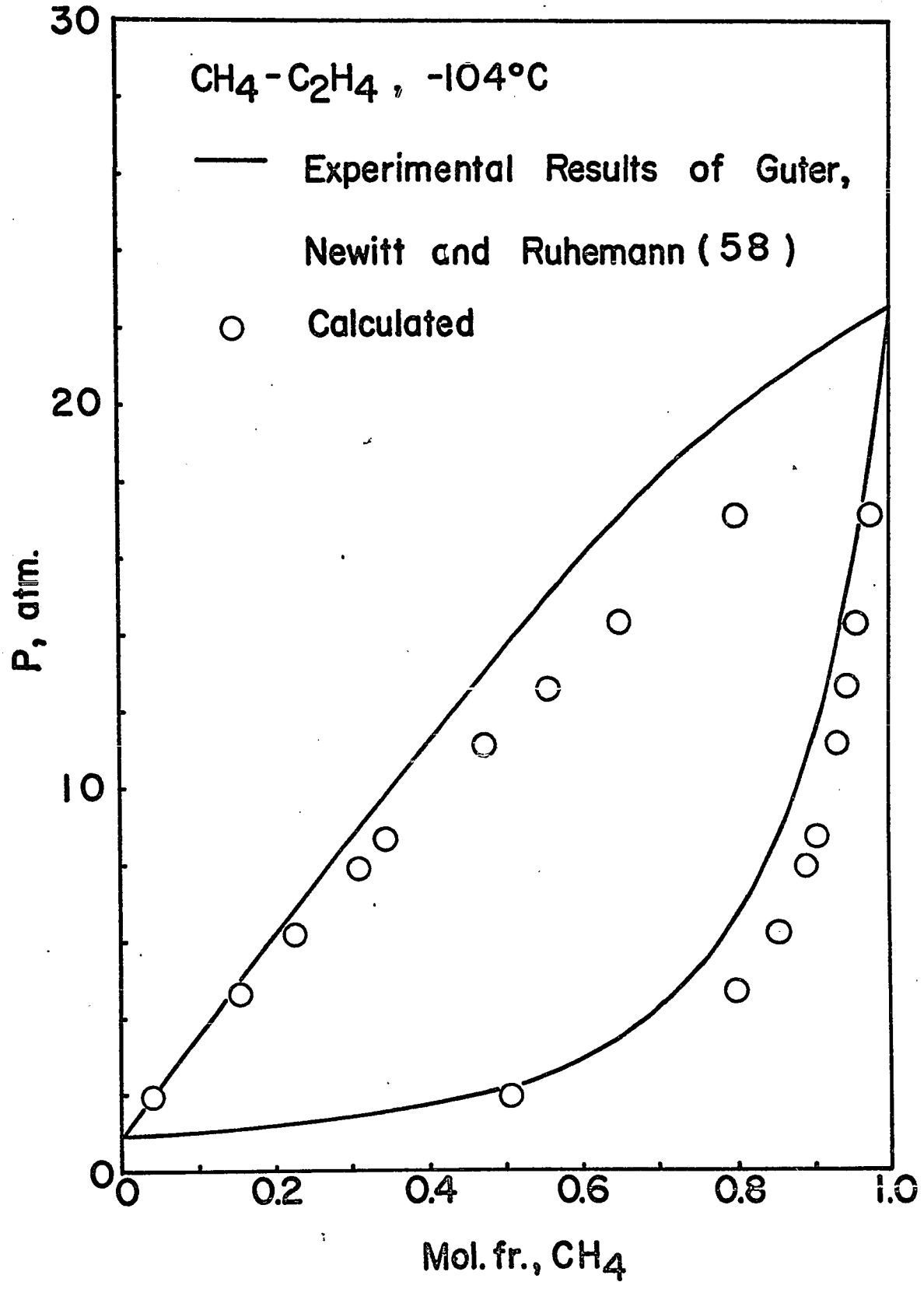

Figure 3-10 Comparison of Calculated and Experimental Vapor-Liquid Equilibria of the Methane-Ethylene System at -104° C

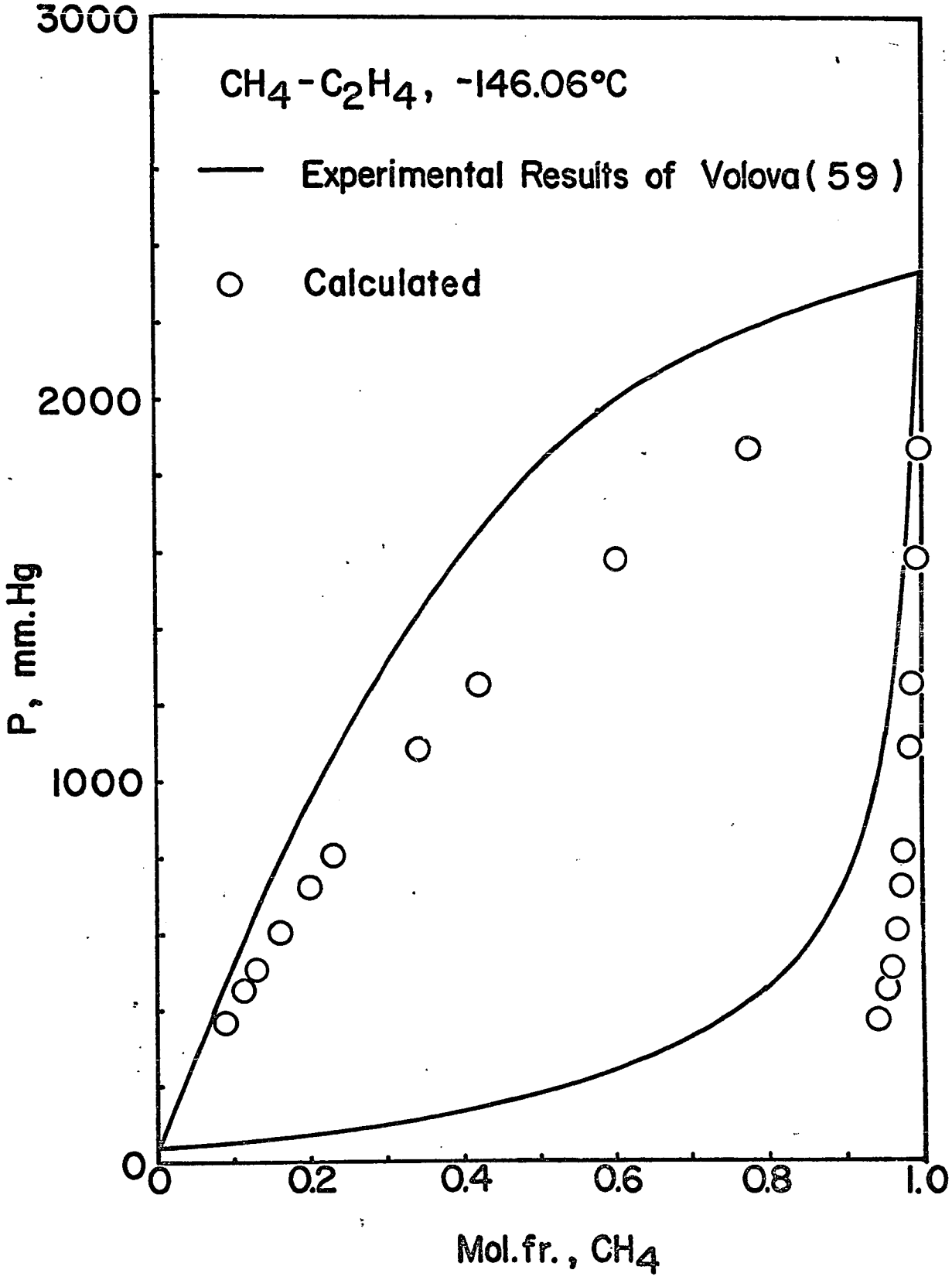

Figure 3-11 Comparison of Calculated and Experimental Vapor-Liquid Equilibria of the Methane-Ethylene System at -146.06°C

Redlich-Kwong equation of state, established for each individual component at the temperature of interest (below its critical point) from its vapor pressure and saturated liquid molal volume, and the binary interaction constant, established from experimental binary equilibrium data, are utilized. The applicability of the method was tested on eleven binary systems at eighteen isothermal conditions from -200° F to 160° F. In general, the agreement between predicted and experimental results is very good. The average deviation in pressure is less than 4% and that in vapor-phase composition is less than 5%. The systems tested contain paraffinic, olefinic, cyclic and aromatic hydrocarbons, carbon dioxide and hydrogen sulfide.

In the calculation, the binary interaction constant has been assumed to be independent of system temperature, pressure and composition. As has been demonstrated in the present work, the method based on this assumption yields satisfactory results. It may be necessary to establish the interaction parameters as temperature or pressure functions rather than pure constants if large changes in temperature and pressure are envisaged.

It has been found from the present work that, in the ethane-propane system, the binary interaction constants, k_{ij}'s are somewhat different with different temperatures. But no definite trend has been observed. It is difficult, at this stage, to draw conclusions with certainty, because the changes with temperature in the value of k_{ij} may be due to the unreliable data for the system studied.

The established binary interaction constants employed in this study are listed in Appendix A.

The disagreement between predicted and observed values for the methane-ethylene system suggests a further experimental investigation in order to justify the applicability of the proposed method.

CHAPTER IV

EXPERIMENTAL STUDY OF VAPOR-LIQUID EQUILIBRIA: SYSTEM METHANE-ETHYLENE-ETHANE

Experimental study of vapor-liquid equilibria for the mixtures containing methane, ethylene and ethane at low-temperature and high-pressure conditions was carried out in this study to serve the following purposes:

(1) The steady growth of ethylene industry requires more and reliable vapor-liquid equilibrium information for the design of fractionation facilities for the efficient separation of ethylene from the cracker effluent. In the industry, demethanization is carried out at temperatures within the range of -90° to -220°F[60]. The determination of vapor-liquid equilibrium data for the mixtures containing methane, ethylene and ethane is favorable within this temperature range.

(2) The disagreement between the predicted and experimental[58, 59] results has been reported in Chapter III. Further experimental investigation is therefore required to justify the validity of the proposed method.

4.1 APPARATUS

The vapor-liquid equilibrium data were measured by means of a forced-recirculation apparatus which was similar to that constructed by Chang[8]. A schematic diagram is shown in Figure 4-1. The general view of the assembly is shown in Figures 4-2 and 4-3.

The equipment assembly consists of a feed charging unit, a closed circulation loop, a cryostat and its temperature control system, sampling facilities, and temperature and pressure measuring devices.

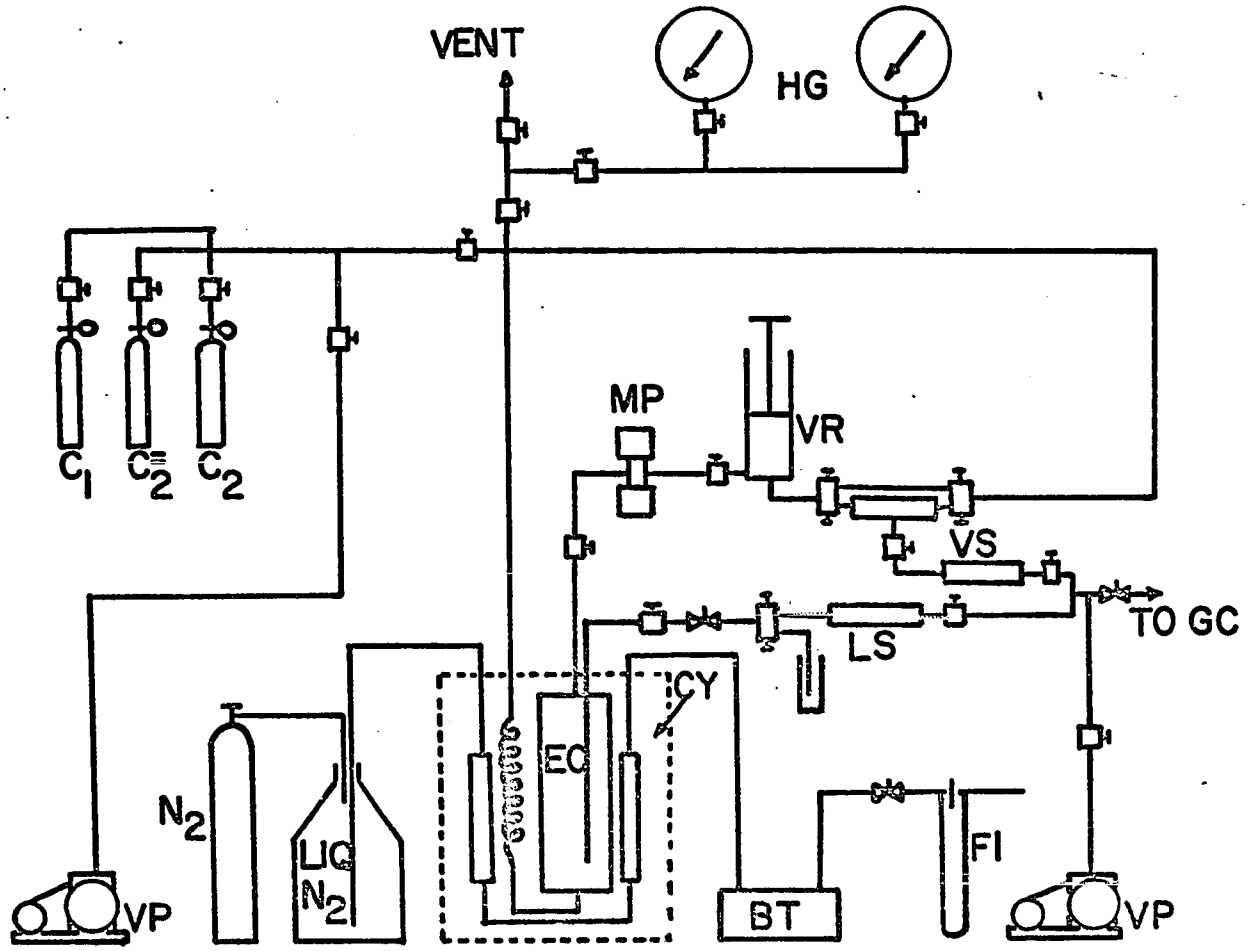

BT	BUFFER TANK	GC	GAS CHROMATOGRAPH
CY	CRYOSTAT	LS	LIQUID SAMPLING BULB
EC	EQUILIBRIUM CELL	MP	MAGNETIC PUMP
FI	FLOW INDICATOR	VP	VACUUM PUMP
HG	HEISE GAUGE	VR	VOLUME REGULATOR
	AUTOCLAVE VALVE	VS	VAPOR SAMPLING BULB
	THREE-WAY VALVE		NEEDLE VALVE

Figure 4-1 Schematic Diagram of Experimental Apparatus

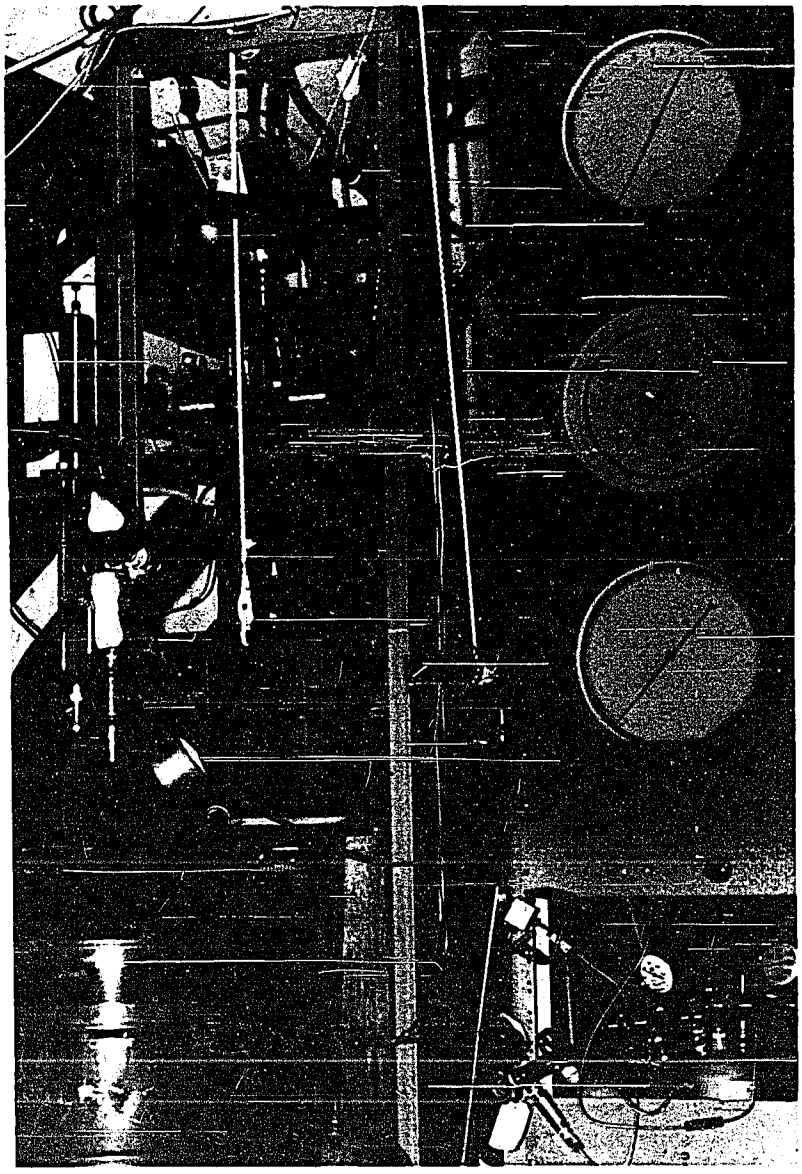

Figure 4-2 Front View of the Equipment Assembly

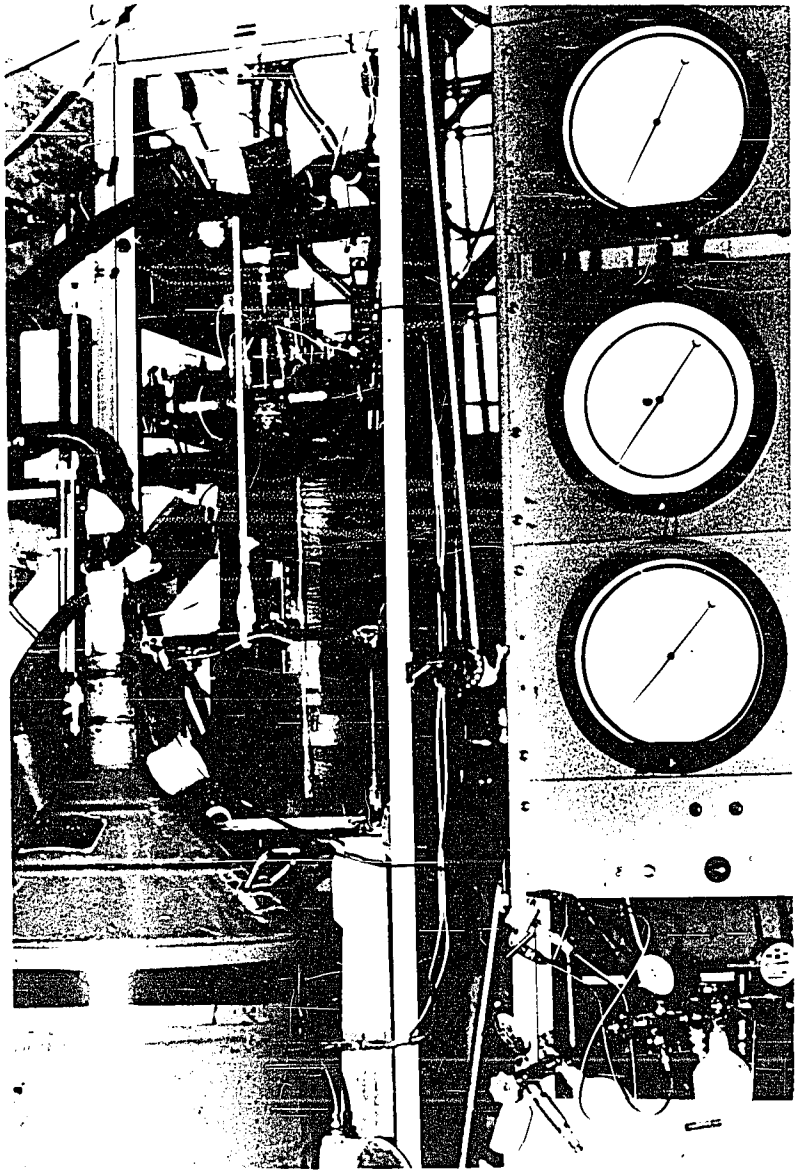

Figure 4-2 Front View of the Equipment Assembly

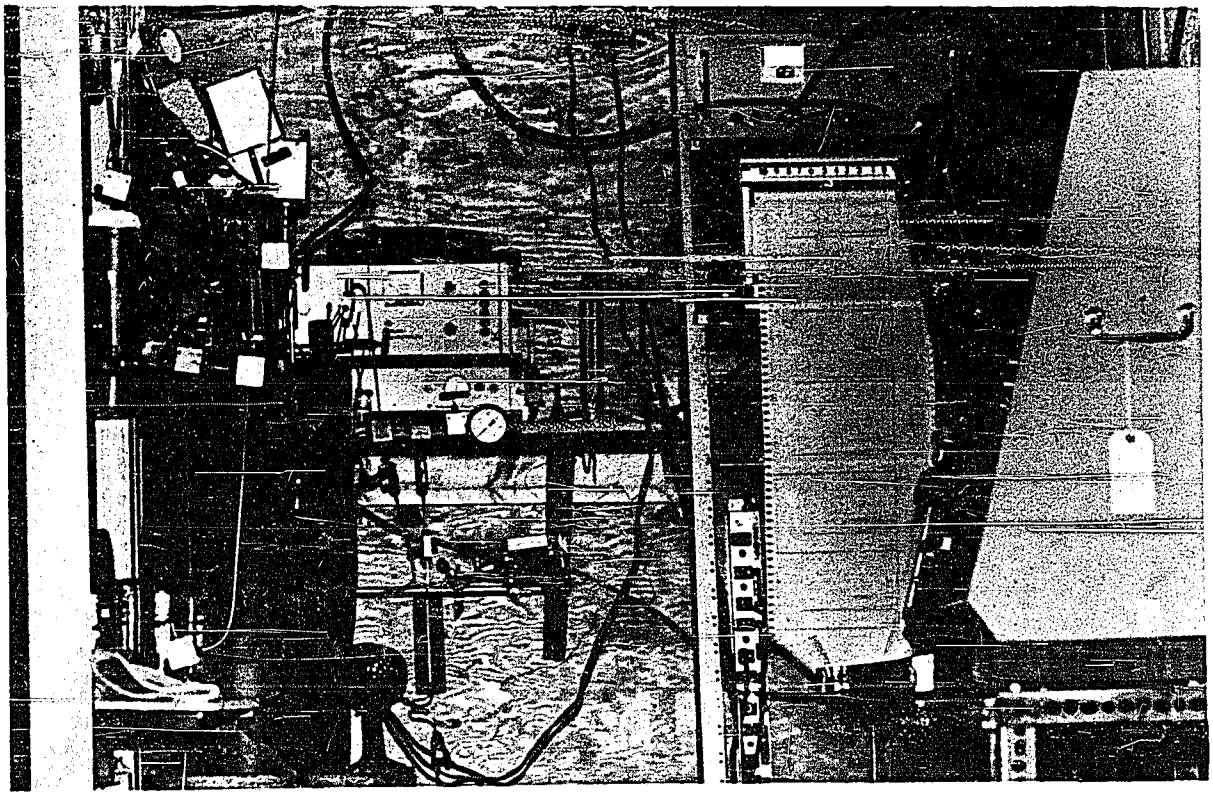

Figure 4-3 Side View of the Equipment Assembly

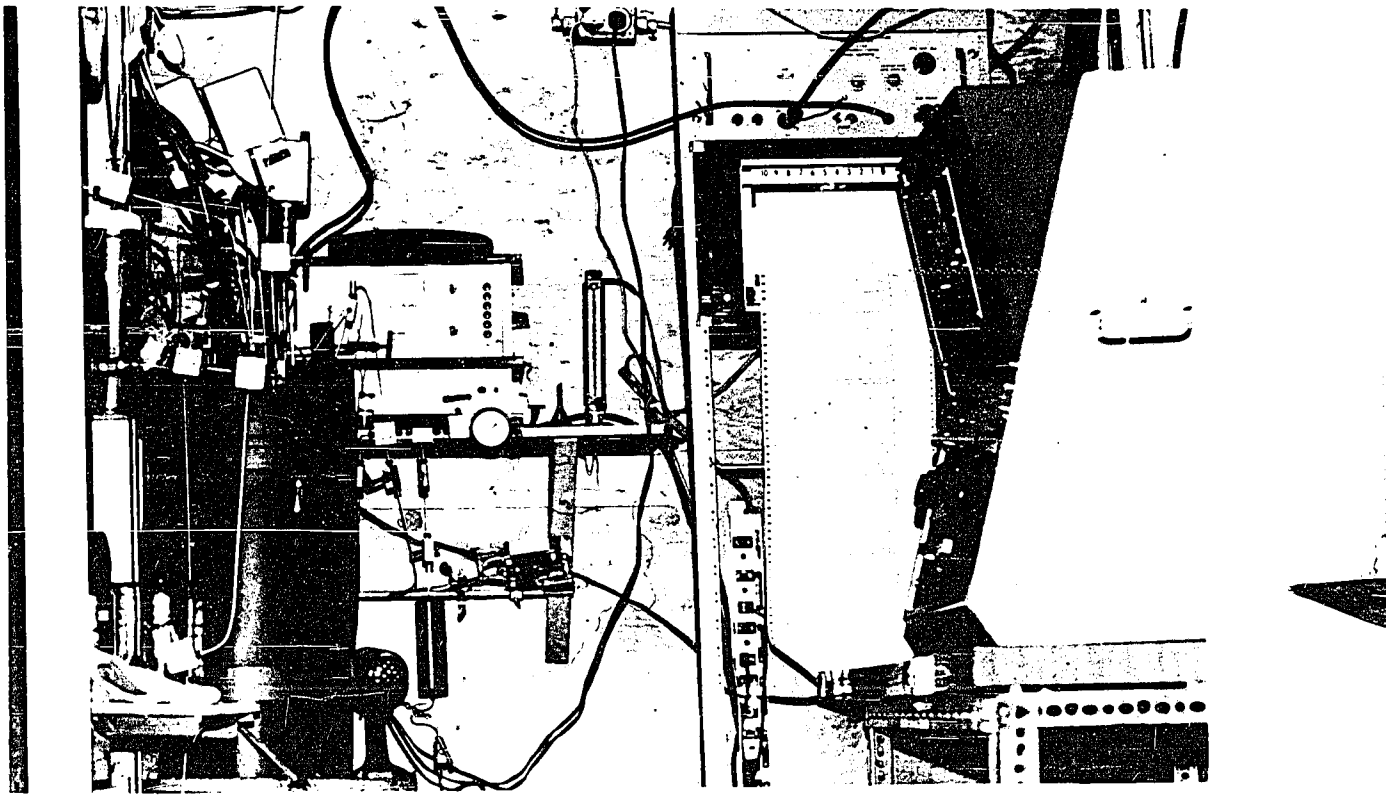

Figure 4-3 Side View of the Equipment Assembly

4.1.1 Feed Charging Unit:

Three gas cylinders, installed with individual pressure regulators and Autoclave valves, were connected to the system.

4.1.2 Closed Recirculation Loop:

The closed recirculation loop mainly consists of an equilibrium cell, an electromagnetic pump, a volume regulator, a vapor sampling tube and a cooling coil.

A 100 ml. Jerguson transparent level gauge with a stainless steel body was used as the equilibrium cell. The top of the cell was fitted with a $\frac{1}{2}$ in. NPT nipple, through which the vapor outlet tube and three 0.036 in. liquid sampling tubes were inserted. A $\frac{1}{2}$ in. NPT connector was fitted to the bottom of the cell. And a $\frac{1}{8}$ in. Autoclave adapter was welded to it and connected to the cooling coil of the vapor inlet line. A view of the cell is shown in Figure 4-4.

The electromagnetic pump is essentially a double acting plunger pump with four check valves in the body, two inlets and two outlets. One permanent magnetic piston rod which travels inside the cylinder is driven by the electromagnetic coils mounted on both ends. The coils are energized by a symmetric flip-flop circuit. The electric circuit is shown in Figure 4-5.

4.1.3 Cryostat and Temperature Control System:

A Dewar flask of 18 liter capacity was employed as the cryostat into which the equilibrium cell was submerged. Isopentane was used as the bath liquid in the cryostat. The cryostat was equipped with a

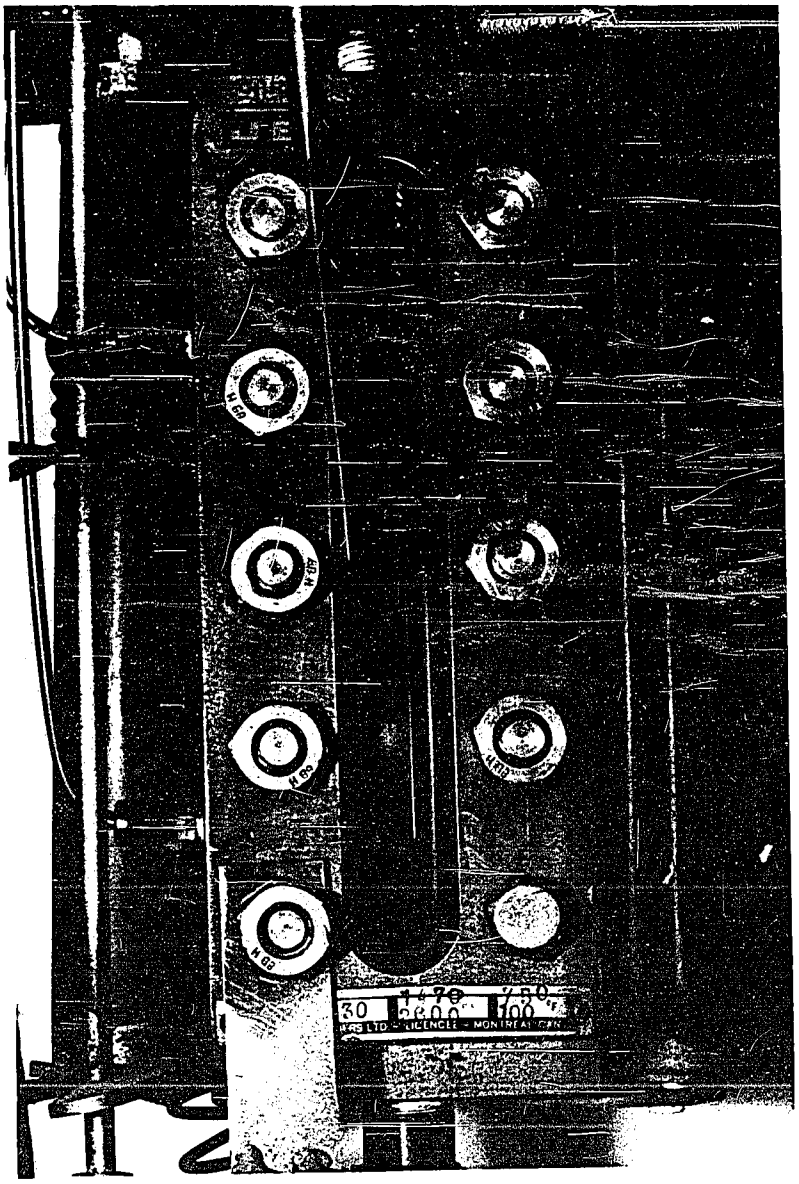

Figure 4-4 A View of Equilibrium Cell

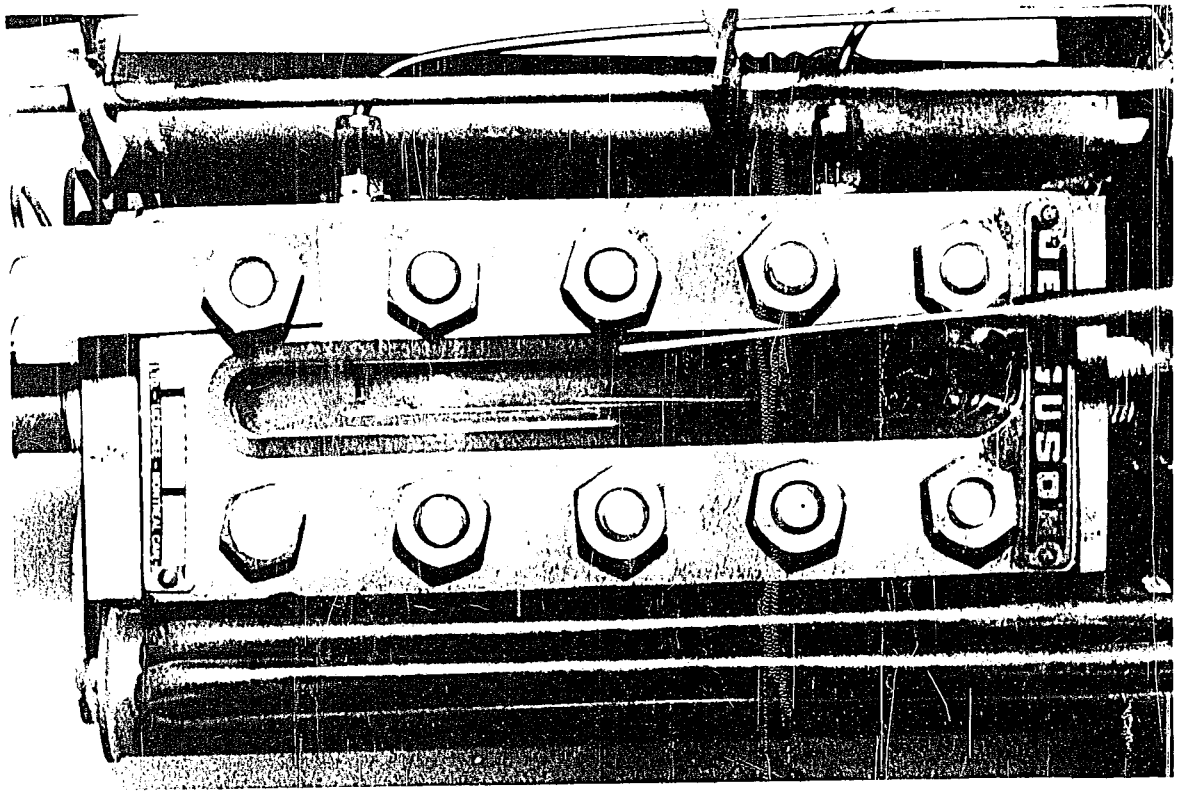
FUSE

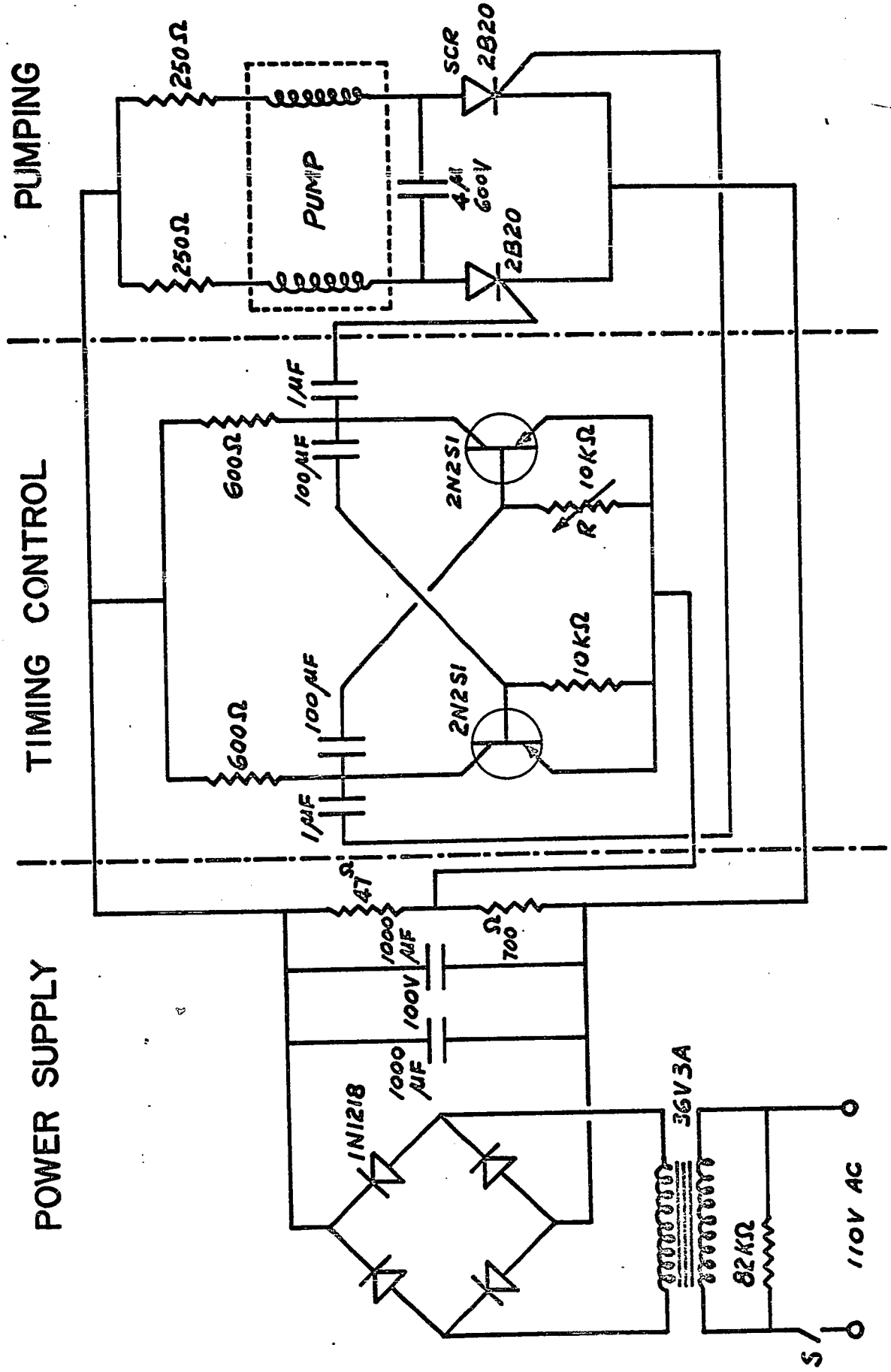

Figure 4-5 Electric Circuit of Electromagnetic Pump

liquid nitrogen evaporation coil, two stirrers, one heater and a resistant-type temperature sensing element. The liquid nitrogen evaporation coil was connected to a buffer tank at the outlet end. A flow indicator and a needle valve were installed in order to keep the nitrogen flow rate constant. A proportional-type Bayley temperature controller, model 250, was used to control the temperature.

4.1.4 Sampling Facilities:

Three 0.036 in.-diameter liquid sampling tubes were extended to different levels in the equilibrium cell. The liquid sampling tubes were installed through a vapor outlet chamber to maintain them at the bath temperature. A needle valve and a three-way valve were installed between the liquid sampling bulb and the equilibrium cell. The vapor sample was trapped in the vapor sampling bulb through the sampling tube. A schematic diagram of the sampling system is shown in Figure 4-6.

4.1.5 Temperature and Pressure Measuring Devices:

Two protected-type copper-constantan thermocouples were installed in the equilibrium cell at two different levels, one located at one-quarter of the height, and the other located at three-quarters of the height. These thermocouples were installed horizontally and their tips were placed at the center of the cell. The equilibrium temperature was measured by means of a Leeds and Northrup K-5 potentiometer facility. The thermocouples were calibrated against the vapor pressure of methane[61].

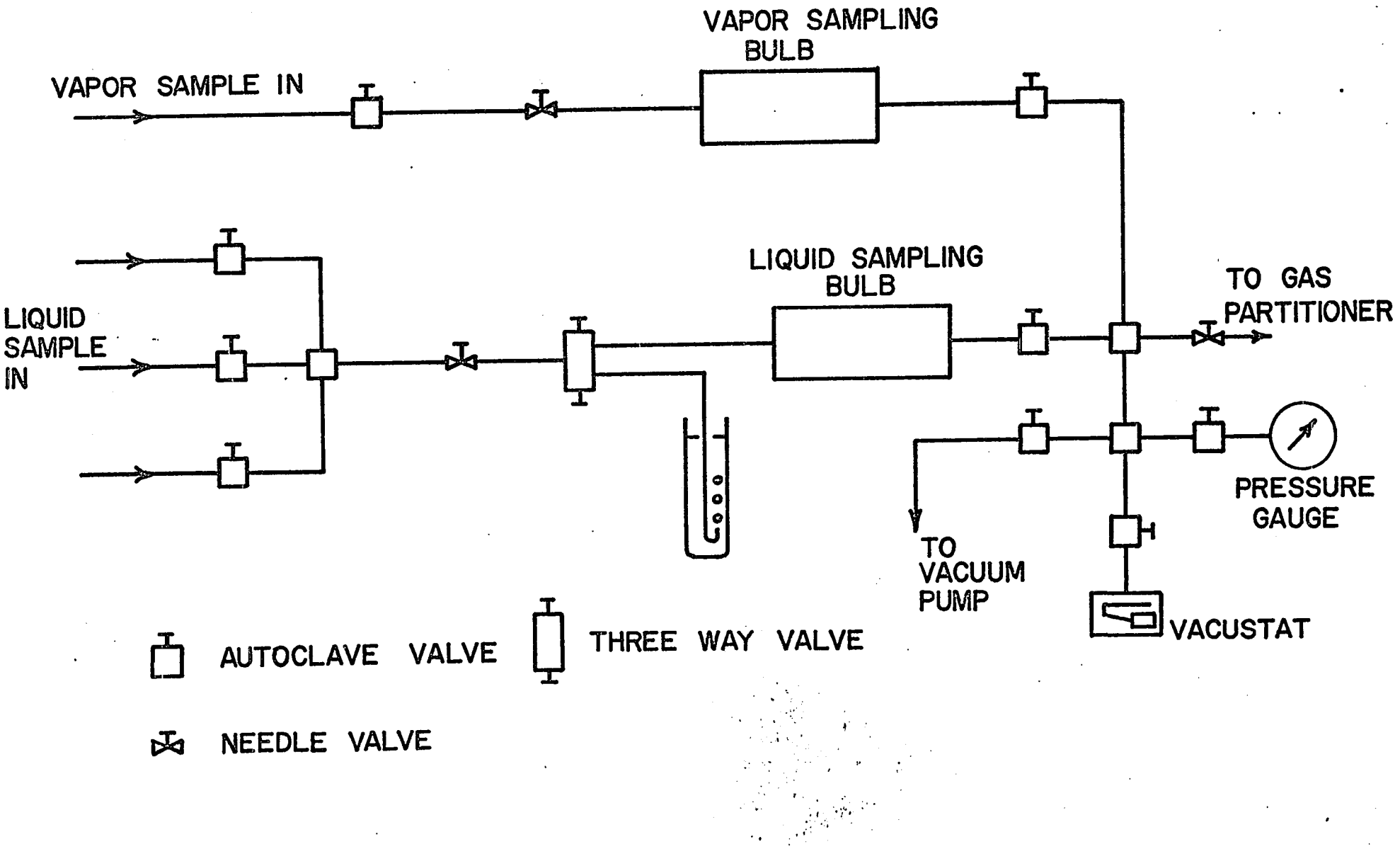

Figure 4-6 Schematic Diagram of Sampling System

The pressure of the system was measured by means of two certified Heise Bourdon gauges. The ranges of the gauges are 0 to 200, and 0 to 1000 lb./sq. in. abs. with 0.2 and 1 lb./sq. in. per division, respectively.

4.2 MATERIALS

Research grade gases supplied by Matheson of Canada, Ltd., were used in this investigation without any further purification. Specified minimum purities of these gases were as follows:

Methane	99.99 mole %
Ethylene	99.98 mole %
Ethane	99.9 mole %

4.3 EXPERIMENTAL PROCEDURES

At room temperature, the system was first evacuated and maintained under the vacuum with a pressure of 0.1 mm. Hg. or less. The Dewar flask was filled with isopentane as the bath liquid. The liquid nitrogen was introduced to the evaporation coil to cool down the cryostat and the equilibrium cell. After a few hours, two stirrers were turned on. In the starting period, the vaporization rate of liquid nitrogen was preferably large in order to reduce the temperature rapidly to a point slightly below the desired level. The temperature of the bath could be adjusted near the desired value by regulating the nitrogen evaporating rate through the needle valve and checking the bath temperature simultaneously.

The various mixtures studied were synthesized and liquefied within the equilibrium cell. The heavier component was first charged

into the cell. As the pressure reached the saturation point, the liquid was formed. The charge was stopped when the liquid level had risen to one-third of the cell capacity. The temperature controller was then turned on and the temperature was controllable to $\pm$ 0.02° F. Then the light component was charged into the cell. As the electromagnetic pump started, the vapor was withdrawn from the cell. The vapor was heated up to room temperature when it passed through the volume regulator and the sampling tube. But it was cooled down to the bath temperature as it passed through the cooling coil inside the cryostat before returning to the equilibrium cell. The returned vapor was bubbling through the liquid phase in the cell. In this study, the circulation was stopped after two or more hours' operation for recording the equilibrium temperature and pressure.

The vapor sample was trapped as soon as the pump was stopped. Then the liquid sampling valve was opened and the sample was withdrawn. The first portion of the liquid sample was totally vaporized to purge the line and to bubble through water in a small flask to estimate the sampling rate. The sudden pressure change during the sampling process was minimized by adjusting the sampling rate. After the sampling rate was appropriately adjusted, the three-way valve was then switched to the liquid sampling bulb which was pre-evacuated. Ten to twenty minutes were required to collect 10-ml. of the sample at room temperature and 20 p. s. i. g. If the system pressure dropped while sampling, the pressure of the system could be kept constant by adjusting the volume regulator.

Analyses of the samples were made with a Fisher Gas Partitioner Model 25V in conjunction with a Texas Instrument potentiorecorder of Model SERVO/RITER II with one millivolt span. The gas partitioner was of dual columns and a double-detector design. The first column

was left empty and the second one was a 4-ft. long column packed with 28-30 mesh silica gel. Helium was used as a carrier gas. The gas partitioner was operated at 55° C. The flow rate of helium was maintained at 75 ml. per minute at 20 p. s. i. g. A retention time of 6 to 8 minutes was required for separating the three components. The peaks were well spaced and completely separated in the sequence of methane, ethane, and ethylene.

The analysis was repeated at least three times for each sample, and then the average value was taken.

After the first experimental point had been determined, the more volatile component was then fed to the system by bubbling it through the liquid. The charging process should be kept as slow as possible. Recirculation was resumed and then the second point was determined by following the same procedure described before. For the ternary system, this process could be repeated several times without disturbing the constant ratio of the two heavy components in the liquid phase.

4.4 MEASUREMENT ERRORS

The principle errors in the measurement of vapor-liquid equilibria can be attributed to: (1) inaccuracy in the temperature measurement; (2) inaccuracy in the pressure measurement; (3) error involved in the analyses of vapor and liquid samples.

Temperature fluctuations of the cryostat were controllable to $\pm$ 0.02° F., and the uncertainty involved in the temperature measurement was believed to be $\pm$ 0.1° F.

The uncertainty involved in the measurement of pressure was $\pm$ 0.1% of the full scale of the pressure gauge. For instance, $\pm$ 1 lb./sq. in. and $\pm$ 0.2 lb./sq. in. uncertainties were involved for the "0 - 1000 p.s.i.a." and the "0 - 200 p.s.i.a." guages, respectively.

The reproducibility of the analysis in general was good to 0.003 mole fraction. Extra care was taken when the sample was in the extreme concentration region so that the reproducibility was improved to 0.001 mole fraction. The comparison between the volumetrically prepared samples and the chromatographic measurements is given in Table 4-1. It is difficult to set forth meaningful average values of the uncertainty of measurements, since the mole fraction of a particular component varies widely over the range of states covered in this investigation. However, it is believed that the uncertainty should not be more than 0.005 mole fraction. At some states, the mole fraction of a given component was below 0.003 mole fractions; under these conditions, the uncertainty in mole fraction was markedly less than the above mentioned value.

4.5 RESULTS AND DISCUSSIONS

Equilibrium measurements were made for the following systems:

(1) Methane - Ethylene system at -193.1°, -173.1°, and -156.1° F.

(2) Methane - Ethane system at -173.1° F.

(3) Methane - Ethylene - Ethane system at -173.1° F.

The vapor pressure of ethylene and ethane were measured and compared with those calculated from the Antoine equation[62, 63]. The results are listed as follows:

TABLE 4 - 1

Analysis of Samples

	Mole Fraction	
	Methane	Ethylene
Sample 1: (prepared)	0.97002	0.02998
	Chromatographic Analysis	
	0.97192	0.02808
	0.97207	0.02793
	0.97180	0.02820
	0.97192	0.02808
	0.97165	0.02835
Deviation*	0.00187	0.00185
Sample 2: (prepared)	0.91262	0.08738
	Chromatographic Analysis	
	0.91237	0.08763
	0.91238	0.08762
	0.91266	0.08734
	0.91282	0.08718
	0.91281	0.08719
Deviation	0.00001	0.00001
Sample 3: (prepared)	0.7260	0.2740
	Chromatographic Analysis	
	0.7248	0.2752
	0.7264	0.2736
	0.7239	0.2761
Deviation	0.0010	0.0010
Sample 4: (prepared)	0.4294	0.5706

(... continuation...) Table 4 - 1

	Mole Fraction	
	Methane	Ethylene
	Chromatographic Analysis	
	0.4300	0.5700
	0.4327	0.5673
	0.4309	0.5691
Deviation	0.0018	0.0018
Sample 5: (prepared)	0.2049	0.7951
	Chromatographic Analysis	
	0.2072	0.7928
	0.2076	0.7924
	0.2072	0.7928
	0.2080	0.7920
	0.2077	0.7923
Deviation	0.0026	0.0026

* Deviation $= \left|\left(\left(\sum_{1}^{NOBS} C_c\right)/NOBS\right) - C_r\right|$

Cr = reference composition (prepared)

Cc = composition obtained from chromatographic analysis

Component	T, °F	Vapor Pressure, p.s.i.a.	
		Measured	Calculated
Ethylene	-193.1	3.45	3.411
	-173.1	7.64	7.695
	-156.1	14.26	14.050
Ethane	-173.1	2.95	2.936

The experimental vapor-liquid equilibrium data were compared with those predicted by means of the method proposed in Chapter III. Close-to-excellent agreement was observed. The comparison is made in Figures 4-7 to 4-9 for the system methane-ethylene at three temperatures, -193.1°, -173.1° and -156.1° F., and in Figure 4-10 for the system methane-ethane at -173.1° F. The results of comparison are also tabulated in Tables 4-2 to 4-4 for the binary and ternary systems. The average deviation in pressure is less than 1% and that in vapor-phase mole fraction for the volatile component (methane) is less than 0.5%. The average absolute deviation obtained in this investigation between the experimental and the predicted values of P and y are summarized as follows:

System	T, °F	Average Absolute Deviation	
		ΔP, p.s.i.a.	Δy
Methane-ethylene	-193.1	0.51	0.0046
	-173.1	0.64	0.0035
	-156.1	1.06	0.0033
Methane-ethane	-173.1	0.96	0.0018
Methane-ethylene-ethane	-173.1	0.38	0.0050

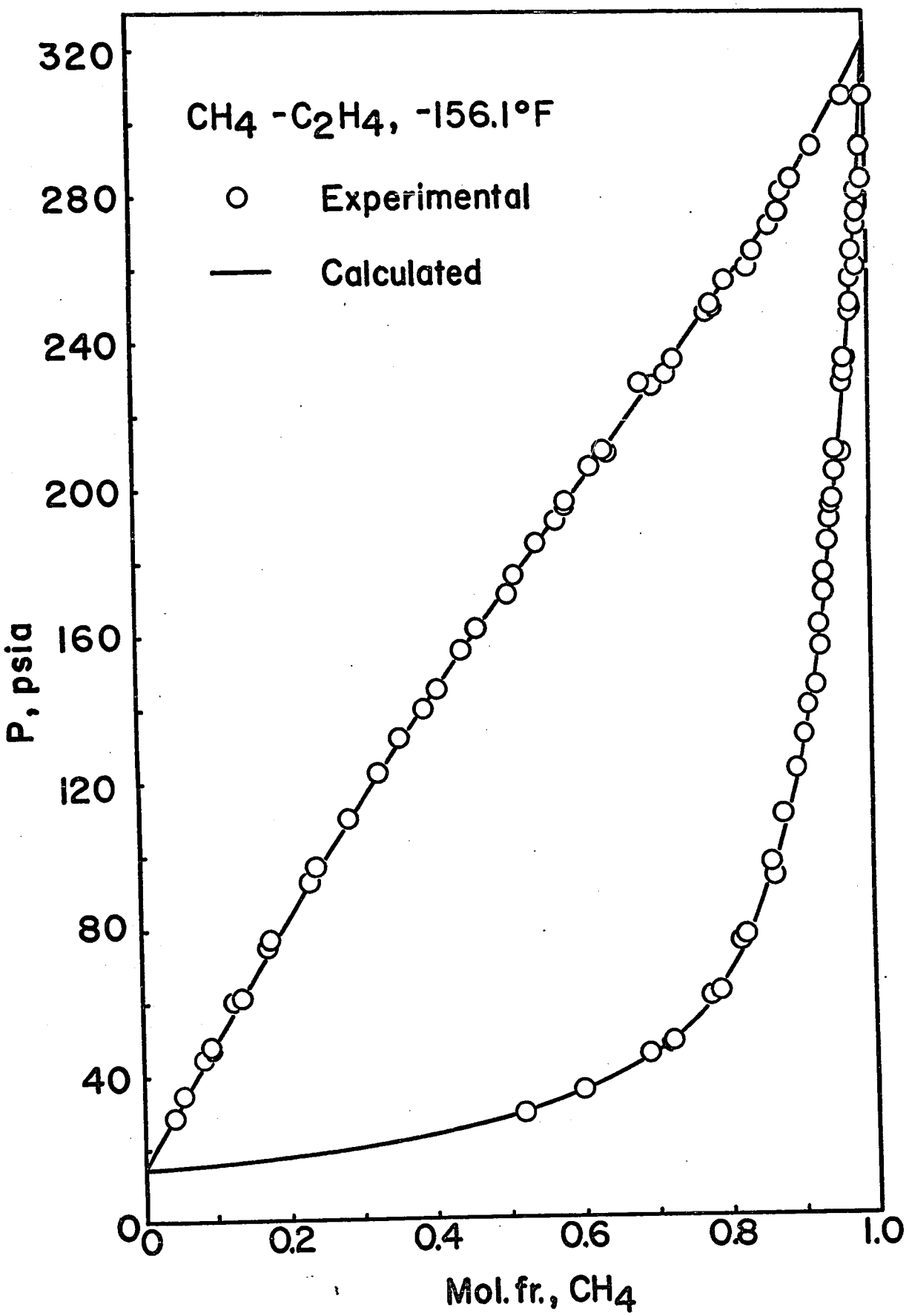

Figure 4-7 Vapor-Liquid Equilibrium Data for the Methane-Ethylene System at -156.1° F

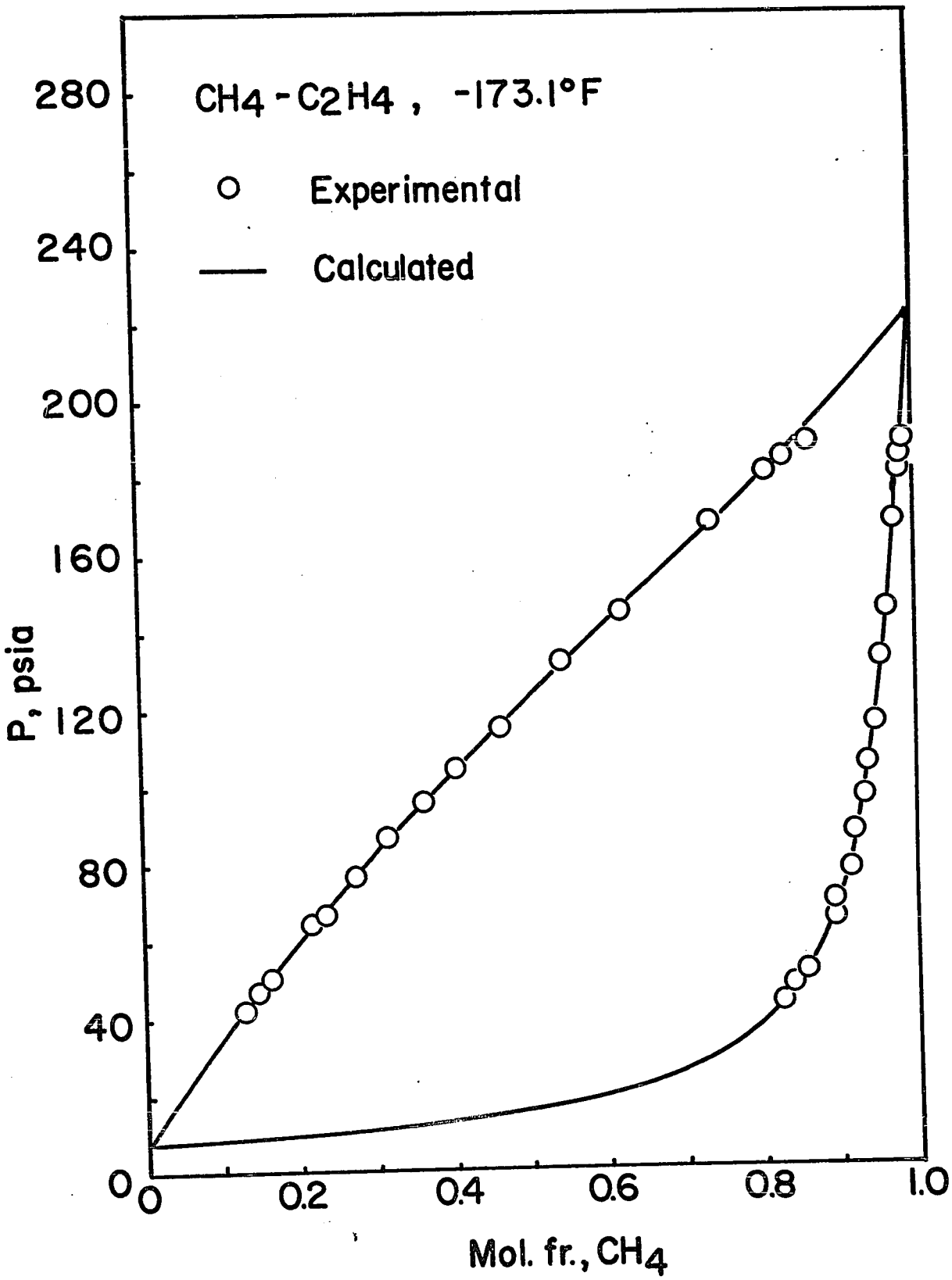

Figure 4-8 Vapor-Liquid Equilibrium Data for the Methane-Ethylene System at -173.1° F

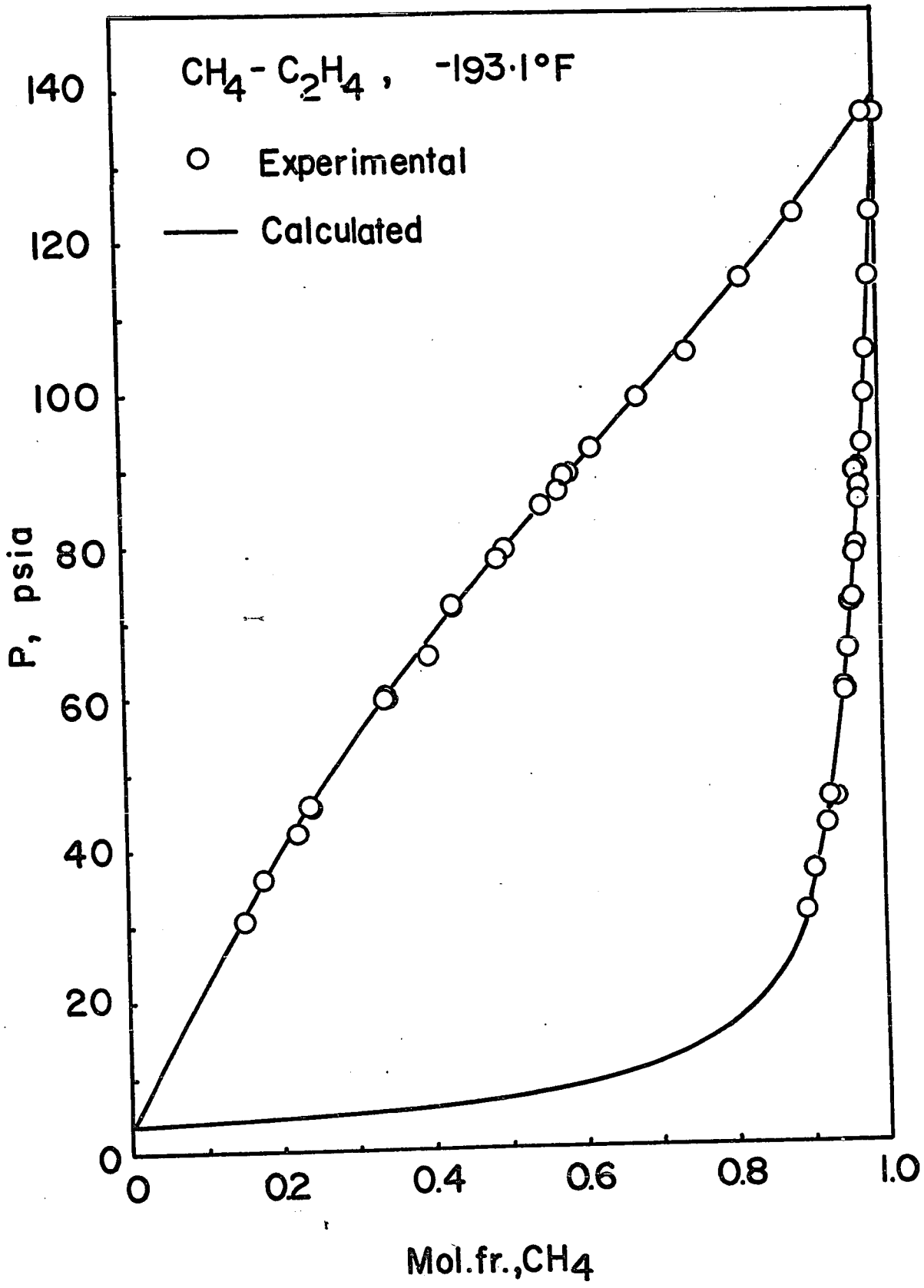

Figure 4-9 Vapor-Liquid Equilibrium, Data for the Methane-Ethylene System at -193.1° F

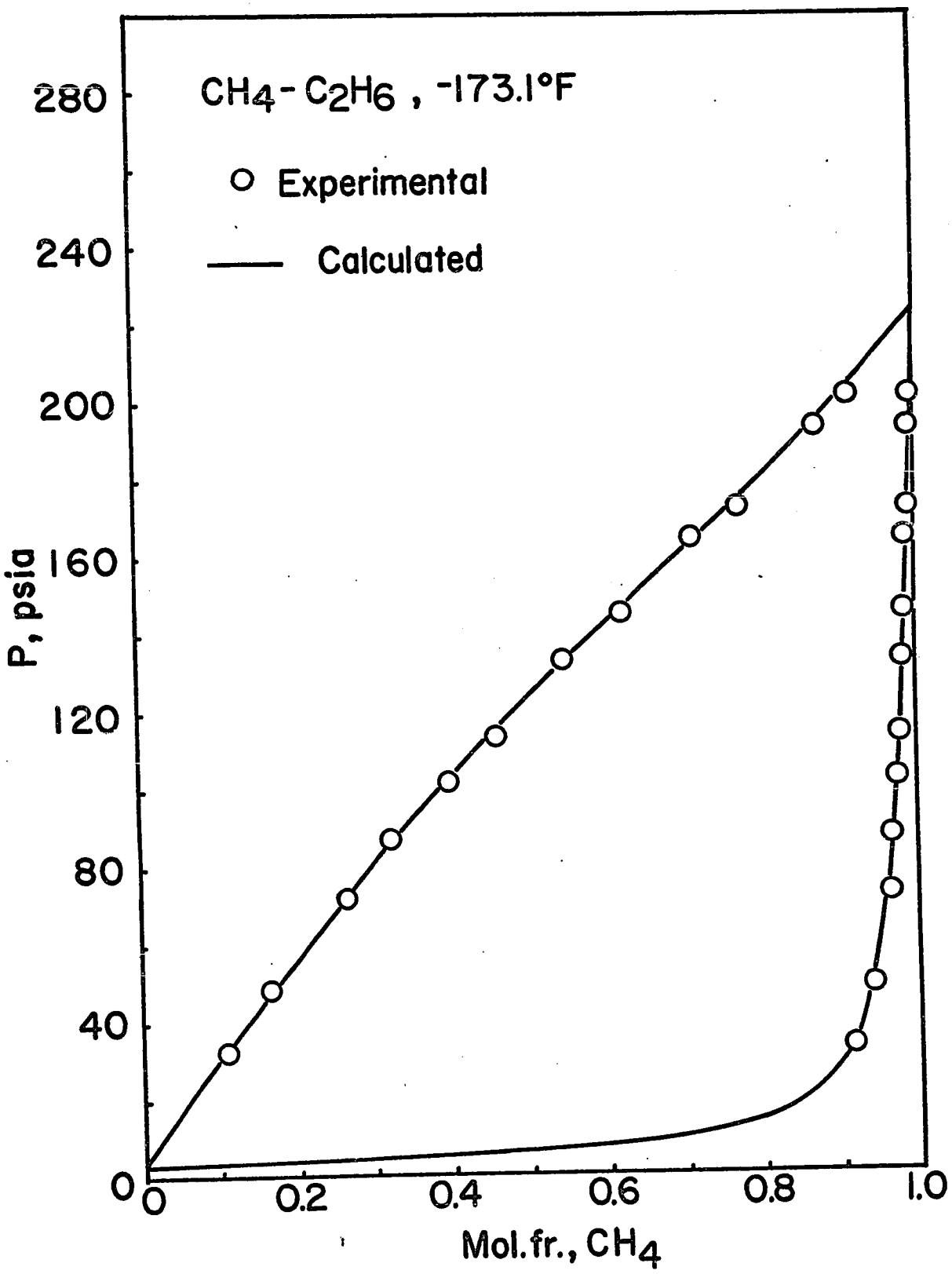

Figure 4-10 Vapor-Liquid Equilibrium Data for the Methane-Ethane System at -173.1° F

TABLE 4 - 2

Comparison of Experimental and Calculated Vapor-Liquid Equilibrium Data for the System Methane (1) - Ethylene (2)

$k_{ij} = 0.0066$

		P, psia		y_1		Deviation	
T, °F	x_1	Expt.	Calc.	Expt.	Calc.	ΔP	Δy_1
-193.1	0.1523	30.50	30.94	0.8969	0.8989	-0.44	-0.0020
	0.1798	36.00	35.42	0.9070	0.9132	0.58	-0.0062
	0.2262	42.10	42.66	0.9240	0.9302	-0.56	-0.0062
	0.2419	45.80	45.20	0.9294	0.9346	0.60	-0.0052
	0.2442	45.55	45.36	0.9374	0.9352	0.19	0.0022
	0.3423	59.90	59.20	0.9510	0.9539	0.70	-0.0029
	0.3448	60.20	59.53	0.9503	0.9543	0.67	-0.0040
	0.3483	60.00	60.00	0.9510	0.9547	0	-0.0037
	0.4004	65.35	66.74	0.9553	0.9611	-1.39	-0.0058
	0.4329	72.00	70.77	0.9619	0.9644	1.23	-0.0025
	0.4359	71.85	71.14	0.9593	0.9647	0.71	-0.0054
	0.4938	78.00	78.03	0.9668	0.9696	-0.03	-0.0028
	0.5034	79.25	79.14	0.9690	0.9704	0.11	-0.0014
	0.5522	85.00	84.70	0.9716	0.9739	0.30	-0.0023
	0.5759	87.00	87.34	0.9730	0.9754	-0.34	-0.0024
	0.5812	89.00	87.93	0.9694	0.9757	1.07	-0.0053
	0.5911	89.30	89.03	0.9733	0.9764	0.27	-0.0031
	0.6197	92.50	92.17	0.9765	0.9781	0.33	-0.0016
	0.6814	99.05	98.90	0.9810	0.9816	0.15	-0.0006
	0.7483	105.00	106.26	0.9832	0.9852	-1.26	-0.0020
	0.8194	114.80	114.39	0.9894	0.9890	0.41	0.0004
	0.8921	123.13	123.33	0.9937	0.9930	-0.20	0.0007
	0.9851	136.30	136.41	0.9975	0.9989	-0.11	-0.0014
-173.1	0.1284	42.25	42.11	0.8263	0.8275	0.14	-0.0012
	0.1469	47.00	46.77	0.8402	0.8461	0.23	-0.0059
	0.1629	50.50	50.73	0.8572	0.8593	-0.23	-0.0021
	0.2153	64.24	63.32	0.8930	0.8906	0.92	0.0024
	0.2335	67.05	67.57	0.8934	0.8985	-0.52	-0.0054
	0.2726	76.80	76.45	0.9150	0.9125	0.35	0.0025
	0.3163	86.76	86.04	0.9202	0.9245	0.72	-0.0043

(... continuation...) Table 4 - 2

T, °F	x_1	P, psia		y_1		Deviation	
		Expt.	Calc.	Expt.	Calc.	ΔP	Δy_1
-173.1	0.3617	96.00	95.65	0.9341	0.9343	0.35	-0.0002
	0.4073	104.50	104.96	0.9377	0.9422	-0.46	-0.0045
	0.4634	115.25	116.01	0.9490	0.9502	-0.76	-0.0012
	0.5458	132.00	131.60	0.9564	0.9597	0.40	-0.0033
	0.6210	145.00	145.41	0.9666	0.9668	-0.41	-0.0002
	0.7385	168.05	166.97	0.9758	0.9767	1.08	-0.0009
	0.8125	180.80	181.14	0.9830	0.9826	-0.34	0.0004
	0.8325	185.00	185.14	0.9850	0.9843	-0.14	0.0007
	0.8653	188.70	191.90	0.9891	0.9870	-3.20	0.0021
-156.1	0.0408	28.41	28.93	0.5197	0.5200	-0.52	-0.0003
	0.0557	35.00	34.27	0.6010	0.5968	0.73	0.0042
	0.0840	44.25	44.26	0.6902	0.6911	-0.01	-0.0009
	0.0919	48.00	47.02	0.7215	0.7101	0.98	0.0114
	0.0938	47.55	47.68	0.7194	0.7143	-0.13	0.0051
	0.1265	60.05	58.94	0.7761	0.7719	1.11	0.0042
	0.1352	61.30	61.89	0.7887	0.7835	-0.59	0.0052
	0.1719	75.42	74.16	0.8165	0.8222	1.26	-0.0057
	0.1772	77.02	75.91	0.8230	0.8268	1.11	-0.0038
	0.2302	93.01	93.05	0.8631	0.8622	-0.04	0.0009
	0.2398	97.00	96.09	0.8575	0.8673	0.91	-0.0098
	0.2811	110.00	108.96	0.8784	0.8855	1.04	-0.0071
	0.3251	122.50	122.30	0.8972	0.9006	0.20	-0.0034
	0.3553	132.00	131.25	0.9070	0.9091	0.75	-0.0021
	0.3875	140.00	140.61	0.9110	0.9170	-0.61	-0.0060
	0.4080	145.69	146.49	0.9237	0.9215	-0.80	0.0022
	0.4403	156.00	155.63	0.9256	0.9279	0.37	-0.0023
	0.4570	160.27	160.29	0.9300	0.9309	-0.02	-0.0009
	0.4617	162.00	161.60	0.9294	0.9318	0.40	-0.0024
	0.5040	170.80	173.25	0.9358	0.9387	-2.45	-0.0029
	0.5132	176.50	175.76	0.9380	0.9401	0.74	-0.0021
	0.5450	185.00	184.35	0.9430	0.9446	0.65	-0.0016
	0.5711	191.00	191.40	0.9449	0.9482	-0.40	-0.0033
	0.5843	195.00	194.95	0.9479	0.9499	0.05	-0.0020
	0.5848	196.50	195.08	0.9483	0.9499	1.42	-0.0016
	0.6192	206.0	204.29	0.9518	0.9542	1.71	-0.0024

(. . . continuation. . .) Table 4 - 2

T, °F	x_1	P, psia		y_1		Deviation	
		Expt.	Calc.	Expt.	Calc.	ΔP	Δy_1
-156.1	0.6380	210.0	209.32	0.9540	0.9564	0.68	-0.0024
	0.6430	209.5	210.66	0.9621	0.9570	-1.16	0.0051
	0.6890	228.3	223.05	0.9615	0.9622	5.25	-0.0007
	0.7042	227.8	227.17	0.9608	0.9639	0.63	-0.0031
	0.7225	230.9	232.18	0.9654	0.9659	-1.28	-0.0005
	0.7320	235.0	234.80	0.9670	0.9670	0.20	0
	0.7327	235.0	234.99	0.9700	0.9670	0.01	0.0030
	0.7794	247.5	248.10	0.9733	0.9721	-0.60	0.0012
	0.7860	250.0	249.98	0.9750	0.9728	0.02	0.0022
	0.7893	249.2	250.93	0.9776	0.9732	-1.73	0.0044
	0.8037	256.5	255.11	0.9767	0.9748	1.39	0.0019
	0.8330	260.1	263.81	0.9850	0.9780	-3.71	0.0070
	0.8424	264.5	266.67	0.9800	0.9791	-2.17	0.0009
	0.8648	271.5	273.65	0.9856	0.9817	-2.15	0.0039
	0.8780	275.0	277.86	0.9860	0.9833	-2.86	0.0027
	0.8816	280.3	279.02	0.9841	0.9837	1.28	0.0004
	0.8962	284.0	283.82	0.9920	0.9855	0.18	0.0065
	0.9250	293.0	293.67	0.9914	0.9891	-0.67	0.0023
	0.9690	306.6	309.94	0.9967	0.9952	-3.34	0.0015

TABLE 4 - 3

Comparison of Experimental and Calculated Vapor-Liquid Equilibrium Data for the System Methane (1) - Ethane (3)

$k_{ij} = 0.0070$

T, °F	x_1	P, psia		y_1		Deviation	
		Expt.	Calc.	Expt.	Calc.	ΔP	Δy_1
-173.1	0.1106	32.54	33.61	0.9130	0.9158	-1.07	-0.0028
	0.1668	48.25	48.26	0.9400	0.9427	-0.01	-0.0027
	0.2658	72.05	72.55	0.9611	0.9636	-0.50	-0.0025
	0.3234	87.10	85.79	0.9676	0.9702	1.31	-0.0026
	0.3990	102.00	102.24	0.9747	0.9762	-0.24	-0.0015
	0.4592	113.60	114.63	0.9791	0.9797	-1.03	-0.0006
	0.5471	133.00	131.77	0.9831	0.9837	1.23	-0.0006
	0.6214	145.50	145.59	0.9863	0.9864	-0.09	-0.0001
	0.7135	164.35	162.35	0.9893	0.9894	2.00	-0.0001
	0.7779	172.22	174.22	0.9916	0.9914	-2.00	0.0002
	0.8766	193.00	193.72	0.9943	0.9946	-0.72	-0.0003
	0.9173	201.4	202.67	0.9963	0.9962	-1.27	0.0001

TABLE 4 - 4

Comparison of Experimental and Calculated Vapor-Liquid Equilibrium Data for the System Methane (1) - Ethylene (2) - Ethane (3) at -173.1° F

		P, psia		y_1		y_2	
x_1	x_2	Expt.	Calc.	Expt.	Calc.	Expt.	Calc.
0.1240	0.6812	38.14	38.70	0.8203	0.8291	0.1572	0.1498
0.2150	0.6116	60.43	60.37	0.8905	0.8957	0.0957	0.0916
0.3147	0.5185	84.31	82.40	0.9251	0.9292	0.0647	0.0614
0.4058	0.4578	102.00	101.65	0.9401	0.9461	0.0528	0.0471
0.4517	0.4161	110.00	110.81	0.9504	0.9528	0.0430	0.0410
0.5367	0.3572	127.97	127.51	0.9596	0.9622	0.0356	0.0331
0.6378	0.2840	147.03	146.77	0.9722	0.9711	0.0246	0.0255
0.7230	0.2163	162.89	162.87	0.9777	0.9778	0.0201	0.0196
0.1241	0.5775	38.00	37.94	0.8268	0.8361	0.1437	0.1333
0.2200	0.5189	59.90	60.63	0.8966	0.9025	0.0830	0.0796
0.3313	0.4422	85.33	85.26	0.9306	0.9358	0.0565	0.0522
0.4241	0.3803	104.95	104.60	0.9505	0.9515	0.0406	0.0394
0.5399	0.2986	127.25	127.48	0.9623	0.9649	0.0302	0.0283
0.5878	0.2706	136.29	136.71	0.9660	0.9690	0.0280	0.0251
0.1297	0.4356	38.70	38.63	0.8516	0.8548	0.1086	0.1046
0.2419	0.3812	64.42	64.97	0.9122	0.9191	0.0611	0.0581
0.3382	0.3280	86.70	86.20	0.9389	0.9433	0.0420	0.0403
0.4136	0.2981	103.00	102.03	0.9520	0.9546	0.0341	0.0325
0.5138	0.2499	123.00	122.13	0.9638	0.9655	0.0260	0.0247
0.6255	0.1911	143.43	143.69	0.9748	0.9747	0.0180	0.0179
0.1196	0.1844	36.00	35.80	0.8787	0.8815	0.0529	0.0548
0.2179	0.1693	60.19	59.77	0.9282	0.9323	0.0314	0.0313
0.3040	0.1453	80.00	79.57	0.9506	0.9525	0.0215	0.0211
0.3990	0.1262	100.86	100.07	0.9637	0.9649	0.0161	0.0153
0.5027	0.1066	121.08	121.06	0.9725	0.9736	0.0117	0.0114
0.6051	0.0814	141.22	140.82	0.9810	0.9802	0.0077	0.0081
0.6761	0.0661	154.16	154.16	0.9839	0.9838	0.0061	0.0064
0.2127	0.2388	58.56	58.29	0.9151	0.9228	0.0445	0.0433
0.2782	0.2101	73.50	73.37	0.9398	0.9421	0.0319	0.0315
0.3574	0.1910	90.62	90.72	0.9540	0.9556	0.0243	0.0241
0.4228	0.1732	105.00	104.42	0.9629	0.9634	0.0204	0.0198
0.4867	0.1575	117.21	117.30	0.9687	0.9692	0.0174	0.0167

(. . . continuation. . .) Table 4-4

		P, psia		y_1		y_2	
x_1	x_2	Expt.	Calc.	Expt.	Calc.	Expt.	Calc.
0.5535	0.1371	130.00	130.38	0.9749	0.9743	0.0140	0.0138
0.6587	0.1056	150.35	150.41	0.9804	0.9808	0.0108	0.0101
0.1143	0.2456	33.95	34.48	0.8551	0.8657	0.0754	0.0727
0.1973	0.2218	54.22	54.71	0.9139	0.9194	0.0451	0.0431
0.2770	0.2060	73.78	73.13	0.9383	0.9422	0.0333	0.0310
0.3526	0.1827	89.75	89.77	0.9563	0.9557	0.0233	0.0234
0.4588	0.1571	111.95	111.81	0.9658	0.9673	0.0184	0.0172
0.5518	0.1281	130.22	130.16	0.9720	0.9748	0.0149	0.0130

It may be found that the equilibrium data of the ternary system methane-ethylene-ethane are successfully predicted without introducing any ternary interaction constants; therefore, the binary interaction constants suffice to describe all interactions in this ternary system.

In conclusion, the phase behaviour of the mixtures containing methane, ethylene and ethane can be predicted with confidence by the proposed method of Chapter III. And the disagreement between the calculated values and the literature values[58, 59] for the system methane-ethylene may be attributed to experimental error.

CHAPTER V

CORRELATION OF VAPOR-LIQUID EQUILIBRIA

In this chapter, the liquid activity coefficients were evaluated from the experimental vapor-liquid equilibrium data and correlated.

5.1 CONSTANT-PRESSURE AND CONSTANT-TEMPERATURE ACTIVITY COEFFICIENT

The liquid activity coefficient depends on the liquid phase composition and saturation pressure at isothermal conditions. For effective thermodynamic analysis and correlation of high-pressure vapor-liquid equilibrium data, it is important to consider the effect of pressure on the liquid activity coefficient.

At low or moderate pressures, liquid activity coefficients are slightly dependent on pressure and, as a result, it has been customary to assume that, for practical purposes, activity coefficients depend only on temperature and composition. Hence, the isothermal and isobaric Gibbs-Duhem equation can be used. However, it can lead to serious error when this assumption is applied to the case of high-pressure phase equilibria. Therefore, it is necessary to adjust the liquid activity coefficient in the following manner. The activity coefficient of component i in the liquid mixture at the system temperature T and reference pressure P° may be defined as:

$$\gamma_i (P^\circ, T, x) = \hat{f}_{iL} (P^\circ, T, x)/x_i f^\circ_{iL} (P^\circ, T) \qquad (5\text{-}1)$$

where f°_{iL} is the reference fugacity of component i at T and P°. The fugacity of any component i of a solution, $\hat{f}_i$, is defined by the following equation[42]:

$$\begin{cases} \mu_i = \mu_i^{\circ} + RT \ln \hat{f}_i \\ \dfrac{\hat{f}_i}{P_i} \rightarrow 1 \quad \text{as} \quad P \rightarrow 0 \end{cases} \tag{3-2}$$

Partial differentiating Equation (3-2) with respect to pressure gives the pressure dependence of the fugacity:

$$\left(\frac{\partial \ln \hat{f}_i}{\partial P}\right)_{T,x} = \frac{1}{RT}\left(\frac{\partial \mu_i}{\partial P}\right)_{T,x} = \frac{\bar{V}_i}{RT} \tag{5-2}$$

Integrating Equation (5-2) from system pressure P to reference pressure P° gives:

$$\hat{f}_{iL}(P^{\circ}, T, x) = \hat{f}_{iL}(P, T, x) \exp \int_{P}^{P^{\circ}} \frac{\bar{V}_i}{RT}\, dP \tag{5-3}$$

Combining Equations (5-1) and (5-3) gives:

$$\gamma_i (P^{\circ}, T, x) = \frac{\hat{f}_{iL}(P, T, x)}{x_i\, f^{\circ}_{iL}(P^{\circ}, T)} \exp \int_{P}^{P^{\circ}} \frac{\bar{V}_i}{RT}\, dP \tag{5-4}$$

This expression is similar to that given by Prausnitz[64]. The activity coefficients are normalized symmetrically; for a component i,

$$\gamma_i \rightarrow 1 \qquad \text{as} \qquad x_i \rightarrow 1 \tag{5-5}$$

It should be mentioned that all components considered are below the critical point of the volatile component of the system concerned. Therefore, the reference fugacity f°_{iL} is simply the liquid fugacity of the pure component i at system temperature T and reference pressure P°.

At equilibrium, the fugacities of component i in both liquid and vapor phases must be identical:

$$\hat{f}_{iL} = \hat{f}_{iV} \tag{5-6}$$

Since:

$$\hat{f}_{iV} = y_i \hat{\varphi}_{iV} P \tag{5-7}$$

therefore, Equation (5-4) becomes:

$$\gamma_i = \frac{y_i \hat{\varphi}_{iV} P}{x_i f^{\circ}_{iL}} \exp \int_{P}^{P^{\circ}} \frac{\bar{V}_i}{RT} dP \tag{5-8}$$

Equation (5-8) may be employed to calculate constant-pressure activity coefficients. Thus the activity coefficients satisfy the isothermal, isobaric Gibbs-Duhem equation. In this work, Equation (5-8) is preferable to Equation (5-4), because Equation (5-8) includes the vapor-phase properties. The final results of calculation would clearly reflect the quality of the experimental data.

5.2 PARTIAL MOLAL VOLUME

The value of the partial molal volume of component i in the liquid mixture is required while the constant-pressure activity coefficient is evaluated. It is necessary to have a reliable method for calculating partial molal volumes from a minimum amount of experimental information.

The partial molal volume of component i in a mixture is defined by:

$$\bar{V}_i = \left(\frac{\partial V_T}{\partial n_i}\right)_{P, T, n_j (i \neq j)} \tag{5-9}$$

The partial molal volume can be evaluated from a suitable equation of state for the liquid mixture. Since most equations of state are explicit in pressure, rather than in volume, it is convenient to rewrite Equation (5-9):

$$\bar{V}_i = \frac{-\left(\frac{\partial P}{\partial n_i}\right)_{T, V_T, n_j (i \neq j)}}{\left(\frac{\partial P}{\partial V_T}\right)_{T, n_i (\text{all } i)}} = f(x, T, V) \tag{5-10}$$

With an equation of state, Equation (5-10) gives $\bar{V}_i$ as a function of the composition, temperature and molal volume of the liquid mixture. Pressure does not appear explicitly in Equation (5-10), but is implicit in the volume, which depends on the pressure.

In the present work, it was decided to follow up the approach of Chang and Lu[5] in which the modified Redlich-Kwong equation of state was employed to evaluate the partial molal volume. Combining

5.2 PARTIAL MOLAL VOLUME

The value of the partial molal volume of component i in the liquid mixture is required while the constant-pressure activity coefficient is evaluated. It is necessary to have a reliable method for calculating partial molal volumes from a minimum amount of experimental information.

The partial molal volume of component i in a mixture is defined by:

$$\bar{V}_i = \left(\frac{\partial V_T}{\partial n_i}\right)_{P, T, n_j (i \neq j)} \tag{5-9}$$

The partial molal volume can be evaluated from a suitable equation of state for the liquid mixture. Since most equations of state are explicit in pressure, rather than in volume, it is convenient to rewrite Equation (5-9):

$$\bar{V}_i = \frac{-\left(\frac{\partial P}{\partial n_i}\right)_{T, V_T n_j (i \neq j)}}{\left(\frac{\partial P}{\partial V_T}\right)_{T, n_i (\text{all } i)}} = f(x, T, V) \tag{5-10}$$

With an equation of state, Equation (5-10) gives $\bar{V}_i$ as a function of the composition, temperature and molal volume of the liquid mixture. Pressure does not appear explicitly in Equation (5-10), but is implicit in the volume, which depends on the pressure.

In the present work, it was decided to follow up the approach of Chang and Lu[5] in which the modified Redlich-Kwong equation of state was employed to evaluate the partial molal volume. Combining

Equation (5-10) with the Redlich-Kwong equation and its mixing rules (Equations (3-7), (3-8) and (3-13) to (3-22)) gives:

$$\bar{V}_i = \frac{\frac{RT}{V-b}\left(1+\frac{b_i}{V-b}\right) - \frac{2\left(\sum_j^C x_j a_{ij}\right) - \frac{ab_i}{V+b}}{V(V+b)T^{\frac{1}{2}}}}{\frac{RT}{(V-b)^2} - \frac{a}{T^{\frac{1}{2}}}\left[\frac{2V+b}{V^2(V+b)^2}\right]} \qquad (5\text{-}11)$$

where V, which is the smallest real root of the Redlich-Kwong equation of state, is the saturated liquid molal volume of the mixture.

5.3 CORRELATION OF ACTIVITY COEFFICIENTS WITH THE REDLICH-KISTER EQUATION

The values of the activity coefficient calculated from Equation (5-8) may then be correlated by means of the Redlich-Kister equation[65] for the binary system,

$$\ln \gamma_1 = x_2^2 \left[B_{12} + C_{12}(3x_1 - x_2) + D_{12}(x_1 - x_2)(5x_1 - x_2) \right]$$

$$\ln \gamma_2 = x_1^2 \left[B_{12} + C_{12}(x_1 - 3x_2) + D_{12}(x_1 - x_2)(x_1 - 5x_2) \right] \qquad (5\text{-}12)$$

The following equation, which was also proposed by Redlich and Kister[65], may be used to correlate the activity coefficients of the ternary system,

$$Q_{123} = Q_{12} + Q_{23} + Q_{31} + x_1 x_2 x_3 \left[C + D_1(x_2 - x_3) + D_2(x_3 - x_1) + D_3(x_1 - x_2) + \cdots\cdots \right] \qquad (5\text{-}13)$$

where:

$$Q_{123} = x_1 \ln \gamma_1 + x_2 \ln \gamma_2 + x_3 \ln \gamma_3 \tag{5-14}$$

$$Q_{12} = x_1 x_2 [B_{12} + C_{12} (x_1 - x_2) + D_{12} (x_1 - x_2)^2] \tag{5-15}$$

$$Q_{23} = x_2 x_3 [B_{23} + C_{23} (x_2 - x_3) + D_{23} (x_2 - x_3)^2] \tag{5-16}$$

$$Q_{31} = x_3 x_1 [B_{31} + C_{31} (x_3 - x_1) + D_{31} (x_3 - x_1)^2] \tag{5-17}$$

The individual activity coefficient can be related with Q_{123} in the following form:

$$\ln \gamma_i = Q_{123} + \frac{\partial Q_{123}}{\partial x_i} - \sum_{i=1}^{3} x_i \frac{\partial Q_{123}}{\partial x_i} \tag{5-18}$$

Combining Equations (5-13) and (5-18) gives[66]:

$$\begin{aligned}
\ln \gamma_1 = {} & B_{12} x_2 (1 - x_1) + C_{12} x_2 (2x_1 - x_2 - 2x_1^2 + 2x_1 x_2) \\
& + D_{12} x_2 (3x_1^2 - 3x_1^3 + 6x_1^2 x_2 - 4x_1 x_2 - 3x_1 x_2^2 + x_2^2) \\
& - B_{23} x_2 x_3 - 2C_{23} x_2 x_3 (x_2 - x_3) - 3D_{23} (x_2 - x_3)^2 \\
& + B_{31} x_3 (1 - x_1) + C_{31} x_3 (x_3 - 2x_1 x_3 + 2x_1^2 - 2x_1) \\
& + D_{31} x_3 (x_3^2 + 6x_1^2 x_3 - 4x_1 x_3 - 3x_2 x_3^2 + 3x_1^2 - 3x_1^3) \\
& + C x_2 x_3 (1 - 2x_1) + D_1 x_2 x_3 (x_2 - x_3 - 3x_1 x_2 + 3x_1 x_3) \\
& + D_2 x_2 x_3 (x_3 - 2x_1 - 3x_1 x_3 + 3x_1^2) \\
& + D_3 x_2 x_3 (2x_1 - x_2 - 3x_1^2 + 3x_1 x_2)
\end{aligned} \tag{5-19}$$

$$\ln \gamma_2 = B_{12} x_1 (1 - x_2) + C_{12} x_1 (x_1 - 2x_2 - 2x_1 x_2 + 2x_2^2)$$
$$+ D_{12} x_1 (x_1^2 - 4x_1 x_2 + 3x_2^2 - 3x_1^2 x_2 + 6x_1 x_2^2 - 3x_2^3)$$
$$+ B_{23} x_3 (1 - x_2) + C_{23} x_3 (2x_2 - x_3 - 2x_2^2 + 2x_2 x_3)$$
$$+ D_{23} x_3 (x_3^2 + 3x_2^2 - 4x_2 x_3 - 3x_2^3 + 6x_2^2 x_3 - 3x_2 x_3)$$
$$- B_{31} x_1 x_3 - 2C_{31} x_1 x_3 (x_3 - x_1)$$
$$- 3D_{31} x_1 x_3 (x_3 - x_1)$$
$$+ C x_1 x_3 (1 - 2x_2)$$
$$+ D_1 x_1 x_3 (2x_2 - x_3 - 3x_2^2 + 3x_2 x_3)$$
$$+ D_2 x_1 x_3 (x_3 - x_1 + 3x_1 x_2 - 3x_2 x_3)$$
$$+ D_3 x_1 x_3 (x_1 - 2x_2 - 3x_1 x_2 + 3x_2^2) \qquad (5\text{-}20)$$

and

$$\ln \gamma_3 = -B_{12} x_1 x_2 - 2C_{12} x_1 x_2 (x_1 - x_2)$$
$$- 3D_{12} x_1 x_2 (x_1 - x_2)^2 + B_{23} x_2 (1 - x_3)$$
$$+ C_{23} x_2 (x_2 - 2x_3 - 2x_2 x_3 + 2x_3^2)$$
$$+ D_{23} x_2 (x_2^2 - 4x_2 x_3 + 3x_3^2 + 3x_2^2 x_3 + 6x_2 x_3^2 - 3x_3^2)$$
$$+ B_{31} x_1 (1 - x_3) + C_{31} x_1 (2x_3 - x_1 - 2x_3^2 + 2x_1 x_3)$$
$$+ D_{31} x_1 (x_1^2 + 3x_3^2 - 4x_1 x_3 - 3x_3^3 + 6x_1 x_3^2 - 3x_1^2 x_3)$$
$$+ C x_1 x_2 (1 - 2x_3)$$

$$+ D_1 x_1 x_2 (x_2 - 2x_3 - 3x_2 x_3 + 3x_3^2)$$

$$+ D_2 x_1 x_2 (-x_1 + 2x_3 - 3x_3^2 + 3x_1 x_3)$$

$$+ D_3 x_1 x_2 (x_1 - x_2 - 3x_1 x_3 + 3x_2 x_3) \qquad (5\text{-}21)$$

5.4 RESULTS AND DISCUSSIONS

In this study, the reference pressure was chosen to be 500 p.s.i.a. which is above the highest saturation pressure encountered in this work. Activity coefficients for the binary systems methane-ethylene and methane-ethane were evaluated by means of Equation (5-8).

The correlation of the ternary system methane-ethylene-ethane at -173.1° F required the information of the ethylene-ethane system. However, available data for the ethylene-ethane binary system in the literature[55, 67] are limited to temperatures at and above -100° F. It is difficult to extrapolate the data to -173.1° F with certainty. On the other hand, the limitations of the sampling system of the existing apparatus prevented the author from determining the equilibrium data directly. Hence, equilibrium data for the ethylene-ethane system at -173.1° F were predicted by employing the method proposed in Chapter III. The predicted results are listed in Table 5-1.

The fitted constants for all the binary systems, which were obtained by the least-squares method for the three-constant Redlich-Kister equation, are presented in Table 5-2. The experimental and calculated liquid activity coefficients are also compared in Figures 5-1 to 5-4, and in Tables 5-3 and 5-4.

TABLE 5-1

Predicted Vapor-Liquid Equilibrium Data for the System Ethylene (2) - Ethane (3)

T, °F	x_2	Predicted			
		$\bar{P}$, psia	y_2	γ_2	γ_3
-173.1	0.05	3.3614	0.1682	1.4880	1.0010
	0.10	3.7501	0.2907	1.4328	1.0040
	0.20	4.4347	0.4591	1.3354	1.0166
	0.30	5.0176	0.5720	1.2528	1.0386
	0.40	5.5214	0.6559	1.1839	1.0706
	0.50	5.9649	0.7233	1.1268	1.1148
	0.60	6.3636	0.7815	1.0811	1.1730
	0.70	6.7278	0.8350	1.0457	1.2478
	0.80	7.0683	0.8873	1.0205	1.3425
	0.90	7.3901	0.9413	1.0052	1.4616
	0.95	7.5447	0.9698	1.0013	1.5351

TABLE 5-2

A Summary of Correlation Results for the Binary Systems

System	T. °F	B_{ij}	C_{ij}	D_{ij}	$\ln \gamma_i^{\infty}$	$\ln \gamma_j^{\infty}$
methane (i)-ethylene(j)	-193.1	0.6109	0.0918	0.0354	0.5545	0.7381
	-173.1	0.5527	0.0897	0.0142	0.4772	0.6566
	-156.1	0.5215	0.0955	0.0203	0.4463	0.6373
methane(i)-ethane (j)	-173.1	0.6001	0.1405	0.0349	0.4945	0.7755
ethylene (i)-ethane (j)	-173.1	0.4562	0.0213	0.0018	0.4367	0.4793

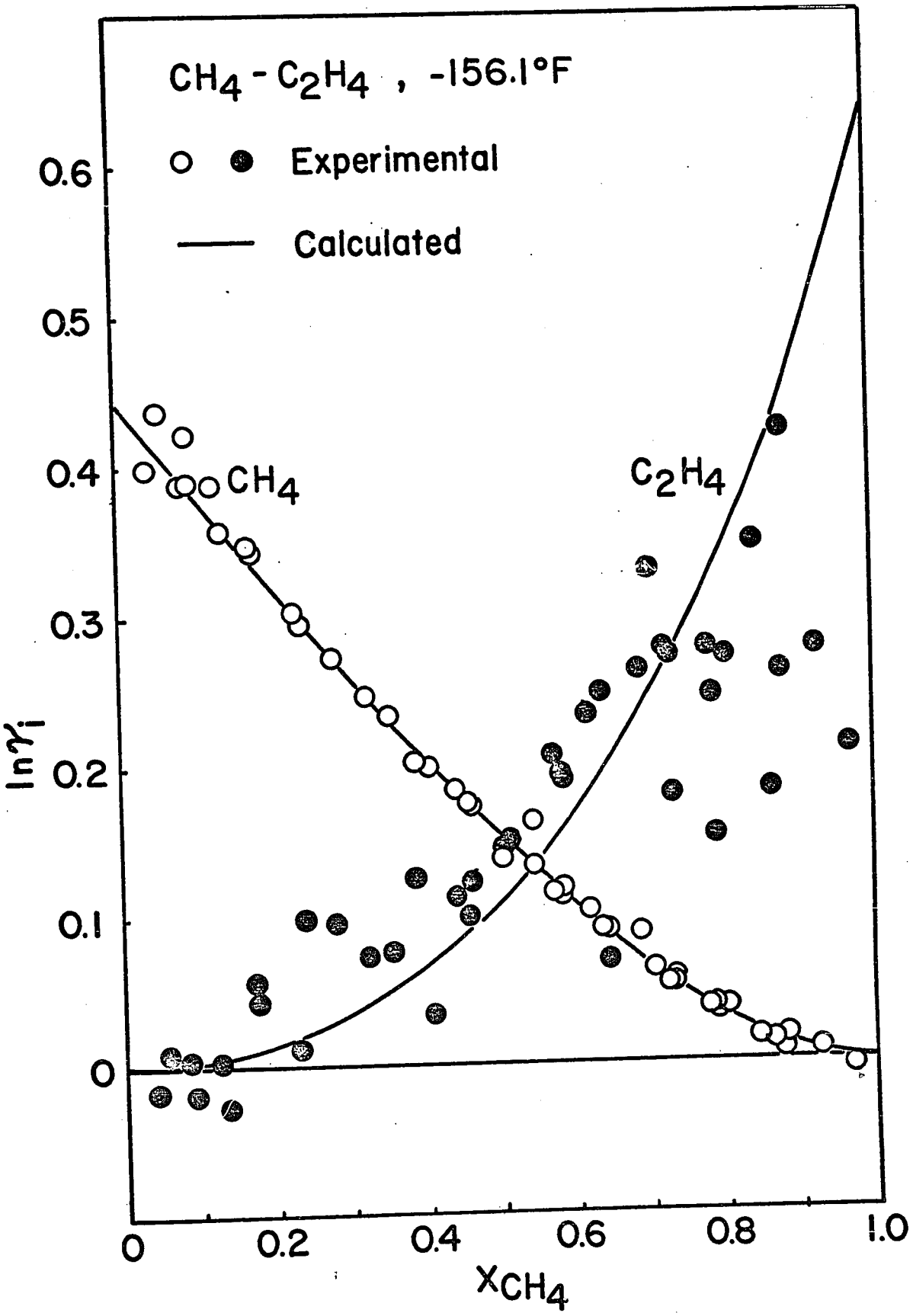

Figure 5-1 Comparison of Experimental and Calculated γ Values for the Methane-Ethylene System at -156.1° F

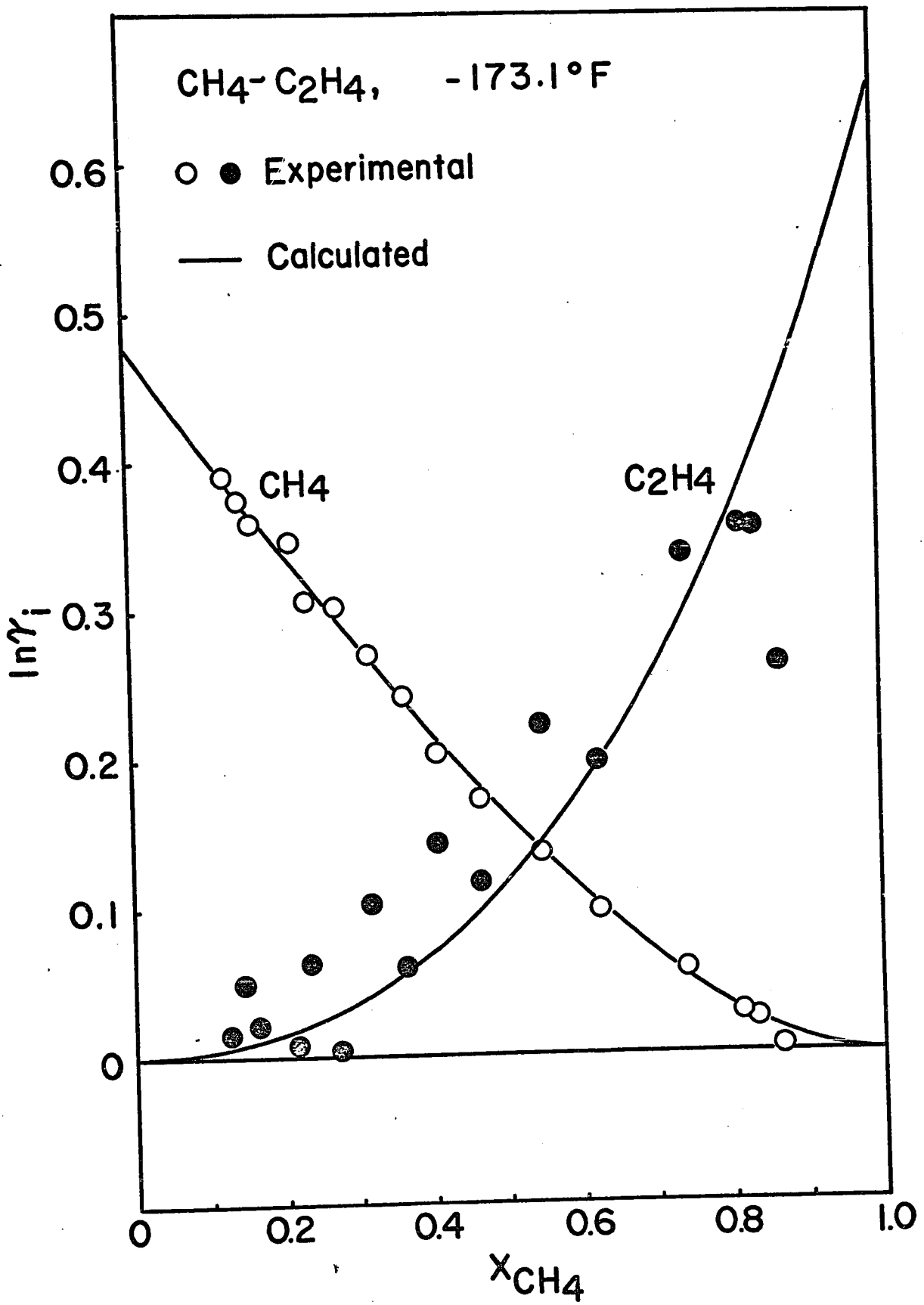

Figure 5-2 Comparison of Experimental and Calculated γ Values for the Methane-Ethylene System at -173.1°F

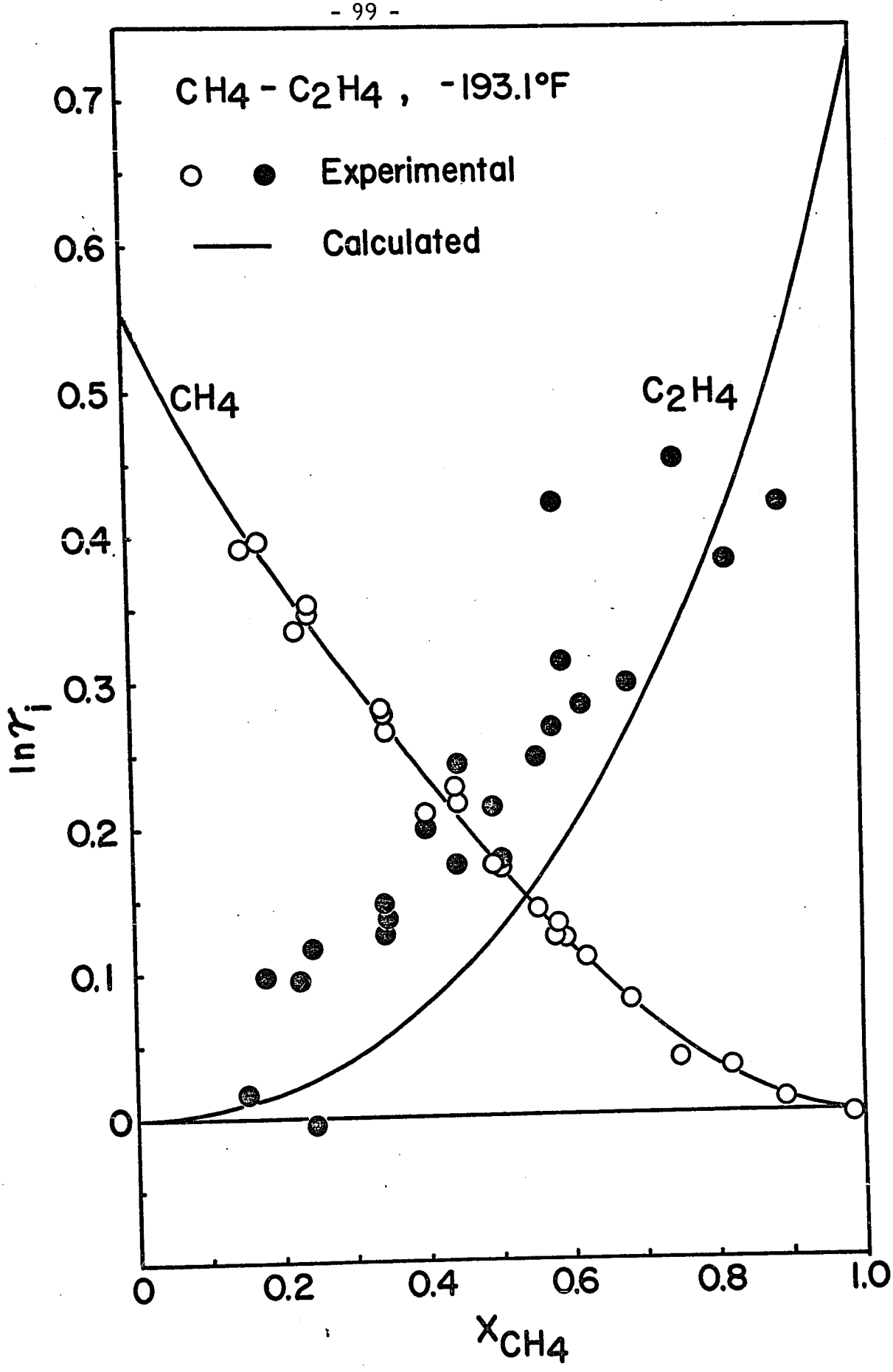

Figure 5-3 Comparison of Experimental and Calculated γ Values for the Methane-Ethylene System at -193.1° F

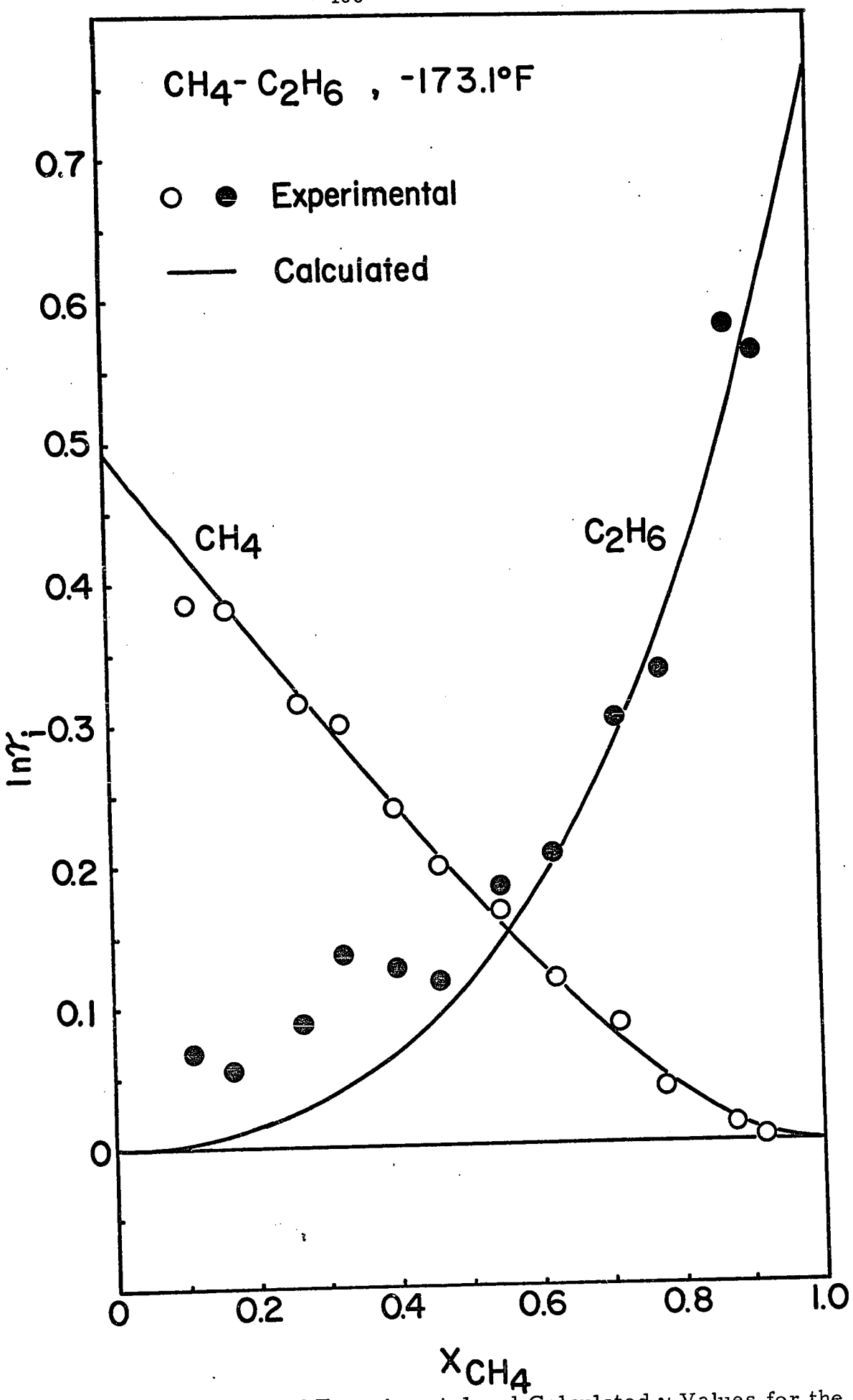

Figure 5-4 Comparison of Experimental and Calculated γ Values for the Methane-Ethane System at -173.1°F

TABLE 5-3

Experimental and Calculated Activity Coefficients for the Binary System Methane (1) - Ethylene (2)

		γ_1		γ_2	
T, °F	x_1	Expt.	Calc.	Expt.	Calc.
-193.1	0.1523	1.4807	1.5140	1.0163	1.0115
	0.1798	1.4872	1.4806	1.1027	1.0160
	0.2262	1.3983	1.4282	1.1000	1.0254
	0.2419	1.4243	1.4115	1.1239	1.0290
	0.2442	1.4157	1.4091	0.9951	1.0296
	0.3423	1.3244	1.3150	1.1339	1.0596
	0.3448	1.3200	1.3128	1.1592	1.0605
	0.3483	1.3037	1.3097	1.1459	1.0619
	0.4004	1.2330	1.2661	1.2199	1.0836
	0.4329	1.2548	1.2406	1.1901	1.0995
	0.4359	1.2405	1.2384	1.2757	1.1010
	0.4938	1.1893	1.1963	1.2383	1.1346
	0.5034	1.1861	1.1897	1.1935	1.1408
	0.5522	1.1548	1.1577	1.2799	1.1761
	0.5759	1.1323	1.1431	1.3076	1.1956
	0.5812	1.1406	1.1400	1.5262	1.2002
	0.5911	1.1294	1.1341	1.3677	1.2090
	0.6197	1.1152	1.1178	1.3288	1.2362
	0.6814	1.0823	1.0856	1.3475	1.3054
	0.7483	1.0395	1.0557	1.5702	1.4003
	0.8194	1.0315	1.0301	1.4662	1.5311
	0.8921	1.0097	1.0113	1.5235	1.7083
	0.9851	0.9982	1.0002	4.6384	2.0279
-173.1	0.1284	1.4779	1.4748	1.0158	1.0062
	0.1469	1.4541	1.4567	1.0512	1.0082
	0.1629	1.4323	1.4413	1.0211	1.0101
	0.2153	1.4160	1.3926	1.0080	1.0183
	0.2335	1.3596	1.3764	1.0662	1.0217
	0.2726	1.3524	1.3425	1.0048	1.0304
	0.3163	1.3107	1.3064	1.1083	1.0442

(. . . continuation. . .) Table 5-3

T, °F	x_1	γ_1 Expt.	γ_1 Calc.	γ_2 Expt.	γ_2 Calc.
-173.1	0.3617	1.2752	1.2708	1.0628	1.0571
	0.4073	1.2266	1.2370	1.1547	1.0751
	0.4634	1.1899	1.1980	1.1235	1.1020
	0.5458	1.1456	1.1463	1.2486	1.1527
	0.6210	1.1025	1.1050	1.2202	1.2136
	0.7385	1.0578	1.0527	1.4004	1.3459
	0.8125	1.0275	1.0281	1.4270	1.4607
	0.8325	1.0233	1.0227	1.4260	1.4971
	0.8653	1.0043	1.0149	1.3007	1.5625
-156.1	0.0408	1.4915	1.5209	0.9841	1.0006
	0.0557	1.5469	1.5062	1.0102	1.0011
	0.0840	1.4767	1.4791	1.0048	1.0024
	0.0919	1.5251	1.4717	0.9816	1.0029
	0.0938	1.4766	1.4699	0.9826	1.0030
	0.1265	1.4749	1.4401	1.0032	1.0056
	0.1352	1.4299	1.4324	0.9742	1.0064
	0.1719	1.4144	1.4006	1.0575	1.0105
	0.1772	1.4103	1.3961	1.0454	1.0112
	0.2302	1.3551	1.3527	1.0124	1.0194
	0.2398	1.3431	1.3451	1.1034	1.0212
	0.2811	1.3153	1.3133	1.1009	1.0298
	0.3251	1.2789	1.2809	1.0774	1.0411
	0.3553	1.2636	1.2595	1.0789	1.0501
	0.3875	1.2253	1.2375	1.1336	1.0611
	0.4080	1.2213	1.2239	1.0354	1.0689
	0.4403	1.2027	1.2031	1.1186	1.0825
	0.4570	1.1914	1.1927	1.1049	1.0902
	0.4617	1.1893	1.1898	1.1319	1.0925
	0.5040	1.1472	1.1645	1.1561	1.1146
	0.5132	1.1606	1.1591	1.1614	1.1199
	0.5450	1.1424	1.1413	1.1758	1.1396
	0.5711	1.1214	1.1273	1.2284	1.1576
	0.5843	1.1183	1.1204	1.2131	1.1673
	0.5848	1.1247	1.1201	1.2106	1.1677
	0.6192	1.1075	1.1030	1.2629	1.1953
	0.6380	1.0941	1.0940	1.2809	1.2119
	0.6430	1.0928	1.0917	1.0706	1.2165

(. . . continuation. . .) Table 5-3

T, °F	x_1	γ_1		γ_2	
		Expt.	Calc.	Expt.	Calc.
-156.1	0.6890	1.0902	1.0714	1.3016	1.2628
	0.7042	1.0643	1.0652	1.3910	1.2799
	0.7225	1.0543	1.0580	1.3178	1.3016
	0.7320	1.0578	1.0544	1.1969	1.3135
	0.7327	1.0378	1.0542	1.3189	1.3144
	0.7794	1.0387	1.0380	1.2785	1.3790
	0.7860	1.0347	1.0359	1.1627	1.3891
	0.7893	1.0371	1.0348	1.3119	1.3942
	0.8037	1.0197	1.0305	0.9991	1.4172
	0.8330	1.0156	1.0225	1.4171	1.4679
	0.8424	1.0139	1.0202	1.2008	1.4854
	0.8648	1.0099	1.0151	1.5239	1.5295
	0.8780	1.0083	1.0124	1.2982	1.5572
	0.8816	1.0158	1.0117	1.5269	1.5650
	0.8962	1.0165	1.0091	0.8815	1.5978
	0.9250	1.0058	1.0048	1.3190	1.6679
	0.9690	0.9953	1.0009	1.2341	1.7911

TABLE 5 - 4

Experimental and Calculated Activity Coefficients for the Binary System Methane (1) - Ethane (3)

		γ_1		γ_3	
T, °F	x_1	Expt.	Calc.	Expt.	Calc.
-173.1	0.1106	1.4710	1.5223	1.0068	1.0038
	0.1668	1.4656	1.4701	1.0565	1.0093
	0.2658	1.3707	1.3831	1.0921	1.0279
	0.3234	1.3500	1.3352	1.1468	1.0429
	0.3990	1.2713	1.2759	1.1344	1.0692
	0.4592	1.2211	1.2315	1.1237	1.0983
	0.5471	1.1805	1.1719	1.2025	1.1533
	0.6214	1.1260	1.1267	1.2299	1.2214
	0.7135	1.0888	1.0781	1.3542	1.3332
	0.7779	1.0404	1.0498	1.4007	1.4419
	0.8766	1.0138	1.0170	1.7885	1.6970
	0.9173	1.0034	1.0081	1.7546	1.8061

Activity coefficients for the ternary system methane-ethylene-ethane at -173.1° F were also evaluated by means of Equation (5-8) and then correlated by Equation (5-13) with the assumption that there was no third component effect. The experimental and calculated γ-values are compared in Table 5-5.

It was found in this investigation that a small difference in vapor-phase composition would give a large difference in the activity coefficient for the less volatile component, because the vapor phase was extremely rich in the volatile component methane. For instance, the binary system methane-ethylene at -193.1° F and 136.3 p. s. i. a. the change of ethylene composition from 0.0011 to 0.0025 mole fraction would cause a change of γ value for ethylene from 2.0279 to 4.6384. Therefore, the activity coefficient for the less volatile component would show a large scattering although the absolute deviation in vapor composition is not very significant.

The $\ln (\gamma_i/\gamma_j)$ vs. composition diagrams for the systems methane-ethylene and methane-ethane are shown in Figures 5-5 to 5-8, with the effect of vapor-phase composition on the $\ln (\gamma_i/\gamma_j)$ values indicated. The maximum values of Δy as indicated in the diagrams are summarized as follows:

System	T, °F	Max. Δy
Methane-ethylene	-193.1	0.0063
	-173.1	0.0052
	-156.1	0.0070
Methane-ethane	-173.1	0.0026

The experimental data are therefore considered thermodynamically consistent.

TABLE 5-5

Experimental and Calculated Activity Coefficients for the Ternary System Methane (1) - Ethylene (2) - Ethane (3) at -173.1°F

		γ_1		γ_2		γ_3	
x_1	x_2	Expt.	Calc.	Expt.	Calc.	Expt.	Calc.
0.1240	0.6812	1.3767	1.4158	1.0717	1.0333	1.3720	1.3193
0.2150	0.6116	1.3350	1.3339	1.0976	1.0490	1.4152	1.3221
0.3147	0.5185	1.2898	1.2530	1.1587	1.0824	1.4249	1.3145
0.4058	0.4578	1.2076	1.1940	1.2447	1.1171	1.3988	1.3323
0.4517	0.4161	1.1729	1.1651	1.1813	1.1438	1.4158	1.3348
0.5367	0.3572	1.1378	1.1212	1.2702	1.1956	1.4188	1.3566
0.6378	0.2840	1.0922	1.0771	1.2114	1.2785	1.3951	1.3887
0.7230	0.2163	1.0553	1.0463	1.3829	1.3749	1.3038	1.4223
0.1241	0.5775	1.3813	1.4092	1.1520	1.0626	1.1702	1.2309
0.2200	0.5189	1.3025	1.3179	1.1139	1.0771	1.3789	1.2494
0.3313	0.4422	1.2460	1.2305	1.1987	1.1118	1.3395	1.2689
0.4241	0.3803	1.1981	1.1706	1.1786	1.1539	1.2487	1.2913
0.5399	0.2986	1.1286	1.1089	1.2848	1.2300	1.4512	1.3243
0.5878	0.2706	1.1040	1.0884	1.3774	1.2661	1.3815	1.3443
0.1297	0.4356	1.3847	1.4179	1.1748	1.1184	1.1020	1.1435
0.2419	0.3812	1.2898	1.2975	1.1896	1.1332	1.3288	1.1759
0.3382	0.3280	1.2489	1.2176	1.2179	1.1649	1.3626	1.2055
0.4136	0.2981	1.2096	1.1670	1.2458	1.1939	1.3055	1.2381
0.5138	0.2499	1.1529	1.1128	1.2916	1.2517	1.3204	1.2821
0.6255	0.1911	1.0932	1.0662	1.2984	1.3427	1.3202	1.3372
0.1196	0.1844	1.4441	1.5405	1.2668	1.2736	1.1083	1.0444
0.2179	0.1693	1.3662	1.3733	1.3003	1.2594	1.1691	1.0799
0.3040	0.1453	1.3062	1.2698	1.3208	1.2743	1.1344	1.1157
0.3990	0.1262	1.2450	1.1829	1.3700	1.3039	1.1360	1.1643
0.5027	0.1066	1.1722	1.1147	1.3501	1.3551	1.2257	1.2250
0.6051	0.0814	1.1218	1.0675	1.2936	1.4308	1.2030	1.2909
0.6761	0.0661	1.0842	1.0436	1.3338	1.4935	1.3593	1.3415
0.2127	0.2388	1.3450	1.3563	1.2747	1.2134	1.2755	1.0987
0.2782	0.2101	1.3054	1.2834	1.2623	1.2288	1.1570	1.1219
0.3574	0.1910	1.2496	1.2093	1.2555	1.2488	1.1846	1.1594
0.4228	0.1732	1.2171	1.1608	1.3037	1.2755	1.1359	1.1929
0.4867	0.1575	1.1725	1.1220	1.3268	1.3077	1.1585	1.2288

(. . . continuation. . .) Table 5-5

		γ_1		γ_2		γ_3	
x_1	x_2	Expt.	Calc.	Expt.	Calc.	Expt.	Calc.
0.5535	0.1371	1.1352	1.0891	1.3198	1.3523	1.1586	1.2679
0.6587	0.1056	1.0860	1.0498	1.4543	1.4399	1.2901	1.3361
0.1143	0.2456	1.3900	1.5139	1.2833	1.2315	1.1602	1.0589
0.1973	0.2218	1.3466	1.3838	1.3003	1.2263	1.1447	1.0860
0.2770	0.2060	1.3135	1.2856	1.3481	1.2315	1.1526	1.1199
0.3526	0.1827	1.2586	1.2145	1.2492	1.2537	1.0747	1.1538
0.4588	0.1571	1.1909	1.1382	1.3602	1.2981	1.1821	1.2105
0.5518	0.1281	1.1372	1.0897	1.5047	1.3591	1.2990	1.2642

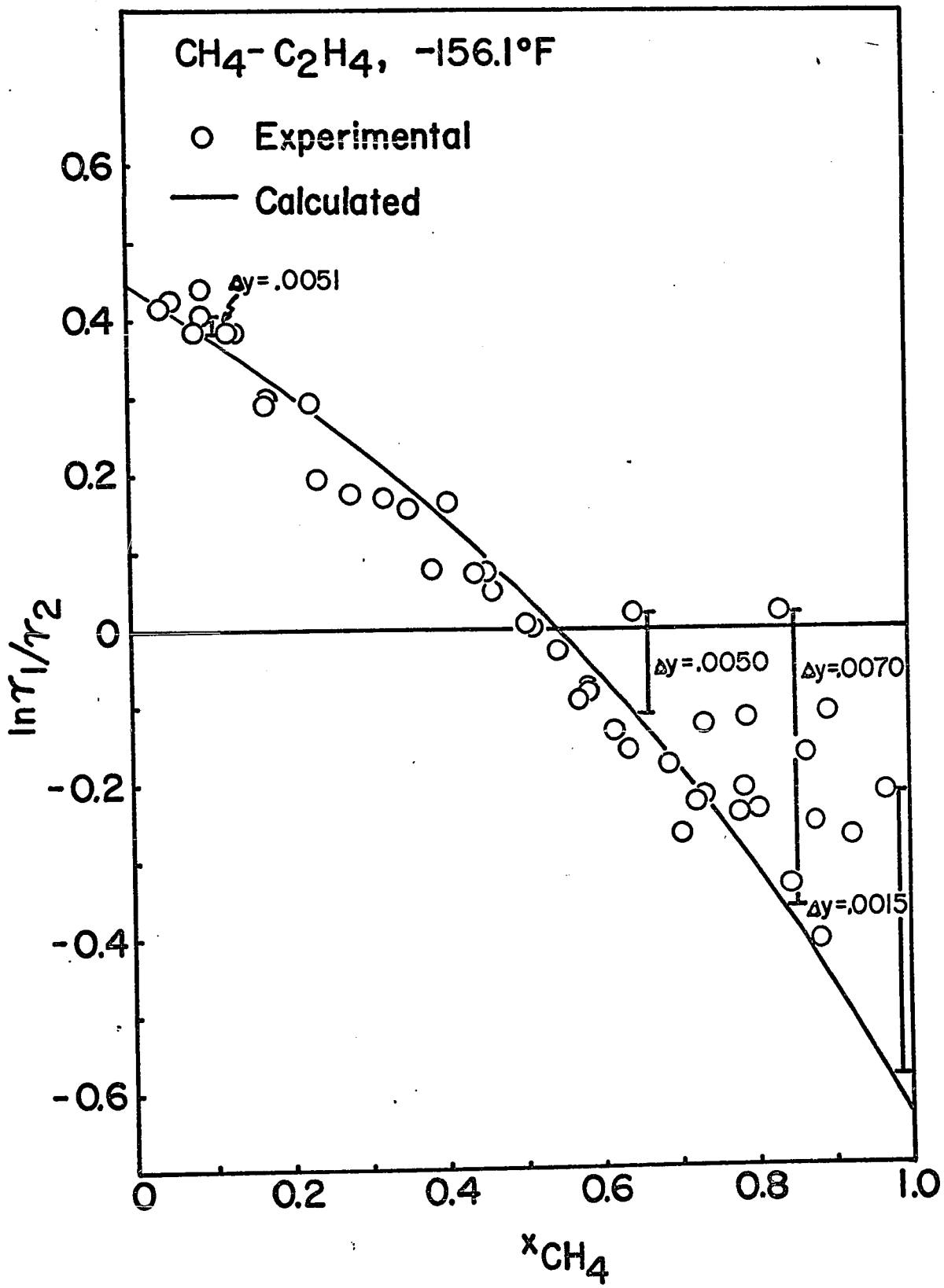

Figure 5-5 Area-test for the Methane-Ethylene System at -156.1° F

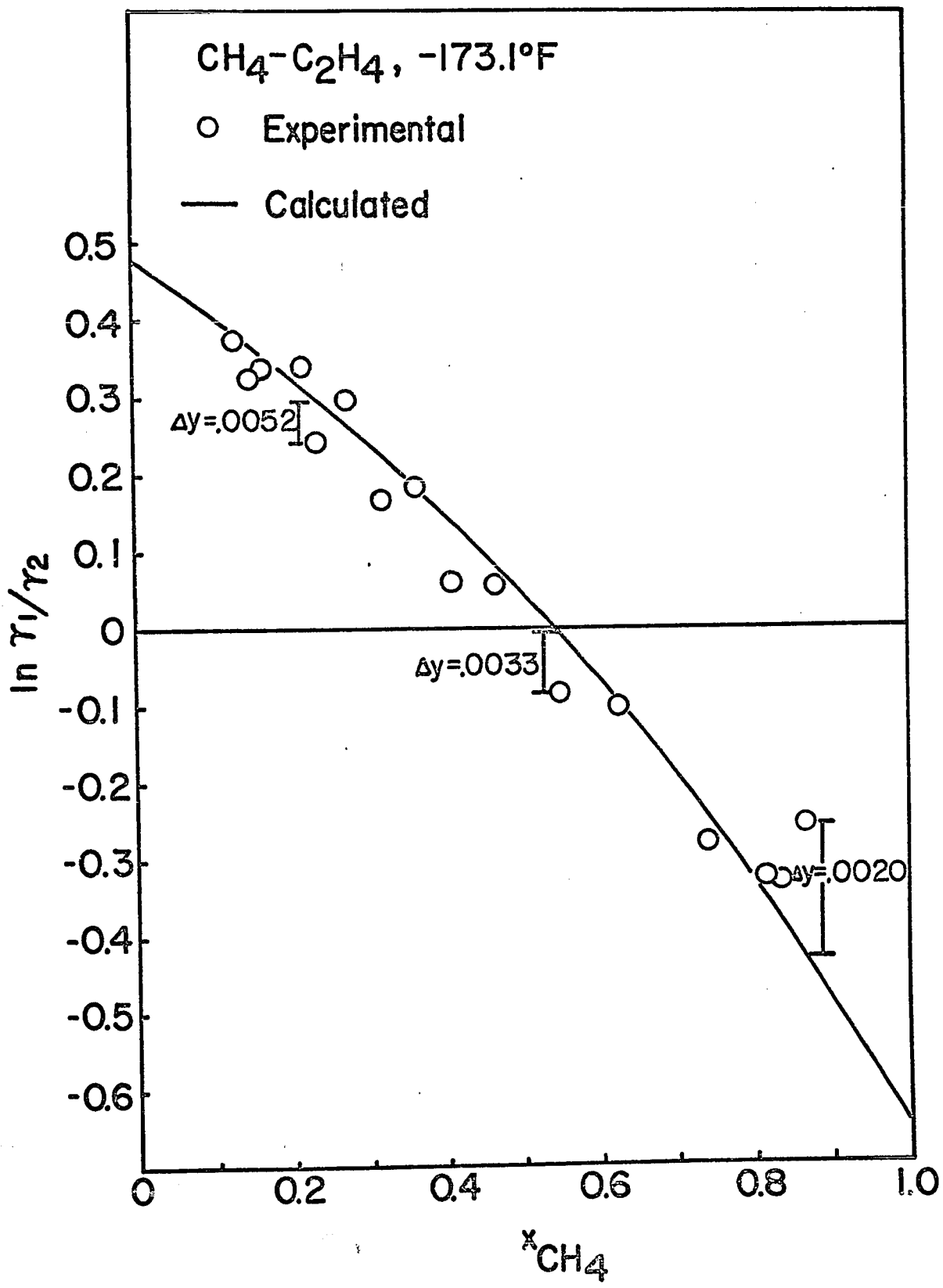

Figure 5-6 Area-test for the Methane-Ethylene System at -173.1° F

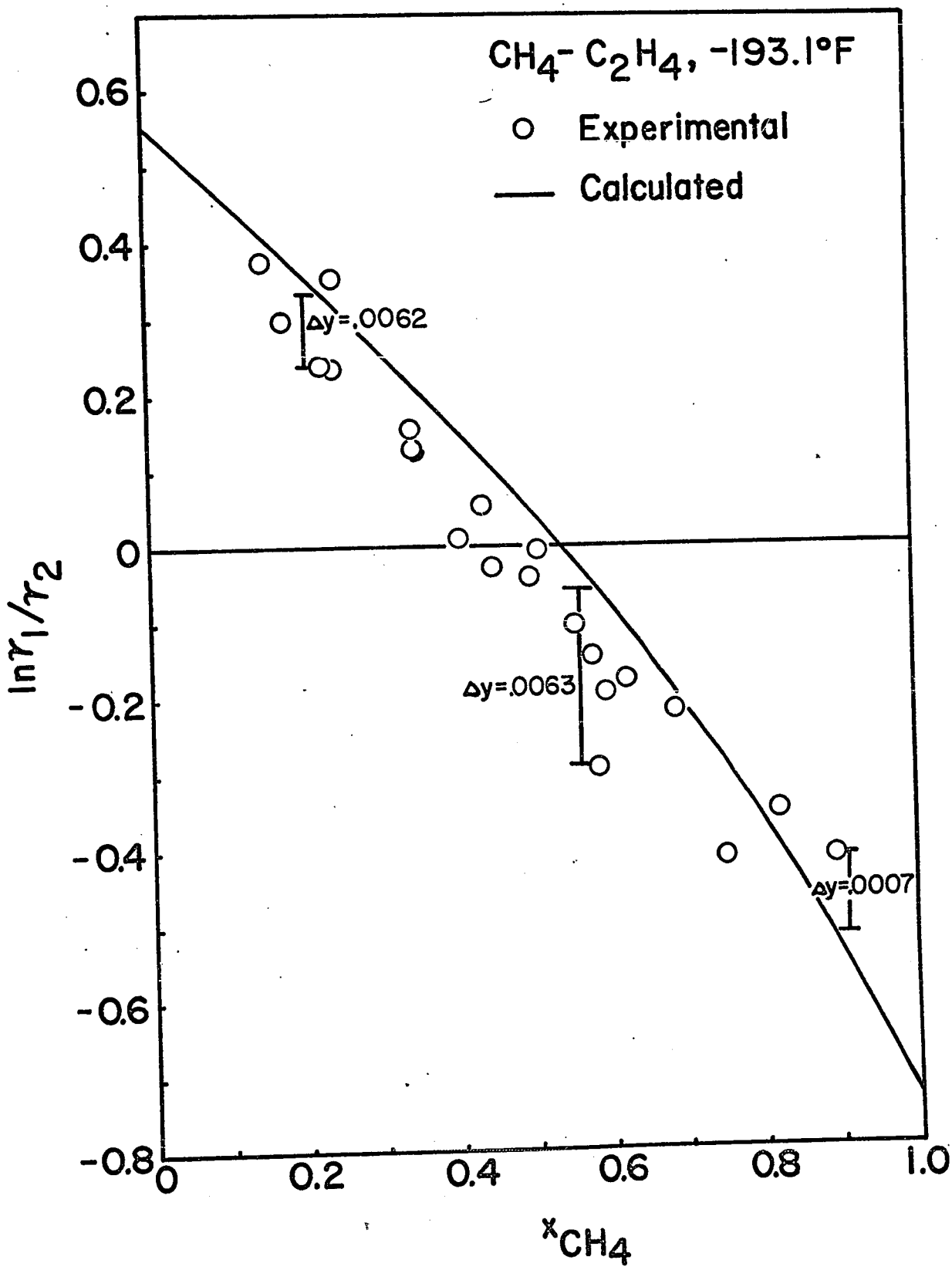

Figure 5-7 Area-test for the Methane-Ethylene System at -193.1° F

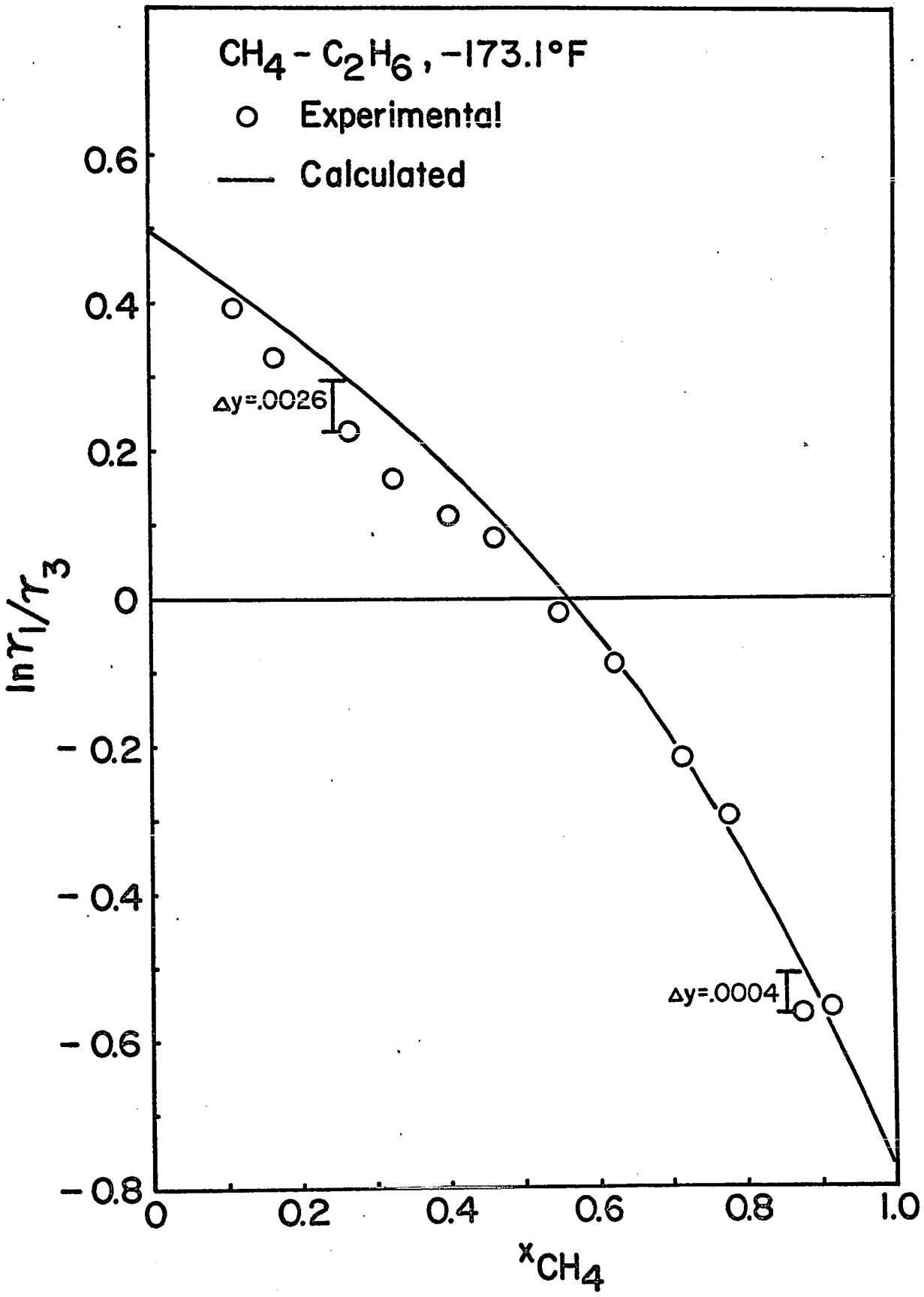

Figure 5-8 Area-test for the Methane-Ethane System at -173.1° F

The super-sensitivity of the γ-value of the less volatile component may be attributed to the major effect of vapor phase composition on the vapor phase fugacity. The average absolute deviations between the experimental γ-values and the values predicted by the modified Redlich-Kwong equation of state are given below:

System	Average Absolute Deviation $\Delta\gamma_1$	$\Delta\gamma_2$	$\Delta\gamma_3$
Methane (1) - ethylene (2)			
-193.1° F	0.0099	0.1075	
-173.1° F	0.0070	0.0525	
-156.1° F	0.0082	0.1004	
Methane (1) - ethane (3)			
-173.1° F	0.0109		0.0495
Methane (1) - ethylene (2) - ethane (3)			
-173.1° F	0.0348	0.0573	0.0673

It should be mentioned that in the comparison, the experimental point discussed above for the binary system methane-ethylene at -193.1° F was not included. The agreement obtained between the experimental and the calculated values is indeed satisfactory.

The limiting values of the activity coefficient are temperature-dependent. They increase with decreasing temperatures as shown in Table 5-2.

Available literature data[58, 59] for the methane-ethylene binary system in the temperature range from -88.56° to -146.06° C have been further examined. The calculated values of the activity coefficient are

listed in Table 5-6. The $\ln \gamma_1/\gamma_2$ vs. x_1 plot is shown in Figure 5-9, the result of the area test[65] indicates that the literature data[58, 59] are not consistent.

Calculated Values of y and ln γ for the System Methane (1) -Ethylene (2) from the Literature Data

Literature Data				Calculated			
T, °C	P, atm.	x_1	y_1	y_1	$\ln \gamma_1$	$\ln \gamma_2$	$\ln \gamma_1/\gamma_2$
- 88.56[58]	5.00	0.058	0.400	0.4841	0.3514	0.2798	0.0716
	6.00	0.079	0.550	0.5603	0.5294	0.1745	0.3549
	8.00	0.132	0.690	0.6806	0.5065	0.1028	0.4037
	10.00	0.185	0.779	0.7495	0.4897	0.0048	0.4849
	12.70	0.260	0.827	0.8090	0.4172	0.0295	0.3877
	15.00	0.325	0.850	0.8424	0.3613	0.0865	0.2748
	17.90	0.408	0.875	0.8724	0.3052	0.1358	0.1694
	20.00	0.470	0.890	0.8895	0.2662	0.1722	0.0940
	22.00	0.525	0.905	0.9019	0.2427	0.1747	0.0680
	24.00	0.585	0.915	0.9141	0.2074	0.2263	-0.0189
	25.00	0.617	0.925	0.9202	0.1928	0.1939	-0.0011
	26.00	0.654	0.925	0.9271	0.1611	0.3012	-0.1401
	30.00	0.774	0.958	0.9478	0.1163	0.1679	-0.0516
	33.00	0.868	0.976	0.9655	0.0725	0.1389	-0.0664
	35.00	0.927	0.982	0.9787	0.0415	0.4266	-0.3851
-104.00[58]	2.00	0.040	0.485	0.5046	0.3941	0.0576	0.3365
	5.00	0.155	0.735	0.7990	0.3316	0.3509	-0.0193
	7.00	0.226	0.812	0.8535	0.3634	0.3747	-0.0113
	9.00	0.310	0.872	0.8905	0.3423	0.2993	0.0430
	10.00	0.347	0.880	0.9017	0.3303	0.3645	-0.0342
	12.80	0.474	0.924	0.9297	0.2745	0.2861	-0.0116
	15.00	0.557	0.942	0.9422	0.2592	0.2752	-0.0160
	17.00	0.650	0.950	0.9543	0.2090	0.4179	-0.2089
	20.00	0.800	0.982	0.9721	0.1509	0.0144	0.1365
-146.06[59]	0.61	0.090	0.802	0.9419	0.6337	1.4566	-0.8229
	0.76	0.115	0.86[illegible]	0.9538	0.6784	1.3120	-0.6336
	0.88	0.130	0.889	0.9588	0.7281	1.2751	-0.5470
	0.98	0.160	0.900	0.9662	0.6380	1.3082	-0.6702

TABLE 5-6 ..... continued.....)

Literature Data				Calculated			
T, °C	P, atm	x_1	y_1	y_1	$\ln \gamma_1$	$\ln \gamma_2$	$\ln \gamma_1/\gamma_2$
-146.06[59]	1.21	0.200	0.935	0.9727	0.6582	1.1254	-0.4672
	1.44	0.230	0.940	0.9761	0.6913	1.2446	-0.5533
	1.93	0.340	0.976	0.9838	0.6199	0.7509	-0.1310
	2.16	0.420	0.980	0.9870	0.5187	0.7966	-0.2779
	2.63	0.600	0.990	0.9917	0.3588	0.6461	-0.2873
	2.88	0.775	0.995	0.9950	0.1932	0.6029	-0.4097

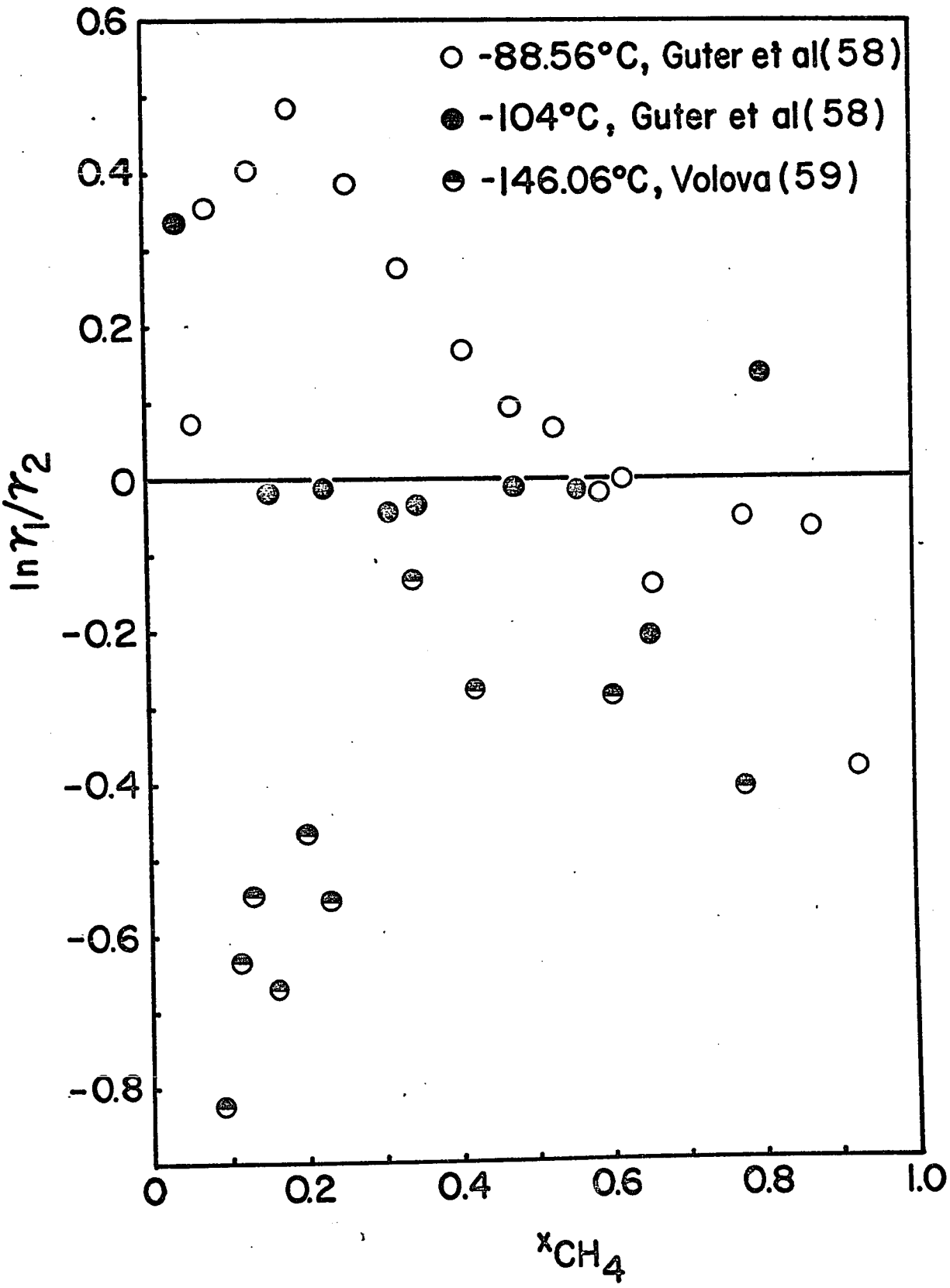

Figure 5-9 ln γ_1/γ_2 vs. x_1 Plot for the Literature Data

CHAPTER VI

PREDICTION OF GAS SOLUBILITIES AND PHASE EQUILIBRIA OF NORMAL FLUID MIXTURES WITH ONE SUPERCRITICAL COMPONENT

As discussed and demonstrated in the previous chapters, the modified version of the Redlich-Kwong equation of state was successfully employed for the prediction and correlation of vapor-liquid equilibria. However, the application of this method is restricted to the situation when all components are in the subcritical region.

The purpose of the present work is to develop a method for the evaluation of the temperature-dependent parameters of the pure component when it is in the supercritical region, so that the modified Redlich-Kwong equation of state can be applied to the prediction of gas solubilities, volumetric properties and phase equilibria of normal fluid mixtures involving one supercritical component.

6.1 FURTHER MODIFICATION OF THE REDLICH-KWONG EQUATION OF STATE

When a pure component is in its supercritical state, saturated liquid properties do not exist. The method proposed by Chang and Lu[5] for evaluating Ω_a and Ω_b for pure component at subcritical conditions cannot be used. Hence, further modification is required.

In the present investigation, it is proposed that values of Ω_a and Ω_b for a supercritical component be evaluated by means of existing binary mixture properties. It is assumed that these obtained values are unique for the component concerned. Therefore, the Ω_a and Ω_b values of a supercritical component A obtained from the properties of the A-B binary can be used for predicting the desired properties for the A-C, A-D, ... systems, the mixing rules used here were identical to those employed in the previous chapters.

The iteration procedure used in the evaluation may be described as follows:

(1) Assuming a value of Ω_b, the available binary properties, such as vapor-liquid equilibrium data, gas solubilities, or saturated liquid molal volumes, are processed through the Equations (3-7) to (3-10) and (3-13) to (3-22) so that a corresponding value of Ω_a may be found to give a minimum deviation between the calculated and the observed value.

(2) Using this obtained value of Ω_a, the same properties are reprocessed in the same manner so that a corresponding value of Ω_b may be obtained to give a minimum deviation between the calculated and the observed value.

(3) Repeat the iteration until the deviation is within the permissible or the estimated experimental error. The final set of Ω_a and Ω_b values are therefore obtained.

It has been observed in this investigation that the parameter Ω_b is less temperature dependent in the vicinity of the critical point.

For this reason, the iteration procedure begins with Ω_b. Its value at the critical point is employed as the initial value.

Based on the proposed procedure the temperature-dependent parameters, Ω_a and Ω_b, were evaluated for the pure component methane from its critical temperature -115.78° F up to 160° F. The vapor-liquid equilibrium data of the methane-propane system[54, 69] were used for determining the Ω_a and Ω_b values of methane in the supercritical region. The values obtained are listed below:

Temperature, °F	Ω_a	Ω_b
-100	0.43444	0.08584
- 50	0.43560	0.08576
0	0.43144	0.08420
50	0.42584	0.08359
100	0.42081	0.08295
130	0.41803	0.08277
160	0.41439	0.08252

The values are also plotted in Figure 6-1 to show the trend of the temperature dependence.

6.2 PREDICTION OF GAS SOLUBILITIES

In this study, the gas solubility is expressed as the mole fraction of the gaseous component in the liquid mixture at its partial pressure of 1 atm. and at the system temperature. The solubility of a gas in a liquid is determined by the equations of phase equilibria as well. If a gaseous phase and a liquid phase are in equilibrium,

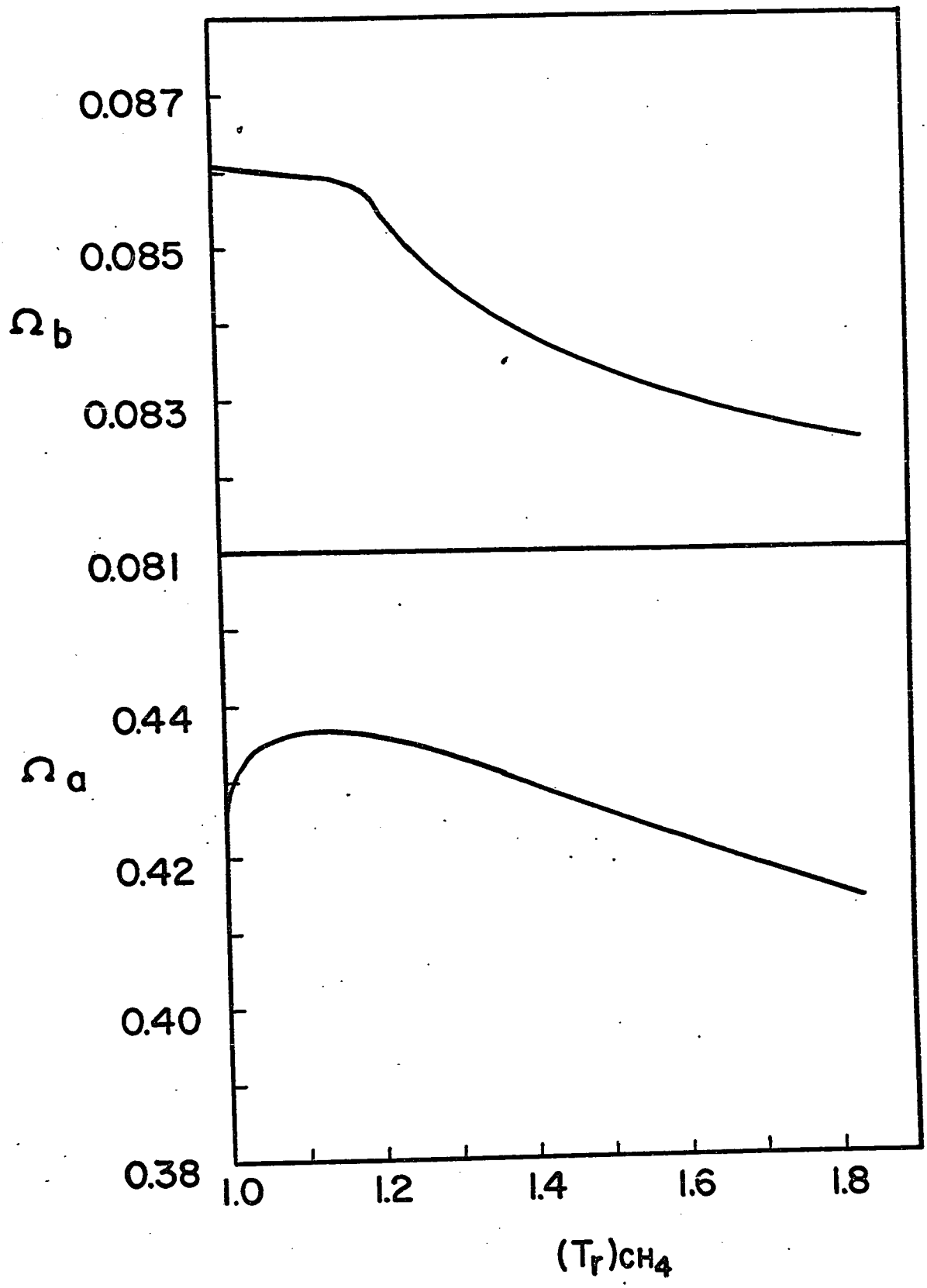

Figure 6-1 Temperature Dependent Characteristics of Ω_a and Ω_b of Methane in the Supercritical Region

then for any component i the fugacities in both phases must be the same:

$$\hat{f}_i^{gas} = \hat{f}_i^{liquid} \tag{6-1}$$

Hence, the method employed for the prediction of gas solubilities is essentially identical to that for vapor-liquid equilibria, provided that the temperature-dependent parameters, Ω_a and Ω_b, of the Redlich-Kwong equation of state of the gaseous component are available. In the calculation, the value of gas solubility is the interpolated mole fraction of the gaseous component in the liquid phase at the partial pressure of 1 atm. The partial pressure is defined by the following equation:

$$p_i = P\, y_i \tag{6-2}$$

In order to test the validity of the proposed method, the solubilities of methane in n-hexane, cyclohexane, benzene and carbon tetrachloride were then predicted and compared with the experimental values reported by Lannung and Gjaldbaek[70]. The reported experimental values are expressed in terms of the Bunsen absorption coefficient, α, i.e. the number of ml. of the gas reduced to 0°C and 1 atm. which can be dissolved in 1 ml. solvent at the temperature concerned when the partial pressure of the gas is 1 atm.[71]. The Bunsen absorption coefficients have been converted into the mole fractions by means of the following equation in order to facilitate the comparison.

$$x = \frac{\alpha/22,360.4}{(\alpha/22,360.4) + (1/V_{solvent})} \tag{6-3}$$

where the molal volume of methane at 0° C and 1 atm., 22, 360. 4 ml./ g. mole, is taken from the compilation of Din[61]. The comparison is made in Table 6-1. The agreement obtained is indeed satisfactory.

6. 3 PREDICTION OF PHASE EQUILIBRIA WITH ONE SUPERCRITICAL COMPONENT

Following the approach employed in Chapter III, the total pressure and vapor-phase compositions were predicted by using the established Ω_a and Ω_b values of methane for the following systems:

(1) Methane - n-butane: The vapor-liquid equilibrium data for the system methane-n-butane at 70° and 100° F were predicted and compared with the experimental values[72, 73]. The comparison is made in Figures 6-2 and 6-3, and also listed in Tables 6-2 and 6-3.

(2) Methane - n-pentane: The predicted vapor-liquid equilibrium data of the methane-n-pentane system at 100° F were compared with the experimental data reported by Sage, Reamer, Olds and Lacey[74] in Figure 6-4 and Table 6-4.

(3) Methane - n-hexane: The vapor-phase compositions and saturation pressures of the methane-n-hexane system at 25° C were predicted and compared with the experimental data of Shim and Kohn[75] in Figure 6-5 and Table 6-5.

(4) Methane - n-heptane: The comparison between the predicted and experimental[76] vapor-liquid equilibrium data for the system methane-n-heptane at 40° F is given in Figure 6-6 and Table 6-6.

(5) Methane - hydrogen sulfide: The methane-hydrogen sulfide system at 40° F was taken as an example of a methane-nonhydrocarbon

TABLE 6 - 1

Comparison of Calculated and Experimental Results for the Solubility of Methane (1) in Various Solvents

Solvent	T, °C	k_{ij}	Solubility, $x_1 \times 10^4$		Deviation, %
			Expt.[70]	Calc.	
n-Hexane	18	0.0623	51.31	52.82	2.94
	25		50.8	50.92	0.24
	37		48.61	48.37	-0.49
Cyclohexane	18	0.0720	33.69	33.63	-0.18
	25		33.7	33.67	-0.09
	37		31.18	31.31	0.42
Benzene	18	0.0760	21.16	21.22	0.28
	25		20.9	20.88	-0.09
	37		20.65	20.43	-1.06
Carbon-tetrachloride	25	0.0603	28.6	28.64	-0.14

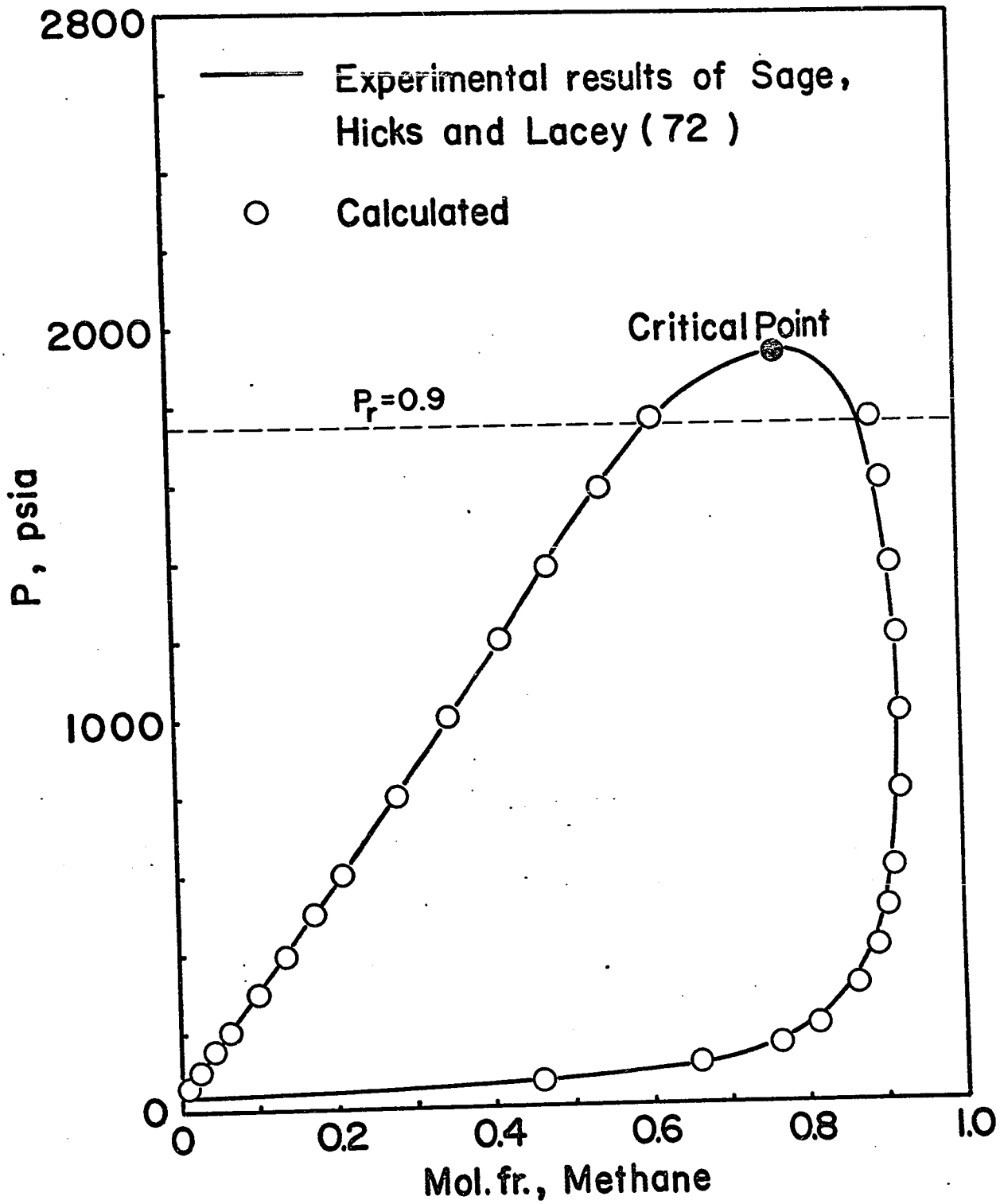

Figure 6-2 Comparison of Calculated and Experimental Vapor-Liquid Equilibria of the Methane-n-Butane System at 70°F

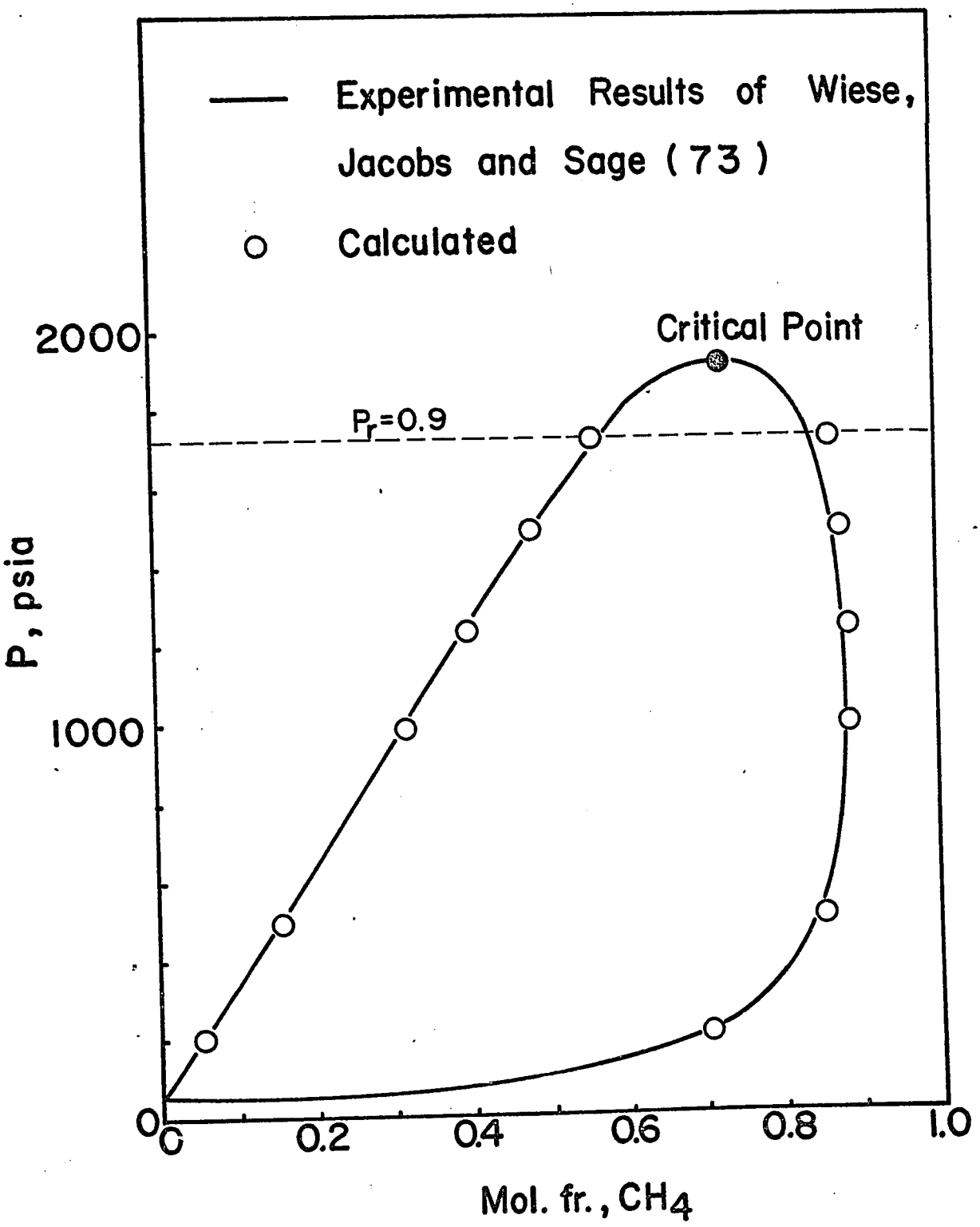

Figure 6-3 Comparison of Calculated and Experimental Vapor-Liquid Equilibria of the Methane-n-Butane System at 100° F

TABLE 6 - 2

Comparison of Calculated and Experimental Results for the System Methane (1) - n-Butane (2) at 70° F

$k_{ij} = 0.0398$

x_1	P, psia		y_1		Deviation	
	Expt.[72]	Calc.	Expt.[72]	Calc.	ΔP	Δy_1
0	31.30	31.30	0	0	0	0
0.0036	40	40.58	0.2103	0.2178	- 0.58	-0.0075
0.0111	60	59.98	0.4593	0.4586	0.02	-0.0007
0.0186	80	79.24	0.5843	0.5823	0.76	0.0020
0.0263	100	99.25	0.6600	0.6603	0.75	-0.0003
0.0452	150	148.66	0.7591	0.7633	1.34	-0.0042
0.0639	200	198.00	0.8088	0.8147	2.00	-0.0059
0.1011	300	297.38	0.8587	0.8658	2.62	-0.0071
0.1379	400	397.47	0.8831	0.8906	2.53	-0.0075
0.1744	500	498.41	0.8978	0.9048	1.59	-0.0070
0.2106	600	600.08	0.9074	0.9134	- 0.08	-0.0060
0.2804	800	800.29	0.9174	0.9218	- 0.29	-0.0044
0.3490	1000	1001.46	0.9202	0.9238	- 1.46	-0.0036
0.4162	1200	1201.21	0.9178	0.9217	- 1.21	-0.0039
0.4305	1250	1243.88	0.9162	0.9207	6.21	-0.0045
0.4775	1400	1383.56	0.9087	0.9163	16.44	-0.0076
0.5100	1500	1479.18	0.9026	0.9121	20.82	-0.0095
0.5450	1600	1580.41	0.8942	0.9063	19.59	-0.0121
0.5863	1700	1695.85	0.8827	0.8976	4.15	-0.0149
0.6105	1750	1760.52	0.8750	0.8913	-10.52	-0.0163
0.6375	1800	1829.31	0.8652	0.8831	-29.31	-0.0179
0.6700	1850	1905.29	0.8511	0.8716	-55.29	-0.0205
0.7152	1900	1993.03	0.8253	0.8524	-93.03	-0.0271
0.7712	1923	1992.34	0.7712	0.8576	-69.34	-0.0864

TABLE 6 - 3

Comparison of Calculated and Experimental Results for the System Methane (1) - n-Butane (2) at 100° F

$k_{ij} = 0.0398$

	P, psia		y_1		Deviation	
x_1	Expt.[73]	Calc.	Expt.[73]	Calc.	ΔP	Δy_1
0.0530	200	200.21	0.7027	0.7040	- 0.21	-0.0013
0.1556	500	497.86	0.8473	0.8503	2.14	-0.0030
0.3171	1000	989.06	0.8809	0.8871	10.94	-0.0062
0.3974	1250	1238.85	0.8786	0.8868	11.15	-0.0082
0.4799	1500	1492.54	0.8665	0.8787	7.46	-0.0122
0.5586	1700	1721.99	0.8440	0.8630	-21.99	-0.0190
0.7236	1912	2003.69	0.7236	0.8357	-91.69	-0.1121

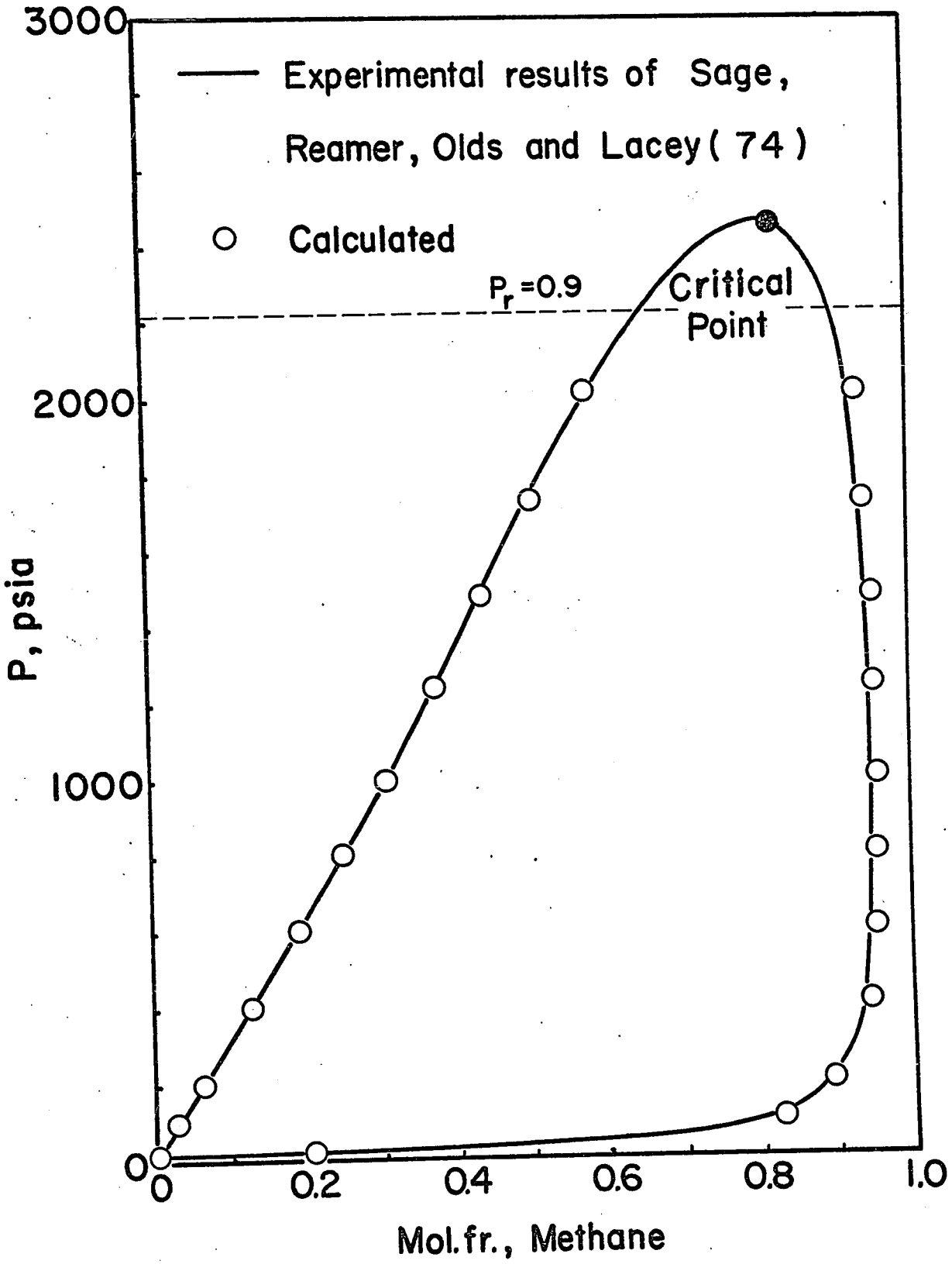

Figure 6-4 Comparison of Calculated and Experimental Vapor-Liquid Equilibria of the Methane-n-Pentane System at 100° F

TABLE 6 - 4

Comparison of Calculated and Experimental Results for the System Methane (1) - n-Pentane (2) at 100° F

$k_{ij} = 0.0474$

	P, psia		y_1		Deviation	
x_1	Expt.[74]	Calc.	Expt.[74]	Calc.	ΔP	Δy_1
0	15.69	15.69	0	0	0	0
0.0015	20	19.95	0.2090	0.2070	0.05	0.0020
0.0085	40	40.30	0.5893	0.5966	- 0.30	-0.0073
0.0154	60	60.13	0.7160	0.7239	- 0.13	-0.0079
0.0221	80	79.63	0.7797	0.7874	0.37	-0.0077
0.0288	100	99.48	0.8178	0.8265	0.52	-0.0087
0.0458	150	149.53	0.8696	0.8790	0.47	-0.0094
0.0625	200	199.52	0.8940	0.9049	0.48	-0.0109
0.0957	300	300.30	0.9195	0.9305	- 0.30	-0.0110
0.1288	400	402.98	0.9323	0.9429	- 2.98	-0.0106
0.1911	600	602.87	0.9430	0.9536	- 2.87	-0.0106
0.2508	800	802.41	0.9460	0.9574	- 2.41	-0.0114
0.3077	1000	999.87	0.9470	0.9582	0.13	-0.0112
0.3748	1250	1241.45	0.9460	0.9564	8.55	-0.0104
0.4390	1500	1480.50	0.9410	0.9524	19.50	-0.0114
0.5041	1750	1728.23	0.9330	0.9457	21.77	-0.0127
0.5788	2000	2013.39	0.9204	0.9337	- 13.39	-0.0133
0.6770	2250	2365.39	0.8972	0.9074	-115.39	-0.0102
0.8236	2455	2411.44	0.8236	0.8986	43.56	-0.0750

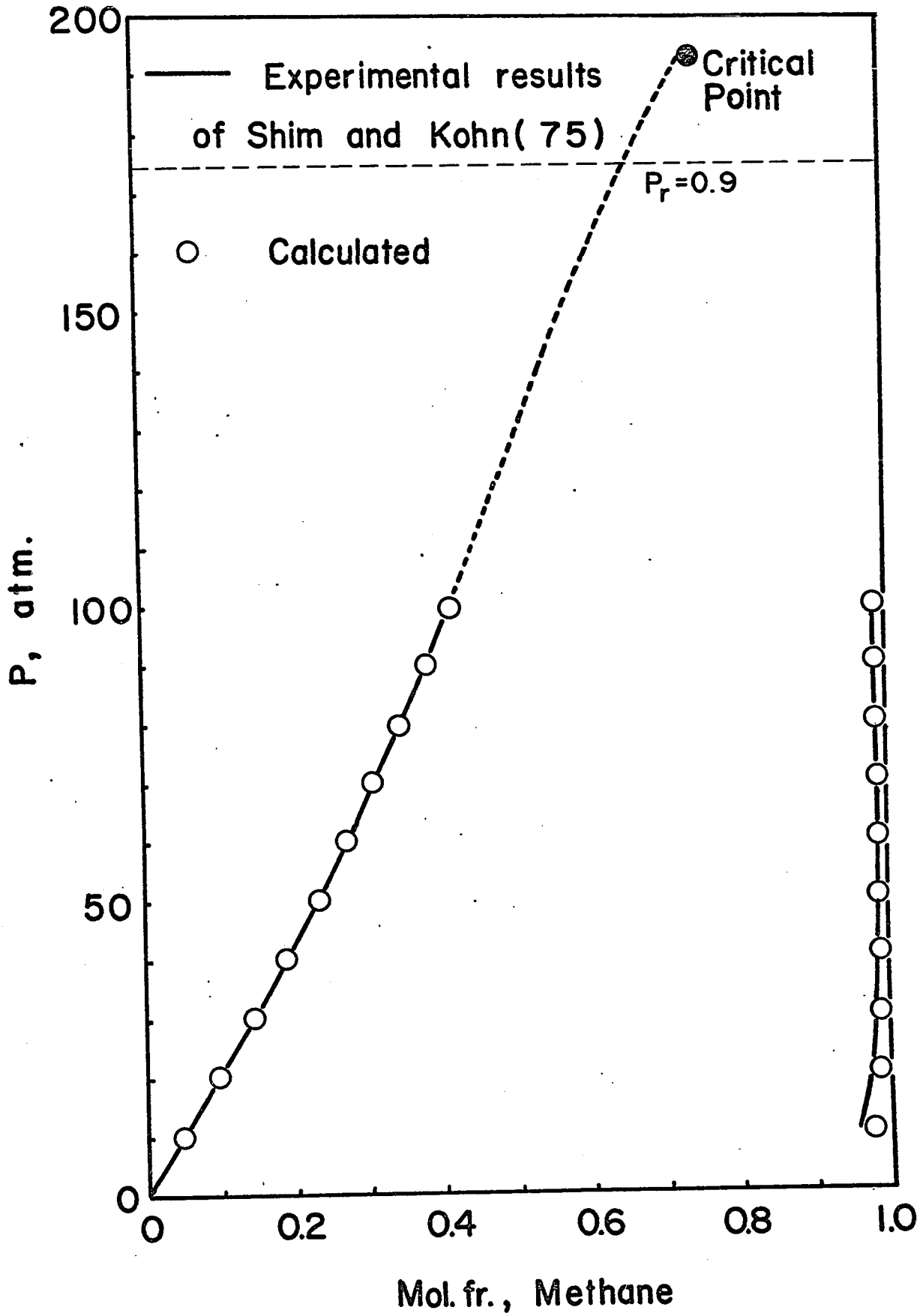

Figure 6-5 Comparison of Calculated and Experimental Vapor-Liquid Equilibria of the Methane-n-Hexane System at 25°C

TABLE 6 - 5

Comparison of Calculated and Experimental Results for the System Methane (1) - n-Hexane (2) at 25°C

$k_{ij} = 0.0623$

	P, atm		y_1		Deviation	
x_1	Expt.[75]	Calc.	Expt.[75]	Calc.	ΔP	Δy_1
0	0.1980	0.1980	0	0	0	0
0.0490	10	10.05	0.9530	0.9762	- 0.05	-0.0232
0.0978	20	20.29	0.9728	0.9857	- 0.29	-0.0129
0.1450	30	30.64	0.9795	0.9885	- 0.64	-0.0090
0.1890	40	40.70	0.9830	0.9894	- 0.70	-0.0064
0.2316	50	50.85	0.9850	0.9897	- 0.85	-0.0047
0.2710	60	60.62	0.9863	0.9895	- 0.62	-0.0032
0.3090	70	70.41	0.9871	0.9889	- 0.41	-0.0018
0.3447	80	79.96	0.9868	0.9881	0.04	-0.0013
0.3810	90	90.01	0.9854	0.9870	- 0.01	-0.0016
0.4125	100	99.04	0.9833	0.9858	0.96	-0.0025
0.4740	120	117.47		0.9823	2.53	
0.5370	140	137.42		0.9769	2.58	
0.6090	160	161.25		0.9673	- 1.25	
0.7446	193.6	205.61	0.7466	0.9306	-12.01	-0.1840

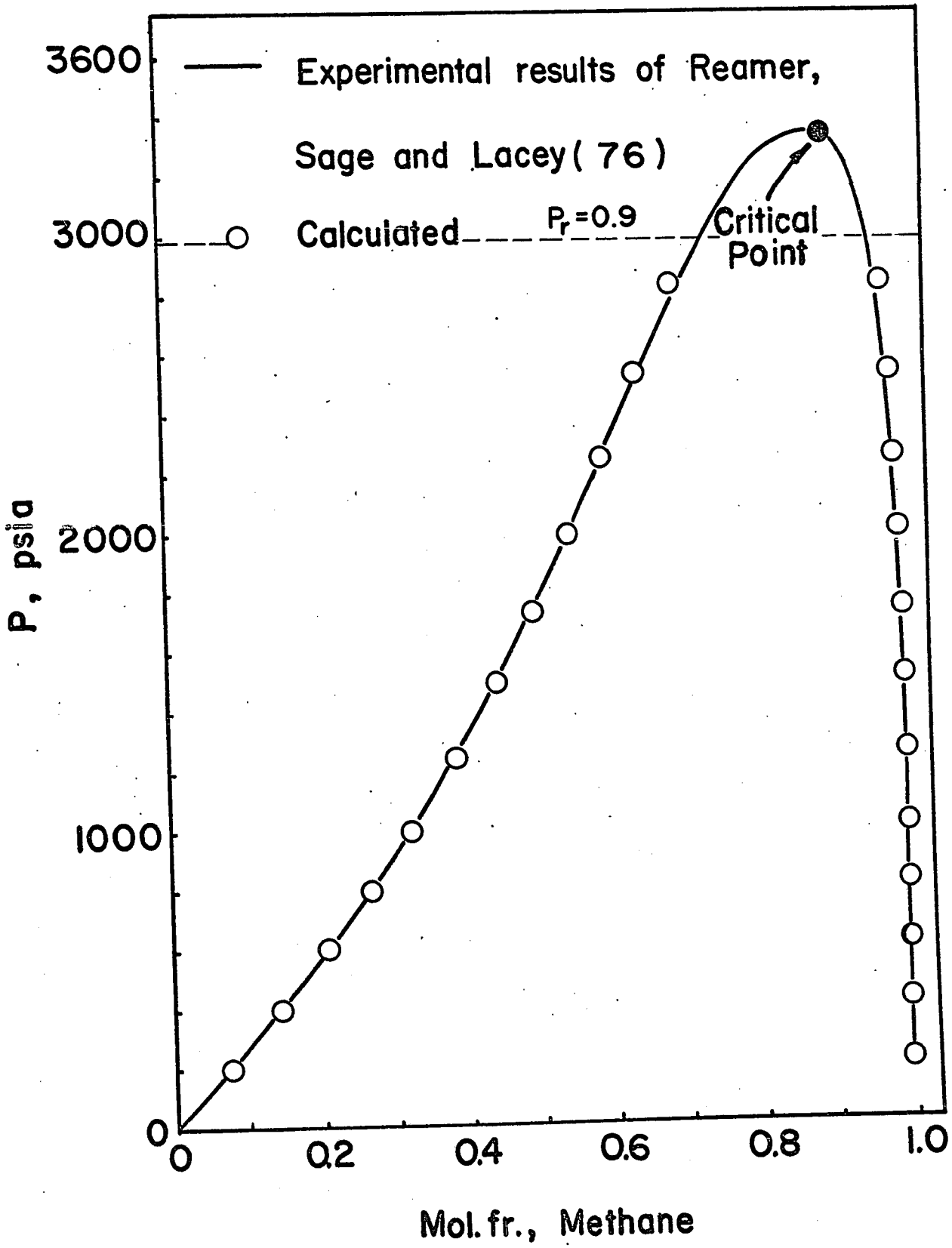

Figure 6-6 Comparison of Calculated and Experimental Vapor-Liquid Equilibria of the Methane-n-Heptane System at 40° F

TABLE 6 - 6

Comparison of Calculated and Experimental Results for the System Methane (1) - n-Heptane (2) at 40° F

$k_{ij} = 0.0705$

x_1	P, psia		y_1		Deviation	
	Expt.[76]	Calc.	Expt.[76]	Calc.	ΔP	Δy_1
0	0.3248	0.3248	0	0	0	0
0.0753	200	202.41	0.9964	0.9977	-1.20	-0.0013
0.1445	400	402.70	0.9974	0.9983	-0.67	-0.0009
0.2084	600	602.10	0.9971	0.9983	-0.35	-0.0012
0.2670	800	799.14	0.9970	0.9982	0.10	-0.0012
0.3215	1000	996.54	0.9966	0.9978	0.34	-0.0012
0.3840	1250	1242.50	0.9957	0.9971	0.60	-0.0014
0.4410	1500	1488.24	0.9940	0.9960	0.78	-0.0020
0.4930	1750	1732.97	0.9920	0.9943	0.97	-0.0023
0.5425	2000	1986.29	0.9890	0.9918	0.68	-0.0028
0.5900	2250	2248.77	0.9850	0.9881	0.05	-0.0031
0.6373	2500	2528.21	0.9780	0.9826	-1.12	-0.0046
0.6870	2750	2836.25	0.9690	0.9743	-3.13	-0.0053
0.7400	3000	3168.23	0.9530	0.9612	-5.60	-0.0082
0.8940	3328	3339.22	0.8940	0.9481	-0.33	-0.0541

system to test the proposed method. The predicted vapor-liquid equilibrium data were compared with the observed data[77] in Figure 6-7 and Table 6-7.

(6) Methane - ethane - propane: The vapor-liquid equilibrium data of the ternary system methane-ethane-propane were predicted and compared with the experimental data[54] for five temperatures from -150° to 50°F. The results are listed in Table 6-8.

(7) Methane - propane - n-butane: The predicted vapor-liquid equilibrium data of the methane-propane-n-butane ternary system at 40°F were compared with the observed data[73] and the results are shown in Table 6-9.

(8) Methane - propane - n-pentane: The vapor-liquid equilibrium data of the methane-propane-n-pentane system at 100° and 160°F were predicted and compared with the observed data[78, 79]. The comparison is made in Table 6-10. The calculated and experimental K-values for each component are also compared in Figures 6-8 and 6-9 to show the good agreement obtained.

It may be seen that at $P_r < 0.9$, the agreement is good. The deviations increase as the critical points are approached. Comparisons shown in Figures 6-2 and 6-7 illustrate the agreement at $P_r < 0.9$ conditions.

6.4 PREDICTION OF VOLUMETRIC PROPERTIES

The volumetric properties such as saturated liquid molal volume and partial molal volumes of each component in liquid mixtures with one supercritical component should be predictable with the established

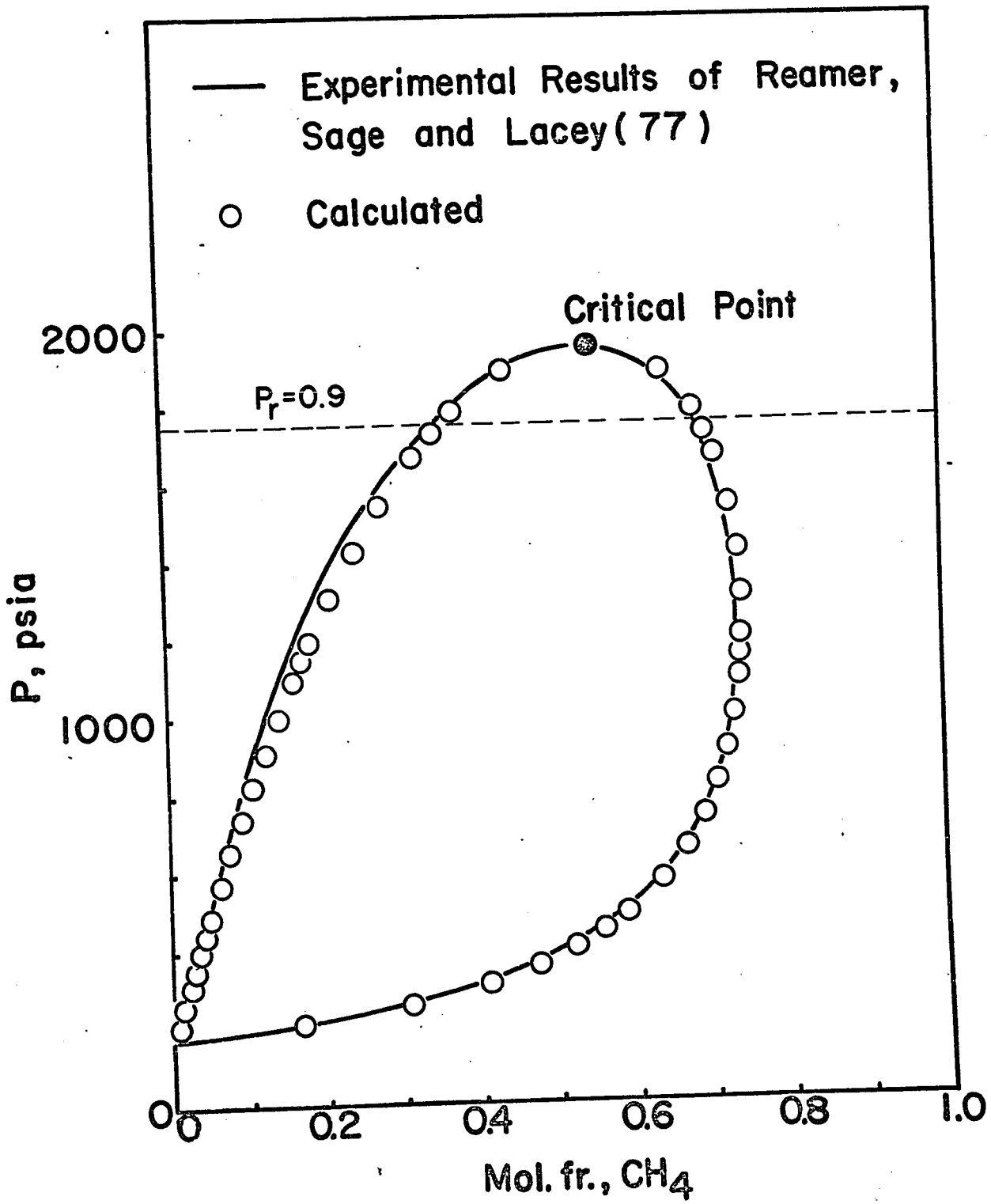

Figure 6-7 Comparison of Calculated and Experimental Vapor-Liquid Equilibria of the Methane-Hydrogen Sulfide System at 40° F

TABLE 6 - 7

Comparison of Calculated and Experimental Results for the System Methane (1) - Hydrogen Sulfide (2) at 40°F

$k_{ij} = 0.050$

	P, psia		y_1		Deviation	
x_1	Expt.[77]	Calc.	Expt.[77]	Calc.	ΔP	Δy_1
0.0057	200	207.38	0.1371	0.1661	- 7.38	-0.0290
0.0132	250	257.18	0.2783	0.3086	- 7.18	-0.0303
0.0212	300	309.44	0.3896	0.4090	- 9.44	-0.0194
0.0284	350	355.72	0.4604	0.4731	- 5.72	-0.0127
0.0354	400	400.04	0.5126	0.5204	- 0.04	-0.0078
0.0424	450	443.67	0.5551	0.5574	6.33	-0.0023
0.0493	500	486.03	0.5879	0.5868	13.97	0.0011
0.0636	600	571.76	0.6394	0.6321	28.24	0.0073
0.0783	700	656.97	0.6755	0.6643	43.03	0.0112
0.0930	800	739.33	0.6989	0.6874	60.67	0.0115
0.1083	900	821.98	0.7141	0.7047	78.02	0.0094
0.1250	1000	908.66	0.7242	0.7183	91.34	0.0059
0.1433	1100	999.46	0.7299	0.7285	100.54	0.0014
0.1635	1200	1094.65	0.7321	0.7357	105.35	-0.0036
0.1750	1250	1146.46	0.7319	0.7382	103.54	-0.0063
0.1868	1300	1197.94	0.7306	0.7398	102.06	-0.0092
0.2137	1400	1308.70	0.7262	0.7404	91.30	-0.0142
0.2450	1500	1426.27	0.7185	0.7365	73.73	-0.0180
0.2798	1600	1542.90	0.7075	0.7275	57.10	-0.0200
0.3240	1700	1669.98	0.6931	0.7097	30.02	-0.0166
0.3492	1750	1731.91	0.6828	0.6968	18.09	-0.0140
0.3758	1800	1789.29	0.6686	0.6811	10.71	-0.0125
0.4401	1900	1891.43	0.6130	0.6398	8.57	-0.0268
0.5500	1949	-	0.5500	-	-	-

TABLE 6 - 8

Comparison of Calculated and Experimental Results for the System Methane (1) - Ethane (2) - Propane (3)

$k_{12} = 0.007, \quad k_{13} = 0.019, \quad k_{23} = -0.015$

T, °F	x_1	x_2	P, psia		y_1		y_2	
			Expt.[54]	Calc.	Expt.[54]	Calc.	Expt.[54]	Calc.
50	0.0022	0.0088	100	100.06	0.0452	0.0433	0.028	0.0296
	0.027	0.160	200	198.85	0.275	0.2670	0.284	0.2928
	0.062	0.553	400	405.38	0.282	0.2792	0.570	0.5798
	0.204	0.178	600	604.08	0.654	0.6692	0.150	0.1455
	0.268	0.359	800	806.10	0.588	0.6126	0.282	0.2655
	0.389	0.169	1000	1012.50	0.707	0.7290	0.126	0.1185
	0.4365	0.0409	1100	1080.86	0.7746	0.7946	0.0306	0.0281
	0.4997	0.0375	1200	1210.59	0.7558	0.7908	0.0302	0.0265
0	0.0335	0.0174	100	100.78	0.5589	0.5681	0.0336	0.0342
	0.0917	0.0127	200	204.79	0.7717	0.7736	0.0133	0.0134
	0.1557	0.5293	400	408.76	0.6003	0.6030	0.343	0.3411
	0.272	0.481	600	608.87	0.6896	0.6984	0.260	0.2587
	0.380	0.5142	800	797.48	0.6795	0.6980	0.296	0.2784
	0.515	0.078	1000	990.71	0.8623	0.8760	0.0443	0.0392
	0.5759	0.0581	1100	1094.06	0.8619	0.8779	0.0341	0.0310
	0.653	0.106	1200	1207.59	0.8158	0.8385	0.0751	0.0681
- 50	0.0486	0.302	100	101.05	0.605	0.6198	0.292	0.2838
	0.125	0.268	200	201.25	0.804	0.8045	0.140	0.1413
	0.271	0.289	400	396.79	0.8791	0.8715	0.0907	0.0983
	0.441	0.366	600	609.44	0.8637	0.8679	0.119	0.1158
	0.611	0.249	800	804.92	0.8901	0.8893	0.0886	0.0918
	0.7609	0.0651	1000	989.65	0.9216	0.9265	0.0331	0.0313

(. . . continuation. . .) Table 6 - 8

T, °F	x_1	x_2	P, psia		y_1		y_2	
			Expt.[54]	Calc.	Expt.[54]	Calc.	Expt.[54]	Calc.
-100	0.110	0.320	100	106.84	0.8651	0.8841	0.110	0.0960
	0.235	0.121	200	211.19	0.9615	0.9636	0.0228	0.0217
	0.496	0.242	400	408.78	0.9562	0.9593	0.0364	0.0343
	0.745	0.052	600	580.31	0.9775	0.9822	0.0119	0.0091
-150	0.242	0.258	100	102.22	0.9686	0.9751	0.0282	0.0222
	0.514	0.208	200	194.51	0.9806	0.9864	0.0167	0.0123

TABLE 6 - 9

Comparison of Calculated and Experimental Results for the System Methane (1) - Propane (2) - n-Butane (3) at 40°F

$k_{12} = 0.019$, $k_{13} = 0.0398$, $k_{23} = 0.0$

x_1	x_2	P, psia		y_1		y_2	
		Expt.[73]	Calc.	Expt.[73]	Calc.	Expt.[73]	Calc.
0.0762	0.1848	200	205.61	0.8273	0.8271	0.0819	0.0873
0.0710	0.3716	200	202.02	0.7636	0.7581	0.1659	0.1744
0.0662	0.5603	200	199.96	0.6990	0.6914	0.2524	0.2609
0.0609	0.7513	200	197.80	0.6327	0.6244	0.3422	0.3500
0.1966	0.1601	500	502.24	0.9102	0.9103	0.0391	0.0423
0.2001	0.3200	500	503.33	0.8825	0.8825	0.0788	0.0838
0.1987	0.4804	500	500.69	0.8523	0.8478	0.1215	0.1258
0.1962	0.6431	500	497.27	0.8180	0.8160	0.1685	0.1698
0.3949	0.1210	1000	1001.43	0.9275	0.9284	0.0281	0.0292
0.4030	0.2388	1000	1003.15	0.9068	0.9068	0.0574	0.0590
0.4071	0.3557	1000	994.71	0.8835	0.8849	0.0904	0.0904
0.4119	0.4705	1000	988.95	0.8567	0.8619	0.1289	0.1244
0.4918	0.1016	1250	1256.49	0.9203	0.9240	0.0276	0.0281
0.5070	0.1972	1250	1263.45	0.9004	0.9025	0.0571	0.0577
0.5154	0.2908	1250	1251.11	0.8749	0.8806	0.0923	0.0899
0.5278	0.3778	1250	1246.57	0.8470	0.8564	0.1335	0.1267
0.5970	0.0806	1500	1527.58	0.9035	0.9099	0.0297	0.0290
0.6157	0.1537	1500	1523.41	0.8747	0.8859	0.0845	0.0612
0.6391	0.2165	1500	1520.19	0.8360	0.8583	0.1114	0.0993

TABLE 6 - 10

Comparison of Calculated and Experimental Results for the System Methane (1) - Propane (2) - n-Pentane (3)

$k_{12} = 0.019, \quad k_{13} = 0.0474, \quad k_{23} = 0.006$

T, °F	x_1	x_2	P, psia		y_1		y_2	
			Expt.[78, 79]	Calc.	Expt.[78, 79]	Calc.	Expt.[78, 79]	Calc.
100	0.152	0.170	500	498.80	0.866	0.8672	0.085	0.0889
	0.306	0.139	1000	997.21	0.901	0.9081	0.056	0.0545
	0.448	0.110	1500	1491.30	0.900	0.9105	0.049	0.0448
	0.606	0.079	2000	2047.39	0.871	0.8890	0.046	0.0418
160	0.124	0.175	500	506.12	0.743	0.7405	0.145	0.1505
	0.266	0.147	1000	996.74	0.826	0.8272	0.080	0.0888
	0.397	0.121	1500	1468.20	0.829	0.8426	0.068	0.0694
	0.546	0.091	2000	1991.33	0.789	0.8276	0.073	0.0593

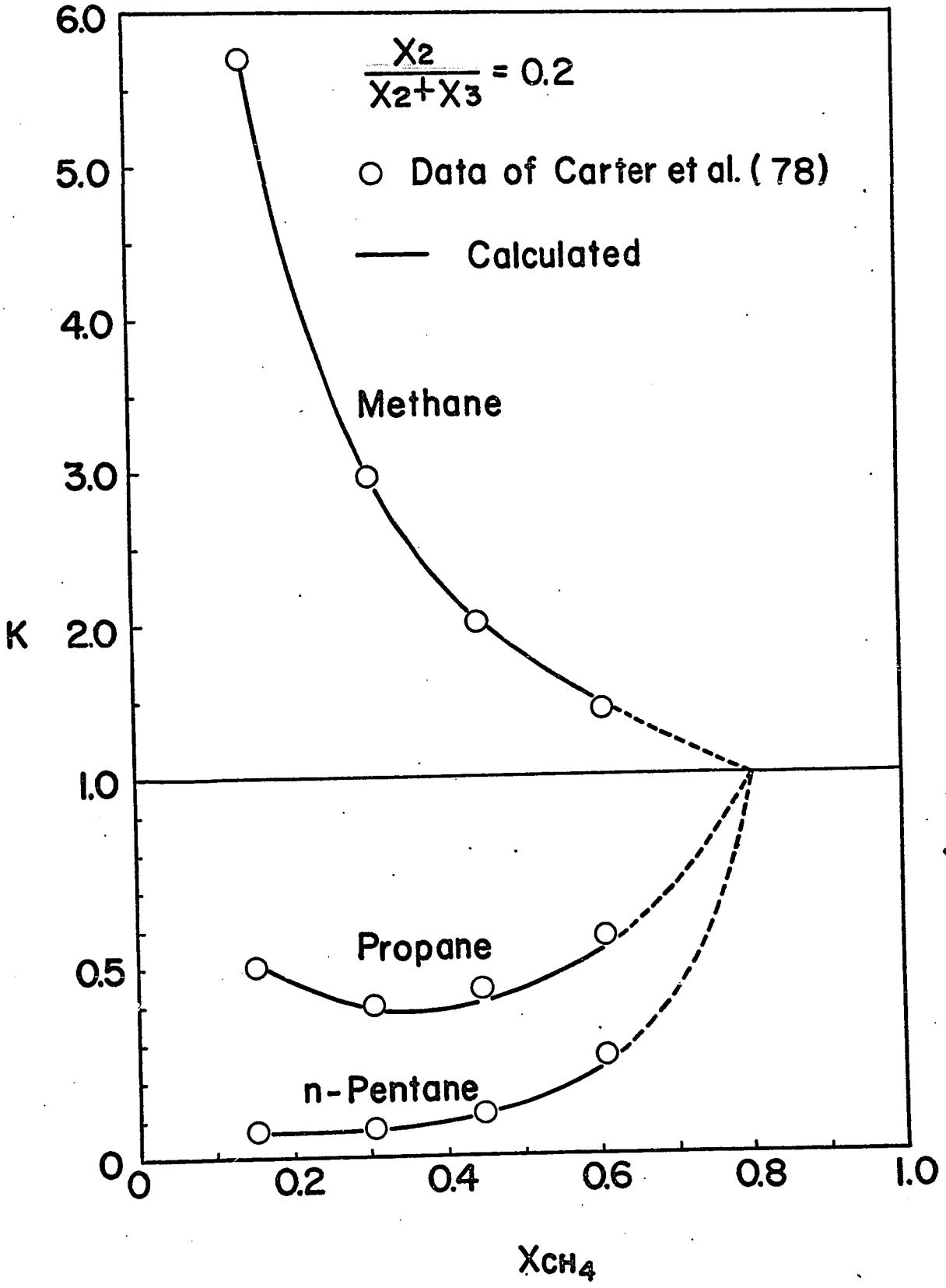

Figure 6-8 Comparison of Calculated and Experimental K-Values for the Methane-Propane-n-Pentane System at 100° F

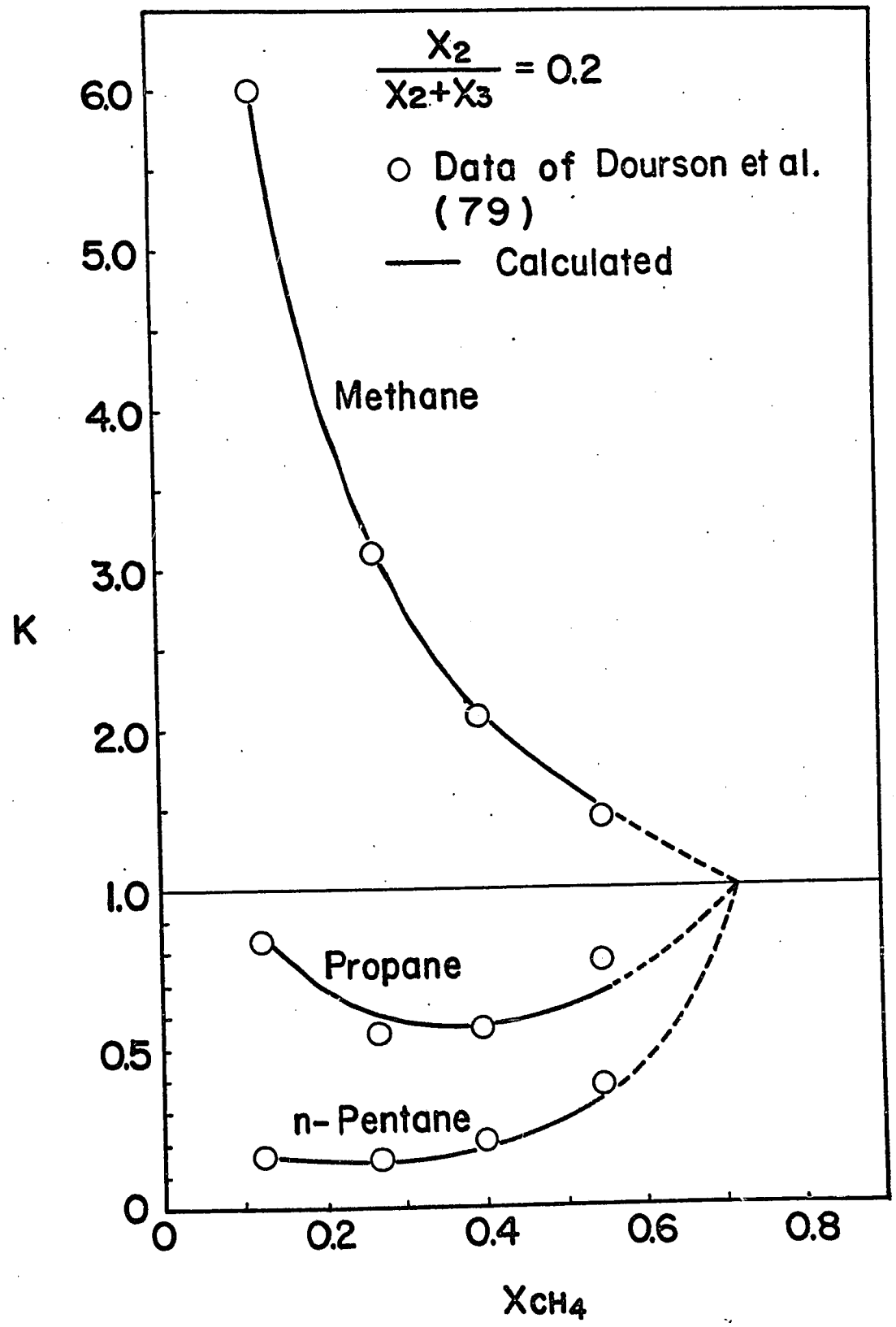

Figure 6-9 Comparison of Calculated and Experimental K-Values for the Methane-Propane-n-Pentane System at 160° F

temperature-dependent parameters of the Redlich-Kwong equation of state. In this section, the saturated liquid molal volume and the partial molal volumes are predicted to illustrate the applicability of the established values of Ω_a and Ω_b of methane.

Saturated Liquid Molal Volume: The saturated liquid molal volume can be evaluated by means of Equation (3-25) along with the mixing rules (Equations (3-13) to (3-22)). The smallest root of Equation (3-25) is taken as the compressibility factor of the saturated liquid, Z_L, therefore,

$$V_L = Z_L RT/P \tag{6-4}$$

The saturated liquid molal volume of seven methane-aliphatic hydrocarbon systems from n-butane to n-decane between 198.16°K and 348.16°K were evaluated. The average difference between the calculated and observed values of V_L is generally less than 1%. A summary of the comparison is given in Table 6-11.

Partial Molal Volume: It has been mentioned in Chapter V that the partial molal volume may be evaluated by means of the following equation:

$$\bar{V}_i = \frac{\dfrac{RT}{V-b}\left(1+\dfrac{b_i}{V-b}\right) - \dfrac{2\left(\sum_j^C x_j a_{ij}\right) - \dfrac{a b_i}{V+b}}{V(V+b)T^{\frac{1}{2}}}}{\dfrac{RT}{(V-b)^2} - \dfrac{a}{T^{\frac{1}{2}}}\left[\dfrac{2V+b}{V^2(V+b)^2}\right]} \tag{5-11}$$

TABLE 6 - 11

Summary of Results of Prediction of Volumetric Behavior

System	T, °K	$\bar{V}^{\infty}_{CH_4}$ ml/g-mole	molal volume of saturated liquid Nobs	av. abs. dev. %	max. dev. %	Ref.
Methane (1) - n-Butane (2)	294.27	68.73	24	0.97	5.50	(72)
Methane (1) - n-Pentane (2)	344.26	86.16	17	0.90	4.22	(74)
	310.93	68.62	19	0.47	3.95	(74)
Methane (1) - n-Hexane	298.16	60.19	15	0.66	1.30	(75)
	273.16	53.83	11	0.19	0.71	(75)
	223.16	45.65	9	0.30	0.66	(75)
	198.16	42.29	13	0.35	1.30	(75)
Methane (1) - n-Heptane (2)	344.26	72.15	16	0.65	2.88	(76)
	310.93	61.09	16	0.40	3.18	(76)
	277.59	53.69	15	0.52	2.95	(76)
Methane (1) - n-Octane (2)	348.16	70.23	8	0.23	0.31	(80)
	323.16	62.51	9	0.59	2.48	(80)
	298.16	56.69	9	0.52	3.99	(80)
	248.16	47.43	8	0.10	0.22	(80)
	223.16	44.42	8	0.21	0.48	(80)
Methane (1) - n-Nonane (2)	298.16	55.44	24	0.75	2.15	(81)
Methane (1) - n-Decane (2)	298.16	54.68	11	0.09	0.87	(82)

In this investigation, partial molal volumes of components in seven systems were evaluated. The partial molal volumes of methane at infinite dilution conditions for the seven systems studied are also listed in Table 6-11. The large temperature effect is shown in Figure 6-10. In addition the partial molal volumes of methane in n-hexane and benzene at 25°C were also calculated. The values obtained are in agreement with the values reported by Gjaldbaek and Hildebrand[83] as follows:

Solvent	$\bar{V}_{CH_4}$, ml./g.mole	
	Literature[83]	This Work
n-hexane	60.0	60.2
benzene	52.0	50.2

For the methane-n-heptane system, partial molal volumes for both of the components were calculated at 40°F. The values obtained are compared with the reported data of Reamer and Sage[84] in Figure 6-11.

The partial molal volumes of methane at infinite dilution conditions and at 25°C in binary mixtures with aliphatic hydrocarbons as the other component are shown in Figure 6-12 as a function of the number of carbon atoms. It is seen that the longer the chain of the solvent, the smaller the value of $\bar{V}^{\infty}_{CH_4}$.

6.5 DISCUSSIONS AND CONCLUSIONS

The modified Redlich-Kwong equation of state has been extended to the supercritical region. A detailed procedure for the evaluation of

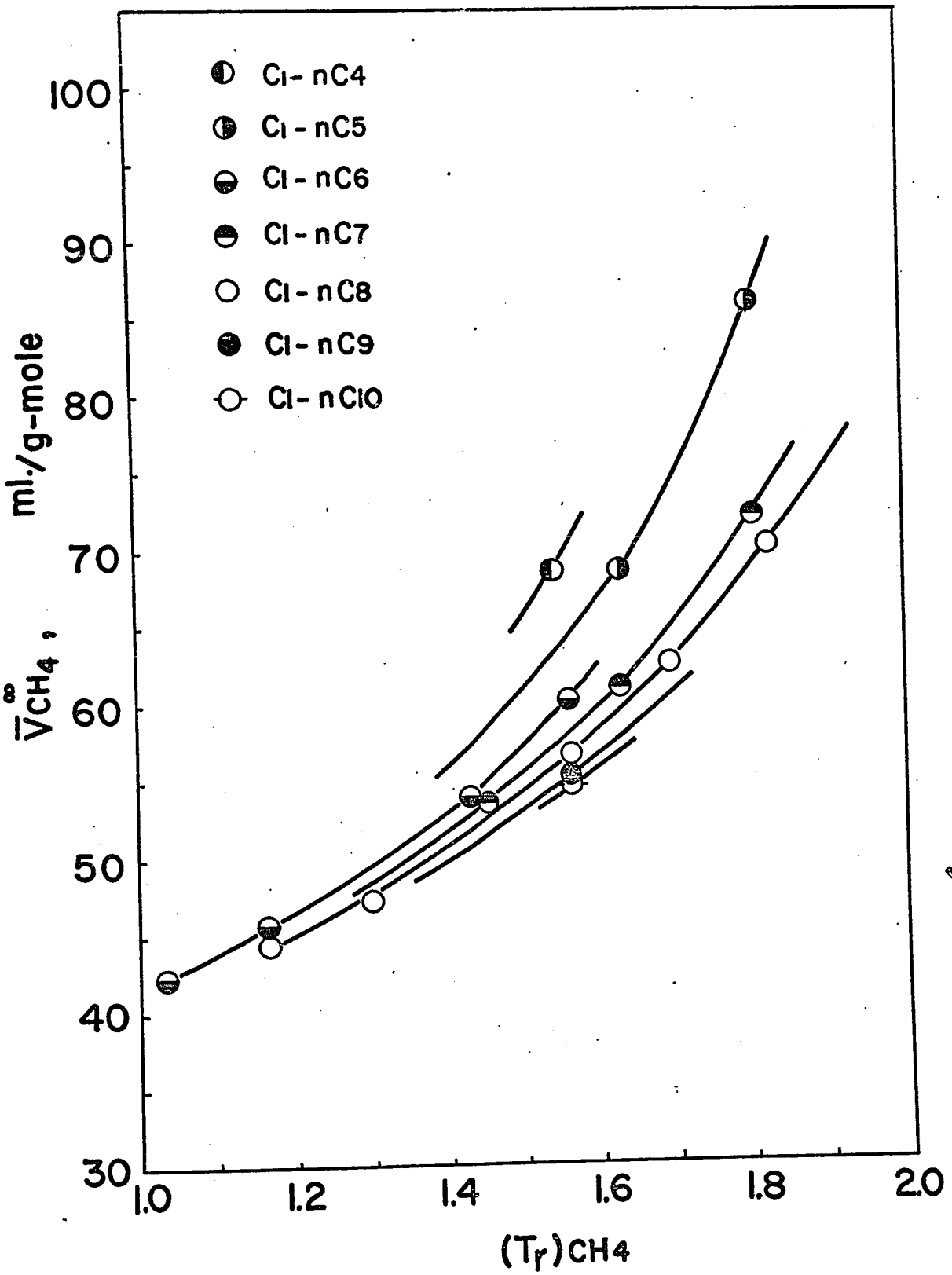

Figure 6-10 Values of $\bar{V}^{\infty}_{CH_4}$ as a Function of $(T_r)_{CH_4}$

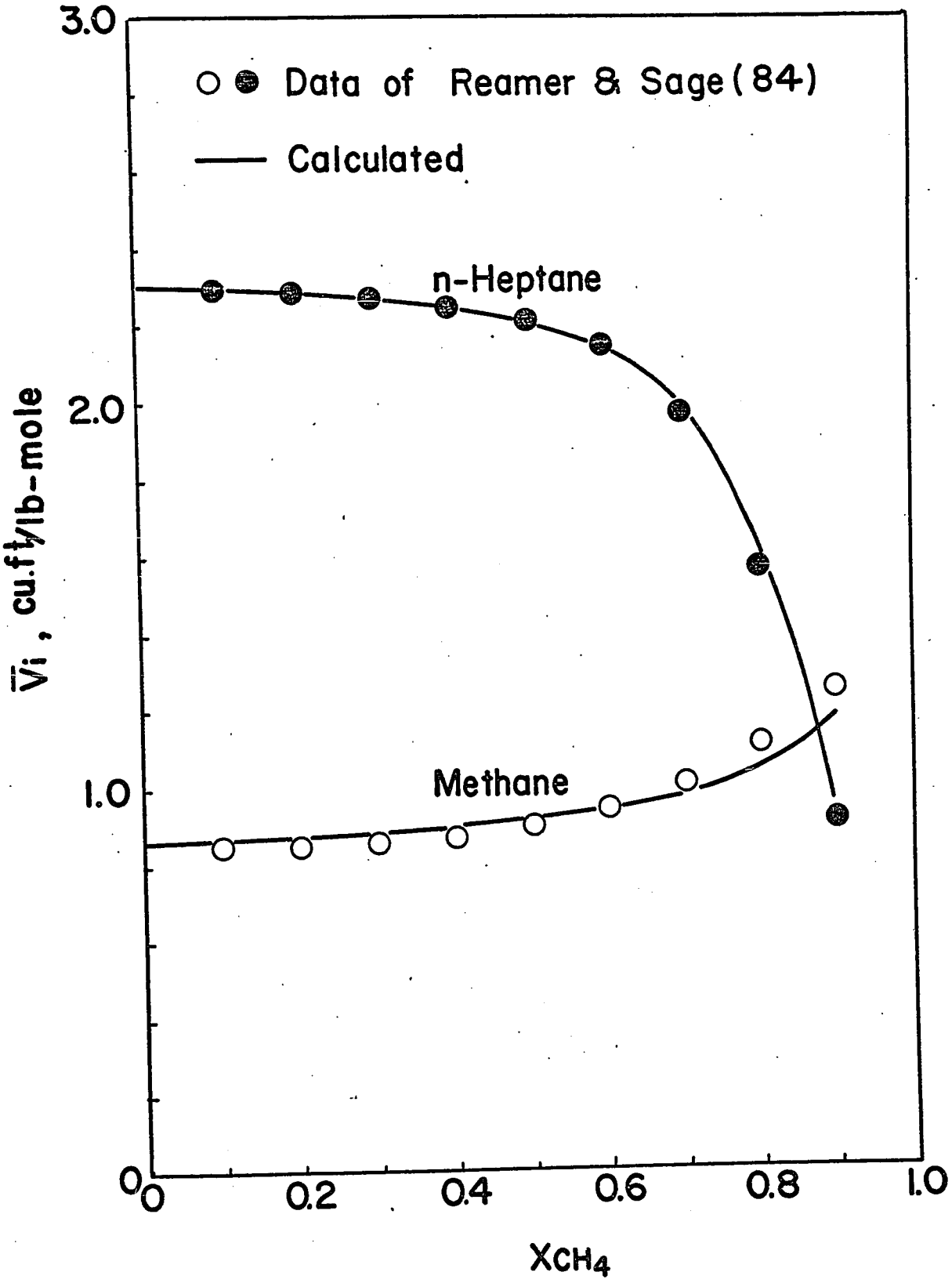

Figure 6-11 Comparison of Calculated and Experimental Partial Molal Volumes of the Methane-n-Heptane System at 40° F

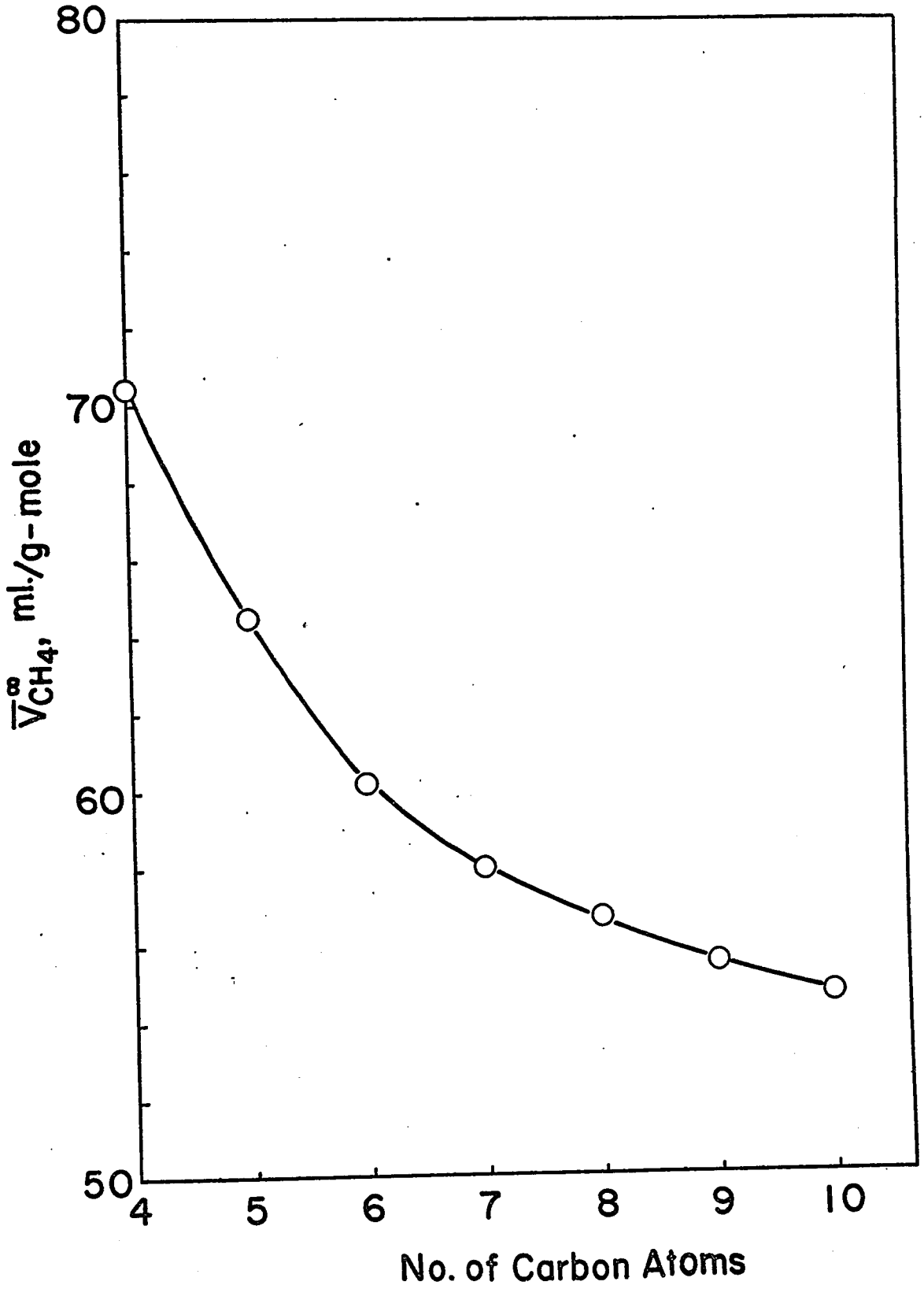

Figure 6-12 A Plot of $\bar{V}^{\infty}_{CH_4}$ vs. the Number of Carbon Atoms of the Aliphatic Hydrocarbon Solvents at 25°C

the temperature-dependent parameters for the supercritical component was proposed and the values of these parameters of pure component methane were evaluated as illustrated. An extensive comparison for gas solubilities, phase equilibria and volumetric properties has been carried out to demonstrate the validity of the proposed method. The examples were chosen to illustrate the versatility of the method. For instance, methane in seven normal paraffins from n-butane through n-decane represent applicability to systems with various differences in boiling points. Mixtures containing nonhydrocarbons are represented by the methane-hydrogen sulfide and methane-carbon tetrachloride binaries. Benzene and cyclohexane are also included in this study.

It has been shown that the proposed method, based on pure component data and some binary data, could be applied to ternary systems without introducing any higher interaction constants.

The binary interaction constants, k_{ij}, employed in this investigation are listed in Appendix A, and those reported by Prausnitz and Chueh[85] are also listed for comparison. The binary interaction constants of the methane-n-paraffin mixtures as a linear function of the ratio of critical volumes is shown in Figure 6-13.

In the critical region, the solution to the equation of equilibrium is very sensitive to small changes in the thermodynamic functions (such as fugacity coefficients and partial molal volumes). Since these functions in the critical region are not known with high accuracy, convergence is difficult and may give incorrect results. Zudkevitch et al.[25] have recently used the experimental data of P-T-x-y as the necessary information to calculate K-values within the critical region. However, in the present investigation, only the specified values of T and x are used in the prediction of saturated pressure and vapor-phase compositions.

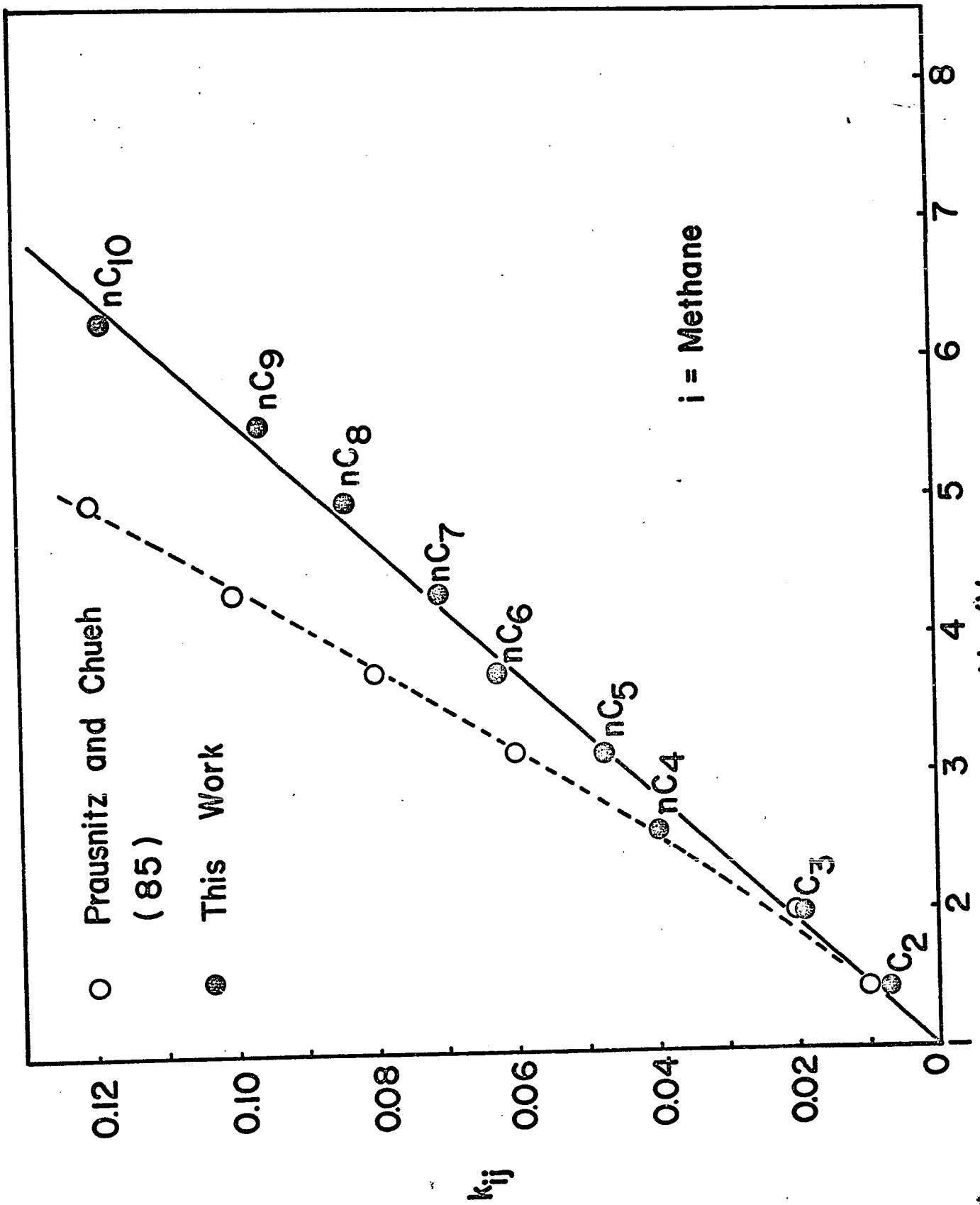

Figure 6-13 Correlation of k_{ij} for the Methane-n-Alkane Binary Mixtures

CHAPTER VII

MISCELLANEOUS WORK

In this chapter, the following two topics are discussed: (1) Evaluation of the excess thermodynamic properties for gaseous mixtures by using a limited amount of information. (2) Method for determining the limiting slopes of binary vapor-liquid equilibrium composition curve.

7.1 EXCESS THERMODYNAMIC PROPERTIES FOR HYDROGEN-NITROGEN MIXTURES

At high pressure and low temperature conditions, the non-ideality of gaseous mixtures cannot be ignored. It is useful to evaluate the excess thermodynamic properties for gaseous mixtures in engineering applications, such as in the design of compressors and pressure vessels.

The purpose of this investigation is to evaluate the excess thermodynamic properties H^E, G^E, and S^E for gaseous mixtures of hydrogen and nitrogen over the complete concentration range. An excess thermodynamic property is defined as the difference between the thermodynamic property of mixing for the system concerned and that for an ideal system at the same temperature, pressure and composition.

Gunn, Chueh and Prausnitz[86] proposed a method for predicting thermodynamic properties of dense gas mixtures containing one or more of the quantum gases. These authors successfully calculated

compressibility factors and H^E values for mixtures of hydrogen-methane, hydrogen-argon and helium-nitrogen at low temperatures. However, when their method was applied to the system hydrogen-nitrogen, it was found in this investigation that the agreement obtained between the calculated and experimental results was not as good. A summary of the deviations obtained from the method of Gunn et al. by using different references[87, 88, 89, 90], including the application of Pitzer's correlation[29], for pure nitrogen enthalpies is shown in Table 7-1. The average absolute deviations obtained vary from 7 to 22%.

Thermodynamic functions of a 1 to 3 nitrogen-hydrogen mixture have been calculated by Michels, deGroot and Lunbeck[91] between 0° to 300°C. These authors based their calculation on the P-V-T data given by Michels and Wassenaar for this mixture[92]. For other compositions of the binary system, P-V-T data are also available in the literature, but limited to temperatures above 0°C[93].

Beenakker et al.[94] indicated that the excess thermodynamic properties V^E and H^E are much more significant at temperatures below 293°K. This investigation is limited to the low-temperature region.

Numerical values of V^E and H^E for the hydrogen-nitrogen system at temperatures below 293°K and pressure up to 100 atm. have been published by Beenakker and his associates[95, 96]. In each case, values were reported for three compositions. Using these limited results, consistent H^E, G^E and S^E values were evaluated for the system over the complete concentration range in this investigation.

7.1.1 Calculation of Excess Thermodynamic Properties

Thermodynamic expressions employed in this investigation are

TABLE 7 - 1

Comparison of Predicted and Experimental H^E Values
Using the Method of Gunn et al. for
A Gaseous Mixture of 47.5% H_2 and 52.5% N_2

		H^E joules/mole				
T, °K	P, atm	Smoothed Expt. (95)	Pure H_2 enthalpy / Pure N_2 enthalpy	(88) (90)	(88) (87)	(88) (89)	(88) (29)
170	95	447		472.7	469.2	467.4	471.8
	80	363		386.5	382.2	374.6	389.9
	60	245		265.7	260.4	264.8	274.9
	40	134		128.8	114.6	125.9	122.8
	20	54		47.7	33.9	45.5	40.7
			av. absolute deviation	7.2%	13.7%	7.5%	11.6%
231	95	162		153.6	170.1	163.1	171.1
	80	137		123.4	146.2	133.2	147.8
	60	102		86.6	107.2	98.0	108.8
	40	66		50.8	63.5	59.5	74.0
	20	31.5		17.1	24.0	18.3	33.2
			av. absolute deviation	19.9%	8.8%	11.9%	7.4%
293	95	99.2		83.5		90.7	98.5
	80	84.5		70.1		77.9	85.1
	60	64.2		52.9		60.8	69.3
	40	43.2		33.2		29.5	51.2
	20	21.3		13.7		24.0	26.6
			av. absolute deviation	21.8%		13.3%	10.5%

well-known and are presented briefly here. At constant temperature and composition,

$$dG^E = V^E \, dP \tag{7-1}$$

where G^E and V^E represent the excess Gibbs free energy and the excess volume of mixing, respectively. They are defined as follows:

$$G^E = \Delta G - \Delta G^{id} \tag{7-2}$$

and

$$V^E = \Delta V - \Delta V^{id} = \Delta V \tag{7-3}$$

since $\Delta V^{id} = 0$.

Integration of Equation (7-1) from the zero-pressure state to a pressure, P, at constant temperature and composition gives

$$G^E = \int_0^P V^E \, dP \tag{7-4}$$

as $G^E = 0$ at the zero-pressure state.

When G^E values are calculated by means of Equation (7-4) at various pressures for fixed temperatures and compositions, the excess entropy of mixing values, S^E, may be obtained at constant pressure and composition by the following equation:

$$S^E = - (\partial G^E / \partial T) \tag{7-5}$$

By definition,

$$H = G + TS \tag{7-6}$$

Hence,

$$H^E = G^E + TS^E \qquad (7\text{-}7)$$

It is, therefore, possible to evaluate G^E, H^E and S^E values if V^E values are available as a function of temperature and pressure at constant compositions.

Primary Information: Since V^E values are very small compared with pure component and mixture V values, V^E values evaluated from P-V-T data generally are of only fair accuracy. It was found that a difference of 0.25% in Z values could give a 40% difference in V^E values. Zandbergen and Beenakker[96] measured the volume change of mixing for the gaseous mixtures of hydrogen and nitrogen, and smoothed V^E values were reported at three temperatures (170.5°, 231.7° and 292.6°K) with pressure up to 100 atm. for three constant-composition mixtures (25%, 50% and 70% hydrogen). These values were employed as the primary information in this calculation.

Procedure: Excess Gibbs free energy values were initially evaluated at the three temperatures at which V^E values were reported by integrating Equation (7-4) graphically. An attempt to obtain G^E values at other temperatures using interpolated V^E values was made, but the results were rejected. As V^E values were only reported at three temperatures over a range of 122°K, the uncertainty involved in the interpolation procedure is reflected in the G^E values. At low temperature and high pressure conditions, a difference of 0.3% in G^E values could give a 20% difference in the calculated S^E values and a 15% difference in the calculated H^E values. These differences decrease, however, with an increase of temperature and decrease

of pressure. The difficulties encountered in the low temperature and high pressure region led to the application of experimentally determined H^E values to the construction of G^E vs. T plots at constant pressure and composition conditions. Knoester, Taconis, and Beenakker[95] measured the H^E values for three hydrogen-nitrogen mixtures at the conditions shown in Table 7-2.

Experimental H^E values were graphically smoothed on H^E vs. P plots at constant temperature and composition conditions. The difference obtained between the smoothed and experimental values are well within the experimental error reported by the authors[95]. Interpolated H^E values obtained from these plots, at the pressure at which the G^E values were computed, were then employed to construct H^E vs. T plots at constant pressure and composition conditions for the purpose of obtaining interpolated H^E values at the temperature at which the G^E values were evaluated. These values were then employed to obtain H^E values at the corresponding compositions on H^E/y_1y_2 vs. y_1 plots at constant temperature and pressure conditions. No difficulties were encountered in these interpolation steps. The interpolated H^E values were considered "true" values and were combined with the calculated G^E values to obtain the S^E values by means of Equation (7-7), hence the $(\partial G^E/\partial T)$ values. The constructed G^E vs. T curves were used to obtain G^E values at regular temperature intervals. They were further smoothed on G^E vs. P plots at constant temperature and composition conditions. The interpolated isothermal G^E curve were slightly adjusted, together with the isobaric G^E curves, until they were consistent with each other and with the $(\partial G^E/\partial T)$ values obtained from the interpolated H^E values. The corresponding S^E values were computed by means

TABLE 7 - 2

Conditions of Experimental H^E Values Reported in the Literature[95]

Temperature, °K	Composition, % Hydrogen	Pressure range atm
293	22	53.7 - 123.7
	47.5	29.0 - 131.0
	75	44.0 - 120.1
231	47.5	9.6 - 123.4
201	22	33.9 - 116.6
	47.5	10.4 - 114.2
	75	29.4 - 116.8
170	47.5	7.8 - 133.0
147	22	34.6 - 113.6
	47	5.6 - 134.0
	75	58.6 - 112.0

of Equation (7-5), and the H^E values by Equation (7-7). A similar cross-plotting procedure was employed to obtain consistent values. Following this procedure, values of G^E, S^E and H^E were obtained at regular intervals of temperature and pressure for the three hydrogen-nitrogen mixtures (25%, 50% and 70% hydrogen). To extend these values over the complete concentration range, the extrapolation method developed by Deshpande and Lu[97] and Jones and Lu[98] was employed.

7.1.2 Results and Discussions

The calculated H^E, G^E and S^E values for the hydrogen-nitrogen binary system between 170° and 290°K at intervals of 10° are presented in Table 7-3 to 7-15. Values are listed at regular intervals of pressure and composition. A typical example is shown in Figure 7-1, in which calculated H^E, TS^E and G^E values are plotted over the complete concentration range for the system at 200°K and 80 atm. The experimental H^E values[95] are compared with the interpolated H^E values, using the calculated results listed in these tables. The average deviation is less than 1%. This is the magnitude of error introduced by the cross-plotting procedure described above. The comparison made for the $y_{H_2} = 0.475$ mixture is shown in Figure 7-2.

Knoester, Taconis, and Beenakker[95] reported that, in general, the errors in the H^E measurements were less than 5%. The uncertainty of the calculated G^E and S^E values was estimated to be of the same magnitude.

TABLE 7-3

Excess Thermodynamic Properties for the Hydrogen-Nitrogen Mixture at 170°K.

	P ATM.	Mole Fraction of Hydrogen								
		0.1	0.2	0.3	0.4	0.5	0.6	0.7	0.8	0.9
H^E	95	218	343	410	446	437	379	322	229	135
	80	164	261	323	354	352	301	262	183	101
	60	99.8	168	215	240	243	212	185	129	68.7
	40	49.1	88.8	120	135	138	125	109	78.8	39.9
	20	19.8	35.9	49.7	55.8	55.7	52.7	45.0	32.4	17.5
	10	9.11	16.2	20.9	24.7	26.6	25.4	20.8	15.2	8.35
G^E	95	45.8	73.0	92.0	103	105	98.6	82.4	58.9	31.3
	80	37.2	60.0	76.0	85.0	87.0	81.5	68.1	49.5	26.3
	60	25.8	42.7	55.2	61.6	62.5	58.5	49.8	37.0	19.7
	40	15.3	26.1	34.4	39.0	40.0	37.4	32.3	24.7	13.2
	20	6.70	12.6	16.5	18.9	19.0	18.0	16.1	12.3	6.60
	10	3.45	6.05	8.00	9.00	9.25	9.00	7.98	6.04	3.30
S^E	95	1.01	1.59	1.87	2.02	1.95	1.65	1.41	1.00	0.609
	80	0.745	1.18	1.45	1.58	1.56	1.29	1.14	0.784	0.437
	60	0.435	0.735	0.940	1.05	1.06	0.905	0.796	0.544	0.288
	40	0.199	0.369	0.501	0.565	0.574	0.514	0.453	0.318	0.157
	20	0.0771	0.137	0.195	0.217	0.216	0.204	0.170	0.118	0.0643
	10	0.0333	0.0599	0.0760	0.0922	0.102	0.0964	0.0752	0.0538	0.0297

TABLE 7 - 4

Excess Thermodynamic Properties for the Hydrogen-Nitrogen Mixtures at 180°K.

Mole Fraction of Hydrogen

	P ATM.	0.1	0.2	0.3	0.4	0.5	0.6	0.7	0.8	0.9
H^E	95	165	266	327	354	352	310	264	188	109
	80	125	204	260	287	287	252	214	151	83.8
	60	78.5	135	177	199	201	180	153	108	57.9
	40	42.1	74.7	100	115	118	109	92.4	66.6	34.6
	20	17.4	31.2	42.6	48.9	49.4	46.8	39.2	28.3	15.6
	10	7.96	14.3	18.4	21.9	23.8	22.6	18.2	13.6	7.54
G^E	95	36.7	61.2	78.7	87.5	89.0	83.5	71.0	51.5	28.3
	80	30.4	50.9	65.8	73.0	74.5	70.0	59.6	43.4	23.9
	60	22.0	37.2	48.0	55.3	54.9	51.9	44.2	32.6	17.9
	40	13.5	23.4	30.0	34.6	35.7	33.8	28.7	21.6	11.9
	20	6.15	11.0	14.3	16.9	16.6	16.0	14.0	10.7	5.98
	10	3.10	5.45	7.10	7.97	8.30	7.97	7.00	5.33	3.00
S^E	95	0.710	1.14	1.38	1.48	1.46	1.26	1.07	0.758	0.451
	80	0.525	0.848	1.08	1.19	1.18	1.01	0.858	0.600	0.333
	60	0.314	0.546	0.717	0.799	0.814	0.713	0.603	0.420	0.222
	40	0.159	0.285	0.391	0.449	0.459	0.415	0.354	0.250	0.126
	20	0.0627	0.112	0.157	0.178	0.182	0.171	0.140	0.0975	0.0535
	10	0.0270	0.0491	0.0630	0.0775	0.0861	0.0811	0.0623	0.0457	0.0252

TABLE 7 - 5

Excess Thermodynamic Properties for the Hydrogen-Nitrogen Mixtures at 190°K.

	P ATM.	Mole Fraction of Hydrogen								
		0.1	0.2	0.3	0.4	0.5	0.6	0.7	0.8	0.9
H^E	95	127	208	266	291	295	263	219	158	90.7
	80	96.5	162	212	237	241	215	179	128	71.0
	60	62.9	110	148	166	171	155	129	92.5	49.6
	40	34.6	62.6	85.5	100	103	94.8	79.6	57.8	30.7
	20	15.2	27.7	37.2	42.9	44.8	42.2	34.9	25.3	14.0
	10	6.97	12.8	16.4	19.7	21.3	20.4	16.4	12.2	6.77
G^E	95	30.4	52.5	68.5	78.2	80.6	76.7	63.8	46.3	25.7
	80	25.1	43.6	57.1	65.4	67.3	63.8	53.3	38.9	21.6
	60	18.2	31.9	42.2	48.3	49.8	47.0	39.5	29.2	16.2
	40	11.4	20.2	27.0	31.3	32.3	30.2	26.0	19.4	10.9
	20	5.45	10.0	12.9	15.0	15.5	14.8	13.0	9.70	5.42
	10	2.75	4.97	6.35	7.25	7.40	7.30	6.45	4.72	2.70
S^E	95	0.510	0.821	1.04	1.12	1.13	0.982	0.818	0.587	0.342
	80	0.376	0.625	0.815	0.905	0.913	0.798	0.663	0.470	0.260
	60	0.235	0.411	0.556	0.617	0.637	0.568	0.471	0.333	0.176
	40	0.122	0.223	0.308	0.362	0.373	0.340	0.282	0.202	0.104
	20	0.0514	0.0930	0.128	0.147	0.154	0.144	0.115	0.0823	0.0450
	10	0.0222	0.0411	0.0530	0.0654	0.0731	0.0687	0.0524	0.0394	0.0214

TABLE 7 - 6

Excess Thermodynamic Properties for the Hydrogen-Nitrogen Mixtures at 200°K.

Mole Fraction of Hydrogen

	P ATM.	0.1	0.2	0.3	0.4	0.5	0.6	0.7	0.8	0.9
H^E	95	99.4	168	218	241	248	224	186	135	76.2
	80	76.8	133	177	200	204	185	153	110	60.0
	60	51.9	92.1	125	142	147	135	111	82.2	42.8
	40	29.7	54.4	73.9	87.7	90.6	84.1	69.7	50.7	26.9
	20	13.5	24.6	33.4	38.7	41.0	38.1	31.0	22.6	12.5
	10	6.05	11.4	15.0	18.2	19.7	18.6	14.9	11.2	6.12
G^E	95	25.2	44.7	60.2	68.9	70.8	67.1	56.3	41.5	22.6
	80	21.2	37.5	50.5	58.0	59.8	56.5	47.5	35.0	19.0
	60	15.7	28.1	37.5	43.3	44.9	42.1	35.6	26.2	14.2
	40	10.2	18.6	24.5	28.5	29.6	27.9	23.7	17.5	9.49
	20	4.96	9.06	12.0	13.9	14.6	13.7	11.6	8.53	4.76
	10	2.35	4.46	5.98	6.97	7.20	6.85	5.91	4.25	2.42
S^E	95	0.371	0.614	0.790	0.859	0.885	0.785	0.648	0.468	0.268
	80	0.278	0.475	0.633	0.708	0.720	0.640	0.527	0.377	0.205
	60	0.181	0.320	0.437	0.491	0.508	0.462	0.379	0.280	0.143
	40	0.0973	0.179	0.247	0.296	0.305	0.281	0.230	0.166	0.0870
	20	0.0428	0.0779	0.107	0.124	0.132	0.122	0.0970	0.0703	0.0385
	10	0.0185	0.0349	0.0451	0.0559	0.0624	0.0588	0.0449	0.0345	0.0185

TABLE 7 - 7

Excess Thermodynamic Properties for the Hydrogen-Nitrogen Mixtures at 210°K.

Mole Fraction of Hydrogen

	P ATM.	0.1	0.2	0.3	0.4	0.5	0.6	0.7	0.8	0.9
H^E	95	80.7	140	184	206	213	196	162	119	66.6
	80	63.2	112	150	172	176	162	134	97.2	53.1
	60	43.8	78.7	108	123	128	119	98.2	71.2	38.6
	40	26.0	47.4	64.8	77.7	81.0	74.8	61.8	44.9	24.4
	20	12.2	22.0	29.7	35.0	37.2	34.6	28.4	20.8	11.5
	10	5.51	10.3	13.4	16.3	18.0	17.2	13.6	10.2	5.64
G^E	95	21.9	39.9	54.5	62.8	63.9	60.5	51.6	38.0	21.2
	80	18.5	33.5	45.7	52.7	53.8	50.9	43.4	31.9	17.8
	60	13.8	24.9	34.1	39.3	40.2	38.3	32.5	23.9	13.4
	40	9.26	16.3	22.4	26.0	27.0	25.4	21.7	15.9	8.96
	20	4.60	8.15	10.7	12.5	13.3	12.5	10.9	7.88	4.50
	10	2.19	4.00	5.18	6.15	6.70	6.41	5.38	3.81	2.20
S^E	95	0.280	0.475	0.619	0.682	0.708	0.643	0.527	0.385	0.216
	80	0.213	0.373	0.499	0.566	0.581	0.527	0.433	0.311	0.168
	60	0.143	0.256	0.351	0.400	0.416	0.383	0.313	0.225	0.120
	40	0.0798	0.148	0.202	0.246	0.257	0.235	0.191	0.138	0.0737
	20	0.0360	0.0661	0.0906	0.107	0.114	0.105	0.0832	0.0613	0.0332
	10	0.0158	0.0301	0.0393	0.0485	0.0539	0.0512	0.0390	0.0303	0.0164

TABLE 7 - 8

Excess Thermodynamic Properties for the Hydrogen-Nitrogen Mixtures at 220°K.

	P ATM	Mole Fraction of Hydrogen								
		0.1	0.2	0.3	0.4	0.5	0.6	0.7	0.8	0.9
H^E	95	67.6	119	158	179	186	174	144	106	58.0
	80	53.5	97.0	129	150	155	144	121	87.7	46.7
	60	37.7	68.9	94.4	110	113	106	88.8	64.6	34.3
	40	22.9	42.5	57.6	69.3	73.2	67.3	55.8	41.0	21.7
	20	10.8	19.9	27.3	32.0	34.3	31.9	25.9	19.1	10.3
	10	4.97	9.48	12.7	15.2	16.4	15.6	12.5	9.64	5.17
G^E	95	19.6	35.9	48.4	56.4	58.2	55.0	47.0	34.3	18.4
	80	16.5	30.3	40.8	47.5	49.0	46.5	39.6	29.0	15.5
	60	12.4	22.7	30.6	35.6	36.9	34.9	29.8	21.9	11.6
	40	8.20	15.0	20.4	23.5	24.6	23.3	19.9	14.6	7.79
	20	4.00	7.35	10.1	11.7	12.3	11.6	9.93	7.27	3.95
	10	1.89	3.69	5.12	5.87	6.03	5.78	5.00	3.74	1.98
S^E	95	0.218	0.377	0.498	0.556	0.580	0.539	0.443	0.328	0.180
	80	0.168	0.303	0.403	0.464	0.480	0.441	0.368	0.267	0.142
	60	0.115	0.210	0.290	0.336	0.346	0.325	0.268	0.194	0.103
	40	0.0669	0.125	0.169	0.208	0.221	0.200	0.163	0.120	0.0634
	20	0.0310	0.0570	0.0784	0.0923	0.0998	0.0921	0.0726	0.0539	0.0290
	10	0.0140	0.0263	0.0346	0.0425	0.0471	0.0448	0.0343	0.0268	0.0145

TABLE 7 - 9

Excess Thermodynamic Properties for the Hydrogen-Nitrogen Mixtures at 230°K.

Mole Fraction of Hydrogen

	P ATM	0.1	0.2	0.3	0.4	0.5	0.6	0.7	0.8	0.9
H^E	95	58.5	105	140	160	166	157	131	98.0	53.3
	80	46.7	86.4	116	134	138	131	109	81.0	42.7
	60	33.5	61.6	84.5	99.1	102	95.7	80.6	59.2	31.2
	40	20.7	38.5	52.2	63.1	66.9	61.8	51.0	37.6	20.2
	20	9.97	18.4	25.2	29.8	31.6	29.5	23.8	17.8	9.56
	10	4.73	8.88	11.7	14.2	15.2	14.6	11.6	8.81	4.79
G^E	95	17.8	32.9	45.4	52.0	53.7	50.7	43.0	32.0	17.2
	80	15.0	27.7	38.0	43.8	45.0	42.6	36.1	26.9	14.2
	60	11.3	20.7	28.4	32.9	33.9	32.0	27.0	20.1	10.8
	40	7.52	13.9	18.9	21.9	22.7	21.5	18.1	13.4	7.22
	20	3.76	6.99	9.40	11.0	11.4	10.6	8.97	6.74	3.67
	10	1.81	3.50	4.50	5.41	5.62	5.45	4.50	3.29	1.80
S^E	95	0.177	0.314	0.411	0.470	0.489	0.462	0.383	0.287	0.157
	80	0.138	0.255	0.337	0.393	0.406	0.383	0.318	0.235	0.124
	60	0.0965	0.178	0.244	0.288	0.298	0.277	0.233	0.170	0.0885
	40	0.0572	0.107	0.145	0.179	0.192	0.175	0.143	0.105	0.0557
	20	0.0270	0.0496	0.0688	0.0818	0.0878	0.0821	0.0645	0.0482	0.0256
	10	0.0127	0.0234	0.0312	0.0380	0.0417	0.0396	0.0307	0.0240	0.0130

TABLE 7 - 10

Excess Thermodynamic Properties for the Hydrogen-Nitrogen Mixtures at 240°K.

	P ATM	Mole Fraction of Hydrogen								
		0.1	0.2	0.3	0.4	0.5	0.6	0.7	0.8	0.9
H^E	95	51.7	94.8	125	145	151	142	120	89.3	49.4
	80	42.1	78.6	105	122	126	119	101	73.8	39.9
	60	30.8	56.2	77.0	90.5	93.6	87.8	74.3	54.2	28.8
	40	19.1	35.4	48.2	57.9	61.3	56.9	47.3	34.8	18.6
	20	9.22	16.9	23.4	27.5	29.2	27.4	22.4	16.7	8.92
	10	4.46	8.13	11.2	13.2	14.2	13.4	11.0	8.41	4.52
G^E	95	16.4	30.0	40.8	47.5	48.9	46.0	39.7	28.6	16.0
	80	13.8	25.3	34.4	40.0	41.2	38.7	33.5	24.1	13.5
	60	10.4	19.0	25.9	30.0	31.0	29.0	25.1	18.2	10.1
	40	6.88	12.6	17.2	20.0	20.7	19.5	16.8	12.2	6.74
	20	3.41	6.25	8.62	10.0	10.4	9.80	8.45	6.20	3.40
	10	1.68	3.04	4.35	5.00	5.20	4.95	4.25	3.18	1.69
S^E	95	0.147	0.270	0.349	0.408	0.425	0.402	0.336	0.253	0.139
	80	0.118	0.222	0.294	0.342	0.354	0.334	0.280	0.207	0.110
	60	0.0848	0.155	0.213	0.252	0.261	0.245	0.205	0.150	0.0780
	40	0.0510	0.0950	0.129	0.158	0.169	0.156	0.127	0.0940	0.0496
	20	0.0242	0.0443	0.0617	0.0730	0.0785	0.0734	0.0581	0.0436	0.0230
	10	0.0116	0.0212	0.0287	0.0341	0.0375	0.0354	0.0280	0.0218	0.0118

TABLE 7 - 11

Excess Thermodynamic Properties for the Hydrogen-Nitrogen Mixtures at 250°K.

	P ATM	Mole Fraction of Hydrogen								
		0.1	0.2	0.3	0.4	0.5	0.6	0.7	0.8	0.9
H^E	95	47.7	86.8	115	133	138	131	110	83.3	45.6
	80	39.1	72.1	96.5	112	116	110	92.3	69.1	37.0
	60	28.5	51.9	71.3	83.5	86.3	81.0	68.5	50.7	26.8
	40	18.0	33.3	45.2	53.8	56.8	52.9	43.9	32.6	17.4
	20	8.66	15.9	22.0	25.8	27.4	25.7	20.9	15.6	8.30
	10	4.27	7.83	11.6	12.5	13.2	12.7	10.3	7.85	4.22
G^E	95	15.2	27.5	38.0	44.0	45.0	42.2	35.7	26.8	14.6
	80	12.8	23.1	32.0	37.0	38.0	35.5	30.0	22.6	12.3
	60	9.57	17.4	24.0	27.7	28.5	26.7	22.5	16.9	9.27
	40	6.40	11.7	15.9	18.5	19.0	17.9	15.1	11.4	6.20
	20	3.18	5.90	8.00	9.25	9.57	9.10	7.68	5.69	3.10
	10	1.59	2.95	3.96	4.71	4.75	4.63	3.94	2.90	1.52
S^E	95	0.130	0.237	0.307	0.357	0.372	0.356	0.298	0.226	0.124
	80	0.105	0.196	0.258	0.300	0.312	0.296	0.249	0.186	0.0988
	60	0.0758	0.138	0.189	0.223	0.231	0.217	0.184	0.135	0.0700
	40	0.0464	0.0865	0.117	0.141	0.151	0.140	0.115	0.0848	0.0448
	20	0.0219	0.0400	0.0560	0.0660	0.0713	0.0664	0.0529	0.0398	0.0208
	10	0.0107	0.0195	0.0264	0.0311	0.0339	0.0321	0.0256	0.0198	0.0108

TABLE 7 - 12

Excess Thermodynamic Properties for the Hydrogen-Nitrogen Mixtures at 260°K.

Mole Fraction of Hydrogen

	P ATM	0.1	0.2	0.3	0.4	0.5	0.6	0.7	0.8	0.9
H^E	95	44.4	80.7	106	123	127	121	103	77.4	43.2
	80	36.6	67.5	89.2	104	108	102	86.6	64.2	34.9
	60	26.9	48.9	66.2	77.3	80.1	74.9	64.5	47.0	25.3
	40	17.1	31.6	42.5	50.3	52.9	49.4	41.2	30.3	16.4
	20	8.23	15.1	20.7	24.2	25.7	23.9	20.0	14.7	7.91
	10	4.03	7.43	10.1	11.8	12.5	11.7	9.81	7.40	4.01
G^E	95	14.2	25.8	34.8	40.5	41.5	38.7	33.6	24.1	13.8
	80	12.0	21.7	29.4	34.1	35.0	32.6	28.4	20.3	11.6
	60	9.00	16.4	22.0	25.6	26.3	24.5	21.3	15.3	8.77
	40	6.00	10.9	14.7	17.0	17.5	16.4	14.2	10.2	5.85
	20	3.00	5.45	7.39	8.60	8.89	8.24	7.30	5.22	2.94
	10	1.49	2.72	3.73	4.37	4.49	4.10	3.65	2.67	1.43
S^E	95	0.116	0.211	0.274	0.317	0.329	0.318	0.268	0.205	0.113
	80	0.0945	0.176	0.230	0.268	0.279	0.265	0.224	0.169	0.0898
	60	0.0689	0.125	0.170	0.199	0.207	0.194	0.166	0.122	0.0636
	40	0.0428	0.0797	0.107	0.128	0.136	0.127	0.104	0.0773	0.0406
	20	0.0201	0.0373	0.0513	0.0601	0.0648	0.0603	0.0487	0.0366	0.0191
	10	0.00975	0.0181	0.0246	0.0287	0.0309	0.0293	0.0237	0.0182	0.00992

TABLE 7 - 13

Excess Thermodynamic Properties for the Hydrogen-Nitrogen Mixtures at 270°K.

	P ATM	Mole Fraction of Hydrogen								
		0.1	0.2	0.3	0.4	0.5	0.6	0.7	0.8	0.9
H^E	95	41.5	74.9	98.6	114	117	112	96.4	73.5	40.4
	80	34.4	61.7	83.3	96.0	99.7	94.1	80.5	61.0	32.8
	60	25.4	46.2	62.2	71.8	74.5	69.8	60.1	44.5	23.7
	40	16.4	30.1	40.4	47.1	49.3	46.6	38.9	28.9	15.3
	20	7.80	14.5	19.6	22.8	24.1	22.6	18.7	14.0	7.42
	10	3.78	7.06	9.62	11.2	11.7	11.2	9.27	6.99	3.77
G^E	95	13.4	23.9	32.2	36.7	37.8	35.0	30.5	23.0	12.6
	80	11.2	20.1	27.1	30.9	31.9	29.6	25.7	19.4	10.6
	60	8.40	15.1	20.3	23.2	24.0	22.3	19.3	14.5	7.98
	40	5.60	10.1	13.5	15.5	16.1	15.0	12.9	9.70	5.32
	20	2.78	5.02	6.74	7.82	8.08	7.65	6.55	4.87	2.67
	10	1.35	2.50	3.36	4.00	4.10	4.00	3.30	2.48	1.30
S^E	95	0.104	0.189	0.246	0.285	0.295	0.287	0.244	0.187	0.103
	80	0.0860	0.154	0.208	0.241	0.251	0.239	0.203	0.154	0.0824
	60	0.0630	0.115	0.155	0.180	0.187	0.176	0.151	0.111	0.0583
	40	0.0399	0.0742	0.0997	0.117	0.123	0.117	0.0964	0.0712	0.0370
	20	0.0186	0.0351	0.0475	0.0554	0.0594	0.0552	0.0450	0.0337	0.0176
	10	0.00900	0.0169	0.0232	0.0266	0.0283	0.0267	0.0221	0.0167	0.00915

TABLE 7 - 14

Excess Thermodynamic Properties for the Hydrogen-Nitrogen Mixtures at 280°K.

	P ATM	Mole Fraction of Hydrogen								
		0.1	0.2	0.3	0.4	0.5	0.6	0.7	0.8	0.9
H^E	95	39.2	70.4	92.5	106	109	105	90.3	68.8	38.4
	80	32.7	59.7	78.1	89.4	93.0	88.2	75.0	56.9	31.2
	60	24.3	43.8	58.6	67.1	69.7	65.7	56.1	41.5	22.5
	40	15.7	29.0	38.6	44.6	46.2	43.8	36.9	27.1	14.4
	20	7.46	13.9	18.7	21.4	22.7	21.0	17.7	13.1	6.96
	10	3.58	6.78	9.25	10.6	11.1	10.3	8.77	6.61	3.59
G^E	95	12.5	22.2	29.5	34.0	34.8	32.5	27.9	20.6	11.7
	80	10.6	18.8	24.9	28.6	29.4	27.4	23.5	17.4	9.90
	60	7.94	14.1	18.6	21.5	22.1	20.6	17.7	13.2	7.40
	40	5.24	9.40	12.5	14.4	14.8	13.8	11.9	8.77	4.92
	20	2.59	4.65	6.20	7.14	7.42	6.90	5.98	4.41	2.45
	10	1.25	2.30	3.12	3.67	3.84	3.45	3.00	2.30	1.22
S^E	95	0.0953	0.172	0.225	0.257	0.265	0.258	0.223	0.172	0.0952
	80	0.0790	0.146	0.190	0.217	0.227	0.217	0.184	0.141	0.0760
	60	0.0585	0.106	0.143	0.163	0.170	0.161	0.137	0.101	0.0540
	40	0.0375	0.0699	0.0931	0.108	0.112	0.107	0.0892	0.0656	0.0340
	20	0.0174	0.0332	0.0446	0.0511	0.0546	0.0505	0.0417	0.0312	0.0161
	10	0.00832	0.0160	0.0219	0.0248	0.0260	0.0246	0.0206	0.0154	0.00846

TABLE 7 - 15

Excess Thermodynamic Properties for the Hydrogen-Nitrogen Mixtures at 290°K.

	P ATM	Mole Fraction of Hydrogen								
		0.1	0.2	0.3	0.4	0.5	0.6	0.7	0.8	0.9
H^E	95	37.4	66.3	87.0	99.3	102	98.1	84.8	64.8	36.1
	80	31.3	56.4	73.6	83.5	86.7	82.8	70.5	54.0	29.5
	60	23.4	41.9	55.9	63.0	65.2	62.0	52.9	39.3	21.3
	40	15.4	28.0	37.0	42.2	43.2	41.4	35.0	25.8	13.5
	20	7.24	13.6	18.0	20.3	21.3	19.9	16.8	12.5	6.52
	10	3.44	6.56	8.86	10.1	10.3	9.81	8.46	6.20	3.35
G^E	95	12.1	20.8	27.5	31.4	32.1	30.2	25.9	19.3	10.7
	80	10.1	17.5	23.1	26.4	27.0	25.4	21.8	16.3	9.00
	60	7.60	13.2	17.3	19.8	20.2	19.1	16.4	12.2	6.72
	40	5.04	8.76	11.5	13.2	13.6	12.8	11.0	8.15	4.48
	20	2.51	4.40	5.76	6.65	6.74	6.48	5.56	4.11	2.20
	10	1.20	2.15	2.80	3.41	3.40	3.23	2.80	2.08	1.09
S^E	95	0.0871	0.157	0.205	0.234	0.240	0.234	0.203	0.157	0.0877
	80	0.0732	0.134	0.174	0.197	0.206	0.198	0.168	0.130	0.0706
	60	0.0546	0.0988	0.133	0.149	0.155	0.148	0.126	0.0935	0.0502
	40	0.0357	0.0662	0.0878	0.100	0.102	0.0987	0.0828	0.0607	0.0311
	20	0.0163	0.0318	0.0421	0.0472	0.0502	0.0463	0.0388	0.0288	0.0149
	10	0.00772	0.0152	0.0209	0.0231	0.0238	0.0227	0.0195	0.0142	0.00781

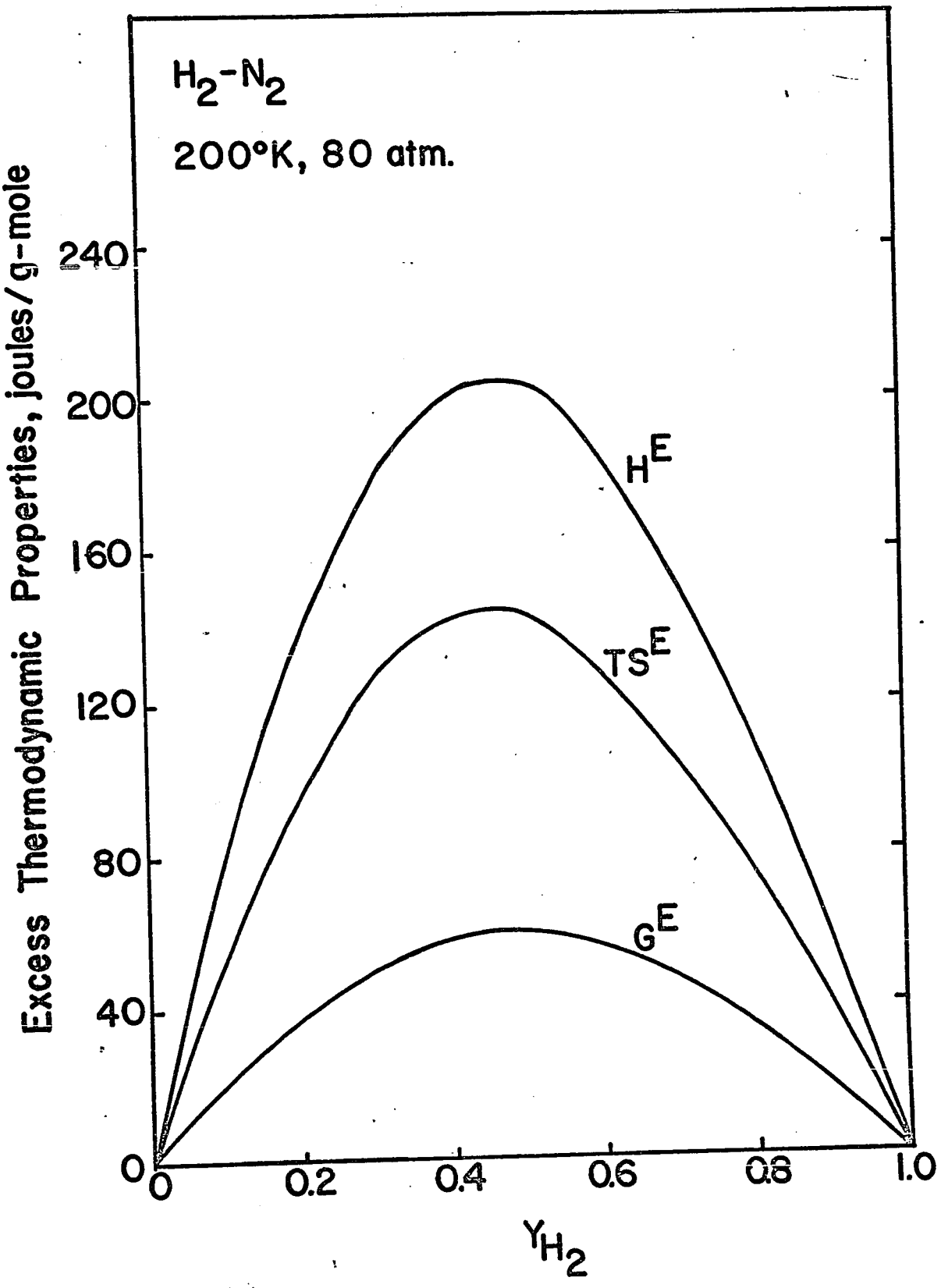

Figure 7-1 Calculated Excess Thermodynamic Properties for the H_2-N_2 Mixtures at 200°K and 80 atm.

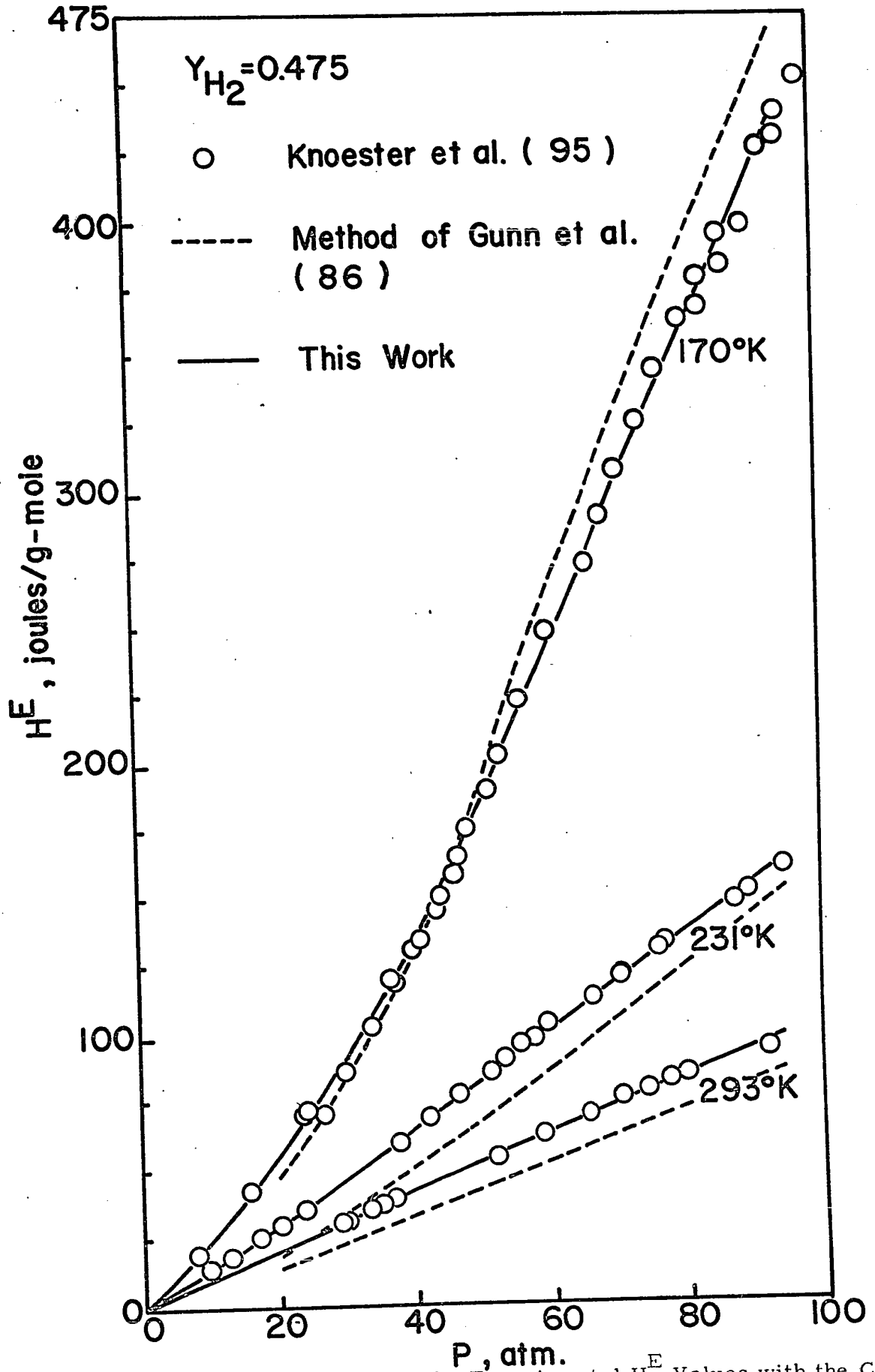

Figure 7-2 Comparison of the Experimental H^E Values with the Calculated Results for Y_{H_2} = 0.475 Mixture

Within the range of this investigation, at constant composition conditions, the calculated H^E, G^E and S^E values increase with increasing pressure, but decrease with an increase in temperature. In all cases, $H^E > TS^E > G^E$, and the quantity TS^E contributes much more than the quantity G^E to the H^E value at a given condition. Hence, gaseous mixtures of hydrogen and nitrogen are neither regular nor athermal solutions.

7.2 DETERMINATION OF LIMITING SLOPES OF BINARY VAPOR-LIQUID EQUILIBRIUM COMPOSITION CURVE

7.2.1 Purpose

Limiting slopes of the vapor-liquid equilibrium composition curve, $\lim_{x_i \to 0} (\partial y_i / \partial x_i)$, are directly related to activity coefficients at infinite dilutions. At the equilibrium conditions,

$$\frac{y_i}{x_i} = \frac{\gamma_{iL} f_{iL}}{\gamma_{iV} f_{iV}} \tag{7-8}$$

As x_i approaches zero, the left-hand side approaches 0/0. Application of l'Hôpital's rule gives

$$\left(\frac{\partial y_i}{\partial x_i}\right)_{x_i = 0} = \left(\frac{\gamma_{iL} f_{iL}}{\gamma_{iV} f_{iV}}\right)_{x_i = 0} \tag{7-9}$$

in which f_{iV} and f_{iL} are pure component properties.

At low pressures, liquid activity coefficient may be represented by[99]:

$$\log \gamma_i = \log \frac{y_i P}{x_i P'_i} + \frac{(P - P'_i)(\beta_i - V_i)}{2.303\, RT} \qquad (7\text{-}10)$$

in which the vapor-phase is assumed to be an ideal solution, but not an ideal gas. For binary systems, as x_i approaches zero, Equation (7-10) gives

$$(\log \gamma_1)_{x_1 = 0} = \log \left[\left(\frac{y_1}{x_1} \right) \left(\frac{P'_2}{P'_1} \right) \right]_{x_1 = 0} + \frac{(P'_2 - P'_1)(\beta_1 - V_1)}{2.303\, RT} \qquad (7\text{-}11)$$

for $\log \gamma_1$; a similar equation may be obtained for $\log \gamma_2$. These limiting $\log \gamma_i$ values may be identified with the constants of any integrated two-constant Gibbs-Duhem equation, such as the equations of van Laar and Margules. They may be obtained directly from the limiting slopes as all the other quantities are pure-component properties. If the vapor phase is assumed to be an ideal gas then Equation (7-11) may be further reduced to

$$(\log \gamma_1)_{x_1 = 0} = \log \left[\left(\frac{\partial y_1}{\partial x_1} \right) \left(\frac{P'_2}{P'_1} \right) \right]_{x_1 = 0} \qquad (7\text{-}12)$$

The limiting slopes are useful in the correlation and prediction of vapor-liquid equilibrium data. Methods are available for correlating limiting slopes and limiting $\log \gamma_i$ values. For example, Carlson and Colburn[100] made an attempt to correlate limiting $\log \gamma_i$ values for homologous series with solubility parameter in 1942. Recently, Tassios and Van Winkle[101] proposed an empirical relationship which also correlates the limiting $\log \gamma_i$ values for homologous series, for the purpose of predicting binary vapor-liquid equilibrium data. Methods are also available for the determination of limiting slopes or limiting $\log \gamma_i$ values. For example, Tassios and Van Winkle[101]

obtained their limiting log γ_i values by extrapolation of log γ_1/γ_2 data in the low concentration range. A new and simple method for obtaining the limiting slopes is proposed in this section.

7.2.2 Method

For binary systems the Clark equation[102] has been used successfully for representing the equilibrium composition data. Clark suggested that the ratio of the mole fractions in one phase is a linear function of the ratio of the mole fraction in the other phase when the ratios are used such that the components in large amounts appear in the numerator. Thus for high values of x_1

$$\frac{y_1}{y_2} = a\left(\frac{x_1}{x_2}\right) + b \qquad (7\text{-}13)$$

and high values of x_2

$$\frac{y_2}{y_1} = a'\left(\frac{x_2}{x_1}\right) + b' \qquad (7\text{-}14)$$

It has been shown by Lu, Li and Ting[103] that the Clark equation may be obtained from the general equation developed from the cluster theory.

It may readily be shown that from Equation (7-13)

$$\left(\frac{\partial y}{\partial x}\right)_{x_1=1} = \frac{1}{a} \qquad (7\text{-}15)$$

and similarly from Equation (7-14)

$$\left(\frac{\partial y}{\partial x}\right)_{x_1 = 0} = \frac{1}{a'} \tag{7-16}$$

The excellent representation of the experimental y - x data by means of Equations (7-13) and (7-14), especially in the low and high x regions, provides a simple and direct method for obtaining the limiting slope values.

As the constants a and a' are directly related to the ratios of the pure-component vapor pressures[104], they may be conveniently correlated with T in the following manner for a homologous series.

$$\log a = A + B/T \tag{7-17}$$

and

$$\log a' = A' + B'/T \tag{7-18}$$

An empirical method, which involves the Redlich-Kister relationships[65] and the van Laar equations as arranged by Carlson and Colburn[100], has been proposed earlier by Lu[104] for evaluating the constants b and b' of Equations (7-13) and (7-14).

7.2.3 Example

Vapor-liquid equilibrium data for the binary systems consisting of p-dioxane with n-hexane, n-octane and n-nonane were reported by Tassios and Van Winkle[101] at 80°C. Using these reported values, limiting slopes (1/a and 1/a') were obtained for the three binary systems, n-hexane - p-dioxane, n-octane - p-dioxane, and n-nonane - p-dioxane.

Logarithms of these values were plotted against 1/T in Figure 7-3, in which T refers to the normal boiling point of the n-alkanes in °K. From this plot, a and a' values were obtained for the binary system n-heptane - p-dioxane as follows:

$$a = 0.379$$
$$a' = 0.278$$

Values of b and b' for the binary system n-heptane - p-dioxane were therefore obtained by the empirical method of Lu[104] as follows:

$$b = 0.722$$
$$b' = 0.632$$

Using the predicted a, a', b and b' values, equilibrium compositions were calculated by means of Equations (7-13) and (7-14). The good agreement obtained between the predicted and the experimental equilibrium compositions is shown in Figure 7-4. It should be mentioned that in this procedure, the vapor phase was assumed to be ideal.

7.2.4 Discussion

For some systems, the three-constant Prahl[105] equation

$$y = \frac{c_3 x (c_1 - x)}{c_3 x (c_1 - x) + (1 - x)(c_2 + x)} \qquad (7\text{-}19)$$

or the equation proposed by Kretschmer and Wiebe[106]

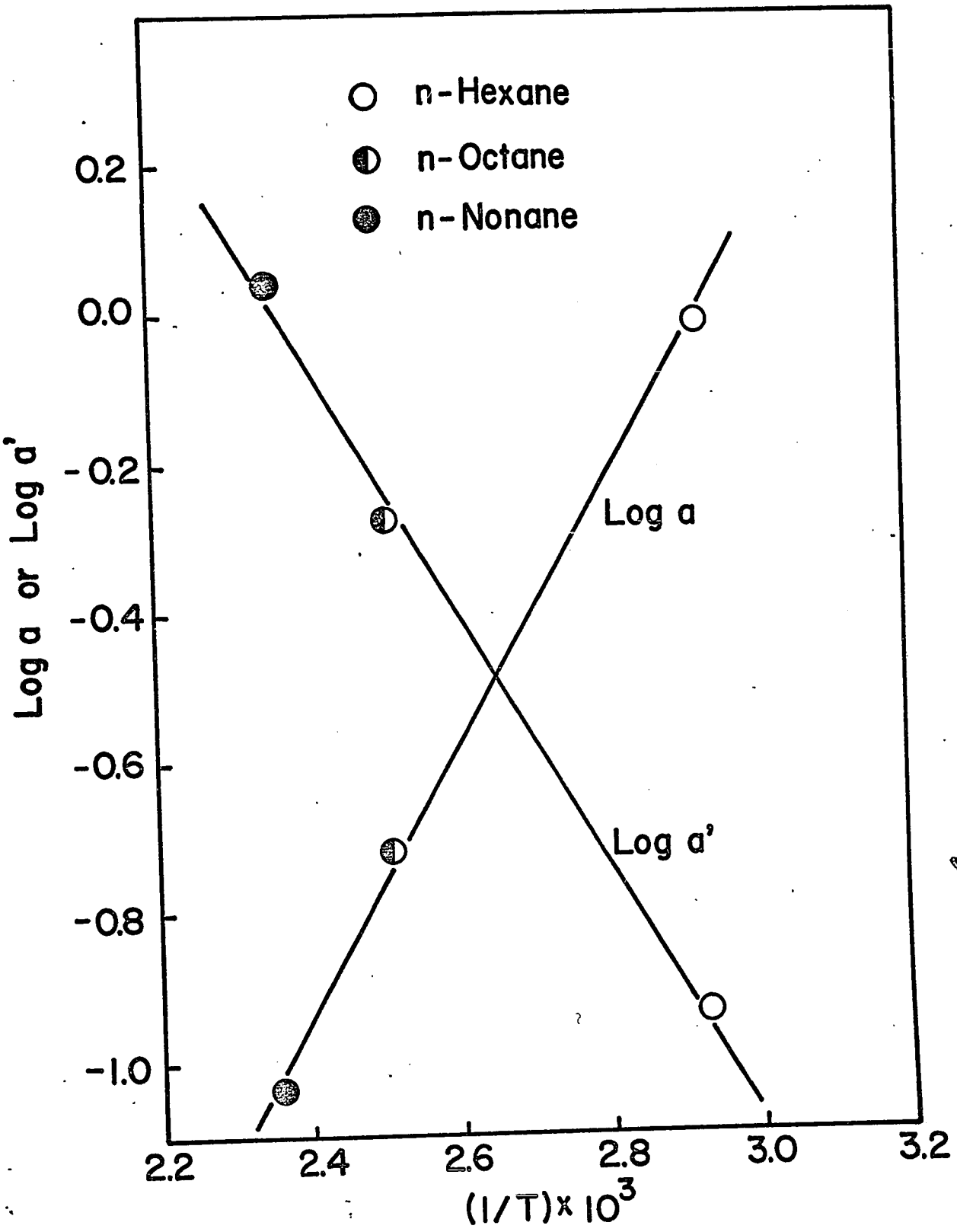

Figure 7-3 Correlation of log a and log a' with Temperature

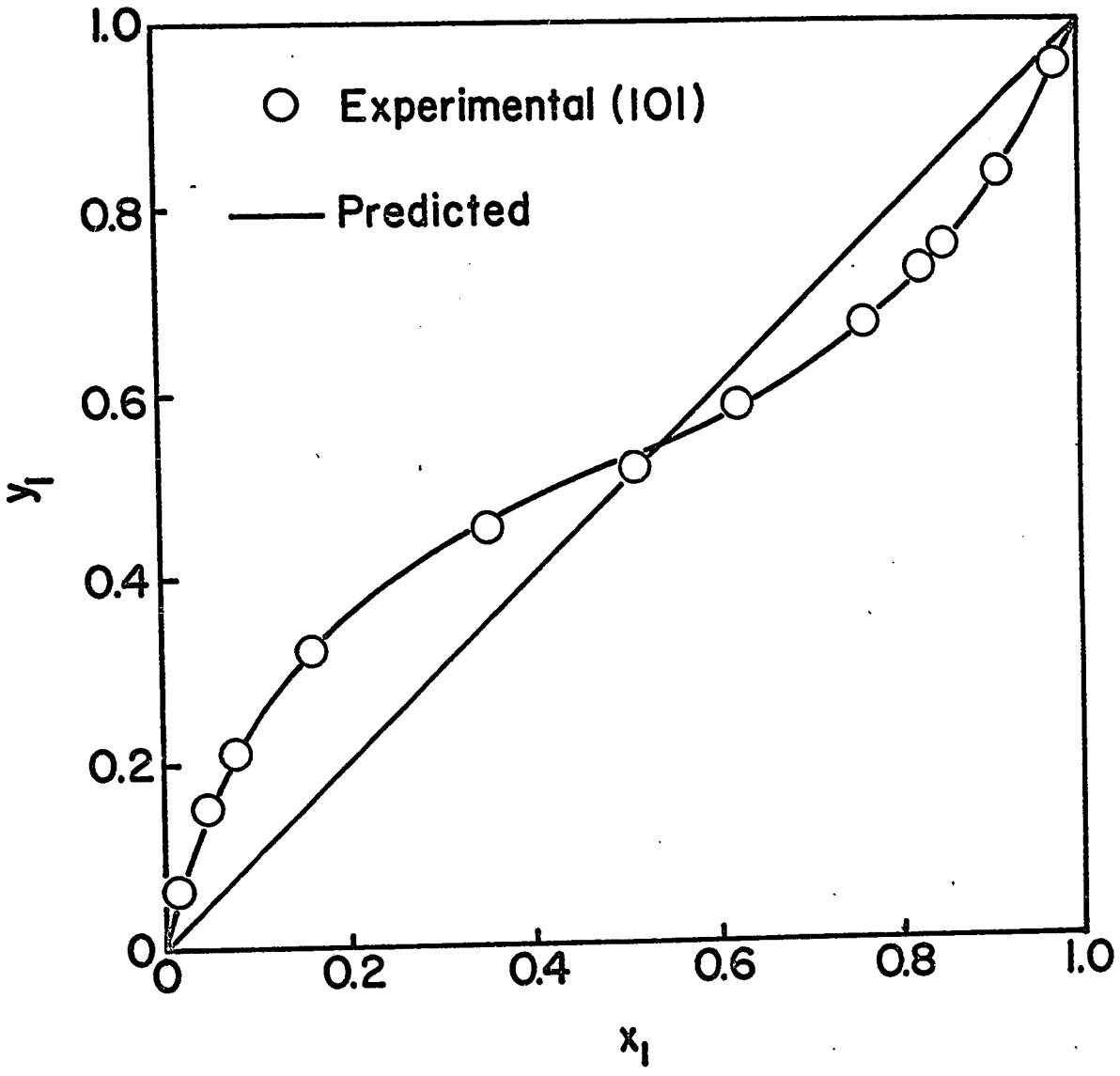

Figure 7-4 Comparison of Predicted and Experimental Equilibrium Compositions for the Binary System n-Heptane (1) - p - Dioxane (2) at 80°C

$$\frac{y_1}{y_2} = \frac{(d_1 - d_2 x_1)}{(x_1 + d_3)(1 - 2d_3 + d_3 x_1)} \cdot \frac{x_1}{x_2} \qquad (7\text{-}20)$$

may be more suitable for representing the equilibrium compositions over the complete concentration range. From Equation (7-19), one may obtain

$$\left(\frac{\partial y}{\partial x}\right)_{x_1 = 1} = \frac{c_2 + 1}{c_3 (c_1 - 1)} \qquad (7\text{-}21)$$

and

$$\left(\frac{\partial y}{\partial x}\right)_{x_1 = 0} = \frac{c_1 c_3}{c_2} \qquad (7\text{-}22)$$

Similarly from Equation (7-20)

$$\left(\frac{\partial y}{\partial x}\right)_{x_1 = 1} = \frac{1 - d_3^2}{d_1 - d_2} \qquad (7\text{-}23)$$

and

$$\left(\frac{\partial y}{\partial x}\right)_{x_1 = 0} = \frac{d_1}{d_3 (1 - 2d_3)} \qquad (7\text{-}24)$$

The predicted limiting slopes using a logarithmic relationship as in Equations (7-17) and (7-18) (i.e., $\log \left(\frac{\partial y}{\partial x}\right)_{x_1 = 0}$ and $\log \left(\frac{\partial y}{\partial x}\right)_{x_1 = 1}$ are linear functions of 1/T) may be substituted into Equations (7-21) and (7-22) or into Equations (7-23) and (7-24) to provide two of the three needed relations for obtaining the three constants. The logarithmic relationship is similar to the assumption made by Tassios and Van Winkle (Equation (8) of reference 101). The third one may be obtained by means of the Redlich-Kister relationship[65].

CHAPTER VIII

SUMMARY AND CONCLUSIONS

The Redlich-Kwong equation of state has been modified and employed for the prediction and extrapolation of industry-needed vapor-liquid equilibrium data.

A detailed calculation procedure for determination of the equilibrium vapor composition and saturated pressure of the system from the given liquid composition and system temperature was proposed. Its applicability was tested on eleven binary systems at eighteen isothermal conditions.

The experimental vapor-liquid equilibrium data were obtained by means of a forced-recirculation apparatus for the following systems:

(1) Methane-ethylene system at -193.1°, -173.1° and -156.1°F,

(2) Methane-ethane system at -173.1°F,

(3) Methane-ethylene-ethane system at -173.1°F.

These data were then employed for further justification of the proposed method.

The constant-pressure and constant-temperature liquid activity coefficients were evaluated for the experimental equilibrium data of the systems containing methane, ethylene, and ethane by means of the following equation:

$$\gamma_i = \frac{y_i \hat{\phi}_{iV} P}{x_i f^{\circ}_{iL}} \exp \int_{P}^{P^{\circ}} \frac{\bar{V}_i}{RT} dP$$

In the calculations, the modified Redlich-Kwong equation of state was again employed for evaluation of the necessary thermodynamic functions, f°_{iL}, $\hat{\varphi}_{iV}$, and $\bar{V}_i$. The reference pressure was taken as 500 p. s. i. a.

The γ values were then correlated by means of the Redlich-Kister relationships for both the binary and ternary systems. It was found that the limiting γ values are temperature-dependent for the methane-ethylene system. The limiting values of γ increase with decreasing temperature.

Because of the limitations of the available method, the Redlich-Kwong equation of state was extended to the supercritical region. Therefore, gas solubilities, volumetric properties, and phase equilibria of normal fluid mixtures involving one supercritical component can be predicted. The applicability was tested on a number of systems. In general, the method yields a satisfactory result of prediction except in the vicinity of the critical point.

In conclusion, the modified Redlich-Kwong equation of state with temperature-dependent parameters and empirically determined binary interaction constants is capable of predicting the gas solubilities, volumetric properties, and phase equilibria. It has been shown that the method is applicable to a wide range of temperature and pressure (temperatures from -200° F to 160° F and pressures from 20 mm. Hg. to 5000 p. s. i. a. have been illustrated in this investigation), and versatile constituents, such as paraffinic, olefinic, cyclic and aromatic hydrocarbons, and carbon dioxide, hydrogen sulfide and carbon tetrachloride non-hydrocarbons. It was also shown that a single binary interaction constant is sufficient to describe the interaction of two components and that binary interaction constants suffice

to describe all interactions in the studied ternary systems. This is particularly useful for engineering work where it is often necessary to predict from binary data the behaviour of a system containing more than two components.

The author wishes to stress that, although progress has been made in this investigation, further improvement can be expected. Such improvement should be directed toward predicting the binary interaction constant from pure molecular properties rather than from experimental binary equilibrium data, and making the interaction constant a temperature- or pressure-dependent parameter. It is also necessary to improve the prediction result in the critical region for future work in this field.

In addition, values of the excess enthalpy of mixing, excess Gibbs free energy of mixing, and excess entropy of mixing for the hydrogen-nitrogen binary system over the complete concentration range between 170° and 290°K and up to 95 atm. were evaluated by using a limited amount of information; and a method for determining the limiting slopes of the binary vapor-liquid equilibrium composition curve was also proposed.

REFERENCES

1. Redlich, O., and Kwong, J. N. S., Chem. Rev., 44, 233 (1949).

2. Shah, K. K., and Thodos, G., Ind. Eng. Chem., 57, No. 3, 30 (1965).

3. Wilson, G. M., Adv. in Cryog. Eng., 9, 168 (1964).

4. Wilson, G. M., Adv. in Cryog. Eng., 11, 392 (1966).

5. Chang, S. D., and Lu, B. C.-Y., Can. J. Chem. Eng., 48, 261 (1970).

6. Pitzer, K. S., Lippmann, D. Z., Curl, Jr., R. F., Huggins, C. M., and Petersen, D. E., J. Am. Chem. Soc., 77, 3427 (1955).

7. Prausnitz, J. M., "Molecular Thermodynamics of Fluid-Phase Equilibria", p. 128 (1969), Prentice-Hall, Inc., Englewood Cliffs, N. J.

8. Chang, S. D., Ph. D. thesis, University of Ottawa (1968).

9. Stewart, R. B., and Timmerhaus, K. D., Adv. in Cryog. Eng., 9, 20 (1964).

10. Martin, J. J., Ind. Eng. Chem., 59, No. 12, 34 (1967).

11. Tsonopoulos, C., and Prausnitz, J. M., Cryogenics, October, 315 (1969).

12. Benedict, M., Webb, G. B., and Rubin, L. C., J. Chem. Phys., 8, 334 (1940).

13. Benedict, M., Webb, G. B., and Rubin, L. C., J. Chem. Phys., 10, 747 (1942).

14. Benedict, M., Webb, G. B., and Rubin, L. C., Chem. Eng. Progr., 47, 419 (1951).

15. Benedict, M., Webb, G. B., and Rubin, L. C., Chem. Eng. Progr., 47, 449 (1951).

16. Benedict, M., Webb, G. B., Rubin, L. C., and Friend, L., Chem. Eng. Progr., 47, 571, 609 (1951).

17. M. W. Kellogg Company, "Liquid-Vapor Equilibria in Mixtures of Light Hydrocarbons", (1950).

18. DePriester, C. L., Chem. Eng. Progr. Symposium Ser., No. 7, 49, 1 (1953).

19. Schiller, F. C., and Canjar, L. N., Chem. Eng. Progr. Symposium Ser., No. 7, 49, 67 (1953).

20. Stotler, H. H., and Benedict, M., Chem. Eng. Progr. Symposium Ser., 49, 25 (1953).

21. Cullen, E. J., and Kobe, K. A., A. I. Ch. E. Journal, 1, 452 (1955).

22. Motard, R. L., and Organick, E. I., A. I. Ch. E. Journal, 6, 39 (1960).

23. Price, A. R., Leland, T. W., and Kobayashi, R., Chem. Eng. Progr. Symposium Ser., No. 21, 55 (1959).

24. Lin, M. -S., and Naphtali, L. M., A. I. Ch. E. Journal, 9, 580 (1963).

25. Zudkevitch, D., Schroeder, G. M., and Joffe, J., paper presented at the International Symposium on Distillation, Brighton, England (Sept. 8, 1969).

26. Hiza, M. J., Heck, C. K., and Kidnay, A. J., Adv. in Cryog. Eng. 13, 343 (1968).

27. Hiza, M. J., Heck, C. K., and Kidnay, A. J., Chem. Eng. Progr. Symposium Ser. 64, No. 88, 57 (1968).

28. Chao, K. C., and Seader, J. D., A. I. Ch. E. Journal, 7, 598 (1961).

29. Curl, R. F., Jr., and Pitzer, K. S., Ind. Eng. Chem., 50, 265 (1958).

30. Hildbrand, J. H., and Scott, R. L., "Solubility of Nonelectrolytes", 3rd ed., Reinhold Publishing Corp., New York, N. Y., (1950).

31. Grayson, H. G., and Streed, C. W., paper 20-PD7, Sixth World Petroleum Conference, Frankfurt, June (1963).

32. Wilson, G. M., Paper presented at the 65th National AIChE Meeting, Cleveland, Ohio, 1969 (quated from reference No. 11).

33. Chang, H. L., Chappelear, P. S., and Kobayashi, R., A. I. Ch. E. Journal, 14, 318 (1968).

34. Guggenheim, E. A., Proc. Roy. Soc. (London), A183, 203 (1944).

35. Miller, A. R., Proc. Cambridge Phil. Soc., 39, 54 (1943).

36. Chueh, P. L., and Prausnitz, J. M., Ind. Eng. Chem., 60, 34 (1968).

37. Zudkevitch, D., and Joffe, J., A. I. Ch. E. Journal, 16, 112 (1970).

38. Lyckman, E. W., Eckert, C. A., and Prausnitz, J. M., Chem. Eng. Sci., 20, 685 (1965).

39. Joffe, J., Schroeder, G. M., and Zudkevitch, D., A. I. Ch. E. Journal, 16, 496 (1970).

40. Dodge, B. F., "Chemical Engineering Thermodynamics", p. 111, McGraw-Hill Book Company, Inc., New York, N. Y., 1944.

41. Prausnitz, J. M., and Chueh, P. L., "Computer Calculations for High-Pressure Vapor-Liquid Equilibria", p. 6, Prentice-Hall, Inc., Englewood Cliffs, N. J., 1968.

42. Denbigh, K., "The Principles of Chemical Equilibrium", p. 123, Cambridge University Press, London, N. W. 1, 1961.

43. Beattie, J. A., Chem. Rev., 44, 141 (1949).

44. Prausnitz, J. M., A. I. Ch. E. Journal, 5, 3 (1959).

45. Scatchard, G., Wood, S. E., and Machel, J. M., J. Phys. Chem., 43, 119 (1939).

46. Nysewander, C. N., Sage, B. H., and Lacey, W. N., Ind. Eng. Chem., 32, 118 (1940).

47. Sage, B. H., and Lacey, W. N., Ind. Eng. Chem., 32, 992 (1940).

48. Reamer, H. H., and Sage, B. H., J. Chem. Eng. Data, 11, 17 (1966).

49. Joffe, J., and Zudkevitch, D., Ind. Eng. Chem. Fundamentals, 5, 455 (1966).

50. Reamer, H. H., Sage, B. H., and Lacey, W. N., Ind. Eng. Chem., 43, 2515 (1951).

51. Robinson, D. B., Hughes, R. E., and Sandercock, J. A. W., Can. J. Chem. Eng., 42, 143 (1964).

52. Reamer, H. H., Sage, B. H., and Lacey, W. N., J. Chem. Eng. Data, 5, 44 (1960).

53. Djordjevich, L., and Budenholzer, R. A., J. Chem. Eng. Data, 15, 10 (1970).

54. Price, A. R., and Kobayashi, R., J. Chem. Eng. Data, 4, 40 (1959).

55. Hanson, G. H., Hogan, R. J., Ruehlen, F. N., and Cines, M. R., Chem. Eng. Progr. Symposium Ser., No. 6, 49, 37 (1953).

56. Ellington, R. T., Eakin, B. E., Parent, J. D., Gami, D. C., and Bloomer, O. T., "Thermodynamic and Transport Properties of Gases, Liquids and Solids", p. 180 (A. S. M. E.), McGraw-Hill Co., New York, N. Y., (1959).

57. Bloomer, O. T., Gami, D. C., and Parent, J. D., Inst. Gas. Tech. Research Bull., No. 22, Chicago, Ill. (1953).

58. Guter, M., Newitt, D. M., and Ruhemann, M., Proc. Roy. Soc. (London), A176, 140 (1940).

59. Volova, I. M., J. Phys. Chem. (U. S. S. R.), 14, 268 (1940).

60. Mark, H. F., McKetta, J. J. Jr., Othmer, D. F., "Kirk-Othmer Encyclopedia of Chemical Technology", Second Ed., Vol. 8, p. 511, Interscience Publishers, New York (1965).

61. Din, F., "Thermodynamic Function of Gases", Vol. 3, Butterworth, London, England, (1961).

62. Dreisbach, R. R., "Advances in Chemistry Series", Vol. 22, American Chemical Society, Washington, D. C. (1959).

63. Rossini, F. D., Pitzer, K. S., Arnet, R. L., Brown, R. M., Pimental, G. C., "Selected Values of Physical and Thermodynamic Properties of Hydrocarbons and Related Compounds", Carnegie Press, Pittsburgh, Pa., (1953).

64. Prausnitz, J. M., Chem. Eng. Sci., 18, 613 (1963).

65. Redlich, O., and Kister, A. T., Ind. Eng. Chem., 40, 345 (1948).

66. Fu, S. J., M. Sc. Thesis, University of Ottawa, 1966.

67. McCurdy, J. L., Katz, D. L., Ind. Eng. Chem., 36, 675 (1944).

68. Lu, B. C. -Y., Chang, S. -D., Elshayal, I. M., Yu, P., Gravelle, D., Poon, D. P. L., proceedings of the First International Conference on Calorimetry and Thermodynamics, paper Q2, August 31 - September 4, 1969, Warsaw, Poland.

69. Reamer, H. H., Sage, B. H., and Lacey, W. N., Ind. Eng. Chem., 42, 534 (1950).

70. Lannung, A., and Gjaldbaek, J. Chr., Acta. Chem. Scand., 14, 1124 (1960).

71. Gjaldbaek, J. Chr., Acta. Chem. Scand., 7, 537 (1953).

72. Sage, B. H., Hicks, B. L., and Lacey, W. N., Ind. Eng. Chem., 32, 1085 (1940).

73. Wiese, H. C., Jacobs, J., and Sage, B. H., J. Chem. Eng. Data, 15, 82 (1970).

74. Sage, B. H., Reamer, H. H., Olds, R. H., and Lacey, W. N., Ind. Eng. Chem., 34, 1108 (1942).

75. Shim, J., and Kohn, J. P., J. Chem. Eng. Data, 7, 3 (1962).

76. Reamer, H. H., Sage, B. H., and Lacey, W. N., Ind. Eng. Chem., Chem. and Eng. Data Series, 1, 29 (1956).

77. Reamer, H. H., Sage, B. H., and Lacey, W. N., Ind. Eng. Chem., 43, 976 (1951).

78. Carter, R. T., Sage, B. H., and Lacey, W. N., Trans. Am. Inst. Mining Met. Engrs., 142, 170 (1941).

79. Dourson, R. H., Sage, B. H., and Lacey, W. N., Trans. Am. Inst. Mining Met. Engrs., 151, 206 (1943).

80. Kohn, J. P., and Bradish, W. F., J. Chem. Eng. Data, 9, 5 (1964).

81. Shipman, L. M., and Kohn, J. P., J. Chem. Eng. Data, 11, 176 (1966).

82. Beaudoin, J. M., and Kohn, J. P., J. Chem. Eng. Data, 12, 189 (1967).

83. Gjaldbaek, J. Chr., and Hildebrand, J. H., J. Am. Chem. Soc., 71, 1077 (1950).

84. Reamer, H. H., and Sage, B. H., J. Chem. Eng. Data, 4, 98 (1959).

85. Prausnitz, J. M., and Chueh, P. L., "Computer Calculations for High-Pressure Vapor-Liquid Equilibria", p. 20, Prentice-Hall, Inc., Englewood Cliffs, N. J., 1968.

86. Gunn, R. D., Chueh, P. L., and Prausnitz, J. M., A. I. Ch. E. Journal, 12, 937 (1966).

87. Bloomer, O. T., and Rao, K. N., Inst. of Gas Tech., Research Bulletin No. 18, (Oct. 1952).

88. Dean, F., Natl. Bureau of Standards, Technical Note, No. 120 (Nov. 1961).

89. Mage, D. T., Jones, M. L., Jr., Katz, D. L., and Roebuch, J. R., Chem. Eng. Progr. Symposium Ser., No. 44, 59, 61 (1963).

90. Pfenning, D. B., and Canfield, F. B., Document No. 7864, Am. Documentation Inst., Lib. Congr., Washington, D. C.

91. Michels, A., de Groot, S. R., and Lunbeck, R. J., Appl. Sci. Res., A1, 378 (1949).

92. Michels, A., and Wassenaar, T., Appl. Sci. Res., A1, 258 (1949).

93. Wiebe, R., and Gaddy, V. L., J. Am. Chem. Soc., 60, 2300 (1938).

94. Beenakker, J. J. M., Van Eijnsbergen, B., Knoester, M., Taconis, K. W., Zandbergen, P., "Advances in Thermophysical Properties at Extreme Temperatures and Pressures", 3rd Symposium on Thermophysical Properties, ASME, p. 114 (1965).

95. Knoester, M., Taconis, K. W., and Beenakker, J. J. M., Physica, 33, 389 (1967).

96. Zanderbergen, P., and Beenakker, J. J. M., Physica, 33, 343 (1967).

97. Deshpande, A. K., and Lu, B. C. -Y., Can. J. Chem. Eng., 41, 84 (1963).

98. Jones, H. K., and Lu, B. C. -Y., J. Chem. Eng. Data, 11, 488 (1966).

99. Van Ness, H. C., "Classical Thermodynamics of Nonelectrolyte Solutions", p. 122, MacMillan Co., New York, 1964.

100. Carlson, H. C., and Colburn, A. P., Ind. Eng. Chem., 34, 581 (1942).

101. Tassios, D., and Van Winkle, M., J. Chem. Eng. Data, 12, 555 (1967).

102. Clark, A. M., Trans. Faraday Soc., 41, 718 (1945).

103. Lu, B. C. -Y., Li, J. C. M., and Ting, T. -W., Ind. Eng. Chem., 51, 219 (1959).

104. Lu, B. C. -Y., A. I. Ch. E. Journal 2, 525 (1956).

105. Prahl, W. H., Ind. Eng. Chem., 43, 1767 (1951).

106. Kretschmer, C. B., and Wiebe, R., J. Am. Chem. Soc., 71, 1793 (1949).

APPENDIX A

Table A-1 Critical Constants and Accentric Factor of Pure Fluids

Table A-2 Values of Ω_a and Ω_b

Table A-3 Binary Interaction Constants k_{12}

TABLE A-1

Critical Constants and Acentric Factor of Pure Fluids

Component	Pc, atm	Vc, ml/g-mole	Tc, °K	ω
Methane	45.8	98.72	191.06	0.013
Ethylene	49.98	127.64	282.66	0.085
Ethane	48.50	141.72	305.50	0.105
Propane	42.10	195.70	370.00	0.152
n-Butane	37.47	254.71	425.17	0.201
n-Pentane	33.27	310.89	469.78	0.252
n-Hexane	29.94	368.50	507.60	0.290
n-Heptane	27.01	425.76	540.17	0.349
n-Octane	24.63	490.06	569.39	0.398
n-Nonane	22.50	543.00	594.60	0.441
n-Decane	20.80	602.00	617.60	0.586
Cyclohexane	40.00	308.28	553.00	0.211
Benzene	48.60	256.69	562.20	0.215
Carbon tetrachloride	45.00	276.00	556.40	0.202
Carbon dioxide	72.90	94.00	304.20	0.225
Hydrogen sulfide	88.90	97.70	373.60	0.100

TABLE A-2

Values of Ω_a and Ω_b

Component	T, °K	Ω_a	Ω_b
Ethane	283.16	0.40222	0.077832
	255.39	0.41212	0.080103
	227.61	0.41833	0.081929
	199.83	0.42151	0.083533
	172.05	0.41834	0.084159
	159.20	0.41499	0.084302
Ethylene	199.83	0.42085	0.083485
	184.56	0.41950	0.083751
	169.16	0.41665	0.083837
	168.69	0.41649	0.083827
	159.20	0.41381	0.083786
	148.13	0.40980	0.083665
	127.10	0.40157	0.083310
Propane	344.26	0.40548	0.078399
	310.93	0.41515	0.079876
	283.16	0.42236	0.081187
	255.39	0.42651	0.081918
	227.61	0.42715	0.082295
	199.83	0.42292	0.082059
	172.05	0.41580	0.081792
n-Butane	344.26	0.41831	0.079053
	310.93	0.42697	0.080206
	294.44	0.42850	0.080326
	277.59	0.43216	0.080956
n-Pentane	344.26	0.43155	0.079427
	310.93	0.43481	0.079369
	277.59	0.43510	0.079081
n-Hexane	310.16	0.44285	0.078134
	298.16	0.44372	0.078023
	291.16	0.44352	0.077934
	273.16	0.44662	0.077803
	223.16	0.43734	0.076671
	198.16	0.43069	0.076025

(... continuation...) Table A-2

Component	T, °K	Ω_a	Ω_b
n-Heptane	344.26	0.44439	0.076623
	310.93	0.44891	0.076325
	277.59	0.44196	0.075655
n-Octane	323.16	0.45388	0.075070
	298.16	0.44962	0.074515
	248.16	0.45057	0.073432
	223.16	0.44562	0.072693
n-Nonane	298.16	0.45907	0.072872
n-Decane	344.26	0.41831	0.079053
	310.93	0.48626	0.073278
	298.16	0.46622	0.071613
Hydrogen Sulfide	277.59	0.42030	0.082641
	310.93	0.41611	0.081686
Carbon Dioxide	277.59	0.40772	0.077838
Cyclo-Hexane	343.14	0.43524	0.080835
	313.15	0.43488	0.080623
	310.16	0.43456	0.080553
	298.16	0.43394	0.080438
	291.16	0.43344	0.080361
Benzene	343.14	0.43086	0.079883
	313.15	0.42996	0.079630
	310.16	0.42291	0.079626
	298.16	0.42893	0.079454
	291.16	0.42823	0.079344
Carbon Tetrachloride	298.16	0.42913	0.080306

TABLE A-3

Binary Interaction Constants, k_{12}

System (1)	System (2)	k_{12} this work	k_{12} Chueh and Prausnitz
methane	ethylene	0.0066	0.01
	ethane	0.0070	0.01
	propane	0.019	0.02
	n-butane	0.0398	0.04
	n-pentane	0.0474	0.06
	n-hexane	0.0623	0.08
	n-heptane	0.0705	0.10
	n-octane	0.0840	0.12
	n-nonane	0.0960	-
	n-decane	0.118	-
	cyclohexane	0.0720	0.08
	benzene	0.0760	0.08
	carbon tetrachloride	0.0603	-
	hydrogen sulfide	0.050	0.05 ± 0.01
ethane	ethylene	0.0	0.0
	propane	-0.015*, -0.025**	0.0
	n-pentane	0.0098	0.02
propane	n-butane	0.0	0.0
	n-pentane	0.006	0.01
	n-decane	0.045	-
	carbon dioxide	0.095	0.11 ± 0.01
n-butane	hydrogen sulfide	0.062	0.090
benzene	cyclohexane	0.0095	-

* evaluated from the data of Price and Kobayashi[54]

** evaluated from the data of Djordjevich and Budenholzer[53]

APPENDIX B

Method for Evaluation of the Temperature-Dependent Parameters, Ω_a and Ω_b, for a Subcritical Component[5].

Evaluation of Ω_a and Ω_b

The method developed by Chang and Lu[5] for evaluation of the temperature-dependent parameters, Ω_a and Ω_b, of the Redlich-Kwong equation of state in the subcritical region is presented in the following:

At equilibrium

$$f_{iV} = f_{iL} \tag{B-1}$$

or in terms of fugacity coefficient

$$\varphi_{iV} = \varphi_{iL} \tag{B-2}$$

The quantity φ_{iV} and φ_{iL} for a pure component may be obtained from the following equations:

$$\ln \varphi_V = Z_V - 1 - \ln Z_V - \ln (1 - h_V) - (A^2/B) \ln (1 + h_V) \tag{B-3}$$

and

$$\ln \varphi_L = Z_L - 1 - \ln Z_L - \ln (1 - h_L) - \left(\frac{A^2}{B}\right) \ln (1 + h_L) \tag{B-4}$$

Combining Equation (B-4) with Equation (B-2) and the Redlich-Kwong equation (Equations (3-7) and (3-8)) gives

$$\ln Z_L \varphi_V + 1 - Z_L + \ln (1 - h_L) + \frac{(1 - Z_L (1 - h_L)) (1 + h_L)}{h_L (1 - h_L)} \cdot \ln (1 + h_L) = 0 \tag{B-5}$$

These equations were employed in the evaluation of Ω_a and Ω_b. The calculation procedure may be briefly outlined as follows:

(1) For a given value of Z_L, and assumed value of φ_V, calculate h_L by means of Equation (B-5).

(2) Calculate B from Equation (3-8) and A from Equation (3-7).

(3) Substitute A and B values obtained from step 2 into Equations (3-7) and (3-8) and solve simultaneously for another set of roots of Z_V and h_V. (As there are three roots of h in Equation (3-7), the largest root is h_L and smallest one is h_V. The approximate numerical values are in the ranges of 0.95 to 0.4 and 0.0 to 0.14 for h_L and h_V respectively. In this investigation, the roots were located by means of the Newton's rule which is quadratically convergent).

(4) Calculate φ_V from Equation (B-3).

(5) Obtain new h_L value from Equation (B-5) and compare it with that obtained in step 1. If not in agreement, repeat the steps 1-5 using the new value of φ_V obtained from step 4.

An iteration loop is thus built up until the change of h_L value is less than the specified tolerance. The final set of A and B values are used to obtain Ω_a and Ω_b values from Equations (3-9) and (3-10), respectively. The tolerance used in this investigation is 0.00005.

The schematic diagram for finding Ω_a and Ω_b by equalizing f_{iV} and f_{iL} is shown in Figure B-1. The computer program is given in APPENDIX C.

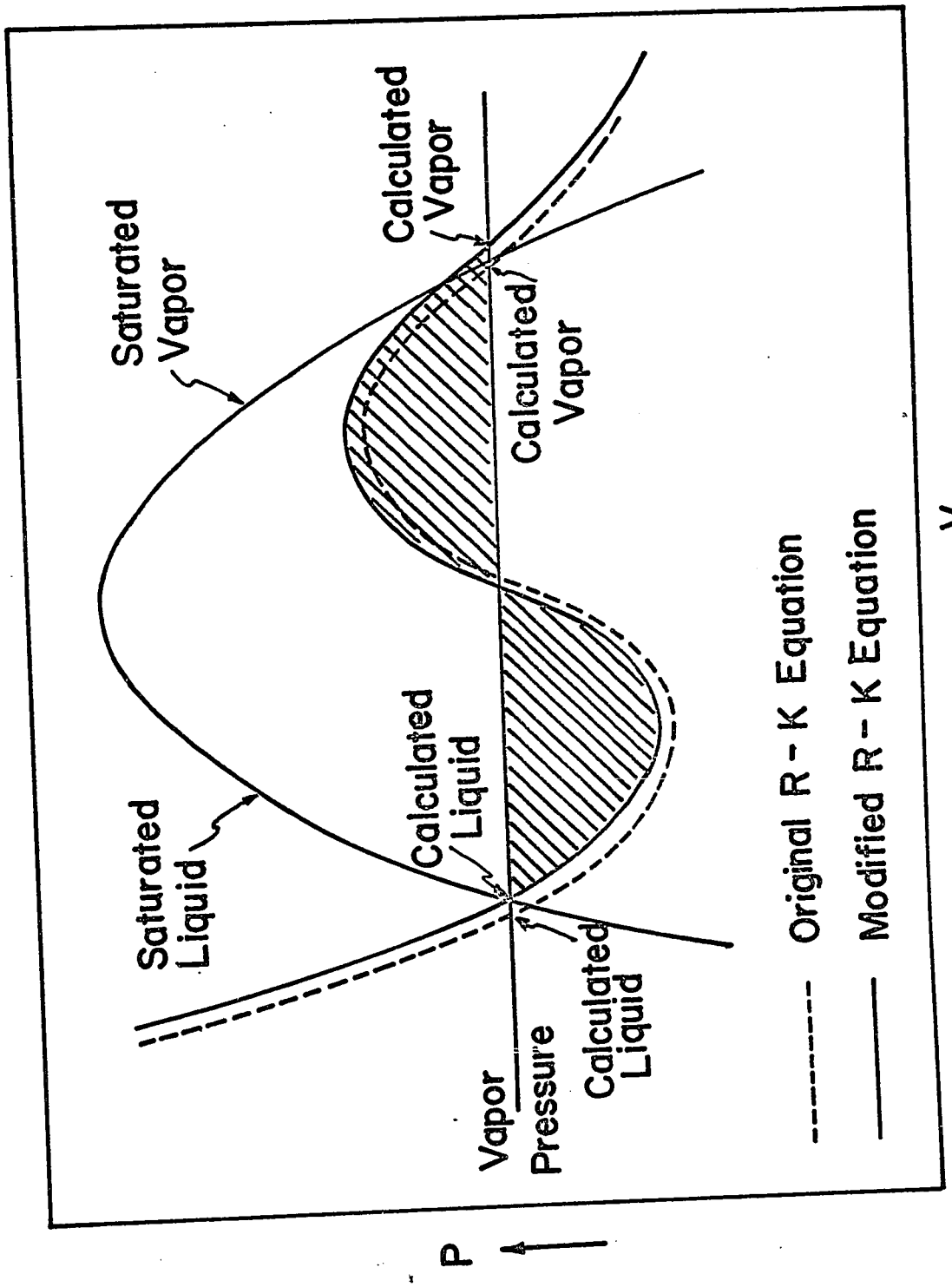

Figure B-1 Schematic Diagram for Comparison of Original and Modified R-K Equation of State

APPENDIX C

COMPUTER PROGRAMS

C-1 Evaluation of Ω_a and Ω_b

C-2 Prediction of Phase Behaviour, Solubilities and Volumetric Properties

C-3 Evaluation of Activity Coefficients

C-4 Evaluation of Supporting Properties (SUBROUTINE SUPT)

C-5 Fitting the Redlich-Kister Equation for Binary System

C-6 Fitting the Redlich-Kister Equation for Ternary System

C-7 Evaluation of Activity Coefficients for Ternary System with the Redlich-Kister Constants

C-1 Evaluation of Ω_a and Ω_b

```
C       EVALUATION OF THE ADJUSTABLE PARAMETER OF  THE REDLICH-KWONG EQUATION
C       OF STATE BY IMPOSING MAXWELL CONDITION.
C       THIS PROGRAM IS SUPPIED BY S. D. CHANG
C       CHU HSI (CHEMICAL ENGINEERING)
C       SEPTEMBER 17,1969.
C       R-K A,B ---VI
C       SUBROUTINE FUG IS REQUIRED.
      DIMENSION TITLE(20),X(8)
      DIMENSION TT(50)
    1 READ(1,300)(TITLE(I),I=1,15)
  300 FORMAT(20A4)
      WRITE(3,400)(TITLE(I),I=1,15)
  400 FORMAT(1H1,10X,51HEVALUATION OF ADJUSTABLE PARAMETERS OF R-K EQN F
     1OR ,15A4///)
      NOBS=3
   10 READ(1,100)PC,VC,TC,W,R,TOL
      IF(PC.LE.0.0)GO TO 800
  100 FORMAT(8F10.4)
      SDTHI=0.0
      SDZV=0.0
      WA=0.4278
      WB=0.0867
   20 READ(1,100)P,V,T,VL
      PR=P/PC
      TR=T/TC
      BATA=(ALOG10(PR)-ALOG10(TR)*8./3.-0.1832*(PR/TR/TR-1.0))/
     1((1.-TR)/TR+ALOG10(TR)*1.8)
      READ(1,100)P,V,T,VL
      TR=T/TC
      ALFA=(VC/VL-1.0-(1.-TR)**(1./3.))/((1.-TR)+(1.-TR)**(1./3.))
      READ(1,100) (TT(I),I=1,NOBS)
      WRITE(3,100)ALFA,BATA
      DO 80 I=1,NOBS
      T=TT(I)
      RT=R*T
      TR=T/TC
      CALL PFK(BATA,TR,PR)
      P=PR*PC
      VL=VC/(1.+ALFA*(1.-TR)+(1.+ALFA)*(1.-TR)**(1./3.))
      V=R*T/P
      ZL=P*VL/R/T
      ZV=P*V/R/T
      A2=WA*TC**2.5/PC/T**2.5
```

```
      B=WB*TC/PC/T
      H=B*P/ZL
      E=B*P/ZV
      CALL FUG(W,PR,TR,THI)
      THI=EXP(2.30259*THI)
C     WRITE(3,100)T,P,VL,V,THI
      ZLL=ZL
      ZVV=ZV
      THIL=THI
      THIV=THI
      HOLD=H
      IJK=0
   39 IJK=IJK+1
      IF(IJK.GE.30) GO TO 49
      J=0
   40 CONTINUE
      IH=0
   41 IF (H.LT.1.0) GO TO 42
      H=H-0.05
      IH=IH+1
      IF(IH.LT.20) GO TO 41
   43 H=0.98
   42 J=J+1
      RH=(1.-ZL*(1.-H))*(1.+H)*ALOG(1.+H)/H/(1.-H)
      FFH=ALOG(ZL*THIV)+1.0-ZL+ALOG(1.-H)+RH
      DFFH=-1./(1.0-H)+RH*(ZL/(1.-ZL*(1.-H))
     1   +(-1.+2.*H+H*H)/H/(1.-H*H)+1./(1.+H)/ALOG(1.+H))
      TEST=FFH/DFFH
      H=H-TEST
      IF(J.GT.40)GO TO 45
      IF(ABS(TEST/H).GT.TCL)GO TO 40
   45 B=H*ZL/P
      A2=B*(1./(1.-H)-ZL)*(1.0+H)/H
      IJ=0
   47 IF(E.GT.0.0) GO TO 46
      E=E+0.01
      IH=IH+1
      IF(IH.LT.20)GO TO 47
      E=0.02
   46 IJ=IJ+1
      IH=0
      FE=-B*P/E+1./(1.0-E)-(A2/B)*E/(1.+E)
      DFE=B*P/E**2+1./(1.-E)**2-(A2/B)/(1.+E)**2
```

```
      TEST=FE/DFE
      E=E-TEST
      IF(IJ.GT.40)GO TO 48
      IF (ABS(TEST/E).GT.TOL)GO TO 47
   48 ZVV=B*P/E
      THIV=ZVV-1.0-ALOG(ZVV*(1.0-E))-(A2/B)*ALOG(1.+E)
      THIV=EXP(THIV)
      WRITE(3,501) J,IJ,IJK
  501 FORMAT(3I5)
      IF(ABS(H-HOLD)/H.LE.TOL*10.)GO TO 49
C     WRITE(3,200)P,T,ZV,ZVV,VL,VLL,THIV,THIL,WA,WB,THI,H,E
      HOLD=H
      GO TO 39
   49 ZLL=B*P/H
      VLL=R*T*ZLL/P
      THIL=ZLL-1.0-ALOG(ZLL-B*P)-(A2/B)*ALOG(1.+B*P/ZLL)
      THIL=1./EXP(-THIL)
      WB=B*PC*T/TC
      WA=A2*PC*T**2.5/TC**2.5
  500 FORMAT(I5,3F10.4,5F10.6)
      DTHI=THI-THIV
      DZV=ZV-ZVV
      SDTHI=SDTHI+ABS(DTHI)
      SDZV=SDZV+ABS(DZV)
   51 WRITE(3,200)P,T,ZV,ZVV,VL,VLL,THIV,THIL,WA,WB,THI,H,E
  200 FORMAT(1H ,F10.4,F8.2,6F9.5,2F10.6,2F8.4,E11.4)
   80 CONTINUE
      ADTHI=SDTHI/NOBS
      ADZV=SDZV/NOBS
      WRITE(3,311) ADTHI,ADZV
      GO TO 1
  311 FORMAT(//20X,'AV. DEV. IN FUGACITY = 'F10.4
     1   ,'AV. DEV. IN ZV = ' F10.4/)
  800 STOP
      END
```

```
      SUBROUTINE FUG(W,PR,TR,THI)
C     GENERALIZED CORRELATION OF FUGACITY COEFFICIENT OF PURE
C     COMPONENTS AT SATURATION.
C     CHU HSI ,CHEMICAL ENGINEERING
C     SEPTEMBER 17, 1969
   10 IF(TR.GT.0.56) GO TO 20
      THI=(PR/2.303)*((.1445-(.330+(.1385+(.0121)/TR)/TR)/TR)/TR
     1+W*(.073+(.460-(.5+(.097+.0073/TR**5)/TR)/TR)/TR)/TR)
      RETURN
   20 IF(TR.GT.0.70) GO TO 30
      THI=(-.53746+(.58798-(.18226-.009499/TR)/TR)/TR)
     1+W*(.11821-(.006542+(.045992-.0116504/TR)/TR)/TR)
      RETURN
   30 IF (TR.GT.0.84) GO TO 40
      THI=(-.65625+(.47890+(.13943-.12167/TR)/TR)/TR)
     1+W*(-.47886+(.53604+(.08951-.14448/TR)/TR)/TR)
      RETURN
   40 THI=(-0.87471+(0.73459-(0.11130-(0.27772-0.20204/TR)/TR)/TR)/TR)
     1+W*(-1.15987+(1.25872-(.13670-(.35086-.34700/TR)/TR)/TR)/TR)
      RETURN
      END
```

```
      SUBROUTINE PFK(BATA,TR,PR)
      ITER=0
      TOL=0.00001
      PRC=-0.1832
   30 PR=BATA*(1.-TR)/TR+(1.8*BATA+8./3.)*ALOG10(TR)+PRC
      PRC=0.1832*(EXP(PR*2.30259)/TR/TR-1.0)
      ITER=ITER+1
      IF(ITER.GT.20) GO TO 32
      IF(ITER.EQ.1) GO TO 31
      IF(ABS((PR-PROLD)/PR).LT.TOL) GO TO 32
   31 PROLD=PR
      GO TO 30
   32 PR=EXP(PR*2.30259)
      RETURN
      END
```

C-2 Prediction of Phase Behaviour, Solubilities and Volumetric Properties

```
C       PREDICT P-X-Y CURVE
C       MODIFIED REDLICH-KWONG EQUATION OF STATE IS USED
C       FOR MULTICOMPONENT  SYSTEMS CALCULATION
C       FROM THE PURE COMPONENT PROPERTIES
C       ONE OF THE COMPONENTS IS AT ITS HYPERCRITICAL STATE
C       WRITTEN BY CHU HSI ,CHEMICAL ENGINEERING DEPARTMENT, UNIV. OF OTTAWA
C       SUBROUTINES SUPT,EQNRK, CUBEQN ARE SUPPLIED BY S.D.CHANG
C       JANUARY 14,1970
        DIMENSION PHI(5),X(5), F( 5),GAMMA(5),FREFER(5),PVOL(5),Y(5),
       1 PC(5),VC(5),TC(5),W(5),C1RKV(5),C2RKV(5),C1RKL(5),C2RKL(5),
        2 AMOLWT(5),COMPA(5),COMPB(5),CORRV(5,5),CORRL(5,5),GAMALN(5),
        3 A(4),Z(3),TITLE(20),D(5),PCO(5),VCO(5),TCO(5),PHIV(5),FREF(5),
        4 PS(5),PP(50),XX(50,5),YY(50,5),YCAL(5),PPVOL(5),DC1DT(5),DC2DT(5),
        5,YD(5),RATIO(5),VVL(50)
        COMMON  /FIRST/ TC,PC,VCO,W,AMOLWT,T,P,R,NCOMP,NQNTUM
       1    /SECOND/ Z,A,MTYPE
  800 READ(1,5)(TITLE(I),I=1,19)
    6 FORMAT(1H1,19A4)
    5 FORMAT(     19A4)
        WRITE(3,6)(TITLE(I),I=1,19)
        READ(1,500)NCOMP,NQNTUM,IJK,R
        IF(NCOMP.LE.0) GO TO 900
        WRITE(3,505)
        DO 210 I=1,NCOMP
        READ(1,510)PCO(I),VCO(I),TCO(I),W(I),C1RKL(I),C2RKL(I),
       1                                 COMPA(I),COMPB(I)
        C1RKV(I)=C1RKL(I)
        C2RKV(I)=C2RKL(I)
  210 WRITE(3,515)PCO(I),VCO(I),TCO(I),W(I),C1RKL(I),C2RKL(I),
       1                                 COMPA(I),COMPB(I)
        CORRL(NCOMP,NCOMP)=0.0
        NCOMP1=NCOMP-1
        WRITE(3,519)
  519 FORMAT(/10X,12HINPUT DATA :///4X,1HP,8X,2HX1,8X,2HX2,9X,1HT,7X,3HRA
       11,7X,3HRB1,7X,3HRA2,7X,3HRB2//)
        DO 9 I=1,NCOMP1
        I1=I+1
        DO 9 J=I1,NCOMP
    9 READ(1,520)CORRL(I,J)
        READ(1,520) TTT,PSI
        I=0
   10 I=I+1
        SX=0.0
```

```
      SY=0.0
C     READ(1,520)TTT,PP(I),(XX(I,J),J=1,NCOMP),(YY(I,J),J=1,NCOMP)
      READ( 1,520) PP(I),(XX(I,J),J=1,NCOMP1),(YY(I,J),J=1,NCOMP1)
     1 ,VVL(I)
      DO 15 J=1,NCOMP1
      SY=SY+YY(I,J)
   15 SX=SX+ XX(I,J)
      XX(I,NCOMP)=1.0-SX
      YY(I,NCOMP)=1.0-SY
      IF(R.LT.11.0) GO TO 16
C     PP(I)=PP(I)/760.
      PP(I)=PP(I)/14.697
      PSI=PSI/14.697
C     PSI=PSI/760.
   16 WRITE(3,520) PP(I),(XX(I,J),J=1,NCOMP ),(YY(I,J),J=1,NCOMP )
     1 ,VVL(I)
      IF(PP(I).GE.0) GO TO 10
   20 NOBS=I-1
      READ(1,525)IJK,KIJ,CINI,CFIN
  525 FORMAT(2I5,2F10.4)
   30 KIJ=KIJ+1
      IF(KIJ.GE.2) GO TO 800
      WRITE(3,525)IJK,KIJ,CINI,CFIN
      K=0
      KK=0
      KK=20
  280 CONTINUE
      WRITE(3,6)(TITLE(I),I=1,19)
      KK=KK+1
      WRITE(3,516)
      DO 220 I=1,NCOMP1
      CORRL(I,I)=0.0
      I1=I+1
      DO 220 J=I1,NCOMP
      IF(KK.GE.20) GO TO 214
      CORRL(I,J)=CINI+(KK-1)*(CFIN-CINI)/10.
  214 WRITE(3,530)I,J,CORRL(I,J)
      CORRL(J,I)=CORRL(I,J)
  220 CONTINUE
      K=0
      SDP=0.0
      SDV=0.0
      SSYD=0.0
```

```
      IF(NQNTUM.GE.1) GO TO 223
      DO 221 I=1,NCOMP
      PC(I)=PCO(I)
      VC(I)=VCO(I)
  221 TC(I)=TCO(I)
  120 T=TTT
      RT=R*T
      WRITE(3,535)
  535 FORMAT(/10X,9HCOMPONENT,1X,1HX,7X,1HY,7X,2HYY,7X,2HYD,4X,4HV(P),6X
     1 ,5HV(PO),5X,4HPHIL,6X,4HPHIV,6X,4HSUMY,6X,4HITER,4X,3HNIY/)
  223 CONTINUE
      NIY=0
      ITER=0
      P=PSI
      K=K+1
      DO 40 J=1,NCOMP
      PHIV(J)=1.0
   40 X(J)=XX(K,J)
   42 CALL SUPT(VL,PHI,PPVOL,C1RKL,C2RKL,CORRL,X,1,KIJ)
   41 SUMY=0.0
      SUMP=0.0
      DO 50 J=1,NCOMP
      Y(J)=PHI(J)*X(J)/PHIV(J)
      SUMY=SUMY+Y(J)
   50 SUMP=SUMP+P*Y(J)
      DO 52 J=1,NCOMP
      Y(J)=Y(J)/SUMY
      IF(X(J).EQ.0.0) GO TO 51
      RATIO(J)=Y(J)/X(J)
      GO TO 52
   51 RATIO(J)=0.0
   52 CONTINUE
      DY=SUMY-1.0
      POLD=P
      P=SUMP
      ITER=ITER+1
      IF(ABS((POLD-P)/P)-1.0E-4) 90,90,56
   56 IF(ITER.GT.150)GO TO 105
      IF(ITER.LE.10) GO TO 80
      IF (ABS(DY).GT.ABS(DYOLD)) GO TO 105
   80 DYOLD=DY
      CALL SUPT(VL,PHIV,PVOL,C1RKL,C2RKL,CORRL,Y,0,KIJ)
      GO TO 42
```

```
 90 IF(ABS(SUMY-1.0)-1.0E-4) 110,110,100
100 NIY=NIY+1
    IF(NIY-1) 91,91,92
 91 P=P+0.01
    GO TO 93
 92 SLOPE=(P-PO)/(SUMY-SYO)
    DELP=SLOPE*DDY
    IF(ABS(DELP)-1.0 ) 79,79,78
 78 DELP=SIGN(1.0 ,DELP)
 79 P=P-DELP
 93 DO 94 J=1,NCOMP
 94 Y(J)=Y(J)/SUMY
    PO=P
    SYO=SUMY
    DDY=SUMY-1.0
    IF(NIY.LE.30) GO TO 95
    IF(ABS(DDY).LE.0.005) GO TO 110
    GO TO 96
 95 CALL SUPT(VL,PHIV,PVOL,C1RKL,C2RKL,CORRL,Y,C,KIJ)
    GO TO 42
105 IF(ABS(DY).LE.0.005) GO TO 110
 96 WRITE(3,601)
110 DP=P-PP(K)
    SDP=SDP+ABS(DP)
    P=P*14.697
C   P=P*760.
    PP(K)=PP(K)*14.697
C   PP(K)=PP(K)*760.
    WRITE(3,600) T,P,PP(K),DP
C   PP(K)=PP(K)/760.
    PP(K)=PP(K)/14.697
600 FORMAT(3X,3HT= ,F8.2,5H  P= ,F10.4,7HPP(K)= ,F10.4,4HDP= ,F10.4)
    SYD=0.0
    DO 111 J=1,NCOMP
    YD(J)=Y(J)-YY(K,J)
    SYD=SYD+ABS(YD(J))
    SSYD=SSYD+SYD
111 WRITE(3,610)COMPA(J),COMPB(J),X(J),Y(J),YY(K,J),YD(J),PPVOL(J),
   1PVOL(J),PHI(J),PHIV(J),SUMY,ITER,NIY
    DV=VL-VVL(K)
    SDV=SDV+ABS(DV)
    WRITE(3,901)VL,VVL(K),DV
901 FORMAT(15X,4HVL= ,F10.4,5HVVL= ,F10.4,4HDV= ,F10.4)
```

```
  610 FORMAT(10X,2A4,4E12.4,4F10.4,F8.4,2I5)
  601 FORMAT(1HO,87HFAILED TO CONVERGE, RESULTS BELOW ARE NOT RELIABLE I
     1F SUMY IS MUCH DIFFERENT FROM UNITY)
C      PSI=P
       IF(K-NOBS) 223, 850,850
  850 CONTINUE
       WRITE(3,620)SDP,SSYD,SDV
  620 FORMAT(/10X,'ACCUM. SUM OF DEV. IN P IS 'E12.4,'ACCUM. SUM OF DEV.
     1IN Y IS ' E12.4,'SDV IS 'E12.4/)
       IF(KK-11)280,30,30
  900 STOP
  500 FORMAT (3I5,F10.4)
  505 FORMAT(1HO,4X,2HPC,10X,2HVC,6X,2HTC,10X,1HW,7X,5HC1RKL,5X,5HC2RKL,
     15X,5HMOLWT,4X,9HCOMPONENT//)
  510 FORMAT(4F8.4,2F8.4,2A4)
  515 FORMAT(1H ,6E12.5,3X,2A4)
  516 FORMAT(1H , /1H ,16X,3HKIJ
  520 FORMAT(14F10.4)
  530 FORMAT(1H ,6X,2I2,F10.4,2F10.4)
       END
```

C-3 Evaluation of Activity Coefficients

```
C    EVALUATION OF ACTIVITY COEFFICIENTS FROM BOTH LIQUID AND VAPOR
C    PROPERTIES OF MIXTURES.
C    MODIFIED REDLICH-KWONG EQUATION OF STATE IS USED.
C    FOR MULTICOMPONENT SYSTEMS CALCULATION.
C    ORIGINALLY WRITTEN BY S. D. CHANG, CHEM. ENG., U. OF OTTAWA
C    MODIFIED BY CHU HSI, CHEM. ENG., U. OF OTTAWA
      DIMENSION PHI(5),X(5), F( 5),GAMMA(5),FREFER(5),PVOL(5),Y(5),
     1 PC(5),VC(5),TC(5),W(5),C1RKV(5),C2RKV(5),C1RKL(5),C2RKL(5),
     2 AMOLWT(5),COMPA(5),COMPB(5),CORRV(5,5),CORRL(5,5),GAMALN(5),
     3 A(4),Z(3),TITLE(20),D(5),PCO(5),VCO(5),TCO(5),PHIV(5),FREF(5),
     4 PS(5),PP(50),XX(50,5),YY(50,5),YCAL(5),PPVOL(5),DC1DT(5),DC2DT(5)
     5 ,PCOR(5)
      COMMON  /FIRST/ TC,PC,VCO,W,AMOLWT,T,P,R,NCOMP,NQNTUM
     1   /SECOND/ Z,A,MTYPE
  800 READ(1,5)(TITLE(I),I=1,19)
    6 FORMAT(1H1,19A4)
    5 FORMAT(    19A4)
      WRITE(3,6)(TITLE(I),I=1,19)
      READ(1,500)NCOMP,NQNTUM,IJK,R
      IF(NCOMP.LE.0) GO TO 900
      WRITE(3,505)
      DO 210 I=1,NCOMP
      READ(1,510)PCO(I),VCO(I),TCO(I),W(I),C1RKL(I),C2RKL(I),
     1   DC1DT(I),DC2DT(I)          ,COMPA(I),COMPB(I)
      C1RKV(I)=C1RKL(I)
      C2RKV(I)=C2RKL(I)
  210 WRITE(3,515)PCO(I),VCO(I),TCO(I),W(I),C1RKL(I),C2RKL(I),
     1   DC1DT(I),DC2DT(I)          ,COMPA(I),COMPB(I)
      CORRL(NCOMP,NCOMP)=0.0
      NCOMP1=NCOMP-1
      WRITE(3,519)
  519 FORMAT(//10X,12HINPUT DATA ://4X,1HP,8X,2HX1,8X,2HX2,9X,1HT,7X,3HRA
     11,7X,3HRB1,7X,3HRA2,7X,3HRB2//)
      DO 9 I=1,NCOMP1
      I1=I+1
      DO 9 J=I1,NCOMP
    9 READ(1,520)CORRL(I,J)
      I=0
   10 I=I+1
      SX=0.0
      SY=0.0
C     READ(1,520)TTT,PP(I),(XX(I,J),J=1,NCOMP),(YY(I,J),J=1,NCOMP)
      READ( 1,520) PP(I),(XX(I,J),J=1,NCOMP1),(YY(I,J),J=1,NCOMP1)
```

```
      DO 15 J=1,NCOMP1
      SY=SY+YY(I,J)
   15 SX=SX+ XX(I,J)
      XX(I,NCOMP)=1.0-SX
      YY(I,NCOMP)=1.0-SY
      IF(R.LT.11.0) GO TO 16
C     PP(I)=PP(I)/760.
      PP(I)=PP(I)/14.697
   16 WRITE(3,520) PP(I),(XX(I,J),J=1,NCOMP ),(YY(I,J),J=1,NCOMP )
      IF(PP(I).GE.0) GO TO 10
   20 NOBS=I-1
      READ(1,520)TTT,PSO,(PS(I),I=1,NCOMP)
      IF(R.LT.11.0) GO TO 21
      PSO=PSO/14.697
   21 WRITE(3,520)TTT,PSO,(PS(I),I=1,NCOMP)
      READ(1,525)IJK,KIJ,CINI,CFIN
  525 FORMAT(2I5,2F10.4)
   30 KIJ=KIJ+1
      IF(KIJ.GE.2) GO TO 800
      WRITE(3,525)IJK,KIJ,CINI,CFIN
      K=0
      KK=0
      KK=20
  280 CONTINUE
      WRITE(3,6)(TITLE(I),I=1,19)
C     WRITE (2,6)(TITLE(I),I=1,19)
      KK=KK+1
      WRITE(3,516)
      DO 220 I=1,NCOMP1
      CORRL(I,I)=0.0
      I1=I+1
      DO 220 J=I1,NCOMP
      IF(KK.GE.20) GO TO 214
      CORRL(I,J)=CINI+(KK-1)*(CFIN-CINI)/10.
  214 WRITE(3,530)I,J,CORRL(I,J)
      CORRL(J,I)=CORRL(I,J)
  220 CONTINUE
      K=0
      SSDY=0.0
  219 CONTINUE
      IF(NQNTUM.GE.1) GO TO 223
      DO 221 I=1,NCOMP
      PC(I)=PCO(I)
```

```
      VC(I)=VCO(I)
  221 TC(I)=TCO(I)
  120 T=TTT
      RT=R*T
      DO 226 I=1,NCOMP
      DO 224 J=1,NCOMP
      X(J)=0.0
  224 CONTINUE
      X(I)=1.0
      P=PSO
      CALL SUPT(VL,  PHI, PVOL,C1RKL,C2RKL,CORRL,X, 1,KIJ)
      FREFER(I)=PHI(I)*X(I)*PSO
  226 D(I)=PVOL(I)
      WRITE(3,521)T,PSO,(FREFER(I),I=1,NCOMP),(D(I),I=1,NCOMP)
  521 FORMAT(//5X,2F10.2, 9E11.4//)
      WRITE(3,535)
  535 FORMAT(/26X,9HCOMPONENT,1X,1HX,7X,4HYCAL,4X,4HYOBS,4X,
     1  6HGAMALN,2X,5HGAMMA,5X,4HV(P),6X,5HV(PO),5X,4HPHIL,6X,
     1  4HPHIV,6X,5HPHILL/)
  223 CONTINUE
      K=K+1
      DO 234 J=1,NCOMP
      Y(J)=YY(K,J)
  234 X(J)=XX(K,J)
      P=PSO
      CALL SUPT(VL,  PHI,PPVOL,C1RKL,C2RKL,CORRL,X, 1,KIJ)
  236 P=PP(K)
      CALL SUPT(VL,  PHI, PVOL,C1RKL,C2RKL,CORRL,X, 1,KIJ)
      DO 237 J=1,NCOMP
  237 PCOR(J)=(PPVOL(J)+PVOL(J))*(PSO-P)/2.0/RT
      CALL SUPT(VL,PHIV,PVOL,C1RKL,C2RKL,CORRL,Y,0,KIJ)
      WRITE(3,789)PP(K),(Y(J),J=1,NCOMP),(PHIV(J),J=1,NCOMP),(PCOR(J),
     1 J=1,NCOMP)
  789 FORMAT(10X,7F10.4)
      RATIO=PHIV(1)*Y(1)/PHI(1)/X(1)
      RATO=PHIV(2)*Y(2)/PHI(2)/X(2)
  266 WRITE(3,600)T,P ,RATIO,RATO
      DO 235 J=1,NCOMP
C     GAMALN(J)=ALOG(PHI(J)*P/FREFER(J)      )
C    1    +(PPVOL(J)+PVOL(J))*(PSO-P)/2.0/RT
      GAMALN(J)=ALOG(PHIV(J)*P*Y(J)/(FREFER(J)*X(J)))+PCOR(J)
      PHIV(J)=1.0
  235 GAMMA(J)= EXP(GAMALN(J) )
```

```
      ITER=0
  240 ITER=ITER+1
      SDY=0.0
      IF(ITER-60)242,242,260
  242 DO 245 J=1,NCOMP
      YCAL(J)=PHI(J)/PHIV(J)*X(J)
      SDY=SDY+YCAL(J)
  245 CONTINUE
      DO 246 J=1,NCOMP
      IF(ITER.LE.1) GO TO 250
  246 YCAL(J)=YCAL(J)/SDY
      DO 247 J=1,NCOMP
      IF(ABS(YCAL(J)-Y(J)) .GT.0.00001) GO TO 250
  247 CONTINUE
      GO TO 260
  250 DO 255 J=1,NCOMP
  255 Y(J)=YCAL(J)
      CALL SUPT(VL,  PHIV,PVOL,C1RKL,C2RKL,CORRL,Y, 0,KIJ)
      GO TO 240
  260 SDY=0.0
      DO 265 J=1,NCOMP
  265 SDY   =SDY   +ABS(YCAL(J)-YY(K,J))
      SSDY=SSDY+SDY
      IF(R.LT.11.) GO TO 266
      P=P*14.697
C     P=P*760.
  540 FORMAT(8F10.4)
      DO 300 J=1,NCOMP
  300 WRITE(3,610)COMPA(J),COMPB(J),X(J),YCAL(J),YY(K,J),GAMALN(J),
     1   GAMMA(J),PVOL(J),PPVOL(J),PHI(J),PHIV(J),     ITER
C     WRITE(2,691)P,(X(J),J=1,NCOMP1),(YY(K,J),J=1,NCOMP1),(GAMALN(J),
C    1 J=1,NCOMP)
C 691 FORMAT(F10.2,7F10.4)
  600 FORMAT(3X,3HT= ,F8.2,5H  P= ,F10.4,8H  RATIO=,F8.4,7H  RATO=,F8.4)
  610 FORMAT(27X,2A4,5F8.4,4F10.4,I5)
  270 IF(K-NOBS)223,850,850
  850 CONTINUE
      WRITE(3,620)SSDY
  620 FORMAT (/ 10X,'ACCUM. SUM OF DEV. IN Y IS 'E12.4/)
      IF(KK-11)280,30,30
  900 STOP
  500 FORMAT (3I5,F10.4)
  505 FORMAT(1H0,4X,2HPC,10X,2HVC,6X,2HTC,10X,1HW,7X,5HC1RKL,5X,5HC2RKL,
```

```
     15X,5HMOLWT,4X,9HCOMPONENT//)
  510 FORMAT(4F8.4,2F8.4,2E12.5,2A4)
  515 FORMAT(1H ,8E12.5,3X,2A4)
  516 FORMAT(1H , /1H ,16X,3HKIJ                    / )
  520 FORMAT(F10.2,12F10.4)
  530 FORMAT(1H ,6X,2I2,F10.4,2F10.4)
  562 FORMAT(45X,2A4,3F10.4)
      END
```

C-4 Evaluation of Supporting Properties

(SUBROUTINE SUPT)

```
      SUBROUTINE SUPT(VL,PHI, PVOL ,C1RKL,C2RKL,CORRL,X,LV,KIJ)
C     EVALUTION OF SUPPORTING PROPERTIES,THE FUGACITY AND THE
C     PARTIAL MOLAL VOLUME OF FLUID MIXTURES.
C     SHINN-DER CHANG, DEPT.OF CHEM.ENG., UNIV. OF OTTAWA.
      DIMENSION TC(5),PC(5),VCO(5),W(5),AMOLWT(5)  ,ARKL(5,5),BRKL(5),
     1  WIJ(5,5),TCOIJ(5,5),TCIJ(5,5),A(4),Z(3),C1RKL(5),C2RKL(5),
     1  PVOL(5),PHI(5),CORRL(5,5),X(5),A2I(5),BI(5),AIRKL(5)
      DIMENSION ZZ(3)
      COMMON  /FIRST/ TC,PC,VCO,W,AMOLWT,T,P,R,NCOMP,NQNTUM
     1   /SECOND/ Z,A,MTYPE
C     LV=0, FOR VAPOR PHASE.
C     LV=1, FOR LIQUID PHASE.
C     KIJ=1, TCIJ=SQRT(TCI*TCJ)*(1.-KIJ)
C     KIJ=2, AIJ=SQRT(AI*AJ)*(1.-KIJ)
C     KIJ=3, AIJ=(AI*KIJ+(1.-KIJ)*AJ)/2.
      RT=R*T
   91 DO 100 I=1,NCOMP
      ARKL(I,I)=C1RKL(I)* R*R     *(TC(I)**2.5)/PC(I)
      BRKL(I)=C2RKL(I)* R    *TC(I)/PC(I)
      IF(I.EQ.NCOMP) GO TO 100
      I1=I+1
      DO 100 J=I1,NCOMP
      IF(KIJ.GT.1) GO TO 97
      TCIJ( I,J)=(TC(I)*TC(J))**0.5*(1.0-CORRL(I,J))
      TCIJ( J,I)=TCIJ( I,J)
      WIJ(I,J)=(W(I)+W(J))*0.5
      ZCOIJ=0.291-0.08*WIJ(I,J)
   94 VCOIJ=(VCO(I)**(1./3.)+VCO(J)**(1./3.))**3/8.0
   96 PCOIJ=ZCOIJ* R    *TCIJ( I,J)/VCOIJ
      PCIJ=PCOIJ
   95 ARKL(I,J)=(C1RKL(I)+C1RKL(J))*0.5* R    **2*TCIJ(I,J)**2.5/PCIJ
      GO TO 98
   97 IF(KIJ.GT.2) GO TO 99
      ARKL(I,J)=(ARKL(I,I)*ARKL(J,J))**0.5*(1.0-CORRL(I,J))
      GO TO 98
   99 ARKL(I,J)=(ARKL(I,I)*CORRL(I,J)+(1.-CORRL(I,J))*ARKL(J,J))
   98 ARKL(J,I)=ARKL(I,J)
  100 CONTINUE
      AMRKL=0.0
      BMRKL=0.0
      DO 120 I=1,NCOMP
      A2I(I)=ARKL(I,I)/RT**2/T**0.5
      BI(I)=BRKL(I)/RT
```

```
      BMRKL=BMRKL+X(I)*BRKL(I)
      AIRKL(I)=0.0
      DO 120 J=1,NCOMP
      AIRKL(I)=AIRKL(I)+X(J)*ARKL(I,J)
  120 AMRKL=AMRKL+X(I)*X(J)*ARKL(I,J)
      A2=AMRKL/RT**2/T**0.5
      B=BMRKL/RT
      A(1)=1.0
      A(2)=-1.0
      A(3)=B*P*(A2/B-1.0-B*P)
      A(4)=-(A2/B)*(B*P)**2
      CALL CUBEQN
      IF(MTYPE)115,140,140
  115 IF(LV.EQ.0) GO TO 145
C     ZL=AMIN1(Z(1),Z(2),Z(3))
      ZL=AMIN1(Z(1),Z(2),Z(3))
C     JJ=0
C     DO 146 I=1,3
C     ZZ(I)=9999.
C     JJ=JJ+1
C     IF(Z(I).LT.0.0) GO TO 146
C     ZZ(JJ)=Z(I)
C 146 CONTINUE
C     ZL=AMIN1(ZZ(1),ZZ(2),ZZ(3))
      GO TO 150
  145 ZL=AMAX1(Z(1),Z(2),Z(3))
      GO TO 150
  140 ZL=Z(1)
  150 H=B*P/ZL
C     WRITE (3,591) H,ZL,B,Z(1),Z(2),Z(3),LV
C 591 FORMAT(5X,6E12.4,I2)
      CALL EQNRK(A2,B,P,H,ZL,LV)
      VL=RT*B/H
  123 CONTINUE
      IF(LV.EQ.0) GO TO 135
      QD=(T**0.5)*VL*(VL+BMRKL)
      QH=(AMRKL/(T**0.5))*((2.*VL+BMRKL)/(VL**2*(VL+BMRKL)**2))
      QK=RT/((VL-BMRKL)**2   )
  135 DO 130 I=1,NCOMP
C     WRITE(3,591)ZL,H
      PHILN =(ZL-1.0)*BI(I)/B-ALOG(ZL)-ALOG(1.0-H)
     1   -(A2/B)*(2.0*AIRKL(I)/AMRKL   -BI(I)/B)*ALOG(1.0+H)
      PHI(I)= EXP(PHILN )
```

```
      IF(LV.EQ.0) GO TO 130
      QE1=0.0
      DO 125 J=1,NCOMP
  125 QE1=QE1+X(J)*ARKL(I,J)
      QE=2.0*QE1-AMRKL*BRKL(I)/(VL+BMRKL)
      QG=(RT/(VL-BMRKL))*(1.0+BRKL(I)/(VL-BMRKL))
      PVOL(I)=((QE/QD)-QG)/(QH-QK)
  130 CONTINUE
  300 RETURN
      END
```

```
      SUBROUTINE CUBEQN
C     SOLVES CUBIC EQUATION OF REDLICH-KWONG EQUATION FOR COMPRESSESSIBILITY
C     FACTORS
      DIMENSION A(4),Z(3) ,B(3)
      COMMON /SECOND/ Z,A,MTYPE
    1 CONTINUE
      B(1)=A(2)/A(1)
      B1OV3=B(1)/3.0
      B(2)=A(3)/A(1)
      B(3)=A(4)/A(1)
      ALF=B(2)-B(1)*B1OV3
      BET=2.0*B1OV3**3  -B(2)*B1OV3+B(3)
      BETOV2=BET/2.0
      ALFOV3=ALF/3.0
      CUAOV3=ALFOV3**3
      SQBOV2=BETOV2**2
      DEL=SQBOV2+CUAOV3
      IF(DEL)40,20,30
   20 MTYPE=0.0
      GAM=SQRT(-ALFOV3)
      IF(BET)22,22,21
   21 Z(1)=-2.0*GAM-B1OV3
      Z(2)=GAM-B1OV3
      Z(3)=Z(2)
      GO TO 50
   22 Z(1)=2.0*GAM-B1OV3
      Z(2)=-GAM-B1OV3
      Z(3)=Z(2)
      GO TO 50
   30 MTYPE=1
      EPS=SQRT(DEL)
      TAU=-BETOV2
      RCU=TAU+EPS
      SCU=TAU-EPS
      SIR=1.0
      SIS=1.0
       IF(RCU)31,32,32
   31 SIR=-1.0
   32 IF(SCU)33,34,34
   33 SIS=-1.0
   34 R=SIR*(SIR*RCU)**0.33333333
      S=SIS*(SIS*SCU)**0.33333333
      Z(1)=R+S-B1OV3
```

```
      Z(2)=-(R+S)/2.0-B10V3
      Z(3)=0.86602540*(R-S)
      GO TO 50
   40 MTYPE=-1
      QUOT=SQB0V2/CUA0V3
      ROOT=SQRT(-QUOT)
      IF(BET)42,41,41
   41 PEI=(1.5707963+ATAN(ROOT/SQRT(1.0-ROOT**2)))/3.0
      GO TO 43
   42 PEI=ATAN(SQRT(1.0-ROOT**2)/ROOT)/3.0
   43 FACT=2.0*SQRT(-ALF0V3)
      Z(1)=FACT*COS(PEI)-B10V3
      PEI2=PEI+2.0943951
      Z(2)=FACT* COS(PEI2)          -B10V3
      PEI4=PEI+4.1887902
      Z(3)=FACT* COS(PEI4)          -B10V3
   50 RETURN
      END
```

```
      SUBROUTINE EQNRK(A2,B,P,E,Z,LV)
      TOL=1.0E-6
      IH=0
      IJ=0
   45 IF(LV.LT.1) GO TO 47
      IF(E.LT.1.0) GO TO 46
      E=E-0.02
      IH=IH+1
      IF(IH.LT.20) GO TO 45
      E=0.98
      GO TO 46
   47 IF(E.GT.0.0) GO TO 46
      E=E+0.01
      IH=IH+1
      IF(IH.LT.20)GO TO 47
      E=0.02
   46 IJ=IJ+1
      FE=-B*P /E+1./(1.0-E)-(A2/B)*E/(1.+E)
      DFE=B*P /E**2 +1./(1.-E)**2-(A2/B)/(1.+E)**2
C     WRITE(3,592)E,FE,DFE,LV
C 592 FORMAT(20X,3E12.4,5X,I2)
C     IF(ABS(DFE).LT.1.0E-20) DFE=DFE/ABS(DFE)*1.0E-20
      TEST=FE/DFE
      E=E-TEST
      IF(IJ.GT.60)GO TO 48
      IF( ABS(TEST/E).GT.TOL) GO TO 45
   48 Z  =B*P/E
      RETURN
      END
```

C-5 Fitting the Redlich-Kister Equation for Binary System

```
C     EVALUATION OF EXCESS FREE ENERGY FROMFITTING REDLICH-KISTER
C     EQUATION IN ONE TO FIVE CONSTANTS
C     PROGRAM COPIED FROM D. GRAVELLE
C     CHU HSI DEPT. OF CHEMICAL ENGINEERING, UNIV. OF OTTAWA
C     FEBUARY 25,1970
      DIMENSION TITLE(20),P(50),X(50),GI(50),GII(50),Y(50),EXCESS(50)
    6 READ(1,1,END=5) (TITLE(I),I=1,20)
    1 FORMAT(20A4)
      WRITE(3,9) (TITLE(I),I=1,20)
    9 FORMAT(1H1,20A4///)
      WRITE(3,8)
    8 FORMAT(1HO,'J      P      X      Y      GI      GII      GE
     1///)
      I=1
    2 FORMAT(5F10.0,I1)
    4 READ(1,2)P(I),X(I),Y(I),GI(I),GII(I),J
C     GI(I)=GI(I)*2.303
C     GII(I)=GII(I)*2.303
      IF(J.EQ.1) GO TO 3
      EXCESS(I)=X(I)*GI(I)+(1.0-X(I))*GII(I)
      WRITE(3,7) I,P(I),X(I),Y(I),GI(I),GII(I),EXCESS(I)
    7 FORMAT(1H ,I2,5X,F10.2,5F10.4)
      I=I+1
      GO TO 4
    3 N=I-1
      CALL RKFIT(TITLE,N,P,X,GI,GII,EXCESS)
      GO TO 6
    5 RETURN
      END
```

```
      SUBROUTINE RKFIT(TITLE,NOBS,P,X,GI,GII,EXCESS)
C     FITTING REDLICH-KISTER EQUATION IN ONE TO FIVE CONSTANTS
      DIMENSION TITLE (20)
      DIMENSION EXCESS(50)
      DIMENSION GAMAI(50),GAMAII(50),A(5,6),H(5,6),F(6)
      DIMENSION P(50),X(50),Y(50),GI(50),GII(50)
      DO 10 I=1,5
      DO 10 J=1,6
   10 H(I,J)=0.0
      DO 20 I=1,NOBS
      XIJ=X(I)*(1.0-X(I))
      F(1)=-(2.0*X(I)-1.0)
      F(2)=6.0*XIJ-1.0
      F(3)=-F(1)*(8.0*XIJ-1.0)
      F(4)=F(1)*F(1)*(10.0*XIJ-1.0)
      F(5)=-F(1)**3*(12.0*XIJ-1.0)
      F(6)=GI(I)-GII(I)
C     F(6)=ALOG(GI(I)/GII(I))
      DO 20 L=1,5
      DO 20 J=L,6
   20 H(L,J)=H(L,J)+F(L)*F(J)
      DO 16 I=1,5
      DO 16 J=I,5
   16 H(J,I)=H(I,J)
      DO 12 I=1,NOBS
      GII(I)=EXP(GII(I))
      GI(I)=EXP(GI(I))
   12 CONTINUE
      NEQ=1
   17 DO 15 I=1,5
      DO 15 J=1,6
   15 A(I,J)=0.0
      NEQ1=NEQ+1
      DO 18 I=1,NEQ
      A(I,NEQ1)=H(I,6)
      DO 18 J=1,NEQ
   18 A(I,J)=H(I,J)
      CALL SOLVE(NEQ,A,INDIC)
      WRITE(3,103)(TITLE(I),I=1,20)
  103 FORMAT(1H1, 'REDLICH-KISTER EQUATION REPRESENTATION OF ',20A4///)
      WRITE(3,106)(A(I,NEQ1),I=1,NEQ)
  106 FORMAT(5X,4H B= ,F8.4,4H C= ,F8.4,4H D= ,F8.4,4H E= ,F8.4,4H F= ,
     1F8.4///)
```

```
      WRITE(3,105)
  105 FORMAT(3X,1HP,7X,1HX,7X,1HY,7X //)
      SSI=0.0
      SSJ=0.0
      SI=0.0
      SJ=0.0
      DO 30 I=1,NOBS
      FF=2.*X(I)-1.
      GAMAI(I)=(1.0-X(I))**2*(A(1,NEQ1)+A(2,NEQ1)*(2.0*FF+1.0)
     1 +A(3,NEQ1)*(3.0*FF+2.0)*FF+A(4,NEQ1)*(4.*FF+3.0)*FF**2
     2 +A(5,NEQ1)*(5.0*FF+4.0)*FF**3)
      GAMAII(I)=X(I)**2*(A(1,NEQ1)+A(2,NEQ1)*(2.*FF-1.)
     1 +A(3,NEQ1)*(3.*FF-2.)*FF+A(4,NEQ1)*(4.*FF-3.)*FF*FF
     2 +A(5,NEQ1)*(5.0*FF-4.0)*FF**3)
      AI=EXP(GAMAI(I))
      AII=EXP(GAMAII(I))
   46 DGI=AI-GI(I)
      DGJ=AII-GII(I)
      SSI=SSI+DGI*DGI
      SSJ=SSJ+DGJ*DGJ
      SI=SI+100.0*ABS(DGI/GI(I))
      SJ=SJ+100.0*ABS(DGJ/GII(I))
      WRITE(3,104)I,P(I),X(I),AI,GI(I),DGI,AII,GII(I),DGJ,
     1 GAMAI(I),GAMAII(I)
  104 FORMAT(1H ,I2,F8.2,F10.4,10X,9F10.4//)
   30 CONTINUE
      SSDI=(SSI/(NOBS-NEQ))**0.5
      SSDJ=(SSJ/(NOBS-NEQ))**0.5
      SDI=SI/NOBS
      SDJ=SJ/NOBS
      WRITE(3,300)SSDI,SSDJ,SDI,SDJ,NOBS,NEQ
  300 FORMAT(/1H ,55H ST.DEV.OF GAMMA VALUES OF THE 1ST & 2ND COMPONENTS
     1 ARE,F15.4,4H AND,F15.4/1H ,58H  AV.% DEV.OF GAMMA VALUES OF THE 1
     2ST & 2ND COMPONENTS ARE,F15.4,4H AND,F15.4/
     3 20H NO.OF OBSERVATION =,I5/31H NO. OF ADJUSTABLE PARAMETERS =,
     4 I5/)
      CALL EXFREE(P,X,GAMAI,GAMAII,EXCESS,NOBS,TITLE)
      NEQ=NEQ1
      IF(NEQ.GT.3) GO TO 800
      GO TO 17
  800 RETURN
      END
```

```
      SUBROUTINE SOLVE(NA,A,INDIC)
      DIMENSION A(5,6)
      NA1=NA+1
      DO 205 I=1,NA
      IF(A(I,I))200,206,200
  200 P=1./A(I,I)
      DO 201 J=I,NA1
  201 A(I,J)=P*A(I,J)
      DO 202 K=1,NA
      IF (I-K) 203,202,203
  203 Q=A(K,I)
      DO 204 J=I,NA1
  204 A(K,J)=A(K,J)-Q*A(I,J)
  202 CONTINUE
  205 CONTINUE
      INDIC=0
      RETURN
  206 IF(NA-1) 300,304,300
  300 I1=I+1
      DO 303 L=I1,NA
      IF(A(L,I)) 301,303,301
  301 DO 302 J=I,NA1
      HOLD=A(I,J)
      A(I,J)=A(L,J)
  302 A(L,J)=HOLD
      GO TO 200
  303 CONTINUE
      INDIC=1
  304 WRITE(3,207) I
  207 FORMAT(//25H DIAGONAL ELEMENT IN EQN ,I4,40H 9S ZERO TRANSPOSE EQN
     1 WITH PREVIOUS ONE//)
      RETURN
      END
```

```
      SUBROUTINE EXFREE(P,X,GAMAI,GAMAII,EXCESS,N,TITLE)
C     PROGRAM TO EVALUATE EXCESS FREE ENERGY
      DIMENSION TITLE(20),EXCALC(50),P(50),X(50),EXCESS(50),GAMAI(50),
     1 GAMAII(50)
      WRITE(3,12)(TITLE(I),I=1,20)
   12 FORMAT(1H1,'PRESSURE-COMPOSITION-EXCESS FREE ENERGY FOR  ',20A4)
      WRITE(3,18)
   18 FORMAT(1HO,
     1     10X,'P',10X,'X',10X,'G/RT',13X,'DELTA',2X,'PER CENT DEV'//)
      SI=0.0
      SII=0.0
      DO 10 I=1,N
      EXCALC(I)=X(I)*GAMAI(I)+(1.-X(I))*GAMAII(I)
      DGI=EXCESS(I)-EXCALC(I)
      CENT=DGI/EXCESS(I)*100.
      WRITE(3,11) I,P(I),X(I),EXCALC(I),DGI,CENT
      SII=SII+ABS(CENT)
   10 SI=SI+DGI*DGI
   11 FORMAT(1H ,I5,F10.2,2F10.4,10X,2F10.4)
      STD=SQRT(SI/N)
      CENT=SII/N
      WRITE(3,13) STD
      WRITE(3,14) CENT
   13 FORMAT(1HO,'STANDARD DEVIATION IN GE/RT' ,F10.4)
   14 FORMAT(1HO,'AVERAGE PER CENT DEVIATION IN GE/RT',F10.4)
      RETURN
      END
```

C-6 Fitting the Redlich-Kister Equation for Ternary System

```
C       EVALUATION OF EXCESS FREE ENERGY FUNCTION
C       FROM REDLICH-KISTER EQUATION
C       FIT REDLICH KISTER EQUATION FOR TERNARY SYSTEM
C       LEAST SQUARE FITTING Q-FUNCTION FOR TERNARY SYSTEM
C       CHU HSI , DEPT. OF CHEM. ENG ,U. OF OTTAWA
C       MARCH 6,1970
        DIMENSION TITLE(20),P(50),X1(50),X2(50),X3(50),Y1(50),Y2(50),
       1Y3(50),GI(50),GII(50),GIII(50),Q12(50),Q23(50),Q31(50),EXCESS(50)
      6 READ(1,1,END=5)(TITLE(I),I=1,20)
      1 FORMAT(20A4)
        WRITE(3,9)(TITLE(I),I=1,20)
      9 FORMAT(1H1,20A4///)
        READ(1,11)B12,C12,D12
        READ(1,11)B23,C23,D23
        READ(1,11)B31,C31,D31
     11 FORMAT(3F10.4)
        WRITE(3,20)B12,C12,D12,B23,C23,D23,B31,C31,D31
     20 FORMAT(10X,'B12= 'F10.4,'C12= 'F10.4,'D12= 'F10.4/10X,'B23= 'F10.4
       1,'C23= 'F10.4,'D23= 'F10.4/10X,'B31= 'F10.4,'C31= 'F10.4,'D31= '
       2F10.4///)
        WRITE(3,8)
      8 FORMAT(1HO,' J          P          X1          X2          Y1
       1 Y2          G1          GII          GIII          GE'///)
        I=1
C     4 READ(1,2)P(I),X1(I),X2(I),Y1(I),Y2(I),GI(I),GII(I),GIII(I),J
      4 READ(1,2)P(I),X1(I),X2(I),Y1(I),Y2(I),GI(I),GII(I),GIII(I)
C     2 FORMAT(F10.0,7F8.4,I1)
      2 FORMAT(8F10.0)
C       IF(J.EQ.1)GO TO 3
        IF(P(I).LE.0.0) GO TO 3
        X3(I)=1.0-X1(I)-X2(I)
        EXCESS(I)=X1(I)*GI(I)+X2(I)*GII(I)+(1.0-X1(I)-X2(I))*GIII(I)
       1+X1(I)*X2(I)*(B12+C12*(X1(I)-X2(I))+D12*(X1(I)-X2(I))**2)
       2+X2(I)*X3(I)*(B23+C23*(X2(I)-X3(I))+D23*(X2(I)-X3(I))**2)
       3+X3(I)*X1(I)*(B31+C31*(X3(I)-X1(I))+D31*(X3(I)-X1(I))**2)
        Q12(I)=X1(I)*X2(I)*(B12+C12*(X1(I)-X2(I))+D12*(X1(I)-X2(I))**2)
        Q23(I)=X2(I)*X3(I)*(B23+C23*(X2(I)-X3(I))+D23*(X2(I)-X3(I))**2)
        Q31(I)=X3(I)*X1(I)*(B31+C31*(X3(I)-X1(I))+D31*(X3(I)-X1(I))**2)
        WRITE(3,7)I,P(I),X1(I),X2(I),Y1(I),Y2(I),GI(I),GII(I),GIII(I),
       1 EXCESS(I)
      7 FORMAT(1H ,I2,5X,F10.2,8F10.4)
        I=I+1
        GO TO 4
      3 N=I-1
        CALL RKFIT(TITLE,N,P,X1,X2,GI,GII,GIII,EXCESS,Q12,Q23,Q31)
        GO TO 6
```

```
      SUBROUTINE RKFIT(TITLE,NOBS,P,X1,X2,GI,GII,GIII,EXCESS,Q12,Q23,Q31
     1)
C     FIT REDLICH KISTER EQUATION FOR TERNARY SYSTEM
      DIMENSION EXCESS(50),Q12(50),Q23(50),Q31(50)
      DIMENSION H(6,6),F(6), A(5,6),TITLE(20),Q123(50)
      DIMENSION P(50),X1(50),X2(50),X3(50),GI(50),GII(50),GIII(50)
   90 CONTINUE
      DO 10 I=1,5
      DO 10 J=1,6
   10 H(I,J)=0.0
  801 FORMAT(1H ,6E15.4)
      DO 20 I=1,NOBS
      X3(I)=1.0-X1(I)-X2(I)
      F(1)=1.0
      F(2)=(X1(I)-X2(I))
      F(3)=(X2(I)-X3(I))
      F(4)=(X3(I)-X1(I))
      F(5)=
     1    ((EXCESS(I)-Q12(I)-Q23(I)-Q31(I))/(X1(I)*X2(I)*X3(I)))
      H(1,1)=H(1,1)+F(1)*F(1)
      H(1,2)=H(1,2)+F(1)*F(2)
      H(1,3)=H(1,3)+F(1)*F(3)
      H(1,4)=H(1,4)+F(1)*F(4)
      H(1,5)=H(1,5)+F(1)*F(5)
      H(2,2)=H(2,2)+F(2)*F(2)
      H(2,3)=H(2,3)+F(2)*F(3)
      H(2,4)=H(2,4)+F(2)*F(4)
      H(2,5)=H(2,5)+F(2)*F(5)
      H(3,3)=H(3,3)+F(3)*F(3)
      H(3,4)=H(3,4)+F(3)*F(4)
      H(3,5)=H(3,5)+F(3)*F(5)
      H(4,4)=H(4,4)+F(4)*F(4)
      H(4,5)=H(4,5)+F(4)*F(5)
   20 CONTINUE
      H(2,1)=H(1,2)
      H(3,1)=H(1,3)
      H(3,2)=H(2,3)
      H(4,1)=H(1,4)
      H(4,2)=H(2,4)
      H(4,3)=H(3,4)
      NEQ=1
C     DO 20 L=1,5
C     DO 20 J=L,6
```

```
C   20 H(L,J)=H(L,J)+F(L)*F(J)
C      DO 16 I=1,5
C      DO 16 J=I,5
C   16 H(J,I)=H(I,J)
C      NEQ=1
    17 DO 15 I=1,5
       DO 15 J=1,6
    15 A(I,J)=0.0
C      IF(NEQ.EQ.2) GO TO 801
       NEQ1=NEQ+1
C      GO TO 802
C  801 NEQ1=NEQ+2
   802 DO 18 I=1,NEQ
       A(I,NEQ1)=H(I,5)
       WRITE(3,801) A(I,NEQ1)
       DO 18 J=1,NEQ
       A(I,J)=H(I,J)
    18 WRITE(3,801) A(I,J)
       CALL SOLVE(NEQ,A,INDIC)
       WRITE(3,103)(TITLE(I),I=1,20)
   103 FORMAT(1H1, 'REDLICH-KISTER EQUATION REPRESENTATION OF ',20A4///)
       WRITE(3,106)(A(I,NEQ1),I=1,NEQ)
   106 FORMAT(5X,'C123= 'F8.4,'D3= 'F8.4,'D1= 'F8.4,'D2= 'F8.4///)
       WRITE(3,105)
   105 FORMAT(3X,1HP,7X,2HX1,7X,2HX2,7X,2HY1,7X,2HY2,7X//)
       SSI=0.0
       SI=0.0
       DO 30 I=1,NOBS
       Q123(I)=Q12(I)+Q23(I)+Q31(I)+X1(I)*X2(I)*X3(I)*(A(1,NEQ1)+A(2,NEQ1
      1)*(X1(I)-X2(I))+A(3,NEQ1)*(X2(I)-X3(I))+A(4,NEQ1)*(X3(I)-X1(I)))
       AI=Q123(I)
    46 DGI=AI-EXCESS(I)
       SSI=SSI+DGI*DGI
       SI=SI+100.0*ABS(DGI/EXCESS(I))
       WRITE(3,104) I,P(I),X1(I),X2(I),AI,EXCESS(I),DGI
   104 FORMAT(1H ,I2,F10.2,5F10.4//)
    30 CONTINUE
       SSDI=(SSI/(NOBS-NEQ))**0.5
       SDI=SI/NOBS
       WRITE(3,300)SSDI,     SDI,    NOBS,NEQ
   300 FORMAT(/1H ,'ST. DEV. OF Q123 VALUES IS 'F15.4/1H ,'AV. % DEV. OF
      1 Q123 VALUES IS 'F15.4/1H ,'NO. OF OBSERVATION= 'I5/1H ,'NO. OF
      2 ADJUSTABLE PARAMETERS = 'I5/)
```

```
      NEQ=NEQ1
      IF(NEQ.GT.4) GO TO 800
      GO TO 17
  800 RETURN
      END
```

```
      SUBROUTINE SOLVE(NA,A,INDIC)
      DIMENSION A(5,6)
    1 CONTINUE
  801 FORMAT(1H ,6E15.4)
      NA1=NA+1
  802 DO 18 I=1,NA
      WRITE(3,801) A(I,N A1)
      DO 18 J=1,NA
   18 WRITE(3,801) A(I,J)
      DO 205 I=1,NA
      IF(A(I,I))200,206,200
  200 P=1./A(I,I)
      DO 201 J=I,NA1
  201 A(I,J)=P*A(I,J)
      DO 202 K=1,NA
      IF (I-K) 203,202,203
  203 Q=A(K,I)
      DO 204 J=I,NA1
  204 A(K,J)=A(K,J)-Q*A(I,J)
  202 CONTINUE
  205 CONTINUE
      WRITE(3,801) (A(I,NA1),I=1,NA)
      INDIC=0
      RETURN
  206 IF(NA-1) 300,304,300
  300 I1=I+1
      DO 303 L=I1,NA
      IF(A(L,I)) 301,303,301
  301 DO 302 J=I,NA1
      HOLD=A(I,J)
      A(I,J)=A(L,J)
  302 A(L,J)=HOLD
      GO TO 200
  303 CONTINUE
      INDIC=1
  304 WRITE(3,207) I
  207 FORMAT(//25H DIAGONAL ELEMENT IN EQN ,I4,40H 9S ZERO TRANSPOSE EQN
     1 WITH PREVIOUS ONE//)
      RETURN
      END
```

C-7 Evaluation of Activity Coefficients for Ternary System With the Redlich-Kister Constants

```
C     EVALUATION OF ACTIVITY COEFFICIENTS FOR TERNARY SYSTEM
C     WITH REDLICH KISTER CONSTANTS
C     CHU HSI, DEPT. OF CHEMICAL ENGINEERING, U. OF OTTAWA
C     MARCH 11,1970
      DIMENSION P(50),X1(50),X2(50),X3(50),Y1(50),Y2(50),Y3(50),
     1GI(50),GII(50),GIII(50),TITLE(20)
  800 READ(1,10)(TITLE(I),I=1,20)
   10 FORMAT(20A4)
      WRITE(3,30)(TITLE(I),I=1,20)
   30 FORMAT(1H1,'ACTIVITY COEFFICIENTS FOR '20A4)
      READ(1,11)B12,C12,D12
      READ(1,11)B23,C23,D23
      READ(1,11)B31,C31,D31
      READ(1,11)C123,D3,D1,D2
   11 FORMAT(4F10.4)
      WRITE(3,31)B12,C12,D12,B23,C23,D23,B31,C31,D31,C123,D3,D1,D2
   31 FORMAT(/10X,'B12= 'F10.4,'C12= 'F10.4,'D12= 'F10.4/
     1  10X,'B23= 'F10.4,'C23= 'F10.4,'D23= 'F10.4/
     2  10X,'B31= 'F10.4,'C31= 'F10.4,'D31= 'F10.4/
     3  10X,'C123= 'F10.4,'D3= 'F10.4,'D1= 'F10.4,'D2= 'F10.4///)
      WRITE(3,32)
   32 FORMAT(/5X,1HP,8X,2HX1,8X,2HX2,8X,2HY1,8X,2HY2,8X,2HGI,8X,3HGII,
     17X,4HGIII//)
      I=0
    1 I=I+1
      READ(1,12)P(I),X1(I),X2(I),Y1(I),Y2(I),GI(I),GII(I),GIII(I)
   12 FORMAT(8F10.0)
      SI=0.0
      SJ=0.0
      SK=0.0
      SII=0.0
      SJJ=0.0
      SKK=0.0
      IF(P(I).GE.0)GO TO 1
      NOBS=I-1
      DO 40 I=1,NOBS
      X3(I)=1.0-X2(I)-X1(I)
      A1=X2(I)*(1.0-X1(I))
      A2=X2(I)*(2.0*X1(I)-X2(I)-2.0*X1(I)**2+2.0*X1(I)*X2(I))
      A3=X2(I)*(3.*X1(I)**2-3.*X1(I)**3+6.*X1(I)*X1(I)*X2(I)-
     14.*X1(I)*X2(I)-3.*X1(I)*X2(I)**2+X2(I)**2)
      A4=X2(I)*X3(I)
      A5=A4*(X2(I)-X3(I))
```

```
      A6=(X2(I)-X3(I))**2
      A7=X3(I)*(1.-X1(I))
      A8=X3(I)*(X3(I)-2.*X1(I)*X3(I)+2.*X1(I)**2-2.*X1(I))
      A9=X3(I)*(X3(I)**2+6.*X1(I)*X1(I)*X3(I)-4.*X1(I)*X3(I)-
     1 3.*X2(I)*X3(I)**2+3.*X1(I)**2-3.*X1(I)**3)
      A10=A4*(1.0-2.*X1(I))
      A11=A4*(X2(I)-X3(I)-3.*X1(I)*X2(I)+3.*X1(I)*X3(I))
      A12=A4*(X3(I)-2.*X1(I)-3.*X1(I)*X3(I)+3.*X1(I)**2)
      A13=A4*(2.*X1(I)-X2(I)-3.*X1(I)**2+3.*X1(I)*X2(I))
      CGI=B12*A1+C12*A2+D12*A3-B23*A4-2.*C23*A5-3.*D23*A6+B31*A7+C31*A8
     1 +D31*A9+C123*A10+D1*A11+D2*A12+D3*A13
      E1=X1(I)*(1.0-X2(I))
      E2=X1(I)*(X1(I)-2.*X2(I)-2.*X1(I)*X2(I)+2.*X2(I)**2)
      E3=X1(I)*(X1(I)**2-4.*X1(I)*X2(I)+3.*X2(I)**2-3.*X1(I)*X1(I)*X2(I)
     1 +6.*X1(I)*X2(I)**2-3.*X2(I)**3)
      E4=X3(I)*(1.0-X2(I))
      E5=X3(I)*(2.*X2(I)-X3(I)-2.*X2(I)**2+2.*X2(I)*X3(I))
      E6=X3(I)*(X3(I)**2+3.*X2(I)**2-4.*X2(I)*X3(I)-3.*X2(I)**3
     1 +6.*X2(I)*X2(I)*X3(I)-3.*X2(I)*X3(I))
      E7=X1(I)*X3(I)
      E8=E7*(X3(I)-X1(I))
      E9=E8*(X3(I)-X1(I))
      E10=E7*(1.0-2.*X2(I))
      E11=E7*(2.*X2(I)-X3(I)-3.*X2(I)**2+3.*X2(I)*X3(I))
      E12=E7*(X3(I)-X1(I)+3.*X1(I)*X2(I)-3.*X2(I)*X3(I))
      E13=E7*(X1(I)-2.*X2(I)-3.*X1(I)*X2(I)+3.*X2(I)**2)
      CGII=B12*E1+C12*E2+D12*E3+B23*E4+C23*E5+D23*E6-B31*E7-2.*C31*E8-
     1 3.*D31*E9+C123*E10+D1*E11+D2*E12+D3*E13
      F1=X1(I)*X2(I)
      F2=F1*(X1(I)-X2(I))
      F3=F2*(X1(I)-X2(I))
      F4=X2(I)*(1.-X3(I))
      F5=X2(I)*(X2(I)-2.*X3(I)-2.*X2(I)*X3(I)+2.*X3(I)**2)
      F6=X2(I)*(X2(I)**2-4.*X2(I)*X3(I)+3.*X3(I)**2+3.*X2(I)*X2(I)*X3(I)
     1 +6.*X2(I)*X3(I)**2-3.*X3(I)**3)
      F7=X1(I)*(1.-X3(I))
      F8=X1(I)*(2.*X3(I)-X1(I)-2.*X3(I)**2+2.*X1(I)*X3(I))
      F9=X1(I)*(X1(I)**2+3.*X3(I)**2-4.*X1(I)*X3(I)-3.*X3(I)**3+
     1 6.*X1(I)*X3(I)**2-3.*X1(I)*X1(I)*X3(I))
      F10=F1*(1.-2.*X3(I) )
      F11=F1*(X2(I)-2.*X3(I)-3.*X2(I)*X3(I)+3.*X3(I)**2)
      F12=F1*(-X1(I)+2.*X3(I)-3.      *X3(I)**2+3.*X1(I)*X3(I))
      F13=F1*(X1(I)-X2(I)-3.*X1(I)*X3(I)+3.*X2(I)*X3(I))
```

```
      CGIII=-B12*F1-2.*C12*F2-3.*D12*F3+B23*F4+C23*F5+D23*F6+B31*F7
     1 +C31*F8+D31*F9+C123*F10+D1*F11+D2*F12+D3*F13
      GAI=EXP(GI(I))
      CGAI=EXP(CGI)
      GAJ=EXP(GII(I))
      CGAJ=EXP(CGII)
      GAK=EXP(GIII(I))
      CGAK=EXP(CGIII)
      DGI=GAI-CGAI
      CENTI=DGI/GAI*100.
      DGJ=GAJ-CGAJ
      CENTJ=DGJ/GAJ*100.
      DGK=GAK-CGAK
      CENTK=DGK/GAK*100.
      WRITE(3,33)I,P(I),X1(I),GAI,CGAI,DGI,CENTI
      WRITE(3,33)I,P(I),X2(I),GAJ,CGAJ,DGJ,CENTJ
      WRITE(3,33)I,P(I),X3(I),GAK,CGAK,DGK,CENTK
   33 FORMAT(1H ,I5,F10.2,6F10.4)
      SII=SII+ABS(CENTI)
      SJJ=SJJ+ABS(CENTJ)
      SKK=SKK+ABS(CENTK)
      SI=SI+DGI*DGI
      SJ=SJ+DGJ*DGJ
   40 SK=SK+DGK*DGK
      STDI=SQRT(SI/NOBS)
      ACENI=SII/NOBS
      STDJ=SQRT(SJ/NOBS)
      ACENJ=SJJ/NOBS
      STDK=SQRT(SK/NOBS)
      ACENK=SKK/NOBS
      WRITE(3,35)STDI,STDJ,STDK
      WRITE(3,36)ACENI,ACENJ,ACENK
   35 FORMAT(1HO,'STANDARD DEVIATION IN GAMAI 'F10.4/1H ,
     1'STANDARD DEVIATION IN GAMAII 'F10.4/1H ,
     2'STANDARD DEVIATION IN GAMAIII 'F10.4)
   36 FORMAT(1HO,'AV.%DEVIATION IN GAMAI 'F10.4/1H ,'AV. % DEVIATION IN
     1GAMAII 'F10.4/1H ,'AV. % DEVIATION IN GAMAIII 'F10.4)
      RETURN
      END
```

APPENDIX D

Calibration Results of the Gas Partitioner

Figure D-1	Calibration of gas partitioner for the methane-ethylene system
Figure D-2	Calibration of gas partitioner for the methane-ethylene system
Figure D-3	Calibration of gas partitioner for the ethylene-methane system
Figure D-4	Calibration of gas partitioner for the ethylene-methane system
Figure D-5	Calibration of gas partitioner for the methane-ethane system
Figure D-6	Calibration of gas partitioner for the ethane-methane system
Figure D-7	Calibration of gas partitioner for the ethane-methane system
Figure D-8	Calibration of gas partitioner for the ethylene-ethane system
Figure D-9	Calibration of gas partitioner for the ethane-ethylene system

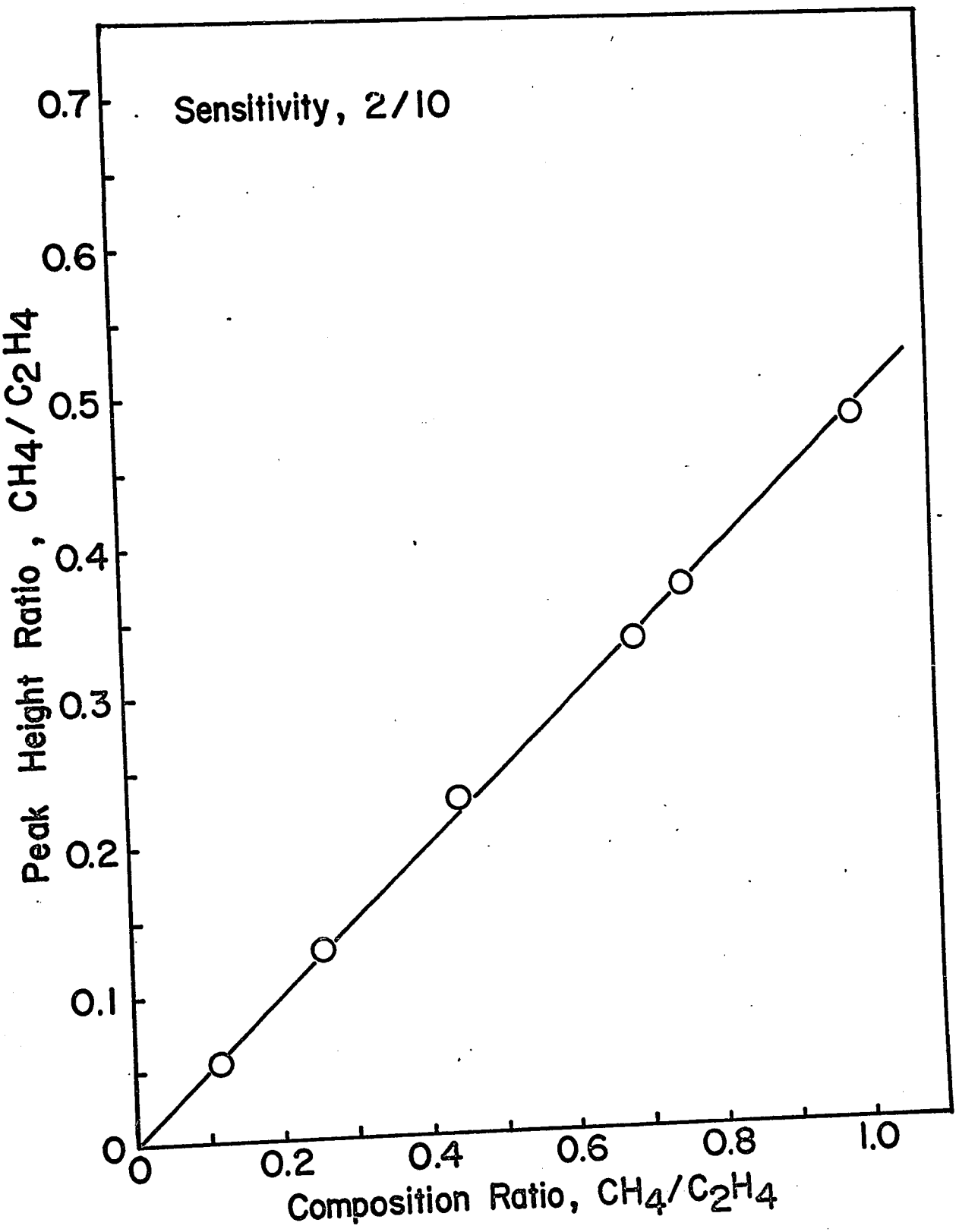

Figure D-1 Calibration of the gas partitioner for the methane-ethylene system

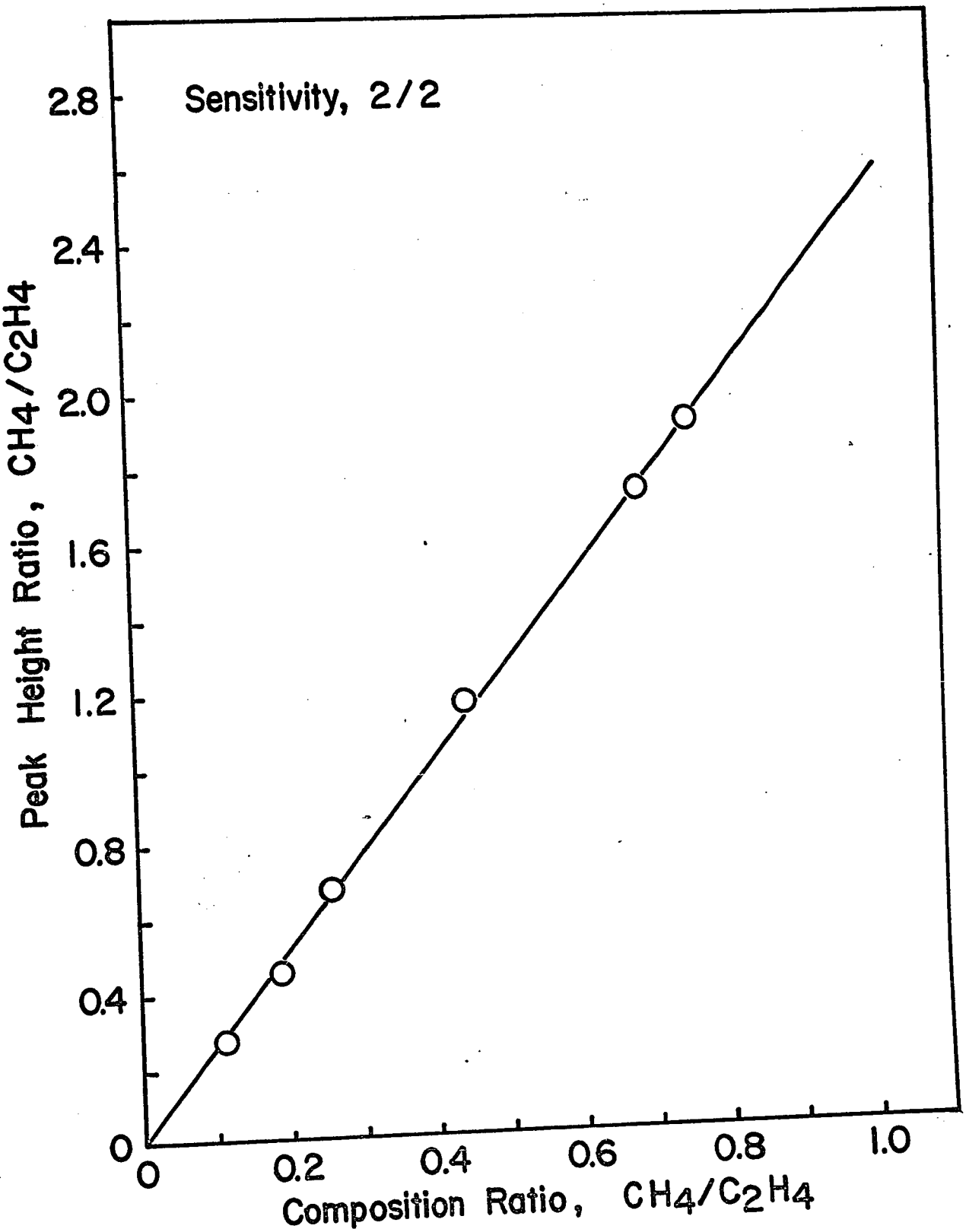

Figure D-2 Calibration of the gas partitioner for the methane-ethylene system

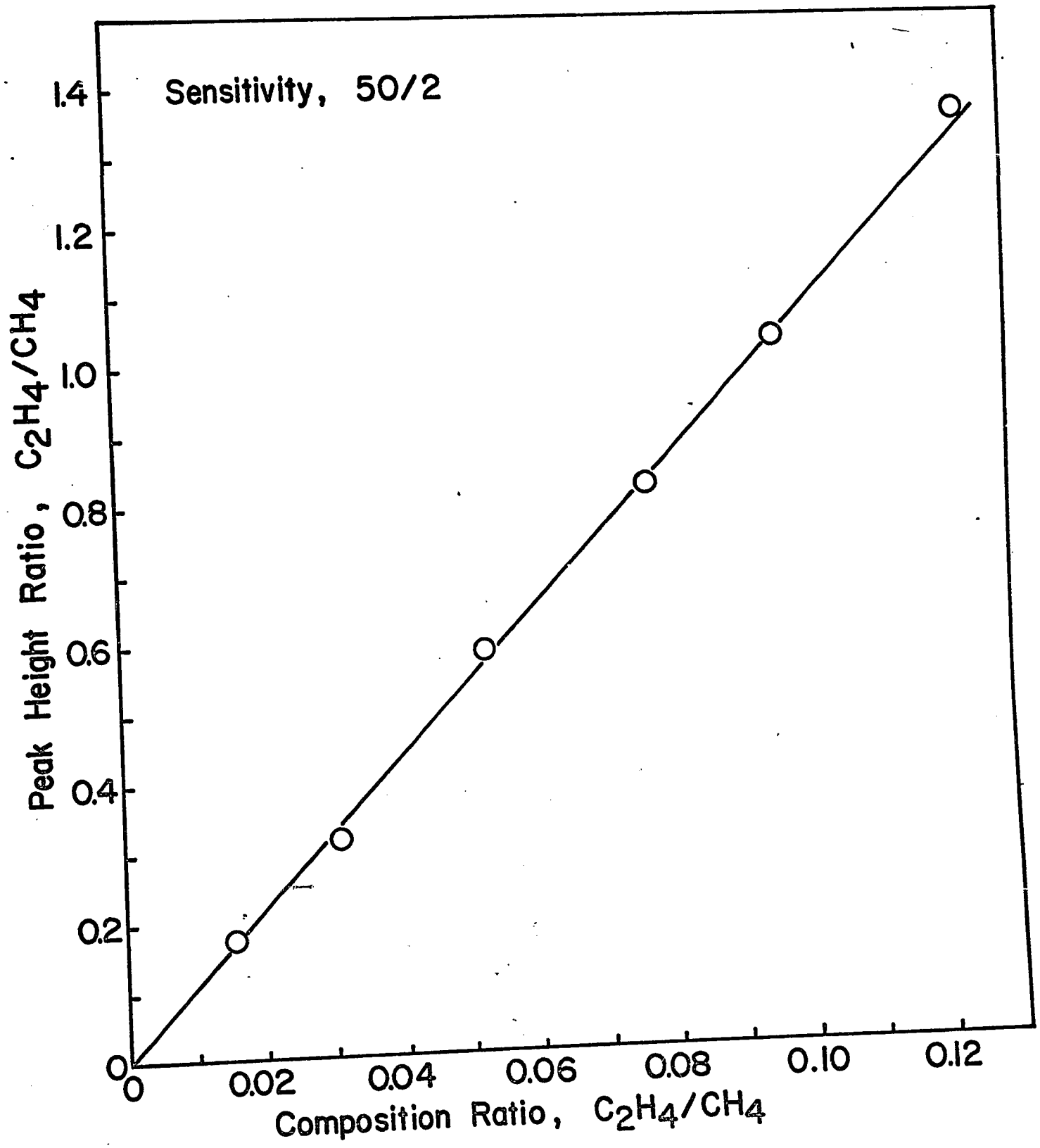

Figure D-3 Calibration of the gas partitioner for the ethylene-methane system

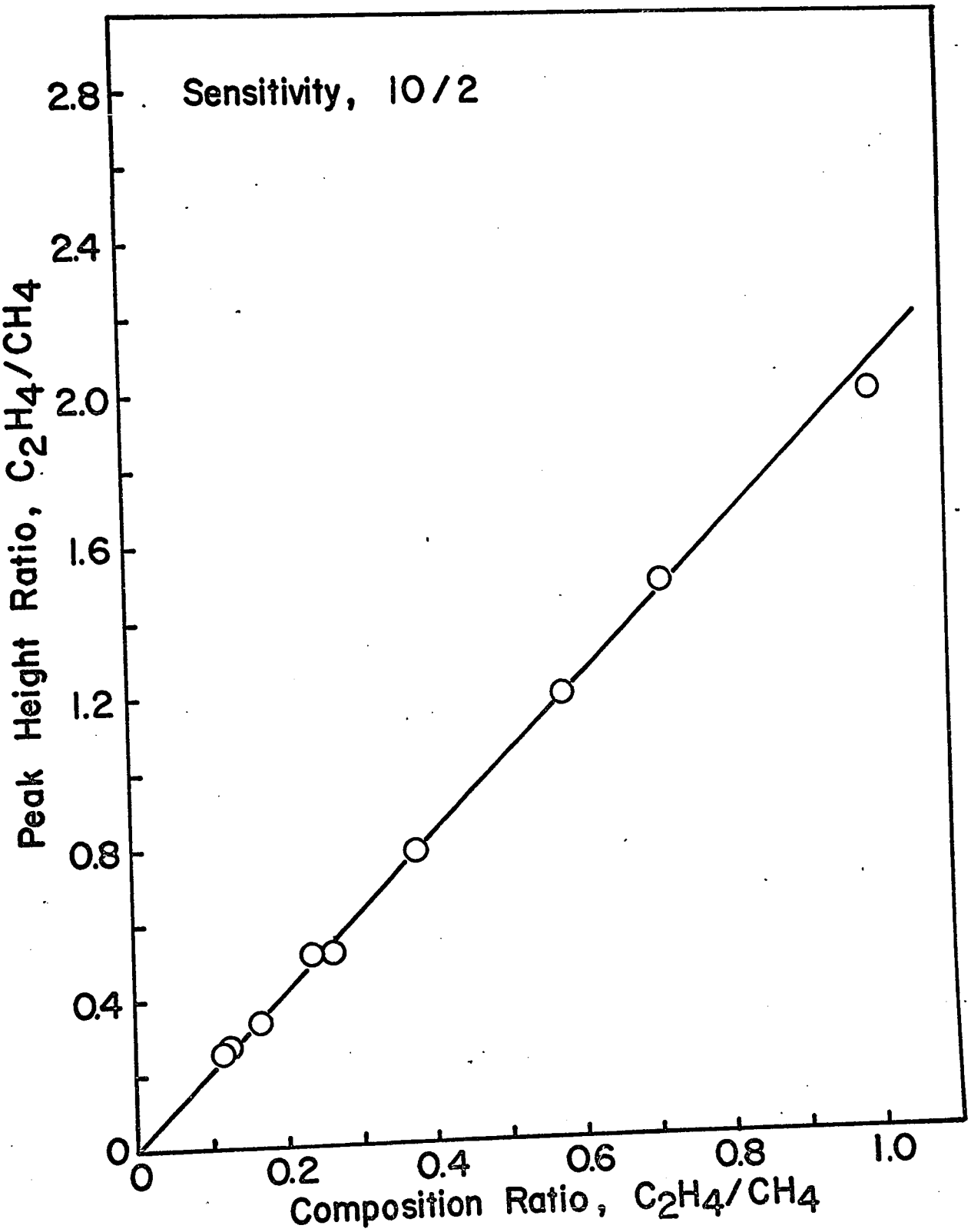

Figure D-4 Calibration of the gas partitioner for the ethylene-methane system

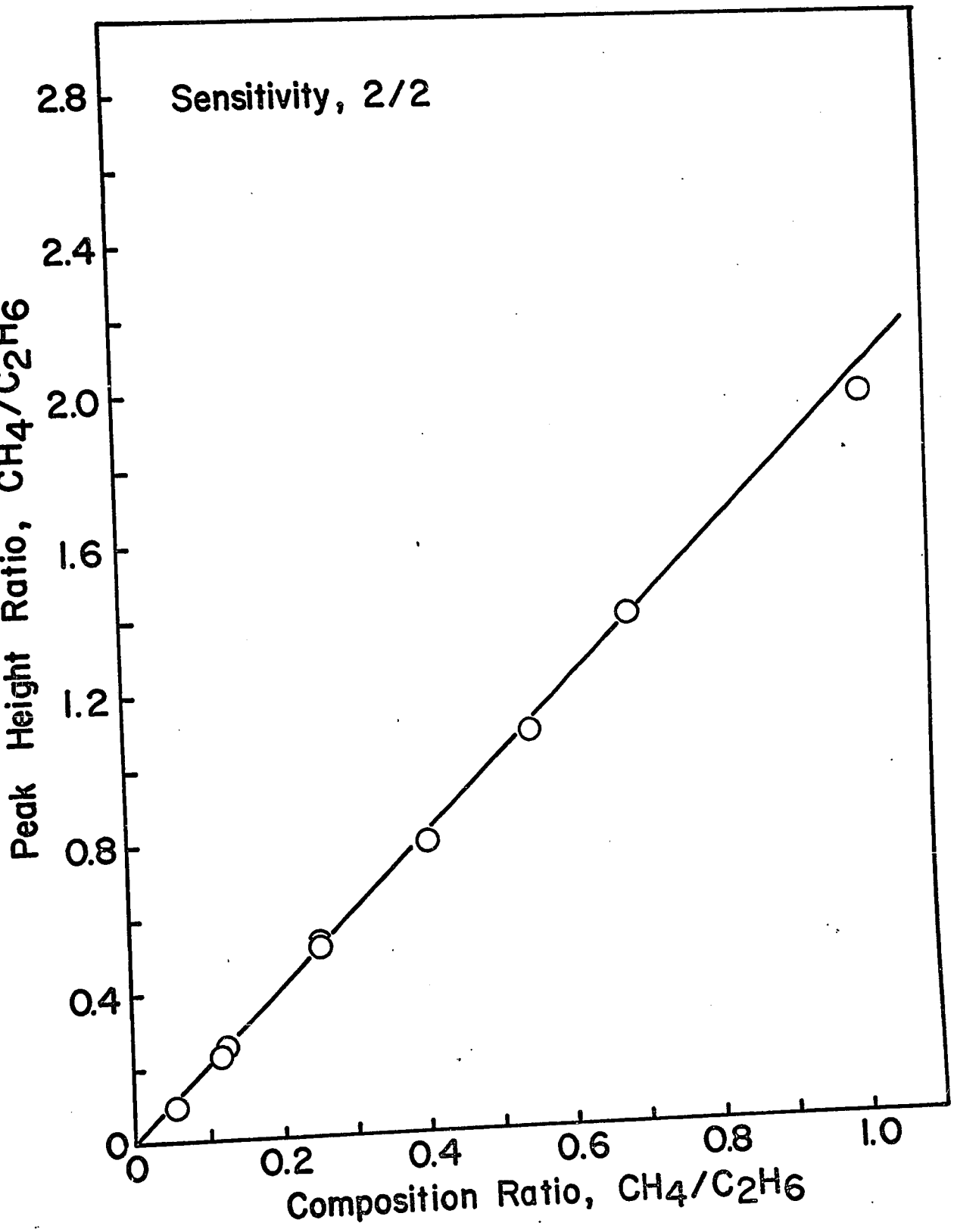

Figure D-5 Calibration of the gas partitioner for the methane-ethane system

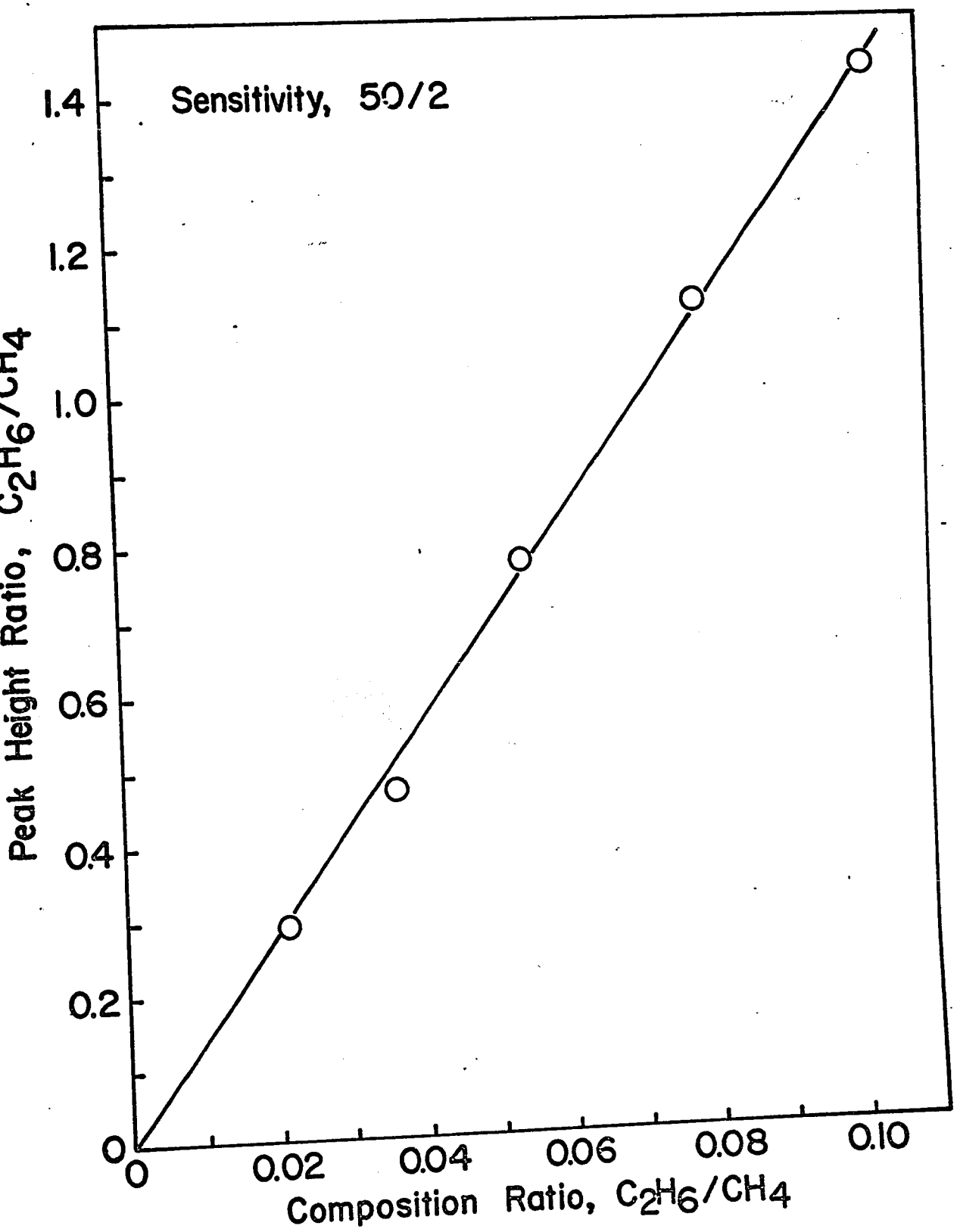

Figure D-6 Calibration of the gas partitioner for the ethane-methane system

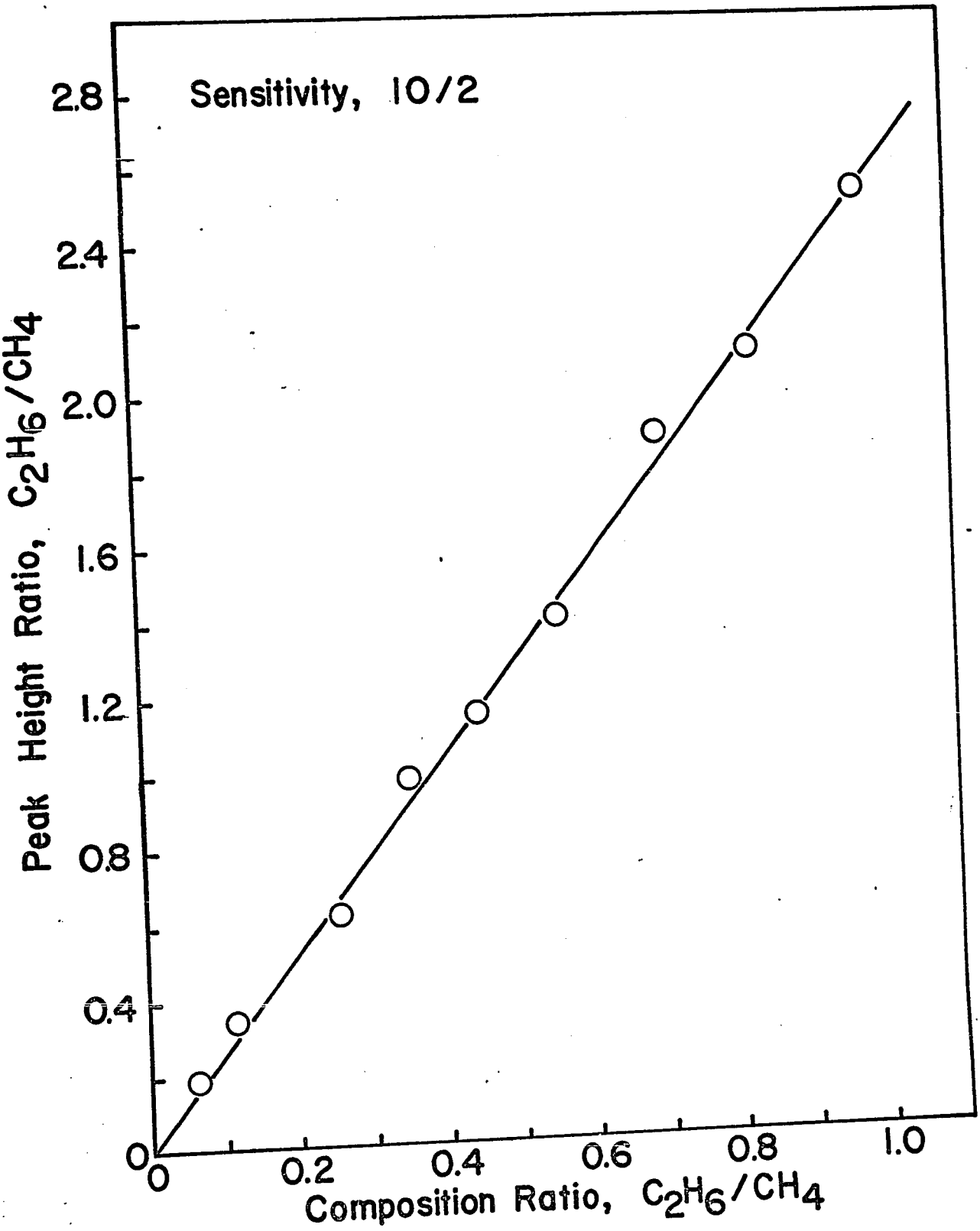

Figure D-7 Calibration of the gas partitioner for the ethane-methane system

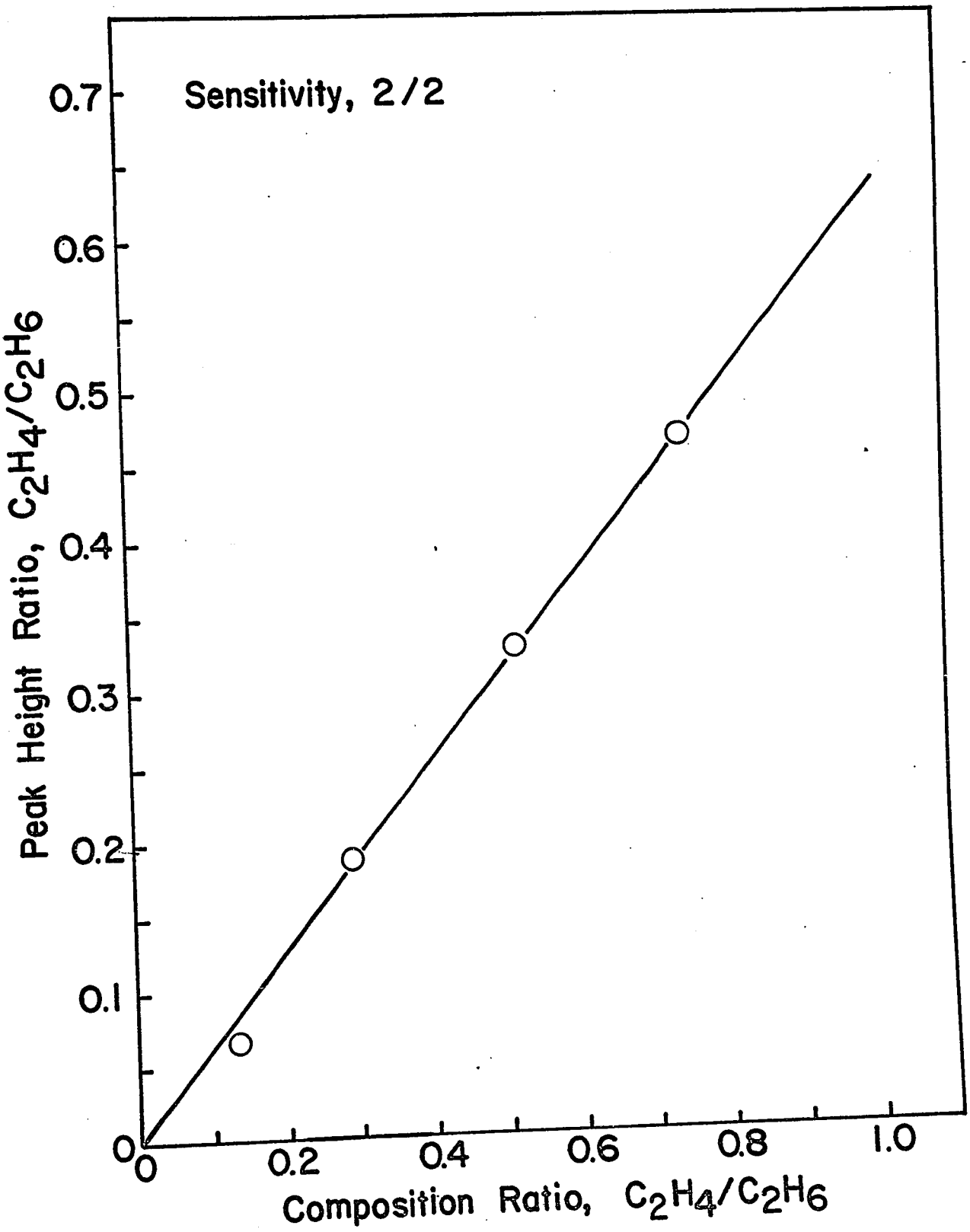

Figure D-8 Calibration of the gas partitioner for the ethylene-ethane system

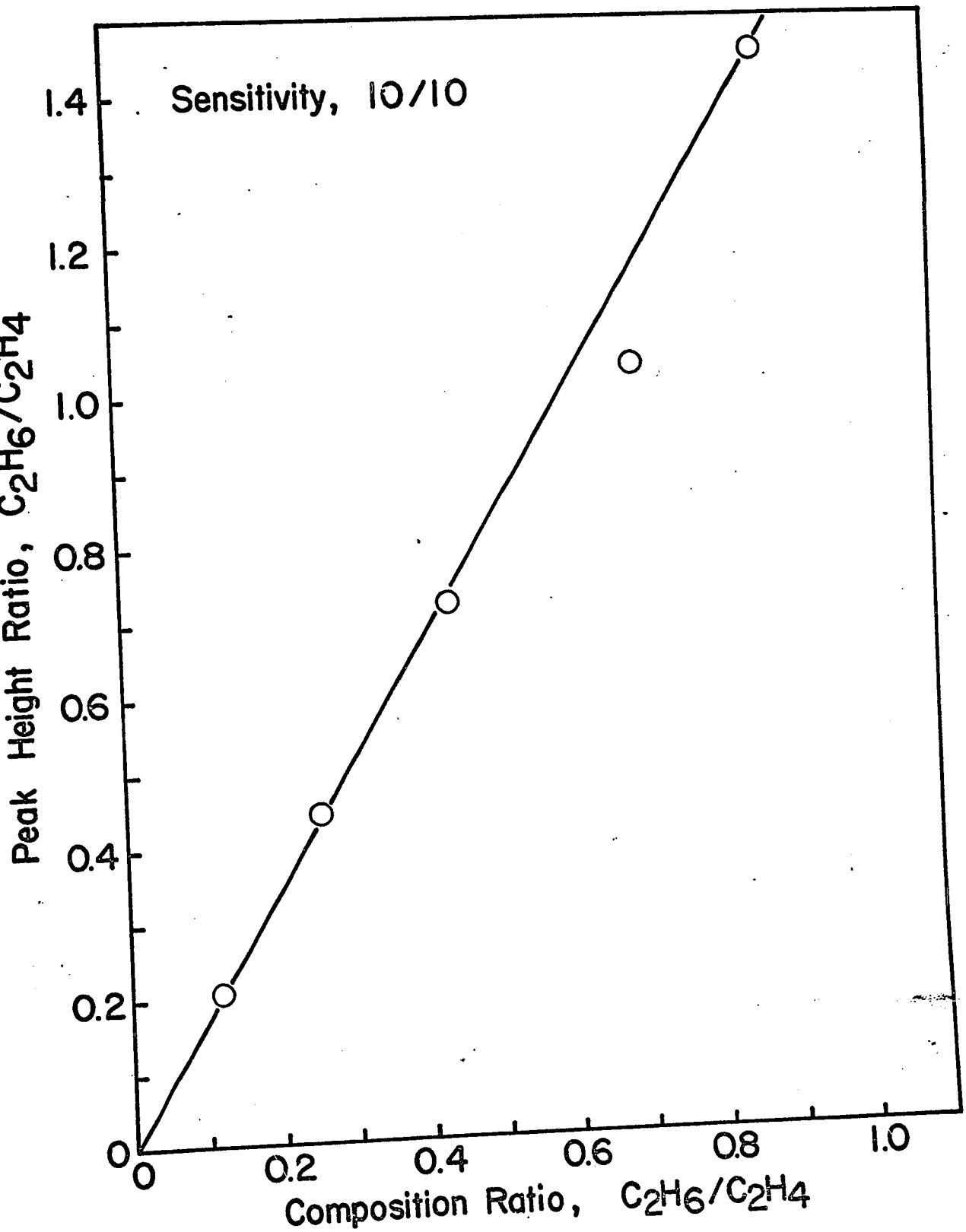

Figure D-9 Calibration of the gas partitioner for the ethane-ethylene system